2007

Effects of Capping on Biodegradation of Organic Contaminants in Sediments

Eun Ju Lee
Louisiana State University and Agricultural and Mechanical College, elee5@lsu.edu

EFFECTS OF CAPPING ON BIODEGRADATION OF ORGANIC CONTAMINANTS IN SEDIMENTS

A Dissertation

Submitted to the Graduate Faculty of the
Louisiana State University and
Agriculture and mechanical College
in partial fulfillment of the
requirements for the degree of
Doctor of Philosophy

in

The Department of Civil and Environmental Engineering

by
Eun Ju Lee
B.S., Gyeong Sang National University, 1995
M.S., Louisiana State University, 2000
December 2007

ACKNOWLEDGMENTS

I would like to express my sincere appreciations to my major professor Dr. John Pardue for his guidance, encouragement and continual support throughout my academic career. I am very grateful for the support and advice from all my committee members, Dr. Donald Dean Adrian, Dr. William M. Moe, Dr. David W. Constant, and Dr. John Scott.

I would like to thank Dr. Gabriel Kassenga and Stephen E. Mbuligwe for tremendous encouragement, experimental help and friendship and extend my thank to my colleagues, wetland research group members, Dr. Xingmao Ma and Dr. Han-Woong Lee, who helped my molecular work. I would like to acknowledge the Dr. Raghunathan Ravikrishna for his guidance using the high pressure liquid chromatography (HPLC) and André Marquette for his help developing the diagenetic model. I would also thank my friends, Elaiza Alvarez, Maria Gabriela Murillo, Dr. Sangjin Lee, Dr. Bing Qi, Dr. Cogna Li, Jun Yan and Kimberly Bowman. Most of all, they made me comfortable.

I would like to extend my appreciation to my parents and brother for their patience and love. Finally, I would like to special thank my husband, Namwon Kim and my son, Leonard Kyungrae Kim, for their encouragement and love.

TABLE OF CONTENTS

ACKNOWLEDGEMENTS……ii

LIST OF TABLES……..v

LIST OF FIGURES…..…….....…..……..…….……..vii

ABSTRACT……xiv

CHAPTER 1. INTRODUCTION……...1
General Description……....1
Literature Review……3
Objectives……..……15

CHAPTER 2. ^{14}C-PHENANTHRENE MINERALIZATION UNDER VARIOUS REDOX CONDITIONS IN ANACOSTIA RIVER SEDIMENTS……17
Introduction……...17
Materials and Methods……..19
Results and Discussion……..25
Conclusions……...45

CHAPTER 3. DIAGENETIC MODEL FOR ASSESSING BIODEGRADATION OF PAHs IN ANACOSTIA SEDIMENTS……....46
Introduction……...46
Mathematical Modeling..……..48
Development of Diagenetic Model……...……53
Calibration of the Model for Anacostia Sediments …..……59
Results and Discussion……..63
Conclusions……108

CHAPTER 4. THE EFFECT ON BIONSOIL ON PAH BIODEGRDATION……..109
Introduction……..……...109
Materials and Methods……111
Results and Discussion……..……..121
Conclusions……140

CHAPTER 5. THE EFFECT ON BIONSOIL ON HCB BIODEGRDATION……..141
Introduction……..……...141
Materials and Methods……143
Results and Discussion……..……..153
Conclusions……171

CHAPTER 6.SORPTIVE REACTIVE CAPPING OF PHENANTHRENE IN ANACOSTIA SEDIMENTS……..172
Introduction……..……...172
Materials and Methods……173
Results and Discussion……..……..186
Conclusions…….216

CHAPTER 7. OVERALL CONCLUSIONS……...…218

LITERATURE CITED……...222

VITA……...……232

LIST OF TABLES

Table 1.1 Biogeochemical reactions (Fossing et al., 2004)……..11

Table 2.1 Oligonucleotide primers used in this study……...24

Table 2.2 First-order rate constants and half-life of phenanthrene in microcosms……...27

Table 2.3 First-order rate constants and half-life of $_{14}CO^2$ production…….30

Table 2.4 Statistical analyses of the PAH mineralization between treatments…….31

Table 2.5 Average hydrogen concentrations associated phenanthrene mineralization and unique range of hydrogen concentrations…….……....39
.

Table 2.6 Bacterial identification by DNA sequencing……44

Table 3.1 Biogeochemical reactions (Fossing et al. 2004)……...49

Table 3.2 Rate expressions in the transport-reaction equations……55

Table 3.3 Input parameters for sediment diagenetic model……..57

Table 3.4 Input data values for the diagenetic model in depth (column 1-105)……...58

Table 3.5 Input data values for Anacostia River sediment model……60

Table 3.6 Sensitivity test from different treatments……..61

Table 3.7 Input data values for the capping simulation (column 1-50; 1.5 cm for cap)…...62

Table 4.1 Properties of the test contaminants (PAHs) (Maagd et al., 1998)……...113

Table 4.2 Oligonucleotide primers used in this study…….120

Table 4.3 First-order rate constants (day^{-1}) and removal efficiency (%) of PAHs…….121

Table 4.4 Sediment TOC and pH values from Anacostia microcosms……...128

Table 4.5 Theoretical stoichiometric equation of PAH compounds……...130

Table 4.6 Real time PCR quantification of bacteria in Anacostia microcosms……..135

Table 4.7 Identification of bacteria from Anacostia microcosms……...136

Table 5.1 Physical and chemical properties of HCB and degradation products…….146

Table 5.2 Oligonucleotide primers used in this study…….151

Table 5.3 First-order rate constants (day^{-1}) of HCB……...160

Table 5.4 Real-time PCR quantification of bacteria, methanogen, and *Dehalococcoides*.166

Table 5.5 Bacterial identification by DNA sequencing……..168

Table 6.1 Assumptions used in the development of RECOVERY (Luiz and Terry, 2001)……181

Table 6.2 Input parameters for phenanthrene transport mathematical model (Lab scale)……...183

Table 6.3 Input for phenanthrene transport mathematical model (Anacostia reactive caps)……184

Table 6.4 Input for phenanthrene transport mathematical model (Anacostia sand caps)...185

Table 6.5 K_d value for phenanthrene among different treatments using linear model…...187

Table 6.6 K_F value for phenanthrene among different treatments using nonlinear Freundlich model……187

Table 6.7 Sediment and water partition coefficient using ^{14}C-phenanthrene…….189

LIST OF FIGURES

Figure 2.1 Degradation of phenantherne and benzo(α)pyrene under different redox conditions 26

Figure 2.2 Mineralization of ^{14}C-phenanthrene in Anacostia sediment under different redox condition 29

Figure 2.3 Nitrate concentrations in Anacostia River sediment microcosms 33

Figure 2.4 Iron concentrations in Anacostia River sediment microcosms 34

Figure 2.5 Manganese concentrations in Anacostia River sediment microcosms 35

Figure 2.6 Sulfate concentrations in Anacostia River sediment microcosms 36

Figure 2.7 Methane concentrations in Anacostia River sediment microcosms 38

Figure 2.8 Hydrogen concentrations in Anacostia River sediment microcosms 40

Figure 2.9 DGGE band with different treatments 43

Figure 3.1 a Concentration profiles of basic diagenetic model 64

Figure 3.1 b Concentration profiles of basic diagenetic model 65

Figure 3.1 c Concentration profiles of basic diagenetic model 66

Figure 3.1 d Concentration profiles of basic diagenetic model 67

Figure 3.1 e Concentration profiles of basic diagenetic model 68

Figure 3.2 a Concentration profiles of Anacostia sediment model as the oxygen rate constant of 0.693 70

Figure 3.2 b Concentration profiles of Anacostia sediment model as the oxygen rate constant of 0.693 71

Figure 3.2 c Concentration profiles of Anacostia sediment model as the oxygen rate constant of 0.693 72

Figure 3.2 d Concentration profiles of Anacostia sediment model as the oxygen rate constant of 0.693 73

Figure 3.2 e Concentration profiles of Anacostia sediment model as the oxygen rate constant of 0.693 74

Figure 3.3 a Concentration profiles of Anacostia sediment model as the nitrate rate constant of 0.693 78

Figure 3.3 b Concentration profiles of Anacostia sediment model as the nitrate rate constant of 0.693 79

Figure 3.3 c Concentration profiles of Anacostia sediment model as the nitrate rate constant of 0.693 80

Figure 3.3 d Concentration profiles of Anacostia sediment model as the nitrate rate constant of 0.693 81

Figure 3.3 e Concentration profiles of Anacostia sediment model as the nitrate rate constant of 0.693 82

Figure 3.4 a Concentration profiles of Anacostia sediment model as the manganic manganese rate constant of 0.693 83

Figure 3.4 b Concentration profiles of Anacostia sediment model as the manganic manganese rate constant of 0.693 84

Figure 3.4 c Concentration profiles of Anacostia sediment model as the manganic manganese rate constant of 0.693 85

Figure 3.4 d Concentration profiles of Anacostia sediment model as the manganic manganese rate constant of 0.693 86

Figure 3.4 e Concentration profiles of Anacostia sediment model as the manganic manganese rate constant of 0.693 87

Figure 3.5 a Concentration profiles of Anacostia sediment model as the ferric iron rate constant of 0.693 88

Figure 3.5 b Concentration profiles of Anacostia sediment model as the ferric iron rate constant of 0.693 89

Figure 3.5 c Concentration profiles of Anacostia sediment model as the ferric iron rate constant of 0.693 90

Figure 3.5 d Concentration profiles of Anacostia sediment model as the ferric iron rate constant of 0.693 91

Figure 3.5 e Concentration profiles of Anacostia sediment model as the ferric iron rate constant of 0.693 92

Figure 3.6 a Concentration profiles of Anacostia sediment model as the sulfate rate constant of 0.693 93

Figure 3.6 b Concentration profiles of Anacostia sediment model as the sulfate rate constant of 0.693 94

Figure 3.6 c Concentration profiles of Anacostia sediment model as the sulfate rate constant of 0.693 95

Figure 3.6 d Concentration profiles of Anacostia sediment model as the sulfate rate constant of 0.693 96

Figure 3.6 e Concentration profiles of Anacostia sediment model as the sulfate rate constant of 0.693 97

Figure 3.7 a Concentration profiles of Anacostia sediment model as the methane rate constant of 0.693 98

Figure 3.7 b Concentration profiles of Anacostia sediment model as the methane rate constant of 0.693 99

Figure 3.7 c Concentration profiles of Anacostia sediment model as the methane rate constant of 0.693 100

Figure 3.7 d Concentration profiles of Anacostia sediment model as the methane rate constant of 0.693 101

Figure 3.7 e Concentration profiles of Anacostia sediment model as the methane rate constant of 0.693 102

Figure 3.8 a Concentration profiles of capping model 103

Figure 3.8 b Concentration profiles of capping model 104

Figure 3.8 c Concentration profiles of capping model 105

Figure 3.8 d Concentration profiles of capping model 106

Figure 3.8 e Concentration profiles of capping model 107

Figure 4.1 Anacostia study sites (From http://www.hsrc-ssw.org/anacostia/) 112

Figure 4.2 Phenanthrene removal in Anacostia sediment microcosm 122

Figure 4.3 Fluoracene removal in Anacostia sediment microcosm..... 123

Figure 4.4 Pyrene removal in Anacostia sediment microcosm 124

Figure 4.5 Benzo(α)anthracene removal in Anacostia sediment microcosm 125

Figure 4.6 Chrysene removal in Anacostia sediment microcosm 126

Figure 4.7 Sulfate concentration changes over time..... 132

Figure 4.8 Methane concentration changes over time..... 133

Figure 4.9 Hydrogen concentration changes over time..... 134

Figure 4.10 PCR amplications of SRB 16S rDNA with SRB specific primers 138

Figure 4.11 Phylogenetic tree using Quantity One® 1-D analysis software..... 139

Figure 5.1 Anacostia study sites (From http://www.hsrc-ssw.org/anacostia/) 145

Figure 5.2 HCB dechlorination in control microcosm 155

Figure 5.3 HCB dechlorination in killed control microcosm 156

Figure 5.4 HCB dechlorination in 20 % BionSoil added microcosm 157

Figure 5.5 HCB dechlorination in 40 % BionSoil added microcosm 158

Figure 5.6 HCB dechlorination in 60 % BionSoil added microcosm 159

Figure 5.7 Sulfate monitoring with time in Anacostia sediment..... 162

Figure 5.8 Methane productions with time in Anacostia sediment 163

Figure 5.9 Hydrogen monitoring with time in Anacostia sediment 164

Figure 5.10 DGGE band 167

Figure 5.11 Phylogenetic tree using Quantity One® 1-D analysis software 170

Figure 6.1 Laboratory Flux Chamber 178

Figure 6.2 Nonlinear Freundlich sorption model for Bionsoil 188

Figure 6.3 Freundlich sorption model using ^{14}C-phenanthrene 190

Figure 6.4 Partition coefficients as function of time 191

Figure 6.5 Desorption in different treatments 192

Figure 6.6 PAH concentrations of cap layer in the sediment with BionSoil cap 195

Figure 6.7 PAH concentrations of sediment layer in the sediment with BionSoil cap 195

Figure 6.8 PAH concentrations of water column in the sediment with BionSoil cap 196

Figure 6.9 PAH concentrations in sediment only without cap 196

Figure 6.10 Aqueous TOC concentrations 197

Figure 6.11 pH value comparisons 197

Figure 6.12 Variation of nitrate flux in sediment with BionSoil cap 199

Figure 6.13 Variation of manganese flux in sediment with BionSoil cap 199

Figure 6.14 Variation of ferric iron flux in sediment with BionSoil cap 200

Figure 6.15 Variation of sulfate flux in sediment with BionSoil cap 200

Figure 6.16 Variation of Nitrate flux in sediment only without cap 201

Figure 6.17 Variation of manganese flux in sediment only without cap..... 201

Figure 6.18 Variation of ferric iron flux in sediment only without cap 202

Figure 6.19 Variation of sulfate flux in sediment only without cap..... 202

Figure 6.20 Flux of phenanthrene from sediment into water in laboratory scale..... 203

Figure 6.21 Flux of phenanthrene from sediment into water without cap 205

Figure 6.22 Flux of phenanthrene from sediment into water with 1 cm BionSoil cap 205

Figure 6.23 Flux of phenanthrene from sediment into water with 5 cm BionSoil cap 206

Figure 6.24 Flux of phenanthrene from sediment into water with 10 cm BionSoil cap ... 206

Figure 6.25 Flux of phenanthrene from sediment into water with 1 cm sand cap 207

Figure 6.26 Flux of phenanthrene from sediment into water with 10 cm sand cap 207

Figure 6.27 a Settling test of BionSoil 210

Figure 6.27 b Settling test of BionSoil 211

Figure 6.27 c Settling test of BionSoil 212

Figure 6.28 a Variation of TSS concentration after re-suspension of BionSoil 213

Figure 6.28 b Variation of TSS concentration after pouring of BionSoil 213

Figure 6.29 a Build up of settled BionSoil layer after re-suspension of previously settled BionSoil 215

Figure 6.29 b Build up of settled BionSoil layer after pouring fresh BionSoil..... 215

ABSTRACT

Sediment capping remains an effective remediation technique for contaminated sediments due to its capability to contain contaminants and provide a sound habitat for indigenous biota. This research investigated the effect of capping on biodegradation of organic contaminants in Anacostia River sediments using both experimental and modeling techniques. ^{14}C–Phenanthrene mineralization was monitored under various redox conditions in Anacostia River sediments. Mineralization of ^{14}C–phenanthrene was strongly linked to sulfate reduction, which was the more energetic process than any other anaerobic condition in Anacostia sediments. Sulfate is a more promising terminal electron acceptor for intrinsic degradation in Anacostia River and other PAH contaminated sites. A sediment flux model was developed as a framework for simulations pertinent to this work and for future use in the field of environmental remediation. The model can be used to predict the response of the primary nutrients and overall sediment redox state after step changes in boundary conditions in sediment.

Further, this study investigated the effects of reactive capping on long-term attenuation of organic contaminants, polycyclic aromatic hydrocarbons (PAHs) and hexachlorobenzene (HCB). Microcosm studies were conducted to investigate the attenuation potential of PAHs and HCB in Anacostia River sediment mixed with BionSoil as a capping material. BionSoil was used because it is rich in organic and carbon sources for driving anaerobic biodegradation and reductive dechlorination reactions. Faster removal kinetics and high sorption potential of HCB were observed in higher ratios of BionSoil than lower ones while for PAHs there were no differences among the treatments. Generally,

degradation kinetics of PAHs and HCB were observed to be the fastest under sulfate-reducing conditions followed by ferric iron-reducing, methanogenesis, and manganic manganese-reducing conditions. Hydrogen concentration trends also suggested that hydrogen was used as an electron donor during both sulfate reduction and methanogenesis. BionSoil was found to be a promising material for *ex-situ* bioremediation in chlorinated solvents contaminated sites. Detection of the 16S rDNA of *Pelobacter sp*. and *Desulfuromonas sp*. by DNA extraction, PCR amplification, cloning and sequencing observed in Anacostia sediment under sulfate reducing conditions. Microbial community analysis results suggested that *Pelobacter sp*. and *Desulfuromonas sp*., which are members of *Geobacteraceae* family, possibly played important roles in the anaerobic degradation of PAHs.

CHAPTER 1
INTRODUCTION

General Description

Hydrophobic organic chemicals, such as polyaromatic hydrocarbons (PAHs) and polychlorinated biphenyls (PCBs), tended to partition to particulate matter and ultimately settle to the bottom sediments. Sediments act as a continual source of contamination to aquatic ecosystem. *In-situ* capping is potentially effective technology to minimize the ecological risk associated with contaminated sediment. *In-situ* capping is the placement of a subaqueous covering or cap of clean isolating material over an *in-situ* deposit of contaminated sediment. It is a potentially effective and economical approach for remediation of contaminated sediment. *In-situ* caps have several primary functions: physical isolation of the contaminated sediment from the benthic environment; stabilization of contaminated sediments, preventing resuspension and transport to other sites, and reduction of the flux of dissolved contaminants into the water column (Azcue et al., 1998; Palermo et al., 1998; U.S. EPA, 1998; Jacobs and Förstner, 1999).

Some caps are designed to act solely as physical barriers to limit migration of pollutants. In these caps no degradation or reaction is encouraged. These caps operate using two mechanisms; (1) to physical contain the contaminated sediment and prevent resuspension and (2) to provide a barrier to the diffusive flux of contaminants to the overlying water. These caps, almost always constructed using sand are an accepted remedial technology for contaminated sediments.

Other caps are designed to provide some additional reactive component to insure that the dissolved contaminant flux is blocked. In these caps degradation of contaminants occurs as the contaminated water passes through whether by diffusion or advection. Reactive caps encourage degradation or sequestration of the contaminants. These capping layers are effective in isolating

contaminated sediments because they are capable of; (1) binding organic-rich capping materials with contaminants, (2) isolating toxic chemicals in sediments, (3) reducing bioturbator activity that release contaminants into water, and (4) promoting natural recovery that degrade contaminants (Azcue et al., 1998; Palermo et al., 1998; Jacobs and Förstner, 1999). The goal of such a cap is to insure elimination of contaminant migration through a cap via sorption, chemical reaction or biodegradation of any contaminants that may migrate. In this study, factors affecting the use reactive caps using biodegradation were investigated in contaminated sediment. The study seeks to provide biogeochemical information on the application of capping technologies to the Anascotia River in Washington, DC where historically industrial, municipal, and military activities have resulted in elevated concentrations of PAHs, PCBs, heavy metals, and other contaminants (http://www.hsrc-ssw.org/anacostia/).

Biodegradation is the biologically catalyzed reduction in complexity of chemicals. In the case of organic compounds, biodegradation leads to conversion of much of the carbon, nitrogen, phosphorous, sulfur (C, N, P, S) and other elements in the original compound to inorganic products (Alexander, 1999). Biodegradation has received particular attention as a clean-up tool for organic compounds because it is destructive rather than simply transferring mass from one location to another. Natural degradation processes lead to the natural attenuation of pollution (Alexander, 1999). Biodegradation in sediments is complicated by the absence of O_2 in many parts of the sediment bed. In the absence of O_2 anaerobic and facultative anaerobic microorganisms have the ability to utilize alternative electron acceptors (AEAs), such as nitrate (NO_3^-), manganese (Mn^{4+}), ferric iron (Fe^{3+}), sulfate (SO_4^{2-}), and carbon dioxide (CO_2). As oxygen is used up, sediment originally in an aerobic state (aerobic respiration) is transformed to anaerobic conditions such as nitrate-reducing conditions, iron-reducing conditions, manganese-

reducing conditions, and sulfate-reducing conditions (Odom and Singleton, 1993; Alexander, 1999; Fossing et al., 2004). The sequence of alternative electron acceptor used is directed related to the energy available to microorganisms that utilize these alternative electron acceptors. In sediments, iron reduction, sulfate reduction and methanogenesis are dominanat. If ferric iron is rich in the system, iron reduction is dominant. If sulfate is rich in the system, sulfate-reducing organisms are dominant. As ferric iron and sulfate are depleted, methanogenic organisms become important with the formation of CO_2 and CH_4 (Odom and Singleton, 1993). Therefore, the ability to monitor anaerobic biodegradation is of prime importance in assessing the fate and biodegradation of organic compounds.

Sorption plays an important role in the physical and biological availability of contaminants in sediments. PAHs, for example, are highly hydrophobic compounds and therefore they tend to partition strongly to solid phase. Biodegradation and sorption will most likely be the important processes that control the natural attenuation of contaminants in the cap material.

Literature Review

Capping Technologies

Capping is defined as the placement of a layer of uncontaminated material over contaminated sediment to isolate the clean medium above the sediment from the contaminated sediment (Brannon et al., 1987; Wang et al., 1991; Thoma et al., 1993; Azcue et al., 1998; Palermo et al., 1998). This covering seals the sediments physically and chemically, preventing pollutants from migrating into the surrounding water. The cap is composed of one or more layers of sand, silt, rock, or geotextile fabrics (Azcue et al., 1998; Palermo et al., 1998; Jacobs and Förstner, 1999). The concept of careful deposition and capping with clean material is a practical

and appropriate measure under favorable conditions. The capping materials are evaluated in terms of coverage, stability, effectiveness in contaminant isolation, and biological potential (Brannon et al., 1986; Sanderson and Mcknight 1986; Wang et al., 1991; Thoma et al., 1993).

Palermo et al. (1998) reports on the description of the capping processes, identification of design requirements and monitoring by conducting *in-situ* capping projects at several sites. To determine the specific capping requirements, contaminant properties such as diffusion coefficients, partitioning coefficients need to be considered. In addition, other parameters such as the cap thickness, consolidation rate, sediment permeability, porosity, and the potential for advective flow condition are required to model long-term cap effectiveness. Long-term monitoring is needed to evaluate performance of the in-situ capping regarding basic cap functions (physical isolation, stabilization, and chemical isolation). Most of all, the thickness of a capping sediment needs to be determined to increase the capping effectiveness (Brannon et al., 1987; Wang et al., 1991; Azcue et al., 1998). Cap design and placement consideration, effective management of a cap, and cost estimation are all important factors for cap properties and thickness (Ravikrishna et al. 2000).

In general, *in-situ* caps have normally ranged from two feet on the low side to between four and five feet on the high side. However, recent research indicates that much thinner caps can be successful in sequestering contaminants for long periods of time. A laboratory study at Louisiana State University (LSU) found that caps as thin as few millimeters drastically reduced the flow of trichlorophenol (TCP) from sediment to water. In containment of PCB study in the New Bedford, Connecticut harbor, LSU research group estimated that 45 centimeter cap would cover the contaminants beneath it for 900 years. They projected that contaminant release would be reduced by 99.9 % even after this time. An Analysis of *in-situ* capping on the Fox River, WI

showed that capping could effectively reduce sediment concentrations and reduce the risk associated eith contaminated sediments as long as cap integrity could be maintained (Reible et al., 2003).

In-situ capping projects have been conducted successfully throughout the world (i.e. The Great Lakes, Long Island Sound, New York Bight, Puget Sound, Los Angeles Harbor, Japan) (http://www.hsrc-ssw.org/anacostia/). Capping works well in sealing a variety of sediment bed types and chemicals. Capping technology is best choice for some of chemicals like aliphatic hydrocarbons, chlorinated solvents, nitrates phosphates, pesticides polychlorinated biphenyls and polynuclear aromatics that they isolates effectively from sediment (http://www.hsrc-ssw.org/anacostia/). The goal of the cap is to insure contaminants migrating through the cap are sorbed, chemically bound, or degraded and not released into the overlying water.

Sand Capping and Reactive Capping

Sand caps are designed to act like physical barriers to limit migration of pollutants. In sand caps, degradation or reaction is not designed to take place. Sand caps are used to retard migration of contaminants from sediments by physically separating contaminants from organisms and the water column (Palermo et al., 1998). No sorption and no biodegradation take place and only physical separation occurs in sand caps.

In the Anacostia capping project, the active capping combines sediment sequestration with contaminant treatment. The treatment of contaminants may migrate through the cap and settle onto the cap from the overlying water. Reactive caps are designed to allow contaminants to pass through. In this type of caps, degradation of contaminants occurs as the contaminated water passes through. Not only physical separation also other destructive technologies such as biodegradation, sorption, and sequestration take place in permeable reactive caps. The

contaminants with alternative materials, such as AquaBlook, Zero-valent iron, Apatite, and BionSoil, can degrade or control more efficiently than sand (http://www.hsrc-ssw.org/anacostia/). The effectiveness of reactive cap using BionSoil was evaluated in this study. BionSoil has potential for nutrient release and is effective primarily against chlorinated organics so, contaminants subject to anaerobic degradation. BionSoil is essentially peat material and a trademark name for a type of processed mixture of animal manure (www.biontech.com). It facilitates sorption of contaminants and can provide a source of carbon for bacteria in waste treatment systems and BionSoil has high organic matter and nutrient content (www.biontech.com). BionSoil encourages degradation of organic contaminants through enhancement of reductive dechlorination and anaerobic degradation of polyaromatic hydrocarbon (PAH) compounds.

In situ treatment of slowly degraded organic contaminants shows a problem due to long time frames necessary for natural bioremediation. A reactive cap could potentially overcome the problem on contaminant flux to the water and the longer time necessary for contaminant removal through biological attenuation processes. The contaminant degradation can be enhanced by reactive cap materials. Reactive caps encourage the fate processes such as degradation or sequestration of the contaminants beneath cap and discourage recontamination of cap. The reactive capping can be extremely effective at reducing the exposure and risk of contaminated sediments.

PAH Biodegradation in Sediments

PAHs are naturally present in crude oil and petroleum products and are also produced during combustion processes. PAHs have been linked with serious ecological damage to the natural environment and adverse health effects to humans. PAHs are common sediment

contaminants and ubiquitously spread worldwide as petroleum sources are used and combustion processes occur. Understanding the fate and transport of PAHs in sediments has drawn the interest of many researchers (Bedessem et al., 1997; Coates et al., 1997; Caldwell et al., 1998; Burland and Edwards et al., 1999; Eriksson et al., 2003). Both aerobic transformation and anaerobic biotransformation of PAHs have been studied (Coates et al., 1996a, Coates et al., 1996b; Coates et al., 1997; Caldwell et al., 1998; Hayes et al., 1999; Rothermich et al., 2002). Under anaerobic or oxygen limited conditions, microbial transformation of aromatic compounds under denitrifying, sulfate-reducing, and methanogenic conditions have been reported (Lovley and Phillips, 1987; Caldwell et al., 1998; Burland and Edwards et al., 1999).

Coates et al. (1996b) were the first to demonstrate the oxidation of PAHs under sulfate-reducing conditions. These researchers documented the oxidation of [^{14}C] naphthalene and [^{14}C] phenanthrene to $^{14}CO_2$ under strict anaerobic conditions in sediments from San Diego Bay, California. Sulfate reduction was necessary for PAH oxidation in these marine sediments. Results from this study suggest that the self-purification capacity of PAH-contaminated, sulfate-reducing environments may be greater than previously recognized (Coates et al., 1996b). Further investigations with the San Diego Bay sediments revealed that methylnaphthalene, fluorene, and fluoranthene were also anaerobically transformed to carbon dioxide, while pyrene and benzo[α]pyrene were not (Coates et al., 1997). Studies with naphthalene indicated that PAH oxidation was sulfate-dependent. Incubating the sediments with additional naphthalene for one month resulted in a significant increase in the transformation of [^{14}C] naphthalene. Results from Coates et al. (1997) study point to the possibility of utilizing sulfate reduction as a treatment strategy for PAH contaminated soil and sediments. Although PAHs entering pristine anaerobic marine sediments may not be degraded immediately, microbial populations capable of utilizing

the abundant sulfate as an electron acceptor can develop over time to metabolize these compounds. In a study conducted by Bedessem et al. (1997) the addition of molybdate, a competitive inhibitor of sulfate reduction, resulted in a 45% reduction in naphthalene degradation in enrichment cultures. Radiolabeled experiments confirmed naphthalene mineralization to CO_2 with simultaneous reduction of sulfate to sulfide. Inhibition of sulfidogenesis by molybdate and a concomitant decrease in naphthalene oxidation provided convincing evidence that naphthalene mineralization was coupled to sulfate reduction (Bedessem et al., 1997). The anaerobic mineralization pathways of PAH compounds are not established to date. Carboxylation has been shown as an initial reaction in the anaerobic transformation by sulfidogenic consortia. Thus, it appears that a sufficiently long adaptation period and the availability of appropriate electron acceptors may be a necessity for the biotransformation of PAHs under anaerobic conditions.

HCB Dechlorination

HCB is very hydrophobic in nature with a low aqueous solubility (0.005 mg/L) at 25°C. The U.S. EPA has classified HCB as a probable human carcinogen and has established national primary drinking water standards as follows: maximum contaminant level (MCL) of 0.001 mg/L (Pavlostathis and Prytula, 2000). HCB is a hydrophobic organic chemical that has shown a lack of toxicity in water at concentrations up to and exceeding the solubility limit (Fuchsman et al., 1998). A potential risk is present in contaminated sediment. HCB is rather persistent and binds to particulate matter and easily bioaccumulates into the organism and food chain (Boese et al., 1996; Nakashima et al., 1997; Fuchsman et al., 1998).

Many studies have shown that anaerobic reductive dechlorination of HCB yields lower chlorinated benzenes (Sims et al., 1991; Beurskens, 1995; Middeldorp et al., 1997; Pavlostathis

and Prytula, 2000). The most often cited predominant pathway of the microbial reductive dechlorination of HCB is as follows: HCB → pentachlorobenzene (PeCB) → 1,2,3,5-tetrachlorobenzene (1,2,3,5-TeCB) → 1,3,5-trichlorobenzene (1,3,5-TrCB). 1,3,5-TrCB usually accumulates, although it can be further reduced via 1,3-dichlorobenzene (1,3-DCB) to monochlorobenzene or even benzene (Beurskens, 1995; Chen et al., 1997; Middeldorp et al., 1997; Pavlostathis and Prytula, 2000). However, these latter reactions tend to occur much more slowly and result in trace levels of dechlorination products. Other possible tetrachlorobenzene (1,2,3,4-TeCB and 1,2,4,5-TeCB), trichlorobenzene (1,2,3-TrCB and 1,2,3-TrCB), and dichlorobenzene (1,4-DCB and 1,2-DCB) isomers have been observed either less frequently or at low levels as compared with the above-discussed predominant HCB sequential dechlorination pathway (Pavlostathis and Prytula, 2000).

Reductive dechlorination of polychlorinated benzene congeners and accumulation of less chlorinated benzene congeners (CBs) has been documented for reduced environments such as soils rich in organic matter and sediments (Sims et al., 1991; Pavlostathis et al., 2000). Since chlorinated compounds are used as electron acceptors during reductive dechlorination, there must be an appropriate source of carbon for microbial growth in order for reductive dehalogenation to occur. Organic matter is one of the potential carbon sources of energy for anaerobic microorganisms. A number of studies have demonstrated that dechlorination kinetics is faster in organic carbon rich soils than in soils poor in organic carbon content because microbial activity depends on the availability of organic carbon (Lorah et al., 1997, Kassenga et al., 2003). Therefore, HCB dechlorination would be expected to be faster in soils rich in organic carbon content.

Redox conditions in soils and sediments can impact HCB dechlorination. Beurskens (1995) reported concomitant dechlorination of HCB with sulfate reduction. The degadation of HCB under sulfidogenesis and methanogenesis is thermodynamically possible since reactions involving HCB conversion to benzene offers more energy (1717.6 kJ/mol) to anaerobic bacteria than the reduction of compounds available naturally in anaerobic environments, such as sulfate to sulfur (551.84 kJ/mol) and carbon dioxide to methane (400.46 kJ/mol) (Sims et al., 1991; Dolfing et al., 1992). Chen et al. (2002) investigated the reductive chlorination of HCB under various redox conditions. Results indicated that level of microbial activity impacted dechlorination (Chen et al., 2002). Researchers have also demonstrated reductive dechlorination of HCB under methanogenic conditions (Beurskens et al, 1994; Chang et al., 1997). Beurskens et al. (1994) determined dechlorination rates. Chang et al. (1997) demonstrated reductive dechlorination of HCB by an anaerobic mixed culture including methane producing bacteria. The chlororespiring anaerobe *Dehaloccoides* sp. strain CBDB1 can degrade chlorinated benzene (CB) compounds. Strain CBDB1 is capable of coupling growth to dechlorination of CBs (Adrian et al., 2000; Jayachandran et al., 2003; Jayachandran et al., 2004).

Redox Changes after Capping

As a cap layer is added over the sediment the sediment interfacr is buried subsequently transformed to a different redox condition. This may be an objective of the reactive capping process or an unintended consequence. For example reactive caps may be developed that enhance redox-driven biological reduction processes since sediments change to more reducing conditions after cap placement.

The degradation of organic matter utilizes oxygen when it is available (Alexander, 1999). Oxygen is typically present in the water column and in the upper few millimeters of the

sediment. When oxygen is reduced and depleted, mineralization continues to proceed through anoxic or anaerobic processes (Odom and Singleton, 1993; Alexander, 1999; Fossing et al., 2004). Respiration with oxygen takes place in the uppermost layers sediment, followed by respiration with nitrate, oxidized iron and manganese compounds and sulfate, respectively. Further down in the sediment, the degradation of organic matter occurs through methane fermentation (Fossing et al., 2004). The primary redox reactions use organic carbon as the reductant and occur through bacterial respiration using these alternate electron acceptors.

The oxidation of organic matter produces the reduced pore water species Mn^{2+}, Fe^{2+}, NH_4^+, H_2S, and CH_4, which may participate in secondary redox conditions (Van Capellen and Wang, 1996). Primary and secondary redox reactions are listed in Table 1. Fossing et al. (2004) reported that secondary reactions are ones that involve the restoration of reduced pore water species to their oxidized state (i.e. NO_3^-, MnO_2, FeOOH, and SO_4^{2-}). Important secondary reactions may include nitrification (eq. 6, Table 1.1), oxidation of ferrous iron to the iron oxyhydroxide form by MnO_2 (eq. 8, Table 1.1) the formation of pyrite (eq. 13 and 14, Table 1.1)

Table 1.1 Biogeochemical reactions (Fossing et al., 2004)

Degradation of organic material

$$(CH_2O)_C\left(NH_4^+\right)_N\left(PO_4^{3-}\right)_P + cH_2O \rightarrow cCO_2 + nNH_4^+ + pPO_4^{3-} + 4ce^- + 4cH^+$$

Primary reactions

(1) *Aerobic respiration*: $O_2 + CH_2O \rightarrow CO_2 + H_2O$

(2) *Denitification*: $4NO_3^- + 5CH_2O + 4H^+ \rightarrow 2N_2 + 5CO_2 + 7H_2O$

(3) *Manganese(hydr)oxide reduction*: $2MnO_2 + CH_2O + 4H^+ \rightarrow 2Mn^{2+} + CO_2 + 3H_2O$

(Table 1.1 cont'd)

(4) *Iron (hydr)oxide reduction*: $4FeOOH + CH_2O + 8H^+ \rightarrow 4Fe^{2+} + CO_2 + 7H_2O$

(5) *Sulfate reduction*: $SO_4^{2-} + 2CH_2O + 2H^+ \rightarrow H_2S + 2CO_2 + 2H_2O$

Secondary reactions

(6) $NH_4^+ + 2O_2 \rightarrow NO_3^- + H_2O + 2H^+$

(7) $(FeOOH)_N + PO_4^{3-} \rightarrow (FeOOH)_N \equiv PO_4^{3-}$

(8) $2Fe^{2+} + MNO_2 + 2H_2O \rightarrow 2FeOOH + Mn^{2+} + 2H^+$

(9) $2Mn^{2+} + O_2 + 2H_2O \rightarrow 2MNO_2 + 4H^+$

(10a) $nH_2S + 2(FeOOH)_N \equiv PO_4^{3-} + 4NH^+ \rightarrow nS^0 + 2nFe^{2+} + 4nH_2O + 2PO_4^{3-}$

(11) $4Fe^{2+} + O_2 + 6H_2O \rightarrow 4FeOOH + 8H^+$

(10b) $H_2S + 2FeOOH + 4H^+ \rightarrow S^0 + 2Fe^{2+} + 4H_2O$

(12) $H_2S + MnO_2 + 2H^+ \rightarrow S^0 + Mn^{2+} + 2H_2O$

(13) $H_2S + Fe^{2+} \rightarrow FeS + 2H^{2+}$

(14) $FeS + S^0 \rightarrow FeS_2$

(15) $SO_4^{2-} + 3H_2S + 4FeS + 2H^+ \rightarrow 4FeS_2 + 4H_2O$

(16) $H_2S + 2O_2 \rightarrow SO_4^{2-} + 2H^+$

(17) $FeS + 2O_2 \rightarrow Fe^{2+} + SO_4^{2-}$

(18) $2FeS_2 + 7O_2 + 2H_2O \rightarrow 2Fe^{2+} + 4SO_4^{2-} + 4H^+$

(19) $4S^0 + 4H_2O \rightarrow 3H_2S + SO_4^{2-} + 2H^+$

The relative location of each primary redox reaction can have a large effect on the degradation of typical zone. Recent researchers have investigated organic degradation related with various redox conditions. Ramsay et al. (2003) showed that PAH mineralization can be linked to wide range of terminal electron acceptors (TEAs): oxygen, nitrate, Fe (III) and sulfate reduction. PAH can be degraded when any of these TEAs were available. The availability of alternate electron acceptors and the link to organic matter oxidation has been widely studied as the area of early diagenesis of sediment organic matter. (Canfield et al., 1993 and Fossing et al., 2004). The hypotheses are listed what happens to the redox processes after putting a cap on the top of the sediment as follows.

1) Sediment will change the strictly anaerobic condition, more anaerobic condition. Oxygen is immediately gone as cap layer blocks the oxygen exposure. Cap will contact with overlying water.

2) Fluxes of solids to sediment surface will cease. No material exchange occurs between cap and sediment and reactions occur within sediment only.

3) System will become closed.

The fate of chemical and possible electron acceptor parameters in contaminated sediment is described during and after capping by determining the PAH mineralization with reodx processes. These results are applied to the model for contaminated sediment management with incorporating redox processes.

Modeling

Mathematical modeling has become an important tool in science and engineering. In recent decades, many researchers performed modeling as an essential component in the fields of fluid mechanics and meteorology. Compared with other fields, the development of mathematical

models for organic matter and nutrient diagenesis in sediments has not had a good improvement (Boudreau, 1996; Berg et al., 2003). Mathematical models of organic matter and nutrient diagenesis in sediments are based on mass conservation approaches expressing balances between vertical transport of selected components and biogeochemical reactions (Berg et al., 2003; Fossing et al., 2004). Modeling of organic matter and nutrient diagenesis is a challenge task to identify and subsequently parameterize the transport processes and biogeochemical reactions to simulate an appropriate fraction of the real and complex world (Berg et al., 2003). The classic book by Berner (1980) contains the analytical transport-reaction models and it presents the advantage of mathematical models for interpretation of measured data and as tools for achieving the various analyses. The transport-reaction models were based on a vertical one-dimensional description of the sediment column (Boudreau, 1996; Soetaert et al., 1996; Dhakar and Burdige, 1996; Van Capellen and Wang, 1996). These diagenetic models account for molecular diffusion, burial, and bioturbation with respect to the vertical transport in the sediment. The model by Van Capellen and Wang (1996) is impressive because of their model parameterization and validation using the measurements by Canefield et al. (1993). In recent, a model of organic matter and nutrient diagenesis in marine sediments describes the oxygen consumption pathways and the cycling of carbon, nitrogen, manganese, iron, and sufur (Berg et al., 2003). This model accounts for molecular diffusion, burial, bioturbation, and irrigation with respect to the vertical transport in the sediment. This model also includes adsorption processes, and the description of organic matter degradation.

Diagenetic models for assessing changes in redox species in sediments can accurately reproduce profiles in a variety of sediment types. The reactive caps are developed with enhancing redox-driven attenuation processes since sediments change to more anaerobic

condition. From Van Capellen and Wang (1996)'s STEADYSED code to the recent model development by Fossing et al. (2004), numerical models of redox processes in sediments are at a fairly advanced state of development. To date, these models have not been extended to contaminated sediments management for organics or metals, despite some obvious needs to have modeling tools that incorporate an understanding of redox processes.

Objectives

The overall objective of the proposed dissertation research is to investigate the reactive capping using highly organic BionSoil as the electron donor in a reactive cap considering anaerobic degradation for PAHs and HCB. Studies identify the dominant processes responsible for attenuation of the test chemicals in the capping material and factors that enhance them and determine fluxes of PAHs and HCB from the capping material. The research work involves:

1) Mineralization of PAH to assess the changes in redox species in sediments for diagenetic models set-up using the radiorespirometry studies.

2) Utilization of a diagenetic model to demonstrate proof of concept.

3) Determination of the degradation kinetics of PAHs and HCB in different ratios of river sediment and BionSoil mixtures using batch microcosms.

4) Evaluation of the reactive capping effectiveness using the potential fluxes of PAHs and nutrients in Anacostia sediment.

Experimental results of the research are presented in the following chapters of this dissertation. The results of study on the mineralization of PAH under various redox conditions and capping model in Chapter 2 and Chapter 3, respectively. In Chapter 4, study on testing the effect of BionSoil on PAH biodegradation is reported. Results of HCB biodegradation with microbial analysis is presented in Chapter 5. Studies on sorptive reactive capping of

phenanthrene using the Anacostia sediments are presented in Chapter 6. Finally, Chapter 7 summarizes major findings and conclusions of this dissertation.

CHAPTER 2
^{14}C – PHENANTHRENE MINERALIZATION UNDER VARIOUS REDOX CONDITIONS IN ANACOSTIA RIVER SEDIMENTS

Introduction

Polycyclic aromatic hydrocarbons (PAHs) are priority pollutants that can cause serious ecological damage to the natural environment and adverse health effects to humans. PAHs are common sediment contaminants and spread worldwide due to the widespread use of petroleum energy sources. The rate and extent of microbial degradation of PAHs is largely determined by different environmental conditions including temperature, salinity, and redox conditions. Specifically the redox conditions are dictated by the availability of oxygen, nitrate, ferric iron, manganic manganese, sulfate and CO_2 in the environment. Understanding the fate and transport of PAHs in sediments under various redox conditions has drawn the interest of many researchers (Bedessem et al., 1997; Coates et al., 1997; Caldwell et al., 1998; Burland and Edwards et al., 1999; Eriksson et al., 2003). Oxygen is typically present in the water column and in the upper few millimeters of the sediment. When oxygen is reduced and depleted, mineralizations continue to proceed through anaerobic processes (Odom and Singleton, 1993; Alexander, 1999; Fossing et al., 2004). Respiration with oxygen takes place in the uppermost layers sediment, followed by respiration with nitrate, oxidized iron and manganese compounds and sulfate in the order of respiratory substrates respectively. Further down in the sediment, the degradation of organic matter occurs through methane fermentation (Fossing et al., 2004).

Researchers have studied anaerobic biotransformation of PAH hydrocarbon contaminants (Coates et al., 1996a, Coates et al., 1996b; Coates et al., 1997; Caldwell et al., 1998; Hayes et al., 1999; Rothermich et al., 2002). Microbial transformation of aromatic compounds under denitrifying, sulfate-reducing, and methanogenic conditions have been reported (Lovley and

Phillips, 1987; Caldwell et al., 1998; Burland and Edwards et al., 1999). Coates et al. (1996b) were the first to demonstrate the oxidation of PAHs under sulfate-reducing conditions. Results from this study suggested that the self-purification capacity of PAH-contaminated, sulfate-reducing environments would be greater than previously recognized (Coates et al., 1996b).

It appears that a sufficiently long adaptation period and the availability of appropriate electron acceptors may be a necessity for the biotransformation of PAHs under anaerobic conditions. The availability of alternate electron acceptors and the link to organic matter oxidization has been widely studied as the area of early diagenesis of sediment organic matter. (Canfield et al., 1993; Fossing et al., 2004). Ramsay et al. (2003) showed that PAH mineralization could be linked to wide range of terminal electron acceptors (TEAs): oxygen, nitrate, ferric iron and sulfate reduction. PAH could be degraded when any of these TEAs were available.

Biodegradation is enhanced when the process is linked with microbial growth. PAH degrading organisms isolated to date ((Lovley et al., 1995; Holmes et al., 2002), they have been observed to use a limited set of electron donors, primarily hydrogen. The hydrogen is produced and consumed by methanogens, nitrate-reducing bacteria, ferric iron –reducing bacteria, and sulfate-reducing bacteria. They compete for hydrogen, and competition can limit anaerobic degradation due to the limited supply of hydrogen (Lovley and Klug, 1983; Lovley and Phillips, 1987).

This radiorespirometry study was performed to assess the mineralization of PAH related to changes in redox species in sediments for diagenetic models. The present study investigated the effect of different redox conditions on PAH degradation in Anacostia River sediment using radiolabelled ^{14}C-phenanthrene. The important environmental conditions were identified by the

effect of reduced form of TEAs on PAH degradation and the microorganisms were determined with relative role of degradation under dominating environments. Furthermore, model can predict reproducing sediment profiles by changing in redox species (Chapter 3).

Materials and Methods

PAH degradation was studied in both laboratory microcosms and radiorespirometers using Anacostia River sediments under a variety of redox conditions. These sediments have past exposure to heavy metals, polychlorinated biphenyls (PCBs), and polyaromatic hydrocarbons (PAHs) due to long-term military and industrial activity. The Anacostia River is one of endangered rivers in U.S. and has large watershed coverage within Maryland and the District of Columbia.

Microcosm Studies

PAH biodegradation experiments were conducted in microcosms under anaerobic conditions. The microcosms contained 125 mL of a 1:1.5 (sediment:water (w/w)) slurry prepared from sediment from the Anacostia site. A 1:1.5 (sediment:water (w/w)) sediment slurry was produced by mixing sediment with sterile water using a low speed blender. One hundred mL of the slurry was placed in 125 mL serum bottles with rubber septa in the anaerobic glove box. Five different redox conditions were established in the microcosms: control (sediment only), nitrate (2.34 mM of nitrate added as $NaNO_3$) (Ramsay *et* al. 2003), ferric iron (25 mM added as amorphous Fe (III) oxyhydroxide (FeOOH) (Lovely et al., 1986), manganese (25 mM added as manganese oxide), and sulfate (1.41 mM of sulfate added as Na_2SO_4) (Ramsay *et* al. 2003) in triplcate. Abiotic controls were established with mercuric chloride (3.89 % wt/vol).

For PAH analysis, one gram of slurry was extracted with an equal mass of HPLC (High Performance Liquid Chromatography) grade hexane (Fisher Scientific, Pittsburgh, PA) in glass scintillation vials. The mixture was then tumbled to extract for 24 hrs. After centrifugation, the extracts were concentrated 10 times under a stream of dry nitrogen and transferred into 1.8 mL glass, crimp-capped vials. HPLC grade acetonitrile was added to make 1 mL for HPLC analysis. The extracts were analyzed using an Agilent 1100 series Π high performance liquid chromatography (HPLC). Concentrations of PAHs were monitored using the gradient method (40:60 (v/v) water:acetonitrile at initial time to 100 % acetonitrile at 25 minutes). A Phenomenex column (Envirosep-PP) was used to separate the individual PAHs in the sample. The column was maintained at 40°C and the flow rate was kept constant at 0.5 ml/min. The analytical column was an HP 5 μm ODS Hypersil 4.6 mm × 25 cm cartridge columns. Selected PAHs were detected using two detectors, UV absorbance using a diode array detector and UV fluorescence detector. Data was collected for both detectors. The fluorescence detector data (operated with a high photo-multiplier-tube (PMT) gain) was used when the concentrations in the sample was below the detection limit for the UV absorbance. These detectors were calibrated regularly with sixteen PAH standards for UV absorbance and different gains for UV fluorescence using at least 4 points.

Phenanthrene, chrysene, and benzo(α)pyrene were selected for monitoring due to their initial concentrations on the slurries. PAH loss over time was fitted using non-linear regression to exponential decay for the first order kinetic equation given below:

$$\frac{C}{C_0} = e^{-kt}$$

where C is a PAH concentrations, C_0 is an initial PAH concentrations, t is a time (days), and k is a pseudo-first order rate constant.

Radiolabelled Carbon Respirometer Studies

A 1:1.5 (sediment:water (w/w)) sediment slurry was produced by mixing sediment with sterile water using a low speed blender. Eighty mL of the slurry was placed in 125 mL serum bottles with Teflon-lined rubber septa in the anaerobic glove box. A total of 30 respirometers were set up using the five different redox conditions plus a control in triplicate, as described above. PAH mineralization was compared between control respirometers and those incubated under different redox conditions. ^{14}C-phenanthrene (8.2 mCi/mmol, 0.5 mCi/mL) greater than 98 % purity and dissolved in methanol was obtained from Sigma (St. Louis, MO). To add the ^{14}C-phenanthrene uniformly, a sediment aliquot (0.2 g) was dried overnight and then autoclaved for 1 h. ^{14}C-phenanthrene in methanol (2 μL, equivalent to 0.1 μCi) was added to the dried, sterile sediment pellets. After the methanol on the pellet was volatilized using a stream of dry N_2 (ca. 30 s) a pellet was added to each respirometer, the serum bottle resealed, vortexed, and incubated **(**Hayes *et* al., 1999; Rothermich *et* al., 2002).

Mineralization rates were determined by trapping volatile $^{14}CO_2$ in 1N NaOH in a 5 mL test tube inside the respirometer. Every three or four days, the NaOH was removed, replaced using a syringe a 15 cm-long needle, and the headspaces of the respirometer was flushed with nitrogen. The spent NaOH was placed in 10 mL of Hionic-fluor (Perkin Elmer, Inc. Shelton, CT) scintillation cocktail. Scintillation counting was performed on Beckman LS 6000 SC. Microcosms were kept in an anaerobic glove bag at room temperature during incubation.

$^{14}CO_2$ generation results were fitted using non-linear regression to a first order production equation below.

$$\frac{C}{C_0} = e^{kt}$$

where C is cumulative trapped $^{14}CO_2$ activity at any time, t, C_0 is an initial background $^{14}CO_2$ activity, t is a time (days), and k is a rate constant for $^{14}CO_2$ production (day^{-1}).

Electron Acceptor Analyses

Electron acceptor analyses were performed on the identically prepared microcosms with no radiolabelled compounds added. The concentrations of nitrate, ferric and ferrous iron, manganic and manganous manganese, and sulfate were analyzed using a Hach DR 2010 spectrophotometer (Hach Co., Loveland, CO). Pore water from the microcosms was taken and diluted with deoxygenated water to 25 mL to analyze using the spectrophotometer. Absorbances were read directly by adding the Hach reagent and inserting the samples into the spectrophotometer. A standard calibration was performed for each lot of reagents. Standards of 5 different points by diluting of the contents of an ampule standard were prepared.

Hydrogen was analyzed using a gas chromatograph equipped with a reduction detector (Trace Analytical, Menlo Park, CA). Headspace samples were injected into a 1 mL gas sampling loop and were separated with a molecular sieve analytical column (Trace Analytical, Menlo Park, CA) at an oven temperature of 40˚C. Ultrahigh purity nitrogen (BOC Gases, Baton Rouge, LA) was used as a carrier gas after it was passed through a catalytic combustion converter to removes traces of H_2. The detection limit for H_2 under these conditions was 1 ppb. Aqueous H_2 concentrations were calculated according to Löffler et al. (1999). Methane was measured using an Agilent 5890 series II gas chromatography / flame ionization detector (GC/FID). One mL of gas was injected onto a 2.4 m × 0.32 mm i.d. column packed with Carbopack b/l % SP-1000 (Supoelco, Bellefonte, PA) from the headspace of the bottle using a gas tight syringe. The

injector and detector temperatures were 375ºC and 325ºC, respectively. The column temperature was held constant (50ºC) for 6.50 min. Ultrahigh purity nitrogen (BOC Gases, Baton Rouge, LA) was used as a carrier gas. Headspace methane concentrations were converted to aqueous phase concentrations using a Henry's Law constant of 0.6364 atm/mol/m^3 in methane.

Microbial Analysis

The protocol of Mo Bio Ultraclean Soil DNA Isolation Kit (Mo Bio Laboratories, Inc., Carlsbad, CA) was followed to extract DNA from 0.25 g of wet sediment slurry from the microcosm bottles. Sediment samples were washed twice with 0.12 M of sodium phosphate buffer to remove extracellular DNA. Extracted DNA was amplified using PCR using 20 μL reaction volume. Each reaction contained DNA Polymerase (1 U), 1x Taq Buffer, 3 mM of $MgCl_2$, 1 μM of each primer, 0.2 mM of deoxynucleoside triphosphate (dNTP) (Promega Corporation, Madison, WI) and 1 μL of extracted DNA. PCR conditions were as reported by Hendrickson et al. (2002) for the bacteria group: initial denaturation at 95ºC for 2 min, followed by 30 cycles consisting of denaturation at 94ºC for 1 min, annealing at 55ºC for 1 min, and extension at 72ºC for 1 min. PCR amplication was performed using a PCR Detection System iCycler iQ (Bio-Rad Laboratories, Inc., Hercules, CA). The PCR products were purified with MoBio PCR Clean-Up Kit (Mo Bio Laboratories, Inc., Carlsbad, CA). The molecular weight of products was determined by electrophoresing portions of extracts on 1.0 % agarose gels with a 1-kb ladder (Promega Corporation, Madison, WI) as a size marker. The oligonucleotide primers are listed in Table 2.1. All these primers were obtained from Alpha DNA (Montreal, Quebec, Canada).

Table 2.1 Oligonucleotide primers used in this study

Primer	Sequence (5´ - 3´)	References
	Universal Primers for 16s rDNA (non GC)	Schafer and Muyzer (2001)
341f	5´-CCTACGGGAGGCAGCAG-3´	
907r	5´-CCGTCAATTCMTTTRAGTTT-3´	
	Universal Primers for DGGE (GC clamp)	Schafer and Muyzer (2001)
341f	5´-GCCCGCCGCGCCCCGCGCCCGTCCCGCC GCCCCCGCCCGCCTACGGGAGGCAGCAG-3´	
907r	5´-CCGTCAATTCMTTTRAGTTT-3´	

Denaturating gradient gel electrophoresis (DGGE) was performed using a D-Code™ Universal Mutation Detection System (Boi-Rad, Hercules, CA). The denaturing gradient gel (6 %, wt/v, acrylamide solution) was used for a particular size range between 300 and 1000 base pairs. The acrylamide gels were made with gradient ranging from 40 % to 70 %, where 100 % denaturant contained 42 % (wt/v) urea and 40 % (v/v) formamide. Polymerization was catalyzed by adding 0.057 % of TEMED (v/v) and 0.85 % of the 10 % ammonium persulfate (v/v) to both denaturant solutions. Gels were cast using a Bio-Rad Model 475 gradient delivery system. Electrophoresis was performed in 1x TAE buffer at 60˚C for 16 hours with an applied current of 0.15 A at 65 V. After electrophoresis, the gel was stained with ethidium bromide (EtBr) for 10 min. then, destained in distilled water for 10 min. The gel was imaged with a UV transilluminator using the Chemidoc XRS system using Quantity One® 1-D Analysis Software (Bio-Rad, Hercules, CA). Significant bands from DGGE profile were chosen for sequencing PCR.

DNA was amplified using PCR reactions with non GC primers, 341F and 907R, for cloning. A ligation reaction was performed using pGEμ-T-vector and transformation was accomplished with *E.coli* competent cells (Promega Coporation, Madison, WI) through the protocol provided by manufacturer. LB (Luria-Bertani) plates with ampicillin/IPTG/X-Gal and liquid LB media with ampicillin were prepared to plate *E.coli* competent cells. The growing white colonies were selected, and transferred into liquid LB medium with ampicillin, and incubated overnight at 37˚C. The plasmid with inserts was extracted from liquid LB medium using the plasmid preparation kit (Mo Bio Laboratories, Inc., Carlsbad, CA). To verify the clone plasmid products, restriction enzyme reactions were conducted and checked with gel electrophoresis. DNA products were purified using the MoBio PCR Clean-Up Kit. Finally, samples were sent to BioMMED (Biotechnology and Molecular Medicine) in the School of Veterinary Medicine of Louisiana State University for sequencing.

Results and Discussion

Microcosm Experiments

The microcosm studies showed anaerobic degradation of PAHs among the different treatments was slow with the extract of degradation generally less than 10 % in treatments for PAHs over the ~200 days of incubation (Figure 2.1). Pyrene and chrysene graphs are not shown. For phenanthrene and benzo(α)pyrene, there was approximately a 20 % reduction when sulfate was added as an electron acceptor. This is consistent with previous reports of degradation of PAHs under sulfate reducing conditions (Coates et al., 1996b; Coates et al., 1997; Caldwell et al., 1998; Rothermich et al., 2002).

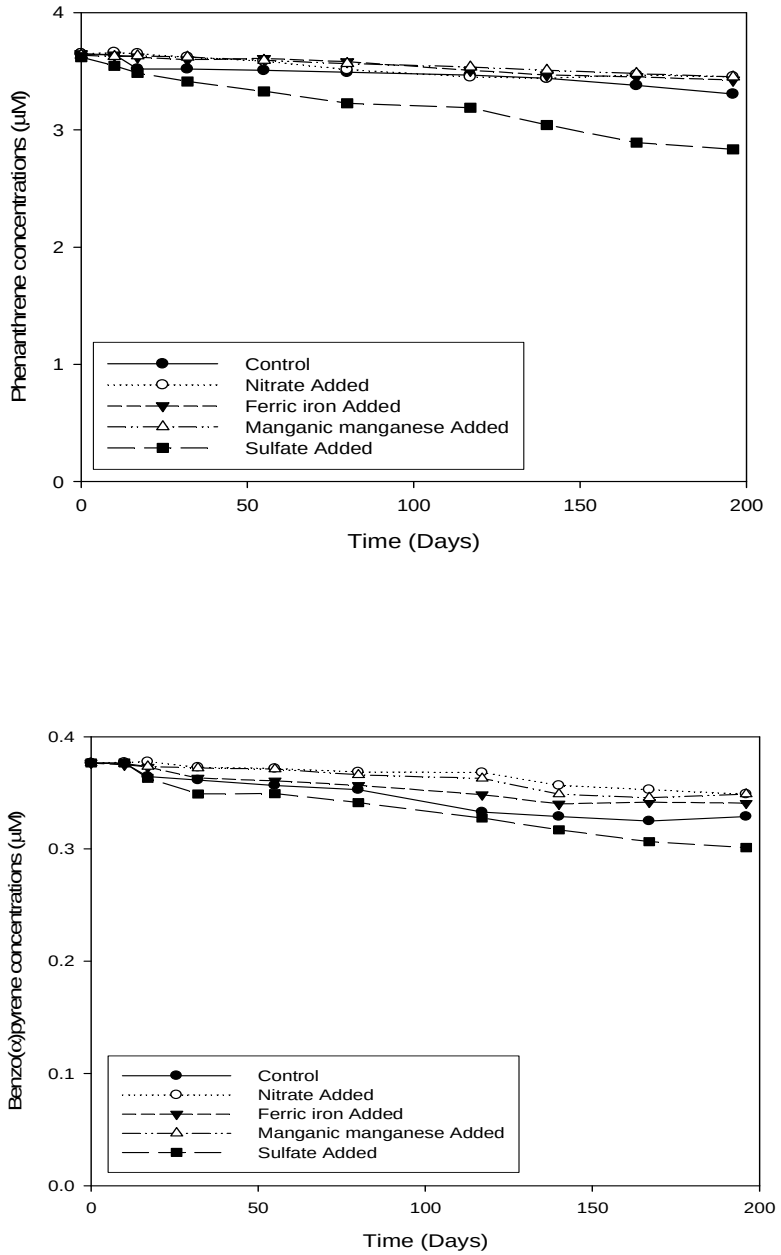

Figure 2.1 Degradation of phenantherne and benzo(α)pyrene under different redox conditions

The rate constants of phenanthrene degradation were different among treatments (Table 2.2). Faster degradation of PAH component was observed in microcosms with sulfate added rather than in microcosms with nitrate, ferric iron, and manganic manganese as terminal electron acceptors. Pyrene, chrysene, and benzo(α)pyrene components had very similar patterns. The first-order kinetic model is able to describe degradation kinetics in most microcosms reasonably well as coefficient of determination (R^2) values show in Table 2.2. Half lives computed from the rate constants ranged from 2.566 days for the nitrate added treatments to 582 days for the sulfate added treatment.

Table 2.2 First-order rate constants and half-life of phenanthrene in microcosms

Treatment	Rate constant (k) (day^{-1})	$t_{1/2}$ (days)	R^2
Control	0.00040	1732	0.87
Nitrate	0.00027	2566	0.99
Ferric iron	0.00032	2165	0.99
Manganic manganese	0.00027	2566	0.98
Sulfate	0.00119	582	0.98

Notably, the rate constant for the sulfate added treatment is 4 times greater than the control (natural attenuation) which had sulfate concentrations of ~1.15 mM. Other treatments which added electron acceptors (nitrate, ferric iron and manganic manganese) slowed down PAH degradation presumably by inhibiting the existing flow of electrons through sulfate reduction where the PAH degrading capability is present. Nitrate, Iron and manganic manganese have

higher energy yields than sulfate and organisms which use these as electron acceptor tend to outcompete sulfate reducers in sediments.

Radiorespirometer Experiments

Extensive mineralization of phenanthrene was observed by production of $^{14}CO_2$ from labelled phenanthrene. The sulfate treatment showed the highest potential for phenanthrene degradation in Anacostia sediments with over 30 % mineralization (Figure 2.2) over the 200 days of incubation. Mineralization ranged from 3-8 % in the nitrate, ferric iron, manganic manganese treatments, and control (methanogenic condition) treatment respirometers. Mineralization rates were quite rapid in the 100-150 days in sulfate treatment. There was 34 % mineralization in the sulfate added treatment while there were approximately 5 % mineralizations with other TEAs.

The rate and extent of mineralization of ^{14}C-phenanthrene in the presence of sulfate was significant (34 % in Figure 2.2) as compared with other treatments. At the time of the sulfate amendment, 92 % over 50 days (first amendment) and 83 % over 130 days (second amendment) of sulfate respectively declined in the microcosms. The third amendment was slower than the first and second. The sulfate concentrations were shown in Figure 2.6.

Mineralization curves for nitrate, ferric iron, manganic manganese treatments as well as the control treatment all seem to have relatively similar linear shapes. For sulfate, a linear rate of degradation was followed by an exponential increase in phenanthrene mineralization from approximately day 100 to the end of the study. This can be interpreted as a period of adaptation of the microbial population followed by more rapid utilization of the phenanthrene by an enhanced microbial population.

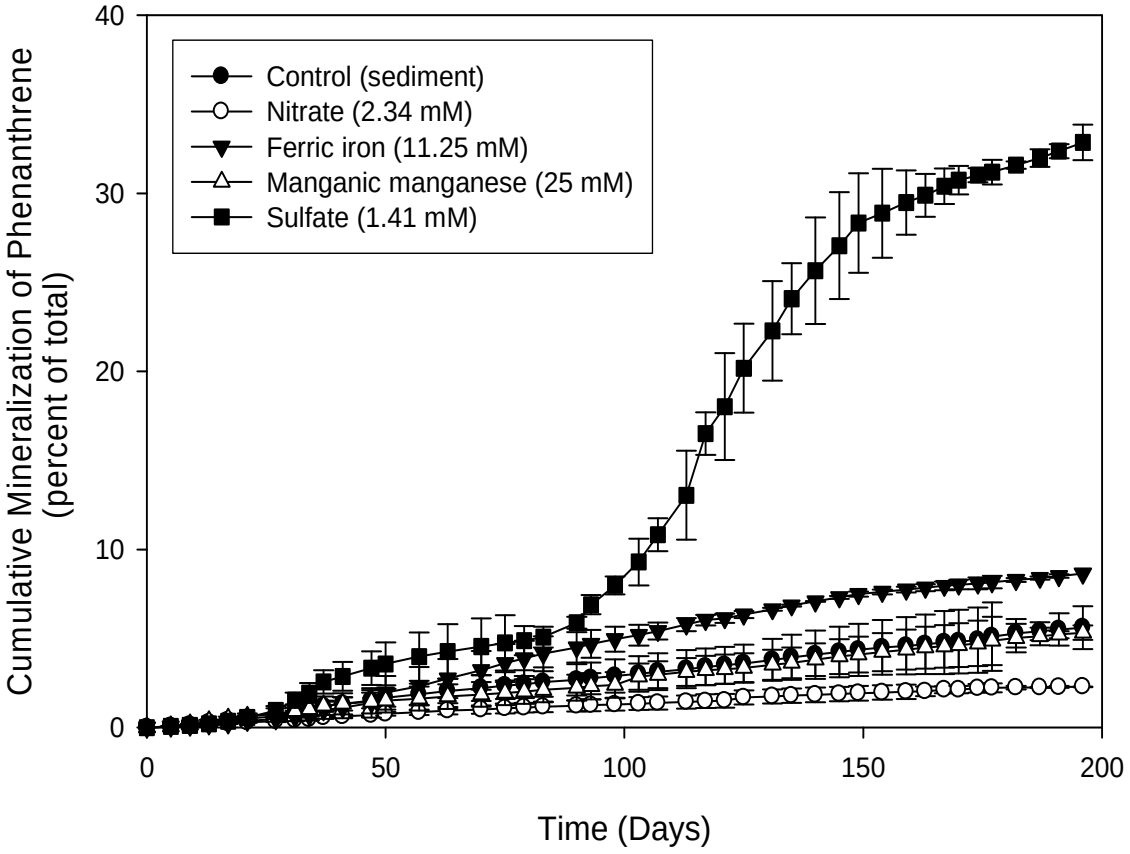

Figure 2.2 Mineralization of 14C-phenanthrene in Anacostia sediment under different redox condition

Table 2.3 presents the observed rates of mineralization with their respective half-lives and correlation coefficients. Additions of sulfate increased the rapid mineralization rate as compared with other treatments. There was no detectable mineralization in the abiotic control with mercuric chloride (3.89 % wt/vol) which causes inhibition of microbial activity. The rate constants of different treatment microcosms are 0.0096 (day^{-1}), 0.0039 (day^{-1}), 0.0130 (day^{-1}), 0.0096 (day^{-1}), 0.0209 (day^{-1}) in control microcosms, nitrate, ferric iron, manganic manganese, sulfate added treatments, respectively.

Table 2.3 First-order rate constants and half-life of $_{14}CO^2$ production

Treatment	Rate constant (day^{-1})	$t_{1/2}$ (days)	R^2
Control	0.0096	72	0.96
Nitrate	0.0039	117	0.73
Ferric iron	0.0130	53	0.93
Manganic manganese	0.0096	72	0.97
Sulfate	0.0209	33	0.95

Results for statistical analysis included nonlinear regression using a first-order growth model were considered statistically significant if $P \leq 0.05$. Many researchers reported that the sulfate reducing condition is dominating when PAH degradation occurs (Coates et al., 1996b; Coates et al., 1997; Caldwell et al., 1998; Rothermich et al., 2002). Statistical analysis was performed on the data set to address the hypothesis that sulfate addition enhanced mineralization of phenanthrene. Rate constants for phenanthrene mineralization in sulfate added treatment were compared with other treatments using paired t-tests. The phenanthrene mineralization rate

constant was significantly greater in the sulfate added treatment than in the any other treatments. An alpha level of 0.05 was used to determine significance. The results of this analysis are summarized in Table 2.4.

Table 2.4 Statistical analyses of the PAH mineralization between treatments

Treatments	t-test results ($\alpha = 0.05$) P(T≤t) (two-tail)	Remarks
Sulfate compared with control	$2.0142\ e^{-8}$	Difference in mean value is highly significant.
Sulfate compared with nitrate	$6.2990\ e^{-9}$	Difference in mean value is highly significant
Sulfate compared with ferric iron	$5.7092\ e^{-8}$	Difference in mean value is highly significant.
Ferric iron compared with manganic manganese	0.6013	Difference in mean value is insignificant.

Alternate Electron Acceptor Data

The concentrations of four different TEAs; nitrate, ferric iron, manganic manganese, sulfate; were monitored in separate microcosms to understand their usage in microbial metabolism. Methane, a product of methanogenesis and hydrogen, an indicator of oxidation reduction status were also measured. Researchers reported that mineralization of naphthalene and anthracene occurred only when a TEA was provided (O_2, NO_3^-, soluble Fe(III), FeOOH or SO_4^{2-}) and did not occur in identical microcosms without a TEA (Ramsay et al., 2003).

Only two percent of added phenanthrene was mineralized with nitrate provided as the TEA over the 200 day incubation period (Figure 2.2). Nitrate concentrations decreased from 2

mM to 1 mM over the first 50 days over the study (Figure 2.3). At that point, further reduction to nitrate stalled and only when nitrate was reamended did nitrate reduction commence again. Under nitrate reducing conditions, there was a stoichiometric conversion of nitrate to nitrite, but mineralization of phenanthrene was slow when nitrate was being reduced.

The mineralization profile of phenanthrene under ferric iron reducing conditions was around 8.6%. The insoluble FeOOH was amended as the TEA to drive phenanthrene degradation. The rate of mineralization changed slightly in the presence of ferric iron. Fe (III) was consumed in the microcosms approximately 20mM as shown in Figure 2.4 while there was no change in the Fe (III) concentration in the abiotic controls. The Fe (III) concentration was calculated the differences between total iron concentrations and soluble iron (Fe (II)) concentrations. The disappearances of manganese (Figure 2.5) as the TEA and mineralization trends were very similar.

The rate and extent of mineralization of ^{14}C-phenanthrene in the presence of sulfate was significant (34 % in Figure 2.2) as compared with other treatments. At the time of the sulfate amendment, 92 % over 50 days (first amendment) and 83 % over 130 days (second amendment) of sulfate respectively declined in the microcosms. The third amendment was slower than the first and second. The sulfate concentrations were shown in Figure 2.6. TEAs indicated that the microbial community was capable of degradation PAH under various conditions. When TEAs present, the PAHs could be intrinsically biodegraded. Sulfate treatment appeared that microbial ability to degrade phenanthrene was stronger than other treatments. Microbial composition for sulfate treatment was compared with Anacostia sediment and control microcosms using the DGGE analysis.

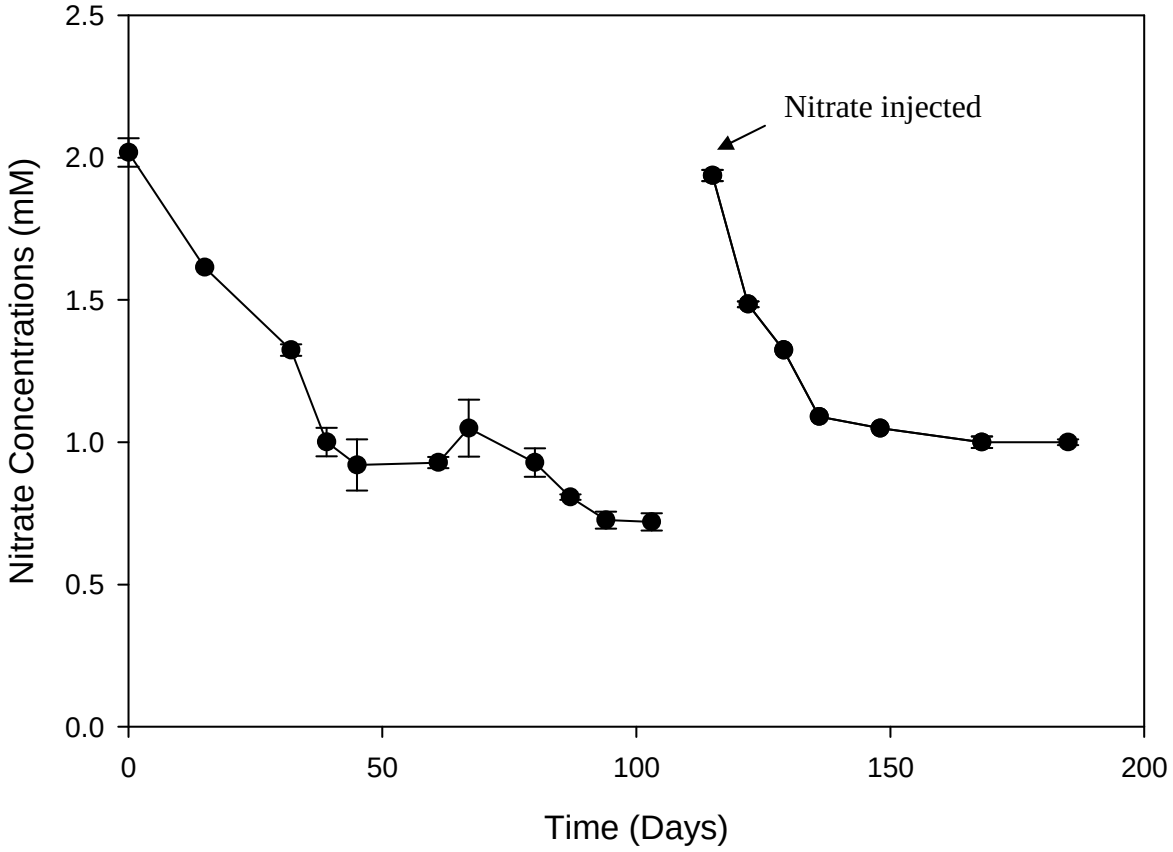

Figure 2.3 Nitrate concentrations in Anacostia River sediment microcosms

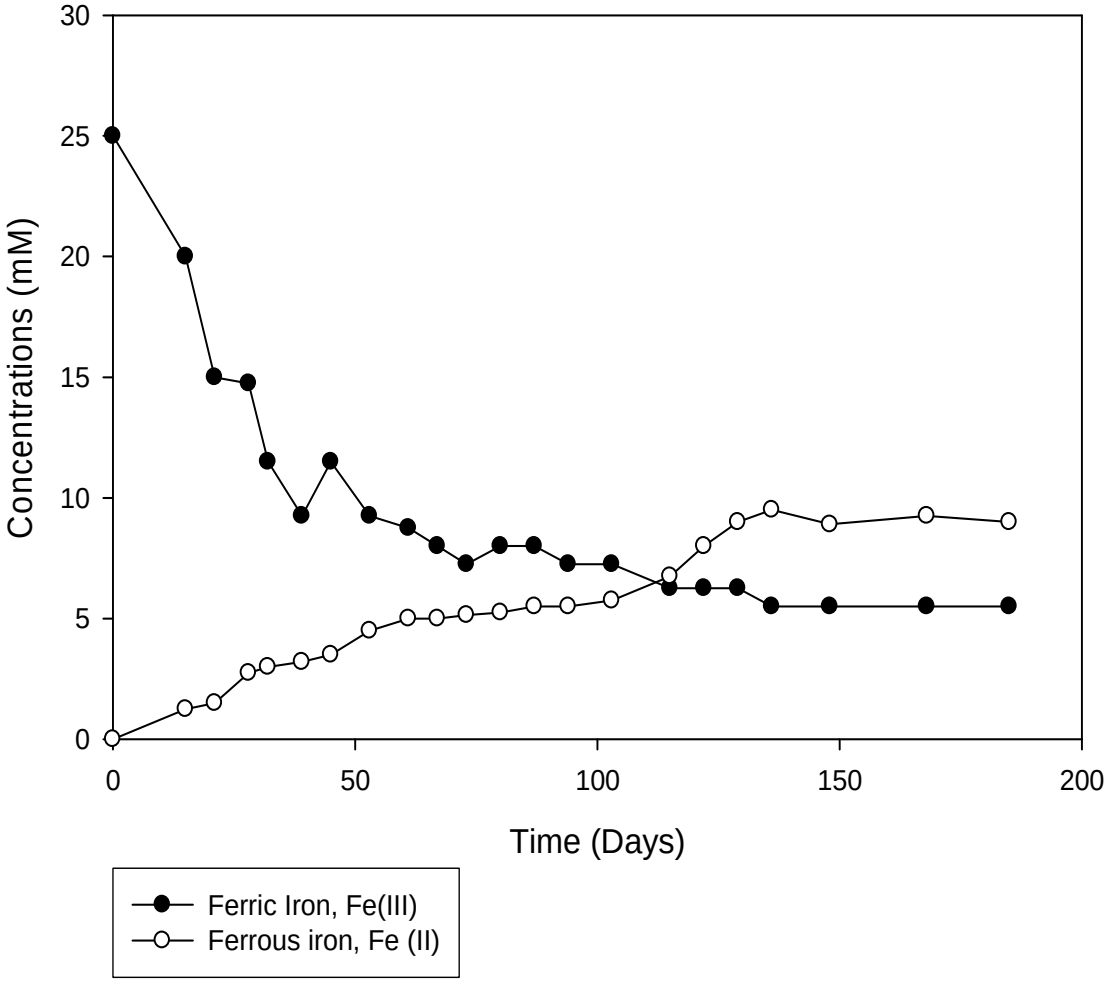

Figure 2.4 Iron concentrations in Anacostia River sediment microcosms

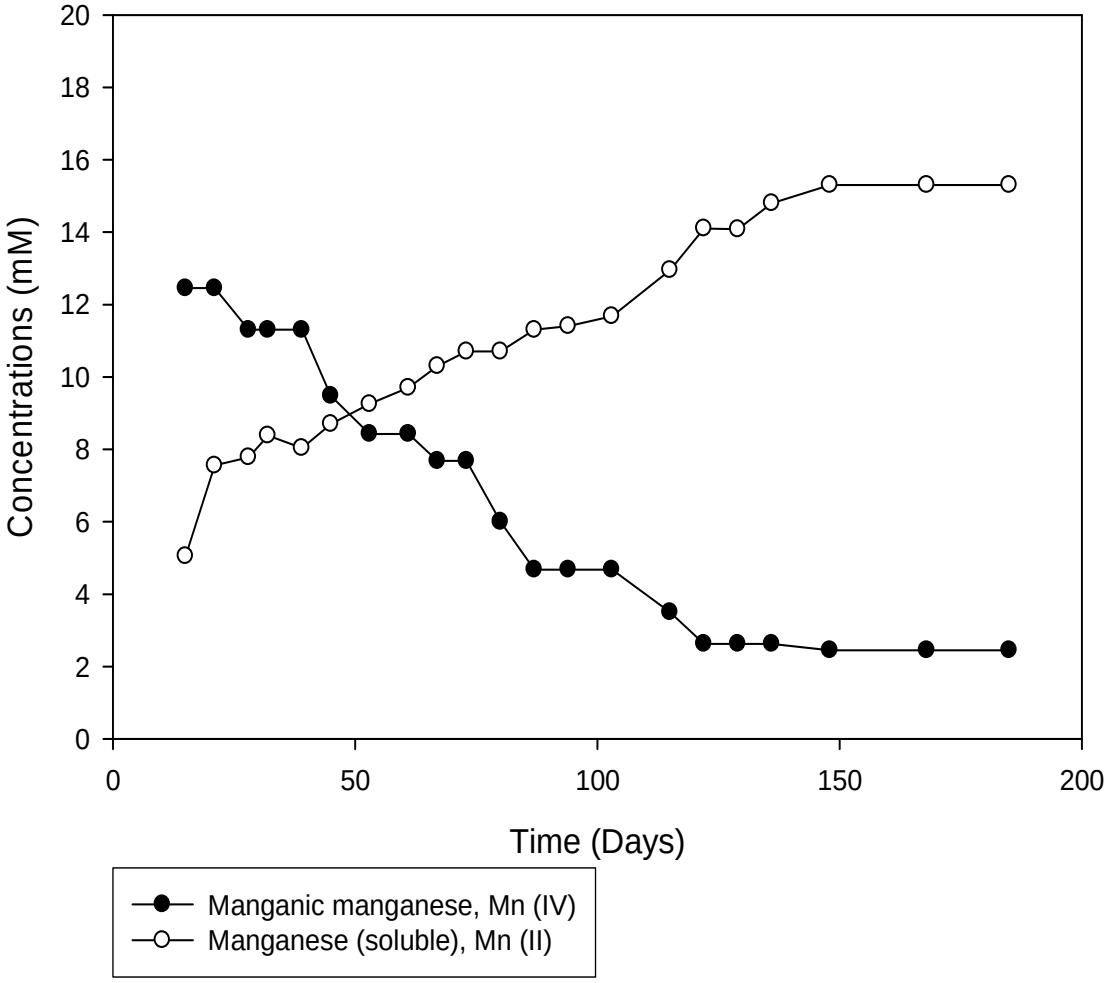

Figure 2.5 Manganese concentrations in Anacostia River sediment microcosms

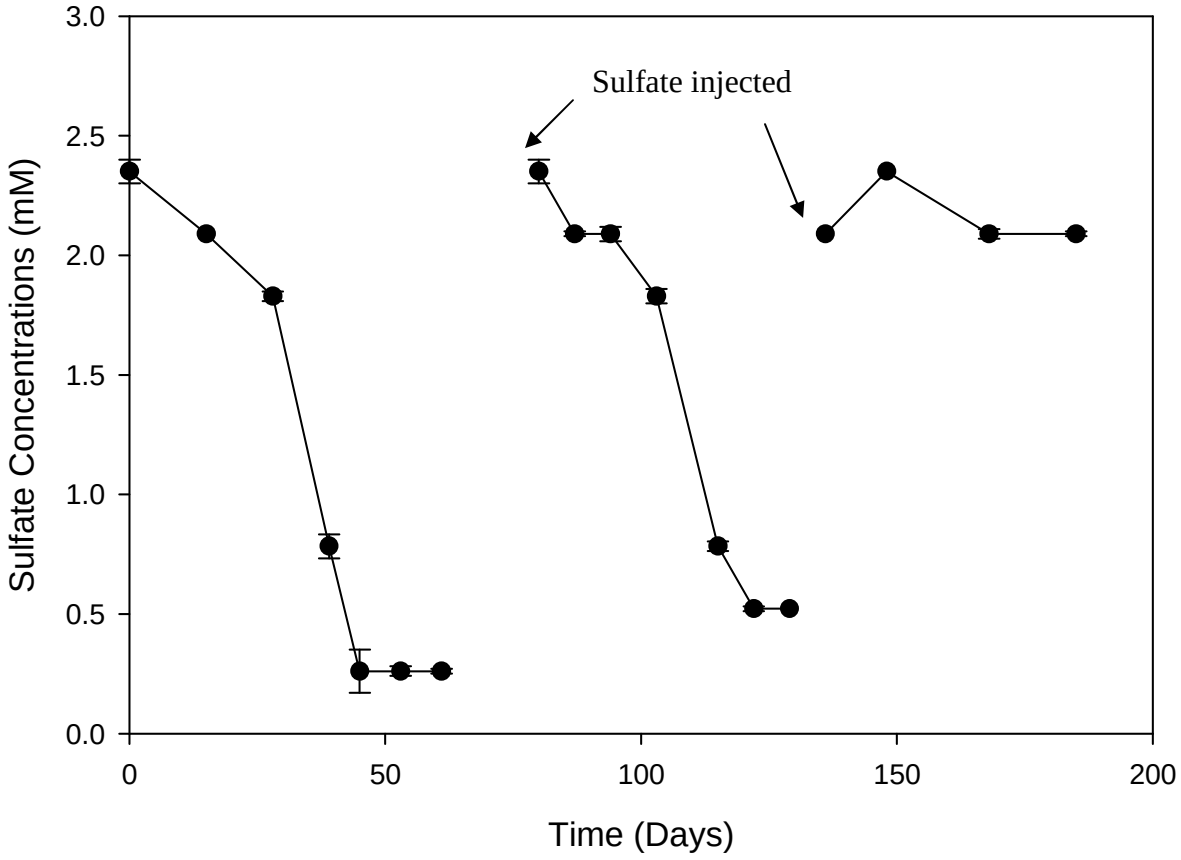

Figure 2.6 Sulfate concentrations in Anacostia River sediment microcosms

Stoichiometry was used to determine that PAH mineralization was occurred with CO_2 release. The amount of CO_2 produced during phenanthrene degradation linked to sulfate reduction was compared to the amount predicted from the theoretical stoichiometric equations.

$$C_{14}H_{10} + 8.25SO_4^{2-} + 16.5H^+ \rightarrow 14CO_2 + 8.25H_2S + 5H_2O$$

Thirty four percentage of $^{14}CO_2$ produced in microcosms during the incubation period over 200 days. 14 moles of CO_2 produced to metabolize 1 mole of phenanthrene. On a mass basis, the ratio of CO_2 to phenanthrene is followed by

Molecular weights: phenanthrene 178.2 gm

CO_2 44 gm

Mass ratio of CO_2 to phenanthrene = 44 : 178.2 = 1 : 4.05

The phenanthrene mineralized to CO_2 as sulfate was terminal electron acceptor. Concentrations of phenanthrene were decreased about 20 % as described previously. Lower initial concentration of phenanthrene (3.7 μM) in natural Anacostia sediment compared to radiolabelled phenanthrene studies may causes slower degradation since additional phenanthrene was not spiked at all. Low concentration limited not only degradation reaction rate also mass transfer rate (Lee et al., 2004).

There was methanogenic activity in the headspace of the anaerobic microcosms. The mineralization rate of ^{14}C-phenanthrene in the methanogenic condition was similar to that observed for manganese reducing condition. Methane produced significantly between 60 and 100 days up to 250 mM in control (methanogenic condition) microcosms. The TEAs depleted between 60 and 80 days in nitrate, manganic manganese, and sulfate treatments. Methane started to increase at the time of TEA decline (Figure 2.7).

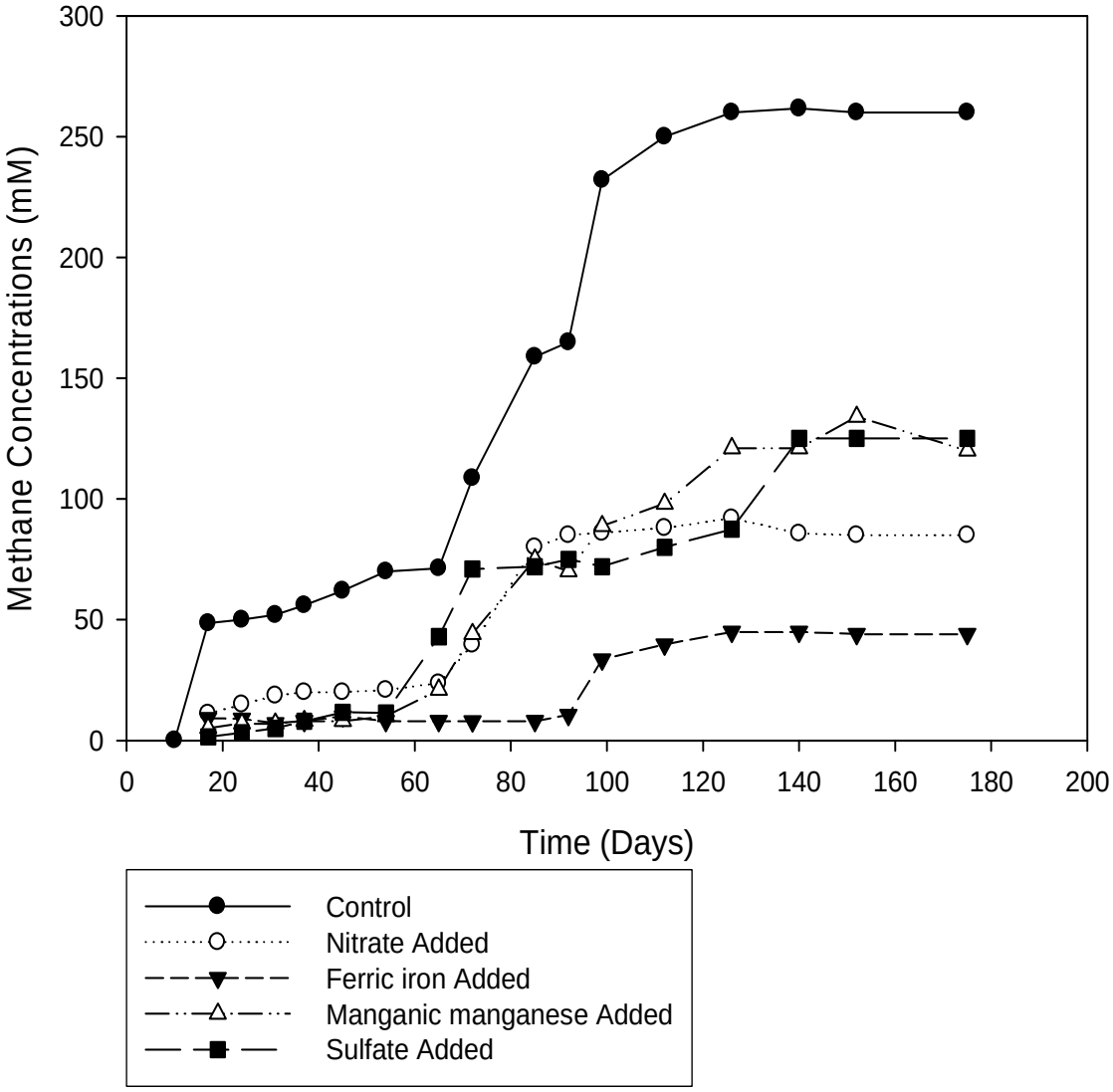

Figure 2.7 Methane concentrations in Anacostia River sediment microcosms

Hydrogen concentration decreased and sustained at low concentration. Hydrogen fluctuated through the entire period. These results indicated that hydrogen was probably used as an electron donor. Hydrogen concentrations decreased from approximately 15 nM to approximately 2 nM within 20 days. Thereafter, hydrogen concentrations stayed nearly constant 2.19 nM, during the period when phenanthrene mineralization was occurring. Hydrogen (~10 nM) was added around 90 days in order to determine the relative role of PAH degradation in the treatment because it is uncertain that hydrogen concentration was enough to drive PAH degradation. Hydrogen concentrations decreased and sustain the lower concentrations in microcosms again (Figure 2.8). The hydrogen concentration remains above the minimum threshold for hydrogen uptake. Therefore, mineralization of PAH components is related with TEAs such as nitrate, ferric iron, manganic manganese, and sulfate by hydrogen as an electron donor. The average hydrogen concentrations between treatments and unique range of hydrogen concentrations listed in Table 2.5.

Table 2.5 Average hydrogen concentrations associated phenanthrene mineralization and unique range of hydrogen concentrations

Treatment	H_2 concentration (nM)	Range of H_2 concentration (Lovley and Goodwin, 1998)
Control	2.82 ± 1.76	7-10
Nitrate	1.93 ± 1.57	< 0.05
Ferric iron	2.00 ± 1.65	0.2
Manganic manganese	2.34 ± 1.47	< 0.05
Sulfate	1.86 ± 1.62	1-1.5

Data represent means ± standard error.

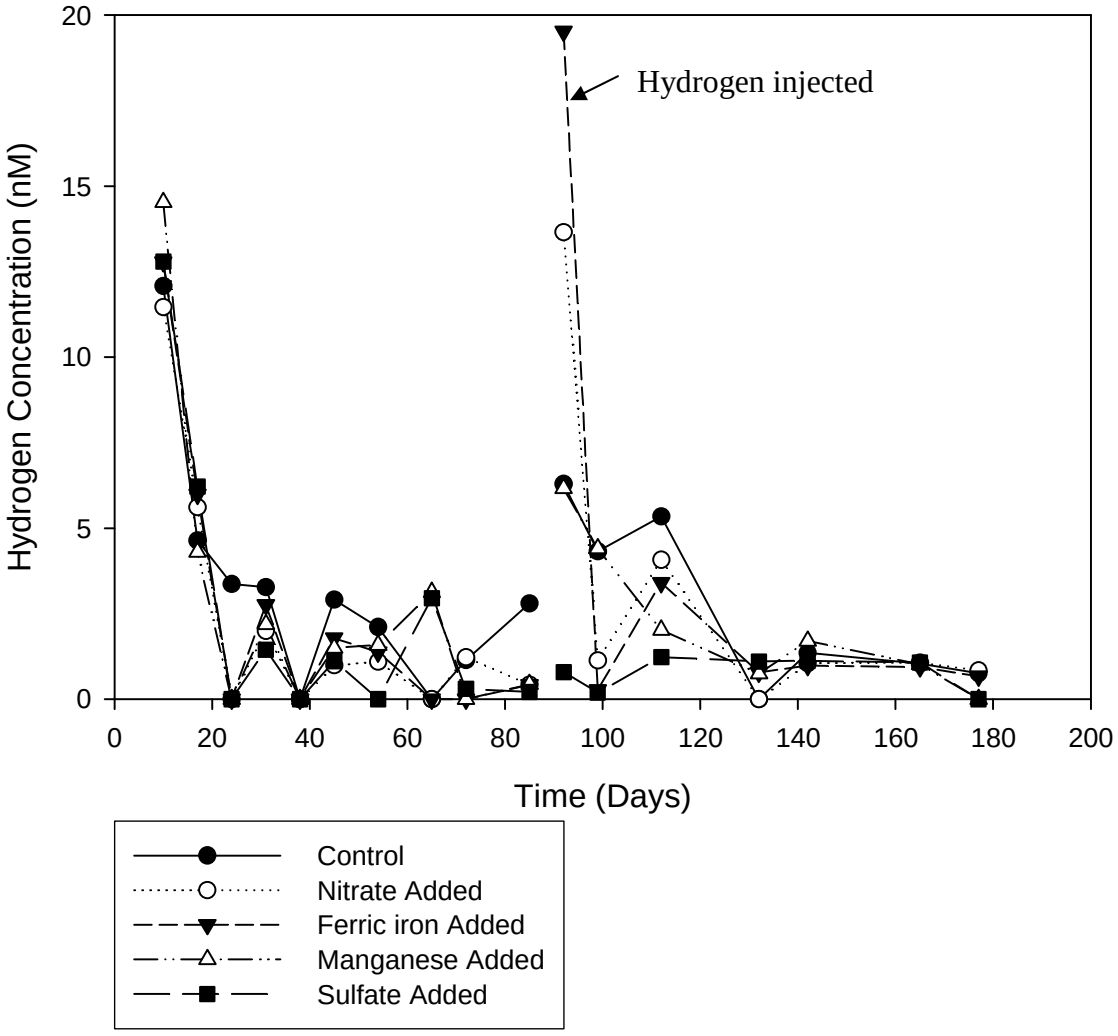

Figure 2.8 Hydrogen concentrations in Anacostia River sediment microcosms

The hydrogen concentrations observed during degradation of phenanthrene under methanogenic conditions was 2.82 ± 1.76 (n = 16, ± standard error of the estimate). While methnogens metabolize hydrogen at concentrations much more than those metabolized by other microorganisms, sulfate-reducing bacteria metabolize hydrogen at concentrations much lower than those metabolized by nitrate reducers, ferric iron reducers, manganic manganese reducers, and methanogens. Sulfate reducers outcompete hydrogen with nitrate reducers, ferric iron reducers, manganic manganese reducers, and methanogens. These observations suggest that microbial degradation of phenanthrene under methanogenic conditions was driven by hydrogen as an electron donor.

The hydrogen concentration between treatments were not much comparable than the range of hydrogen concentrations of Lovley and Goodwin (1998). Each terminal electron-accepting reaction had a unique range of steady-state hydrogen concentrations associated with it and hydrogen concentrations measurements can estimate terminal electron-accepting reactions. But, hydrogen concentrations also vary in response to change in the predominant terminal electron-accepting process in subsurface environments (Lovley and Goodwin, 1998). These concentrations are similar to those reported by Kassenga et al. (2004) of between 2.4 and 2.6 nM but significantly higher than those reported by Löffler et al. (1999) of between 0.27 and 0.31 nM.

Microbial Analyses

Soil slurry samples from microcosms were analyzed to compare the diversity of microbial communities under different conditions and to specifically investigate the effect of the sulfate treatment on microbial consortia. DNA from soil slurry samples was extracted and amplified for DGGE analyses.

DGGE band profiles of the PCR amplification products obtained with target DNA of bacteria extracted from microcosms and Anacostia sediment that had not been incubated in microcosms are shown in Figure 2.9. Comparing the banding patterns, Anacostia sediment (Lane 1 in Figure 2.9), sediment only (control) microcosm (Lane 2 in Figure 2.9), and sulfate reducing condition microcosm (Lane 3 in Figure 2.9) had different microbial composition. Band (a) was significantly visible in sediment, the control microcosm and sulfate amended microcosm and band (b) was dominant in the sediment and control microcosms. The bands (c), (d), and (e) were more intense in control microcosms. The band (f) was very intense in the sulfate microcosms but not in any other samples.

DNA sequences of the cloned DNA fragments were edited using Chromas software (http://www.mb.mahidol.ac.th/pub/chromas/chromas.htm) and was compared using BLAST (http://www.ncbi.nlm.nih.gov/BLAST/) maintained by the National Center of Biotechnology Information (NCBI). Identified sequences are presented in Table 2.6. The result of the DGGE profile indicated that strain (f) and (g), *Pelobacter sp*. and *Desulfuromonas sp*., were in sulfate treatment microcosms. *Desulfuromonas sp*. stimulates a sulfate reduction and iron reduction (Lovley et al., 1995) and metal reduction from contaminated aquifer sediments (Holmes et al., 2002). *Desulfuromonas sp*. also participates in dechlorination of TCE (tetrachloroethene) (Löffler et al., 2000; Lorah and Voytek, 2004). The characterization of both strains *Pelobacter sp*. and *Desulfuromonas sp.* are very similar. Starin (f) and (g) were potentially contributed the faster phenanthrene mineralization under sulfate-reducing conditions. These observations suggest that *Pelobacter sp*. and *Desulfuromonas sp.* have a possible capability to accelerate phenanthrene mineralization as a microbial source.

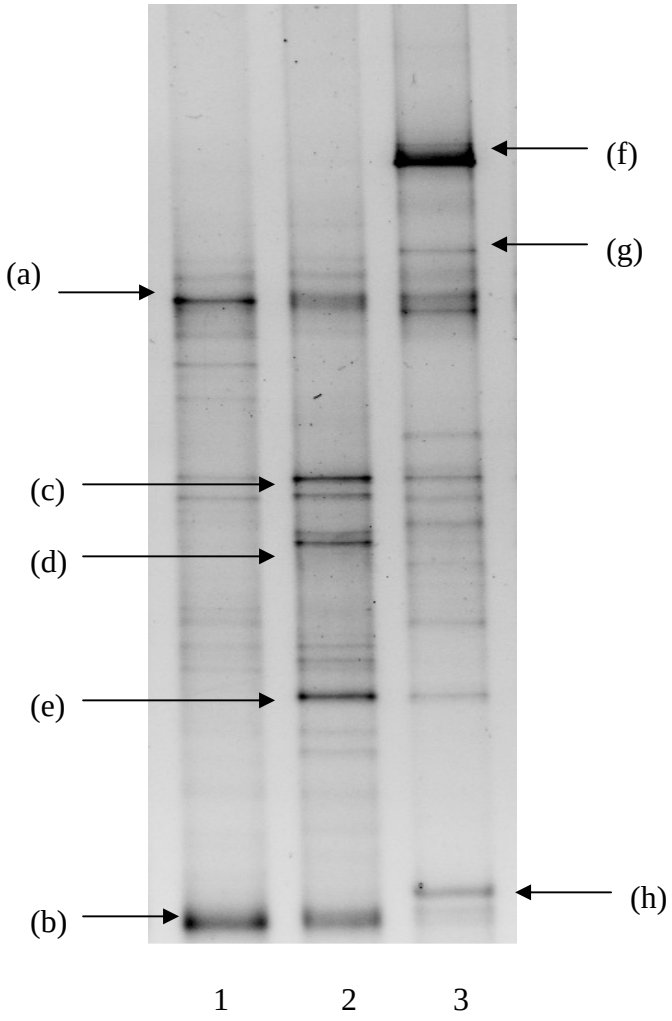

Figure 2.9 DGGE band with different treatments 1: Anacostia sediment, 2: Control microcosm (sediment only), 3: Sulfate reducing condition

Table 2.6 Bacterial identification by DNA sequencing

DGGE band	Bacterial species (% of similarity)
(a)	*Lactobacillus sp.* (100 %)
(b)	*Clostridium sp.* (96 %)
(c)	*Desulfuromonas sp.* (98 %)
(d)	*Leucobacter sp.* (98 %)
(e)	*Aquamonas fontana* (99 %)
(f)	*Pelobacter sp.* and *Desulfuromonas sp.* (98 %)
(g)	*Pelobacter sp.* and *Desulfuromonas sp.* (98 %)
(h)	*Clostridium sp.* (96 %)

Recently, researchers have reported that the members of the *Geobacter* family of the *Geobacteraceae* have a important role in the anaerobic degradation of petroleum contaminated aquifers and in other metal-contaminated subsurface environments or landfill leachate (Cummings et al., 2003; Nevin et al., 2005; Anderson et al., 2007). They found that *Geobacteraceae* have the potential to degrade aromatic compounds using phylogenetic analyses of DNA sequences and *Geobacter* species play in Fe (III) reduction in the environment related to anaerobic PAH degradation. *Geobacteraceae* includes the four genera *Geobacter, Pelobacter, Desulfomonas*, and *Desulfuromusa* (Cummings et al., 2003; Nevin et al., 2005). These indicate that *Pelobacter* and *Desulfomonas* observed in this study may have a role in the anaerobic activities of PAH contaminated sites.

Conclusions

This study observed ^{14}C–Phenanthrene mineralization under various redox conditions in Anacostia river sediments with providing TEAs. Mineralization was examined to demonstrate the comparable effectiveness using the nitrate, ferric iron, manganese, sulfate, and methane production conditions.

Mineralization of phenanthrene component was strongly linked to sulfate reduction since 34 % of mineralization was occurred when sulfate was provided as TEA. The mineralization of phenanthrene was less than 10 % in other treatments entire study period. The sulfate was electron acceptor in biodegradation processes. Sulfate reduction was the more energetic process than any other condition in Anacostia sediments. Sulfate treatment had more microbial ability to degrade phenanthrene than other treatments.

Faster degradation of phenanthrene was possibly mediated by microbial communities such as *Pelobacter sp*. and *Desulfuromonas sp*. in the sulfate treatment microcosms. The microbial consortia may have a relation with the degradation potential and these organisms can possibly help facilitate PAH mineralization. *Pelobacter sp*. and *Desulfuromonas sp*. are members of the *Geobacteraceae* family which have an important role in the anaerobic degradation of PAHs. These sulfate reducers use hydrocarbon substrates as electron donors and sulfate is used as an electron acceptor. Mineralization monitoring data suggested that the population of sulfate-reducing bacteria were involved with PAH degradation. Therefore, sulfate is a more promising TEA for intrinsic degradation in Anacostia River and other PAH contaminated sites.

CHAPTER 3
DIAGENETIC MODEL FOR ASSESSING BIODEGRADATION OF PAHs IN ANACOSTIA RIVER SEDIMENTS

Introduction

The understanding of biochemical reactions within a complex physical system in the natural environment requires an ability to apply measurable characteristics to mathematical models. The goals of these models are to verify our understanding of the physical system, to determine parameters which are not measurable, and to predict the future status of a system. Assessing the biodegradation of organic contaminants such as PAHs in sediments requires this type of approach.

The rate and extent of microbial degradation of organics is largely determined by environmental conditions such as temperature, pH, salinity and the presence of electron acceptors such as oxygen, nitrate, ferric iron, manganese, sulfate and methane in the environment. In sediments, electron acceptor availability at any point in the bed is the result of a complex series of transport and mixing processes, primary biological reactions and secondary chemical transformations. In the simplest models, respiration with oxygen takes place in the uppermost sediment, followed by respiration with nitrate, oxidized iron and manganese compounds and sulfate in the order of the availability of energy from these electron acceptors, respectively. Further down in the sediment, the degradation of organic matter occurs through methane fermentation (Fossing et al., 2004). Organic carbon and nutrient cycles control the redox (reduction and oxidation) state and microbial activity of the surface layers of sediment affecting metal speciation and the degradation of organic contaminants. Such sediment processes are involved in “diagenesis”, which is the conversion into sedimentary organic matter by physical, chemical and biological alteration at relatively low temperatures and pressures. After deposition,

sediments are compacted and buried beneath successive layers of sediment. Diagenesis processes are complex mixtures of primary biological reactions, chemical reactions and, transport processes. Understanding PAH degradation and diagenetic modeling is at a very advanced level and a number of model formulations are available that accurate reproduce porewater profiles (Berner, 1980; Berg et al., 2003). Van Capellen and Wang (1996) provided a thorough description of diagenetic processes and many key parameters in developing the model. Diagenetic models for assessing changes in redox species in sediments can reproduce profiles accurately in a variety of sediment types. From Van Capellen and Wang (1996)'s STEADYSED code to the recent model development by Fossing et al. (2004), numerical models of redox processes in sediments are at a fairly advanced state of development. To date, these models have not been extended to contaminated sediment management for organics or metals, despite some obvious needs to have modeling tools for these contaminants that incorporate an understanding of redox processes. Important applications where a model would have some impact include monitoring the natural recovery of organics in sediments, development of reactive caps for enhancing redox-driven (i.e., biodegradation processes) attenuation processes, and predicting the fate of metals in sediments after capping (not considered here). Each of these applications would require a different but overlapping modeling effort that would require parameter estimation and specification of any new transport processes. Here are some of the modeling and parameter estimation tasks required for each application. This chapter presents the development of models which are consistent with the available dataset and desired modeling. The reactive caps are developed with enhancing redox-driven attenuation processes since sediments change to more anaerobic condition.

1) Nutrient flux and redox conditions in the sediments. A model is developed for the simulation of the fate and transport of organic carbon, oxygen, nutrient, and contaminant within sediments. Numerical model is developed based on an existing conceptual framework and solution structure.
2) Diagenetic model applied into Anacostia sites. A model is developed for the Anacostia River conditions based on measured value from literatures. The governing equations of an Anacostia system are solved with the use of a numerical solver using the MATLAB.

Mathematical Modeling

Diagenetic Processes

Organic matter reacts via oxygen respiration, denitrification, manganese reduction, iron reduction, sulfate reduction, and methanogenesis in sediments. These primary redox reactions use organic carbon as the reductant and accomplish the degradation of organic material through bacterial respiration.

The oxidation of organic matter produces the reduced pore water species Mn^{2+}, Fe^{2+}, NH_4^+, H_2S, and CH_4, which may participate in secondary redox conditions (Van Capellen and Wang, 1996). Reduced end products from these primary reactions may react to reform the primary constituents (Fossing et al., 2004). Oxidation of ions is limited to the upper reaches of the sediment, whereas hydrogen sulfide is present for the reduction of iron and manganese oxides. Other secondary reactions include the formation of minerals, such as pyrite, and the morphing of solid oxides into a crystalline form. The primary and secondary redox reactions identified by Fossing et al. (2004) are listed in Table 3.1.

Table 3.1 Biogeochemical reactions (Fossing et al. 2004)

Degradation of organic material

$$(CH_2O)_C\left(NH_4^+\right)_N\left(PO_4^{3-}\right)_P + cH_2O \rightarrow cCO_2 + nNH_4^+ + pPO_4^{3-} + 4ce^- + 4cH^+$$

Primary reactions

(1) *Aerobic respiration*: $O_2 + CH_2O \rightarrow CO_2 + H_2O$

(2) *Denitification*: $4NO_3^- + 5CH_2O + 4H^+ \rightarrow 2N_2 + 5CO_2 + 7H_2O$

(3) *Manganese(hydr)oxide reduction*: $2MnO_2 + CH_2O + 4H^+ \rightarrow 2Mn^{2+} + CO_2 + 3H_2O$

(4) *Iron (hydr)oxide reduction*: $4FeOOH + CH_2O + 8H^+ \rightarrow 4Fe^{2+} + CO_2 + 7H_2O$

(5) *Sulfate reduction*: $SO_4^{2-} + 2CH_2O + 2H^+ \rightarrow H_2S + 2CO_2 + 2H_2O$

Secondary reactions

(6) $NH_4^+ + 2O_2 \rightarrow NO_3^- + H_2O + 2H^+$

(7) $(FeOOH)_N + PO_4^{3-} \rightarrow (FeOOH)_N \equiv PO_4^{3-}$

(8) $2Fe^{2+} + MNO_2 + 2H_2O \rightarrow 2FeOOH + Mn^{2+} + 2H^+$

(9) $2Mn^{2+} + O_2 + 2H_2O \rightarrow 2MNO_2 + 4H^+$

(10a) $H_2S + 2FeOOH \equiv PO_4^{3-} + 4NH^+ \rightarrow S^0 + 2Fe^{2+} + 4H_2O + 2PO_4^{3-}$

(10b) $H_2S + 2FeOOH + 4H^+ \rightarrow S^0 + 2Fe^{2+} + 4H_2O$

(11) $4Fe^{2+} + O_2 + 6H_2O \rightarrow 4FeOOH + 8H^+$

(11b) $H_2S + 2FeOOH + 4H^+ \rightarrow S^0 + 2Fe^{2+} + 4H_2O$

(12) $H_2S + MnO_2 + 2H^+ \rightarrow S^0 + Mn^{2+} + 2H_2O$

(13) $H_2S + Fe^{2+} \rightarrow FeS + 2H^{2+}$

(14) $FeS + S^0 \rightarrow FeS_2$

(15) $SO_4^{2-} + 3H_2S + 4FeS + 2H^+ \rightarrow 4FeS_2 + 4H_2O$

(16) $H_2S + 2O_2 \rightarrow SO_4^{2-} + 2H^+$

(17) $FeS + 2O_2 \rightarrow Fe^{2+} + SO_4^{2-}$

(18) $2FeS_2 + 7O_2 + 2H_2O \rightarrow 2Fe^{2+} + 4SO_4^{2-} + 4H^+$

(Table 3.1 cont'd)

(19) $4S^0 + 4H_2O \rightarrow 3H_2S + SO_4^{2-} + 2H^+$

(20) $MnO_{2\ A} \rightarrow MnO_{2\ B}$

(21) $FeOOH_{\ A} \rightarrow FeOOH_{\ B}$

A diagenetic model requires dynamic parameters and boundary conditions, modular programming, standardized input file, and compatibility. The goal of this study is to implement a diagenetic model capable of predicting organic carbon, nutrient, and contaminant concentrations with depth. The study is focused on the implementation of the model framework and the development of boundary condition that can be used in diagenetic models for future research.

Mathematical Modeling

Chemical fate and transport processes are described with, not only diagenesis, but also molecular diffusion, burial, biodiffusion, and sorption. These processes are mathematically described by the mass conservation equation, which presents the changes in concentration over time. These process terms are developed into a numerical model, solved, and then compared with measured data to verify the understanding of diagenetic processes. The model is then available for use to predict the outcome of previously unexplored scenarios, such as contaminant degradation in sediments.

A mass balance equation describes the chemical fate and transport of all components in the system.

$$R\ \frac{\partial C}{\partial t} + \nabla \bullet J\ = S$$

where C is the concentration in μmol/cm^3 or μmol/g, R is retardation factor, J is total flux of component in μmol/cm^2-s, and S is source term in μmol/cm^3-s. The eighteen aqueous and solid bound components included in the diagenetic models have a significant role in the involved chemical reactions.

Molecular Diffusion

The flux of a solute transported by diffusion is given by Fick's Fisrt Law

$$F_D = -\varphi D_S \frac{\Delta C}{\Delta x}$$

where φ is porosity, D_S sediment diffusivity and $\frac{\Delta C}{\Delta x}$ the concentration gradient.

Bioturbation and Bioirrigation

The flux of a solute by bioturbation can be described by

$$F_{Bw} = -\varphi D_{Bw} \frac{\Delta C}{\Delta x}$$

where D_{Bw} is the coefficient of biodiffusion and $\frac{\Delta C}{\Delta x}$ the concentration gradient.

The flux of a solid by bioturbation can be expressed as

$$F_{Bs} = -\rho_s (1-\varphi) D_{Bs} \frac{\Delta C}{\Delta x}$$

where ρ_s is the density of the solid sediment.

Burial of Components

The burial flux of solutes and solids can be expressed as

$$F_{Cw} = \varphi u C$$

$$F_{Cs} = \rho_s (1-\varphi) w C \text{ (Solids)}$$

where w and u are the burial rates of solutes and solids, respectively.

Adsorption

The adsorption model assumes that all adsorption is reversible and in equilibrium with water. Thus, the concentration of the absorbed component can be calculated as

$$C_{ads}=K'C$$

where K' is the adsorption coefficient and C the total pore-water concentration. The total flux of a dissolved component becomes:

$$F_{Bw}=-\varphi D_{Bw}\frac{\Delta C}{\Delta x}--\rho_s(1-\varphi)D_{Bs}\frac{K'\Delta C}{\Delta x}$$

where the first term presents bioturbation and second term is the adsorption term.

The General Mass Balance

The governing mass balance equation (Fossing et al., 2004) is important for the purpose of numerical modeling for both soluble and solid bound components. Hence, a coefficient (ζ) is used to differentiate between soluble and solid terms.

$$(\xi\varphi+\rho_s(1-\varphi)K')\frac{\partial C}{\partial t}=\frac{\partial}{\partial x}\left((\xi\varphi(D_{Bw}+D_s)+\rho_s(1-\varphi)D_{Bs}K')\frac{\partial C}{\partial x}\right)-$$
$$\frac{\partial}{\partial x}((\xi(\varphi u)_x+\rho_s((1-\varphi)w)_xK')C)+\xi\varphi\alpha(C_0-C)+R$$

where R is net production (negative: consumption), ξ is 1 when a substance is a solute and 0 when a substance is a solid. The left side expresses that adsorbed concentration changes with time with respect to solute or solid. In the first term on the right side is shown the variation of the flux involved in bioturbation coefficient and sediment diffusivity of the adsorbed concentration of a component with depth.

Development of Diagenetic Model

To monitor the natural recovery of organics in sediments, the target organic contaminant (PAH) was added as both a sorbed and dissolved species to an existing calibrated redox model. The dissolved and sorbed organic contaminant was connected with transport processes for dissolved and sorbed species. Diagenetic models generally have molecular diffusion and bioirrigation which affect dissolved species and bioturbation and sedimentation which affect both sorbed and dissolved species. The kinetic reactions of the organic contaminant were established with sorbed and dissolved species.

The five primary biodegradation reactions were set up using the target organic as an electron donor based on limiting value approach used in Van Cappellen's model. It assumes that there exists a critical or limiting concentration of the oxidant in each of the five respiratory pathways. When the concentration of the oxidant exceeds the limiting value, the rate of the metabolic pathway is assumed to be independent of concentration of the oxidant (Van Cappellen and Wang, 1996). When the external oxidant concentration decreases below the limiting value, the rate is calculated by:

$$R_i = R_{\max} \frac{[EA]}{[EA]_{\lim}} \qquad for\ [EA] < [EA]_{\lim}$$

where $[EA]$ is the concentration of external oxidant, $[EA]_{\lim}$ is the limiting concentration, and $R_{\max}$ is the rate of oxidation when the supply of oxidant is not limiting ($[EA] \geq [EA]_{\lim}$) (Van Cappellen and Wang, 1996). The value of the limiting concentrations, $[EA]_{\lim}$, control the extent of vertical overlap between the successive organic matter degradation pathways. The calculation require values for the limiting concentrations of the successive external electron acceptors, O_2, NO_3^-, Mn(IV), Fe(III), and SO_4^{2-} (Van Cappellen and Wang, 1996). For compounds used as

electron acceptors, a similar approach was developed to turn reactions off and on in non-ideal redox zones. Additionally, methanogenesis reactions were established as the final stage of biodegradation in freshwater sediments. Methane production and methane oxidation were considered as components of the system.

For target organic PAH compounds (C_aH_b),

(22) $\left(\frac{4a+b}{4}\right)O_2 + C_aH_b \rightarrow aCO_2 + \frac{b}{2}H_2O$

(23) $\left(\frac{2a+b}{3}\right)NO_3^- + bH^+ + C_aH_b \rightarrow aCO_2 + bH_2O + \left(\frac{2a+b}{6}\right)N_2$

(24) $\left(\frac{2a+b}{2}\right)MnO_2 + 5bH^+ + C_aH_b \rightarrow aCO_2 + 3bH_2O + \left(\frac{2a+b}{2}\right)Mn^{2+}$

(25) $5bFe(OH)_3 + (14b-4a)H^+ + C_aH_b \rightarrow aCO_2 + (15b-2a)H_2O + 5bFe^{2+}$

(26) $\left(\frac{4a+b}{8}\right)SO_4^{2-} + \left(\frac{4a+b}{4}\right)H^+ + C_aH_b \rightarrow aCO_2 + \frac{b}{2}H_2O + \left(\frac{4a+b}{8}\right)H_2S$

(27) $\left(\frac{4a-b}{4}\right)H_2O + C_aH_b \rightarrow \left(\frac{4a-b}{8}\right)CO_2 + \left(\frac{4a+b}{8}\right)CH_4$

(28) $2CH_2O \rightarrow CO_2 + CH_4$

(29) $CH_4 + O_2 \rightarrow CO_2 + 4H^+$

Rate expressions in the biochemical reaction of each component are presented in Table 3.2 and input parameters and data values for the model are listed in Table 3.3 and 3.4. The chemical transport and cycling takes place in the sediment domain of 0-20 cm below the sediment:water interface. The sediment model is divided into 105 layers (representing depth of 20 cm). The top layer represents the very lowest part of the water column while the underlying layers represent the sediment (Fossing et al., 2004). The model calculates the cycling of

components in the bed and the exchange of components between the sediment and bottom water through the diffusive boundary layer (DBL) which is in the uppermost layer of the model.

Table 3.2 Rate expressions in the transport-reaction equations

Component	Rate expression, R
CH_2O fast	$R_{CH_2O\ \ fast} = -(R_{1f} + R_{2f} + R_{3f} + R_{4f} + R_{5f})$
CH_2O slow	$R_{CH_2O\ \ slow} = -(R_{1s} + R_{2s} + R_{3s} + R_{4s} + R_{5s})$
O_2	$R_{O_2} = -\left(R_1 + 2R_6 + \frac{R_9}{2} + \frac{R_{11}}{4} + 2R_{16} + 2R_{17} + \left(\frac{4a+b}{4}\right)R_{22}\right)$
NO_3^-	$R_{NO_3^-} = -R_2 + R_6 - \left(\frac{2a+b}{3}\right)R_{23}$
MnO_2	$R_{MnO_2} = -R_3 + R_9 - R_{12} - R_{20} + \left(\frac{2a+b}{2}\right)R_{24}$
FeOOH	$R_{FeOOH} = -R_4 - R_7 + R_8 - 2R_{10b} + R_{11} - R_{21} - 5bR_{25}$
SO_4^{2-}	$R_{SO_4^{2-}} = -R_5 - R_{15} + R_{16} + R_{17} + 2R_{18} + \frac{R_{19}}{4} - \left(\frac{4a+b}{8}\right)R_{26}$
NH_4^+	$R_{NH_4^+} = \left(R_1 + \frac{5R_2}{4} + R_3 + R_4 + 2R_5\right) \times \left(\frac{1}{C:N\ ratio}\right) - R_6$
PO_4^{3-}	$R_{PO_4^{3-}} = -R_7 + 2R_{10a} + (R_1 + \frac{5R_2}{4} + R_3 + R_4 + 2R_5) \times \left(\frac{1}{C:P\ ratio}\right)$
Fe^{2+}	$R_{Fe^{2+}} = R_4 - R_8 + 2R_{10a} + 2R_{10b} - R_{13} + R_{17} + R_{18} - R_{11} + 5bR_{25}$
Mn^{2+}	$R_{Mn^{2+}} = R_3 + \frac{R_8}{2} - R_9 + R_{12} + \left(\frac{2a+b}{2}\right)R_{24}$

(Table 3.2 cont'd)

H_2S	$R_{H_2S} = R_5 + \frac{3R_{19}}{4} - R_{10a} - R_{10b} - R_{13} - R_{15} - R_{16} + \left(\frac{4a+b}{8}\right)R_{26}$
$=PO_4^{3-}$	$R_{=PO_4^{3-}} = R_7 - 2R_{10a}$
FeS	$R_{FeS} = R_{13} - R_{14} - 4R_{15} - R_{17}$
FeS_2	$R_{FeS_2} = -2R_{18} + 4R_{15} + R_{14}$
S	$R_S = R_{10a} + R_{10b} + R_{12} - R_{19} - R_{14}$
PAHs	$R_{PAHs} = -(R_{22} + R_{23} + R_{24} + R_{25} + R_{26} + R_{27})$
CH_4	$R_{CH_4} = \left(\frac{4a+b}{8}\right)R_{27} + R_{28} - R_{29}$

The model requires boundary conditions that specify characteristics for the top of the uppermost layer and the bottom of the lowest layer. Boundary conditions of each component are given in terms of either a flux or a concentration. Organic matter comes in from the overlying water column with the flux of particles via sedimentation. Soluble component transfer at the sediment:water interface is presented as a diffusive flux with a constant concentration in the overlying water. The solid-bound components are defined at the boundaries by an incoming flux that represents settling from the water column. The incoming flux is always zero or positive under normal conditions because the sediment is not subject to resuspension. At the bottom of the control volume, all components have a zero concentration gradient. Initial concentrations are simply defined as a concentration profile for components. The initial concentrations may be zero, a constant, or a function of sediment depth.

Table 3.3 Input parameters for sediment diagenetic model

Parameter	value	Source
Sedimentation rate (*w*)	0.064 cm yr^{-1} ($1e^{-10}$ m s^{-1})	www.hsrc.org
Temperature (T)	14℃	air annual mean
Density (ρ_s)	2.04 g cm^{-3}	Fossing et al. (2004)
Bioirrigation parameter	α_0 = 200 yr^{-1}, α_1 = 0.28 cm^{-1}	Van Cappellen and Wang (1996)
Ratios	C:N = 10.0	Fossing et al. (2004)
	C:P = 80.0	
	$F_{OM\ n}$ /$F_{OM\ total}$ = 0.08	
	$F_{OM\ f}$ /$F_{OM\ total}$ = 0.42	
External fluxes	F_{POC} = 35 mmol m^{-2} day^{-1}	
	F_{MnO2} = 3.5 e^{-6} nmol cm^{-2} s^{-1}	Fossing et al. (2004)
	F_{FeOOH} = 2.05 e^{-4} nmol cm^{-2} s^{-1}	
Limiting concentrations	$[O_2]_{lim}$ = 20 μM	
	$[NO_3^-]_{lim}$ = 5 μM	
	$[MnO_2]_{lim}$ = 10 μmol g^{-1}	
	$[FeOOH]_{lim}$ = 50 μmol g^{-1}	
	$[SO_4^{2-}]_{lim}$ = 1600 μM	

Table 3.4 Input data values for the diagenetic model in depth (column 1-105)

Components	Initial Condition (μmol/cm^3)				Boundary Condition
	1-32	33-64	65-96	97-105	(μM)
1. CH_2O *fast*	34.97-0			0	
2. CH_2O *slow*	872-690	682-361	349-25	21.5-0.71	
3. O_2	0.38-0			0	389
4. NO_3^-			0		6.2
5. MnO_2	82.5-50.7	47.1-2.81	2.47-0.52	0.63-1.92	
6. FeOOH	107.5-100	99.47-42.2	27.7-3.68	4.91-9.10	
7. SO_4^{2-}			28-26.6		28000
8. NH_4^+	0-0.03	0.03-0.14	0.15-0.35	0.35	0.58
9. PO_4^{3-}	0-0.01	0.01-0.06	0.07-1.8	1.8-0.95	0.526
10. Fe^{2+}		0-0.02		0.016-0	0
11. Mn^{2+}	0-0.07	0.08-0.28	0.28-0.08	0.08-0.06	1
12. H_2S			0		0
13. $=PO_4^{3-}$	0.04	0.04-0.06	0.06-5.98	8.39-16.2	0
14. FeS	0-0.07	0.08-2.66	2.88-0.56	0.25-0	0
15. FeS_2	1.3-17	18.2-81.8	84.9-182	181.3-161.5	0
16. S	4-5.64	5.7-15.7	16.5-6.2	4.9-1.7	0
17. Phenanthrene			0.0006		0
18. CH_4			0.16		160

Calibration of the Model for Anacostia Sediments

The diagenetic model was calibrated for Anacostia River condition using experimentallymeasured values and literature values from the Anacostia River or the adjacent Potomac River.

External flux for POC was calculated as

$$F_{POC} = \frac{w \times \rho_b \times C_{f_{OC}}}{mw}$$

where w is the sedimentation rate, ρ_b is bulk density, $C_{f_{OC}}$ is the organic carbon concentration, and mw is the molecular weight.

An external flux for POC of 472.5 mmol m^{-2} day^{-1} was selected based on the assumption that sedimenting particles contain 5 % organic carbon. The sedimentation rate used was 0.064 cm yr^{-1}, which was defined from the Hazardous Substance Research Centers/South & Southwest adopted documents (http://www.hsrc-ssw.org/). For the PAH flux, an experimental value of the phenanthrene concentration, approximately 92 ± 8.2 (mg/Kg), from Anacostia sediment was used.

Sources for boundary conditions for soluble components were from a U. S. Geological Survey (USGS) report (Miller and Klohe, 2003). The sources for initial conditions for solid components, FeOOH and MnO_2 were from Lovley and Phillips (1986), whereas those for FeS and FeS_2 were from Wallmann et al. (1993). Sources for initial conditions for Fe^{2+} was from Phillips et al. (1993). The overview of initial conditions and boundary conditions to the Anacostia River sediment model is presented in Table 3.5.

Table 3.5 Input data values for Anacostia River sediment model

Components	Initial Condition (μmol/cm^3)				Boundary Condition
	1-32	33-64	65-96	97-105	(μM)
1. CH_2O *fast*	106-0		0		
2. CH_2O *slow*	2720-2156	2131-1128	1090-90	65-0.21	
3. O_2	0.38-0		0		315
4. NO_3^-		0			110
5. MnO_2	23.6-0		0		
6. FeOOH	245-0		0		
7. SO_4^{2-}		1.3			1000
8. NH_4^+	0-0.03	0.03-0.14	0.15-0.35	0.35	83
9. PO_4^{3-}	0-0.01	0.01-0.06	0.07-1.8	1.8-0.95	4.25
10. Fe^{2+}	0-2	5-25	25-50-20	20-5	420
11. Mn^{2+}	0-2.4	2.4-2.8	2.8-0.8	0.8-0.6	3.8
12. H_2S			0		0
13. $=PO_4^{3-}$	0-0.07	0.07-0.08	0.08-5.98	5.98-16.2	0
14. FeS			0		0
15. FeS_2			0		0
16. S	4-5.64	5.64-15.06	15.06-7.41	7.41-1.7	0
17. Phenanthrene			0.0006		0
18. CH_4			0.16		160

Sensitivity Analysis

A sensitivity analysis was conducted to identify the location of primary phenanthrene mineralization reactions using a variety of electron acceptors. A rate constant of 0.693 (day^{-1}) was used in order to observe phenanthrene mineralization rate over the simulation times possible using the model (Table 3.6). The rate constants of 0.693 (day^{-1}) corresponds to a half-life of 1 day.

Table 3.6 Sensitivity test from different treatments

Treatments	Rate constants (day^{-1})	Model trial	Simulation time (s)
Oxygen	0.01	0.693	1.6072 e^5
Nitrate	0.0039	0.693	3.3367 e^5
Manganic manganese	0.0096	0.693	1.4529 e^5
Ferric iron	0.013	0.693	1.7163 e^5
Sulfate	0.0209	0.693	1.9209 e^5
Methane	0.0096	0.693	1.5907 e^5

Capping Simulations

A cap of 1.5 cm was added on the top of the sediment in order to simulate sediment concentration profile with capping. The cap layers are 0.3 mm in thickness with 50 model layers, while the underlying layers represent the sediment. At the top of the sediment, the layers are 0.3 mm thickness, but at a depth of 0.8 mm the thickness of the layers begins to increase linearly reaching 7 mm at a depth of 14 cm. The overview of initial conditions and boundary conditions for capping simulation is presented in Table 3.7.

Table 3.7 Input data values for the capping simulation (column 1-50; 1.5 cm for cap)

Components	Initial Condition (μmol/cm^3)					Boundary
	1-50	51-82	83-114	115-146	147-155	Condition (μM)
1. CH_2O *fast*	349.76	34.97-0		0		
2. CH_2O *slow*	8728.49	872-690	682-361	349-29.5	21.5-0.71	
3. O_2	0	0.38-0		0		389
4. NO_3^-	0		0			6.2
5. MnO_2	0	82.5-50.7	47.1-2.81	2.47-0.52	0.63-1.92	
6. FeOOH	0	107.5-100	99.47-42.2	27.7-3.68	4.91-9.10	
7. SO_4^{2-}	28		28-26.6			28000
8. NH_4^+	0	0-0.03	0.03-0.14	0.15-0.35	0.35	0.58
9. PO_4^{3-}	0	0-0.01	0.01-0.06	0.07-1.8	1.8-0.95	0.526
10. Fe^{2+}	0		0-0.02		0.016-0	0
11. Mn^{2+}	0	0-0.07	0.08-0.28	0.28-0.08	0.08-0.06	1
12. H_2S	0		0			0
13. $=PO_4^{3-}$	0	0-0.04	0.04-0.06	0.06-5.98	8.39-16.2	0
14. FeS	0	0-0.07	0.08-2.66	2.88-0.56	0.25-0	0
15. FeS_2	0	1.3-17	18.2-81.8	84.9-182	181.3-161.5	0
16. S	0	4-5.64	5.7-15.7	16.5-6.2	4.9-1.7	0
17. PAH	0		0.0006			0
18. CH_4	0		0.16			160

Result and Discussion

Baseline Diagenetic Model

The sediment flux model is time-dependent, one-dimensional transport/reaction model (Fossing et al., 2004). The model consists of 105 layers including a 0.3 mm water layer overlying the sediment in order to describe mathematically the transport and nutrient cycling taking place in the depth range of 0-20 cm. Pore water profiles for the primary reactants (O_2, NO_3^-, MnO_2, FeOOH and SO_4^{2-}) are presented in Figure 3.1 and are similar in both shape and magnitude to those produced by Fossing et al. (2004) using the same calibration parameters. SO_4^2 and Fe^{2+} increased slightly and PO_4^{3-} and FeOOH are equal to the initial condition. These profiles match with actual data profile by Fossing (2004). Model was developed and PAH reactions added into model. The sediment flux model can simulate concentration profiles in the sediment actually, the sediment flux model can respond dynamically to addition of organic matter to the sediment, and the sediment flux model can simulate the response of the seabed to changes in organics, oxygen, and nutrient concentrations.

The sediment flux model could also reproduce the profiles of secondary reactants such as ammonium (NH_4^+), dissolved reduced manganese (Mn^{2+}), hydrogen sulfide (H_2S), phosphate (PO_4^{3-}), and iron sulfides (FeS and FeS_2). A significant limitation of the model in its current form is that the simulation time of the model and the run (clock) time of the model within MATLAB are very closely linked and therefore, simulation of month to years are not possible in the current coding. For example, the simulation time of this basic diagenetic model presented in Figure 3.1 is 2.74 e^5 seconds or ~2 days. This limits the ability of the model to examine the impact of longer term processes in the bed but allow some analysis of the PAH equations, themselves, which are the focus of this chapter.

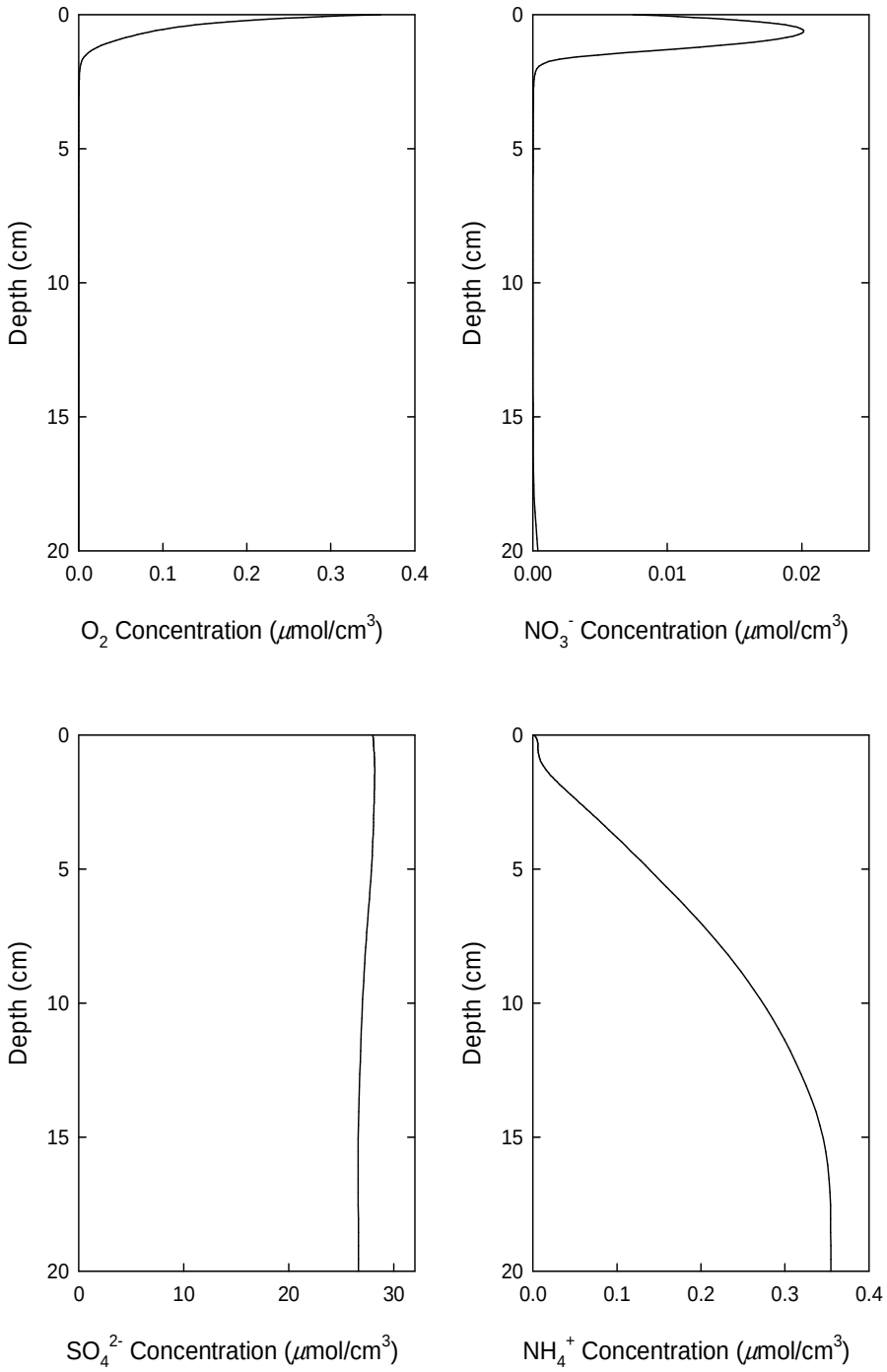

Figure 3.1 a Concentration profiles of basic diagenetic model

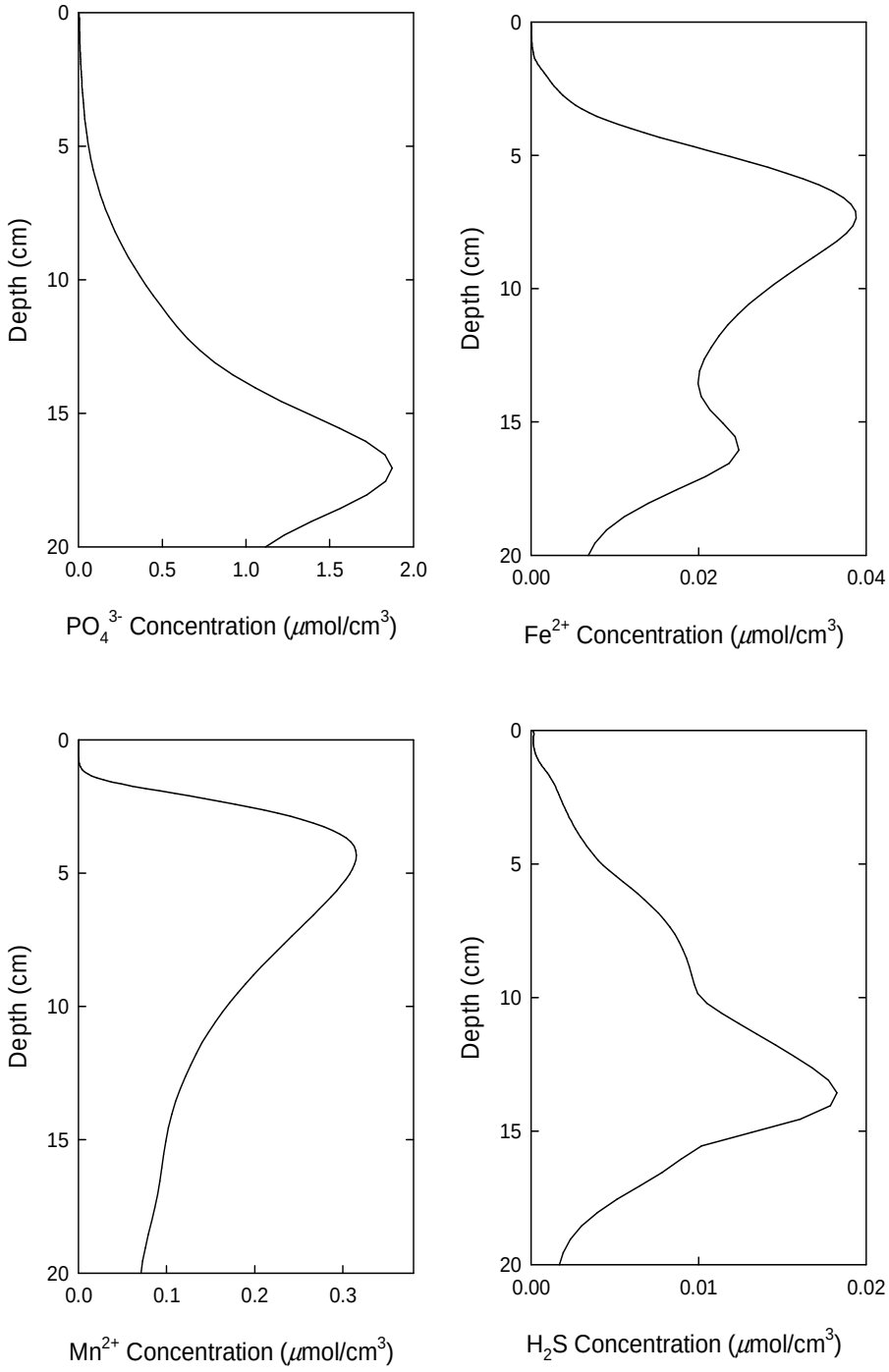

Figure 3.1 b Concentration profiles of basic diagenetic model

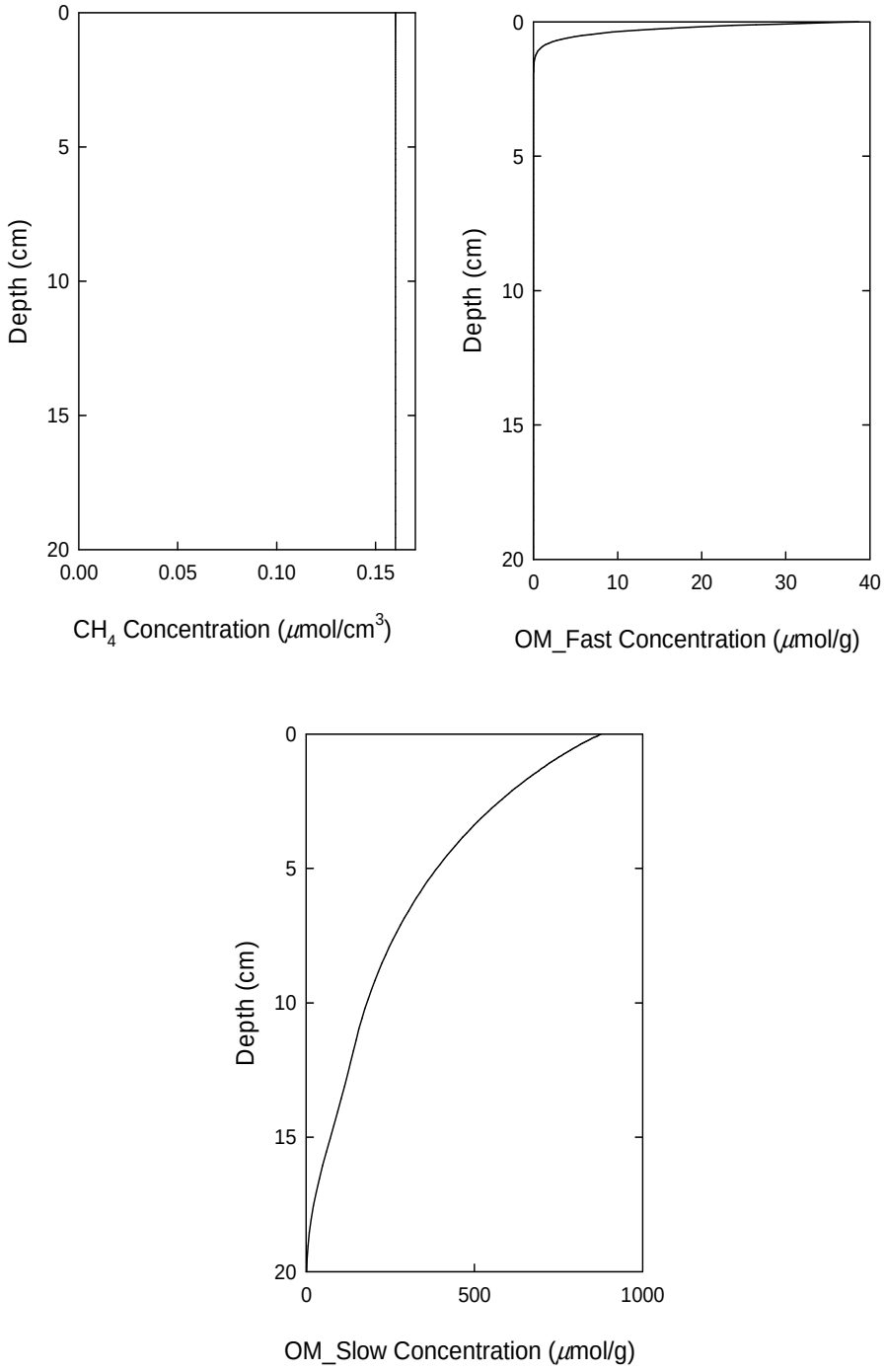

Figure 3.1 c Concentration profiles of basic diagenetic model

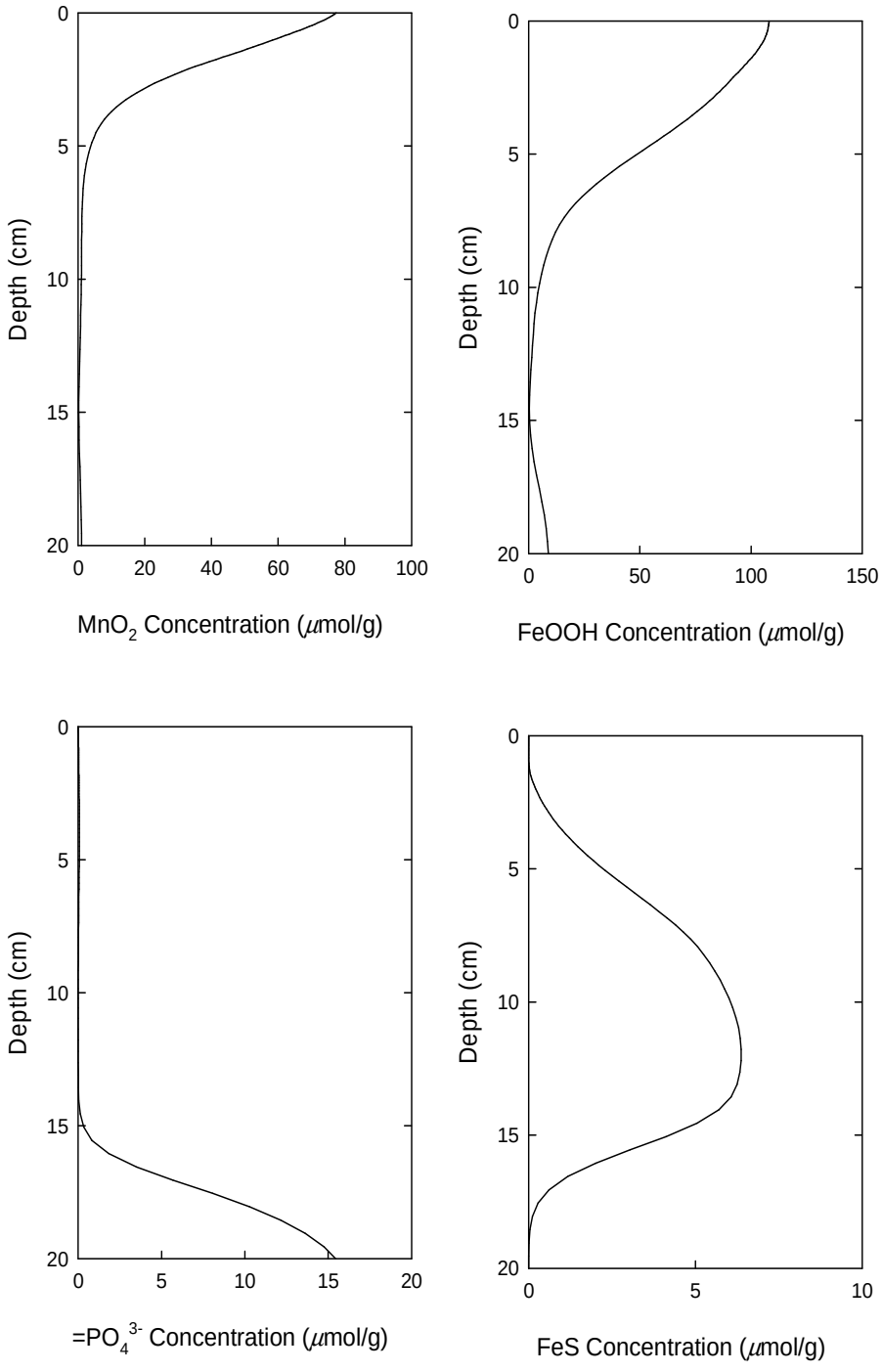

Figure 3.1 d Concentration profiles of basic diagenetic model

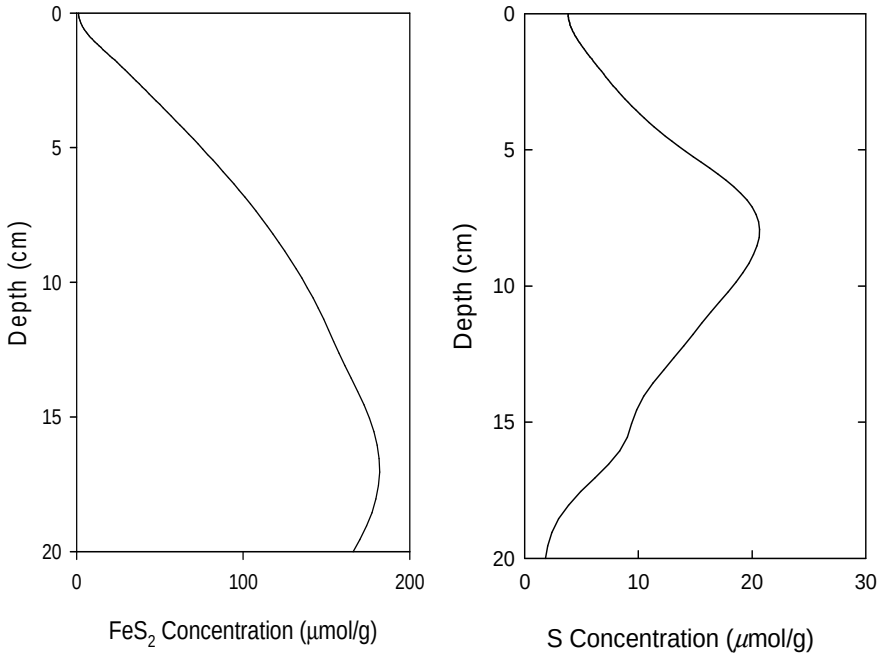

Figure 3.1 e Concentration profiles of basic diagenetic model

Anacostia River Sediment Model Sensitivity

The diagenetic model was calibrated the Anacostia River condition using experimental values and literature values from Anacostia River or adjacent Potomac River (Table 3.5). First, the model was calibrated by adding the biodegradation rate of each phenanthrene biodegradation reaction determined in Chapter 2. As expected, runs using these biodegradation rates showed no PAH biodegradation over the short simulation time given that half-lives of PAHs in Anacostia sediment under anaerobic conditions are months to years. The PAH biodegradation equations were tested by adjusting the biodegradation rate of each reaction involving an electron acceptor as a rate constant of 0.693 day^{-1}, corresponding to a 1 day half-life. This allows us to examine the depth of the different redox-linked PAH degradation reactions in the bed. The simulation time and run time are very closed. Since long time simulation is not possible, the rate constant was speed up to 0.693 day^{-1}. The location of PAH reactions was identified in the Anacostis sediment bed.

As long as oxygen is present, organic matter degradation takes place by bacterial respiration with oxygen, it called aerobic respiration. Oxygen is typically present in the water column and in the uppermost few millimeters of sediment (i.e 0–5 mm), followed by respiration with nitrate, oxidized iron, manganese, and sulfate. Under oxygen reduction condition, PAH was degraded just in the uppermost millimters of the bed as shown the Figure 3.2 c. Oxygen is present in the 0.045 centimeters of sediment and there is 0.7 years for aerobic biodegradation to take place based on Anacostia River sedimentation rate, 0.064 cm/year. Comparing the initial condition of each component (Figure 3.2), SO_4^{2-} reduced in the 1-4 cm of sediment, H_2S, FeS, and FeS_2 are formed in the 1–2 cm, 2–4 cm, and 5 cm, respectively. Then FeOOH is formed in the 5–10 cm layer, and it turns off PAH and sulfate concentration.

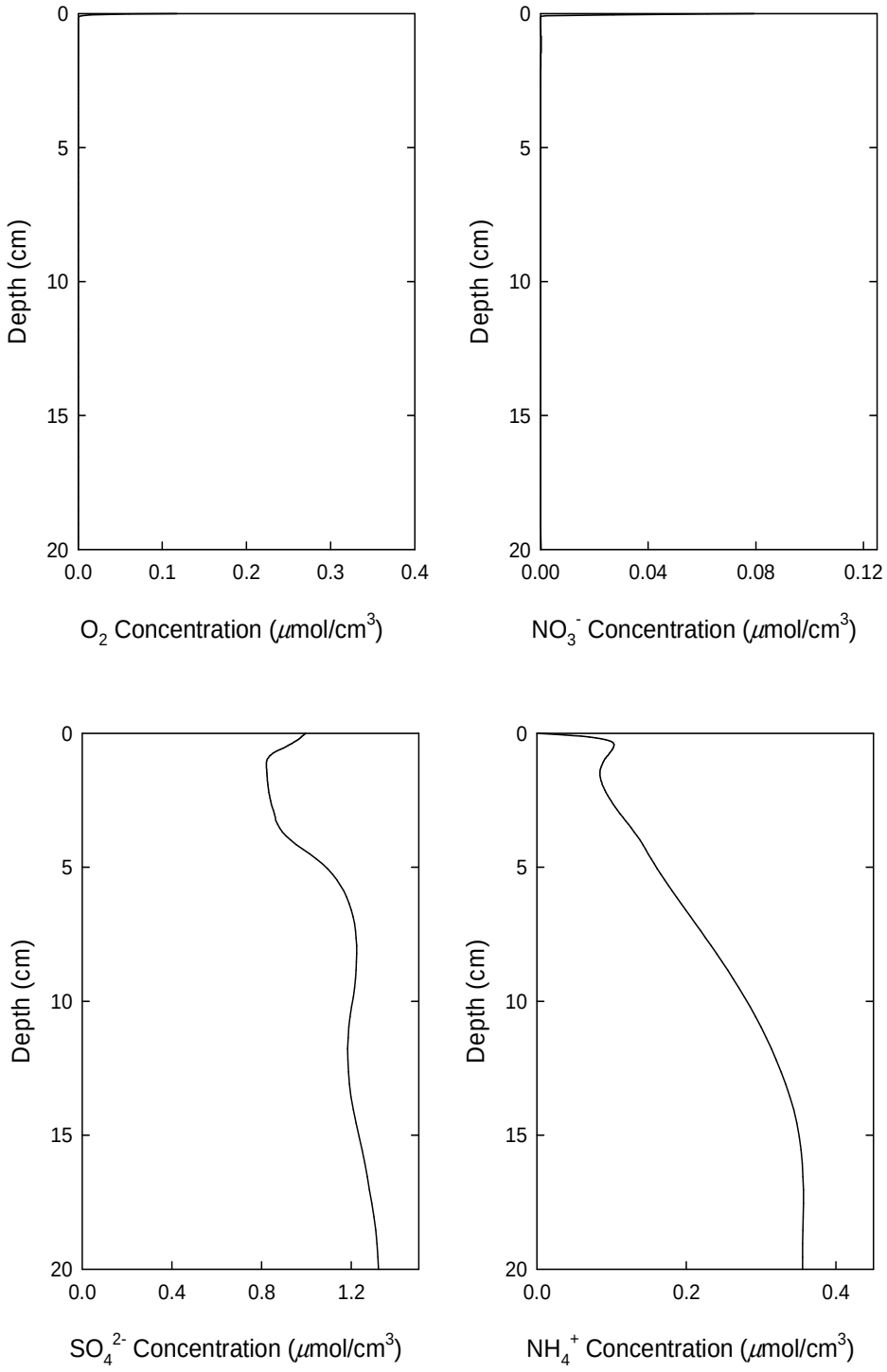

Figure 3.2 a Concentration profiles of Anacostia sediment model as the oxygen rate constant of 0.693

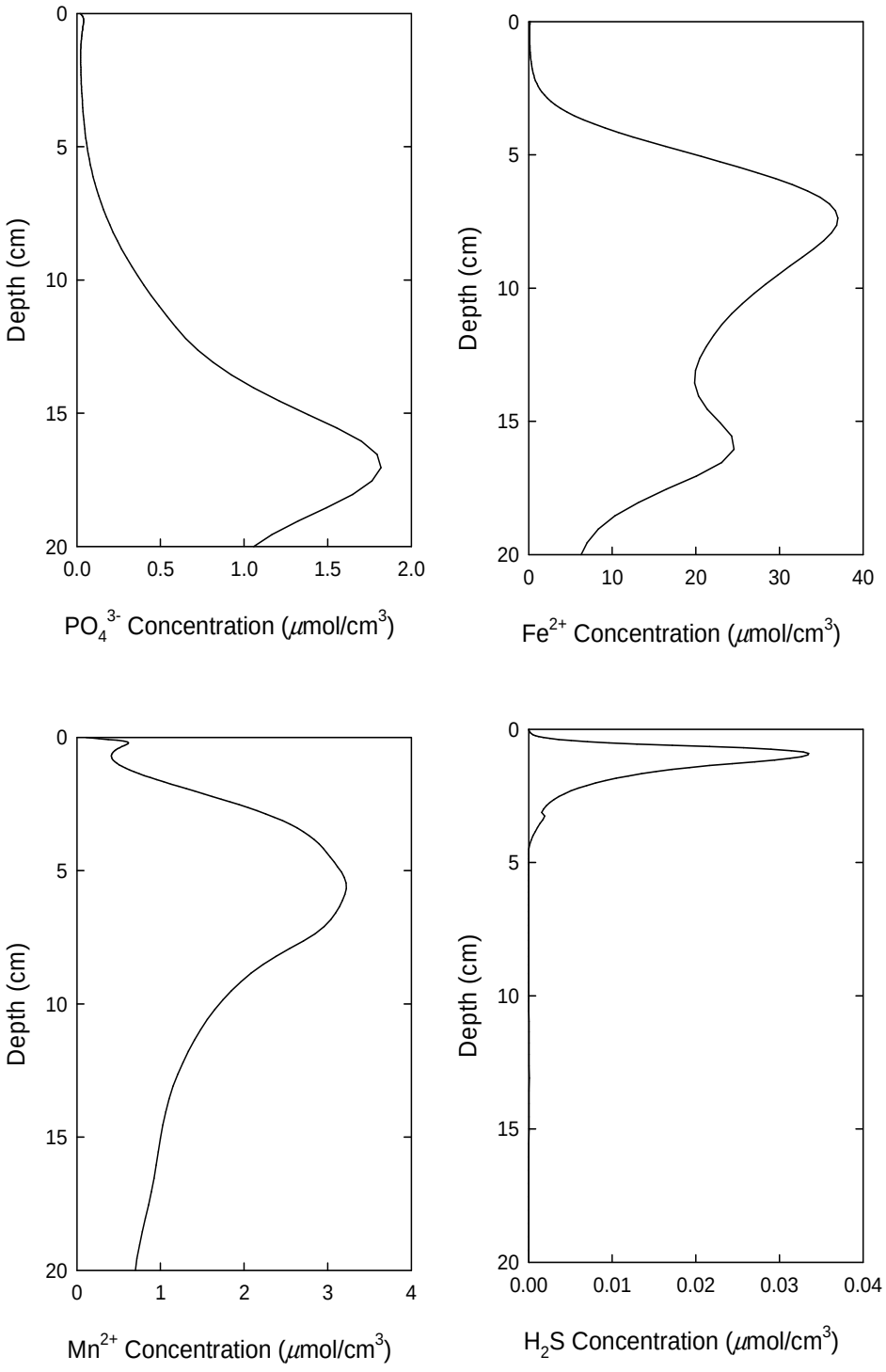

Figure 3.2 b Concentration profiles of Anacostia sediment model as the oxygen rate constant of 0.693

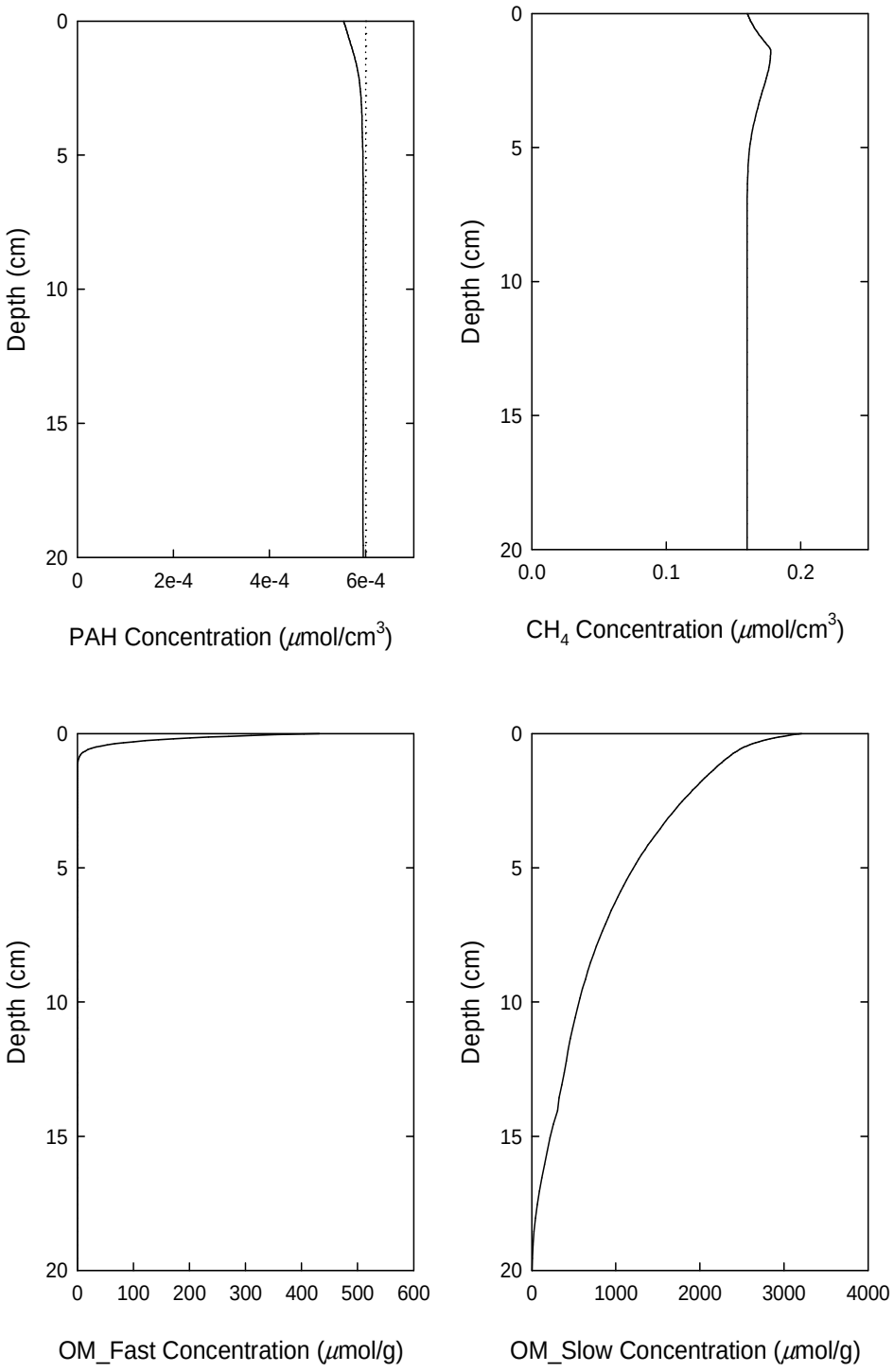

Figure 3.2 c Concentration profiles of Anacostia sediment model as the oxygen rate constant of 0.693

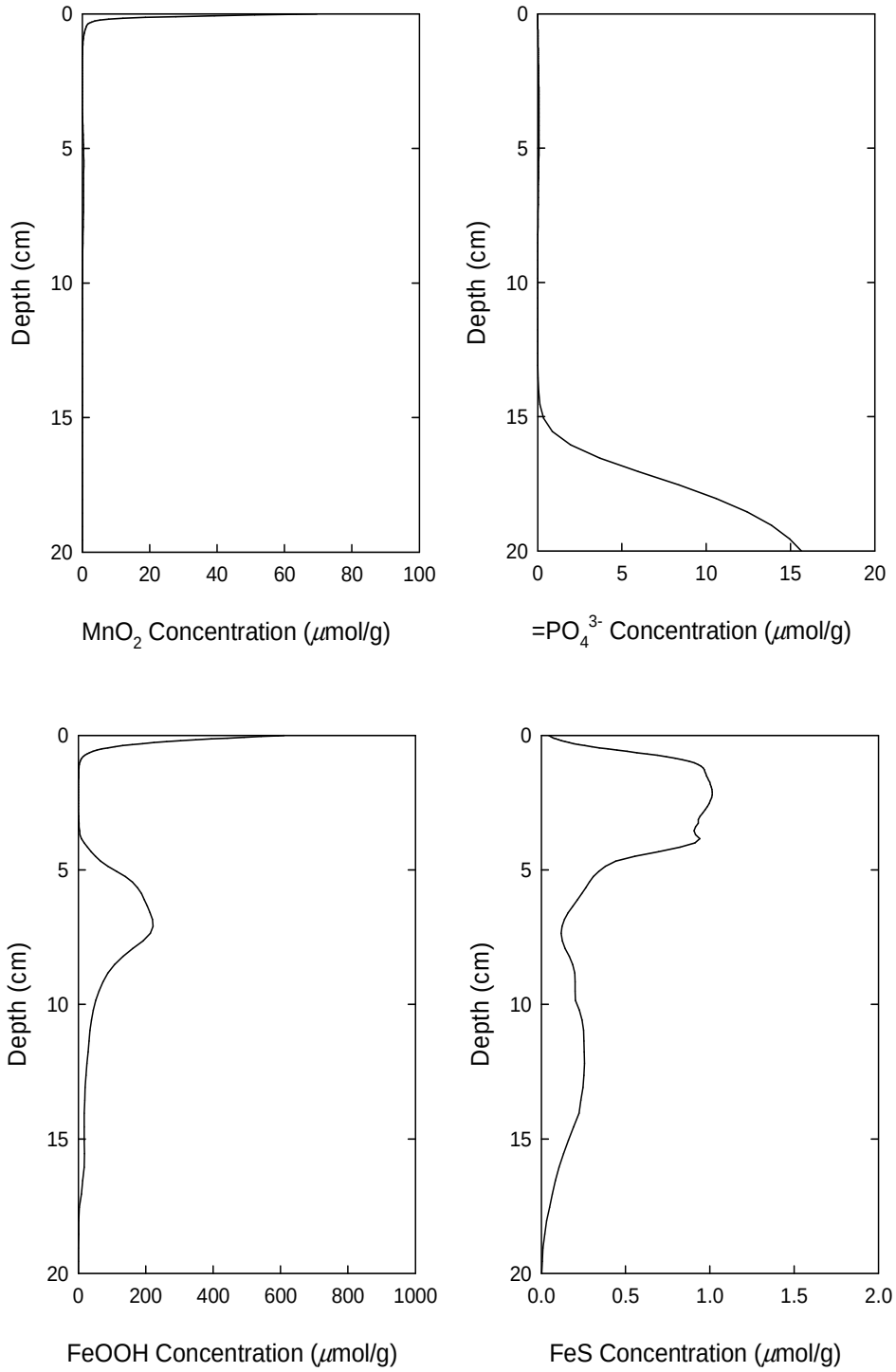

Figure 3.2 d Concentration profiles of Anacostia sediment model as the oxygen rate constant of 0.693

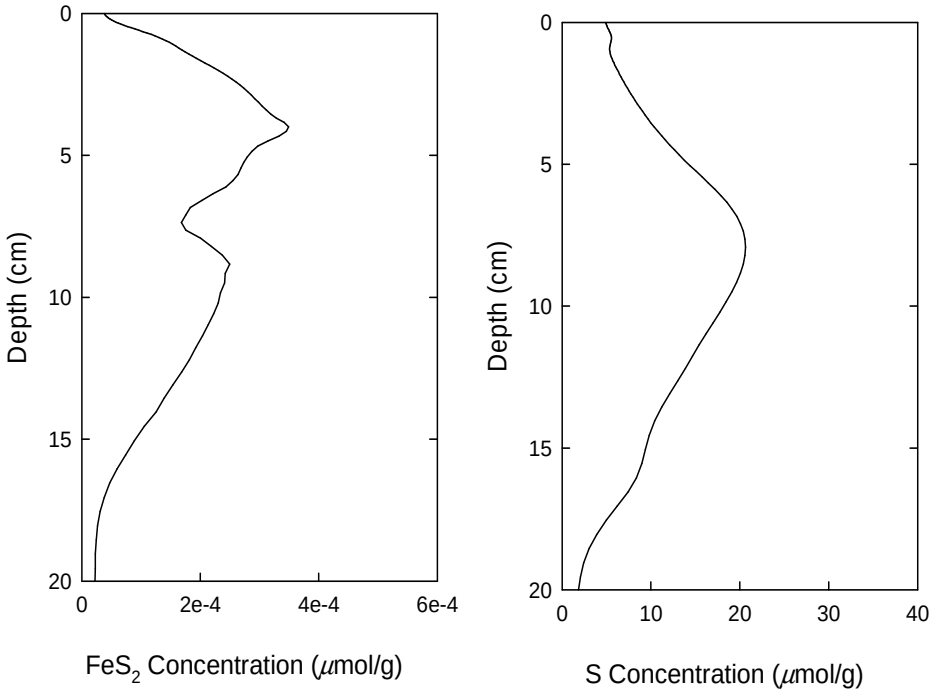

Figure 3.2 e Concentration profiles of Anacostia sediment model as the oxygen rate constant of 0.693

The respiration processes are distributed in a characteristic vertical pattern within the seabed. When oxygen is depleted, mineralization continues to proceed through anaerobic respiration. Nitrate reduction takes place slightly deeper into the seabed than oxygen and also disappears within the upper few millimeters (i.e. 5–10 mm). Under nitrate reduction condition, PAH concentration didn't change in the Figure 3.3 c. Nitrate is present in the 0.075 centimeters of sediment and there is 1.2 years for anaerobic biodegradation to take place based on Anacostia River sedimentation rate, 0.064 cm/years. Comparing the initial condition of each component (Figure 3.3), there are very similar patterns of SO_4^{2-}, H_2S, FeS, FeS_2, and FeOOH in the oxygen reduction. The presence of NO_3^- is required for the denitrification process to take place. Nitrate for denitrification is formed in the sediment by oxidation of NH_4^+ to NO_3^-. As long as sediment contains oxygen and NH_4^+, denitrification can still occur. There is ammonium in the seabed as shown in the Figure 3.3 a while NO_3^- and oxygen concentration is very low. This causes the denitrification activity to decrease.

Manganic manganese reduction takes place slightly below the nitrate zone (i.e. 1–1.5 cm). PAH concentration didn't change in the Figure 3.4 c under manganic manganese reduction condition. Manganese is present in the 3.39 centimeters of sediment and there is 53 years for anaerobic biodegradation to take place based on Anacostia River sedimentation rate, 0.064 cm/years. Comparing the initial condition of each component (Figure 3.4), SO_4^{2-} reduced in the 1-4 cm of sediment, H_2S, FeS, and FeS_2 are formed in the 1–2 cm, 2–4 cm, and 5 cm, respectively. Then FeOOH is formed in the 5–10 cm. Manganese (oxidized form) reacts with H_2S to form Mn^{2+} and reduced manganese oxidized to MnO_2 in the presence of the oxygen.

Iron reduction also takes place slightly below the nitrate zone (i.e. 1.5–2.5 cm). PAH removal was observed in the 3–7 cm in the sediment in the Figure 3.5 c under iron reduction

condition. Iron is present in the 2.87 centimeters of sediment and there is 45 years for anaerobic biodegradation to take place based on Anacostia River sedimentation rate, 0.064 cm/years. Reduced iron reacts with both MnO_2 and O_2 to form FeOOH and iron sulfide (FeS) is formed by reaction Fe^{2+} with H_2S. Comparing the initial condition of each component (Figure 3.5), H_2S and FeS are formed in the 1–2 cm, and 2–4 cm, respectively. FeOOH is formed in the 5–10 cm.

Sulfate penetrates as far as 1-4 cm into the sediment. Oxygen consuming bacteria degrade less than half of the organic material that reaches the seabed. Anaerobic bacteria take care of the reminder of the organic material. Approximately 60 % of anaerobic degradation takes place through sulfate reduction in the marine environment, while all the rest takes place through iron reduction (Fossing et al., 2004). PAH component removed in the 0–4 cm in the sediment and then below 10 cm removed again in the Figure 3.6 c under sulfate reduction condition. Sulfate is present in the 2.11 centimeters of sediment and there is 33 years for anaerobic biodegradation to take place based on Anacostia River sedimentation rate, 0.064 cm/years. Considering the sulfate dominating condition (Figure 3.6), the reactants react in the order of FeOOH, H_2S, and CH_4 in the top 4 cm and down below secondary reactions happen. PAH decreased in the upper 0-4 cm with fast organic carbon reaction and PAH is back in 5–10 cm due to FeOOH forming. Then, further down slow decreased. FeOOH formed in 5–10 cm of sediment depth and turns off SO_4^{2-} and PAH. The concentration profiles under sulfate-reducing conditions are very similar with concentration profile under iron-reducing conditions. Literatures have been reported that Anacostia River sediment is iron rich sediment and contaminant degradation was linked with iron reduction. (Lovley and Phillips, 1986; Phillips et al., 1993).

Biodegradation processes take place in the order with oxygen followed by with nitrate, maganic manganese, ferric iron, and sulfate in the sediment. Further down in the sediment, the

degradation of organic matter takes place through fermentation. Methane is formed by this reaction. Deepest down in the sediment, below the sulfate zone, methane is produced by fermentation of organic material. PAH removal was observed in the 1-3 cm in the sediment in the Figure 3.7 c under methanogenesis condition. Methane is produced between 1.5 and 7.5 centimeters in the sediment and anaerobic biodegradation takes 94 to 118 years to take place based on Anacostia River sedimentation rate, 0.064 cm/years.

Capping Simulations

Capping simulation model was developed in Figure 3.8. The layer of uncontaminated material was added on top and then rerun the simulation. Capping simulation was run with the initial condition of the maring system plus a cap to observe the changes with elevated sulfate concentration with a cap. Sediment profiles can be reproduced by changes in redox species with adding the cap layer. As cap layer is added over the sediment originally in an aerobic state on the surface are buried and subsequently transformed to anaerobic condition. The primary reactants (MnO_2, FeOOH and SO_4^{2-}) react with organic matter whereas other primary reactants (O_2 and NO_3^-) are not. Ten times of organic carbon added on initial condition that drives more sulfate reduction. PAH decline at the surface due to the cap and then degraded in an area just below the cap and deeper below the iron zone. Sulfate concentration decreased rapidly in the cap layer and then slowly reduced below 5 cm of sediment. The cap will inhibit the flux of organic matter to contaminated sediment and force the microorganism to degrade the contaminants. The reactions of secondary reactants (NH_4^+, Fe^{2+}, Mn^{2+}, H_2S, PO_4^{3-}, FeS and S) happedned near the capping region in the sediment. We could not observe the much differences in the redox conditions from the capping simulation since thise changes would occur over months. The simulation time of capping model is 2.95 e^5 with sulfate reaction rate of 0.693.

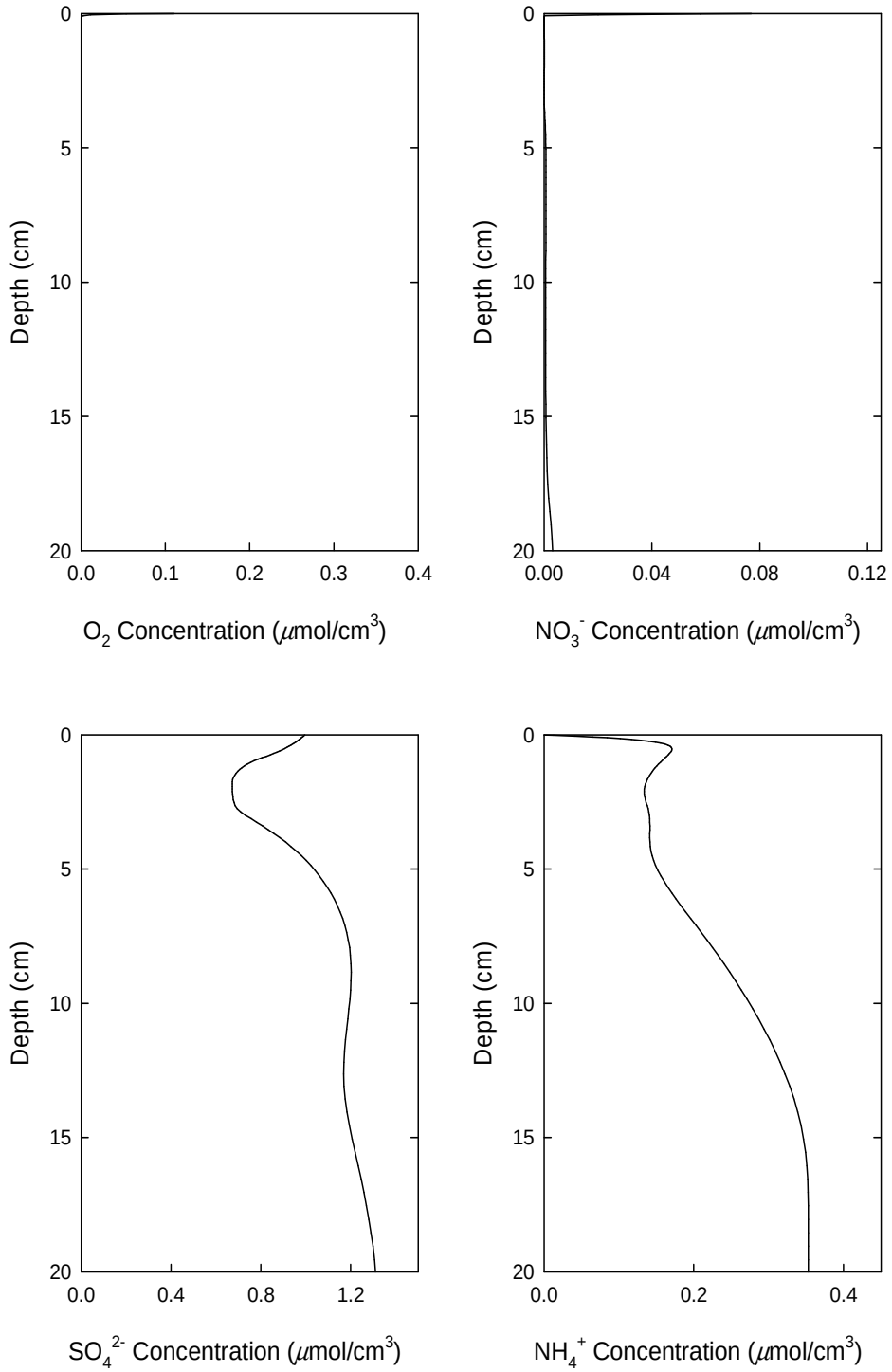

Figure 3.3 a Concentration profiles of Anacostia sediment model as the nitrate rate constant of 0.693

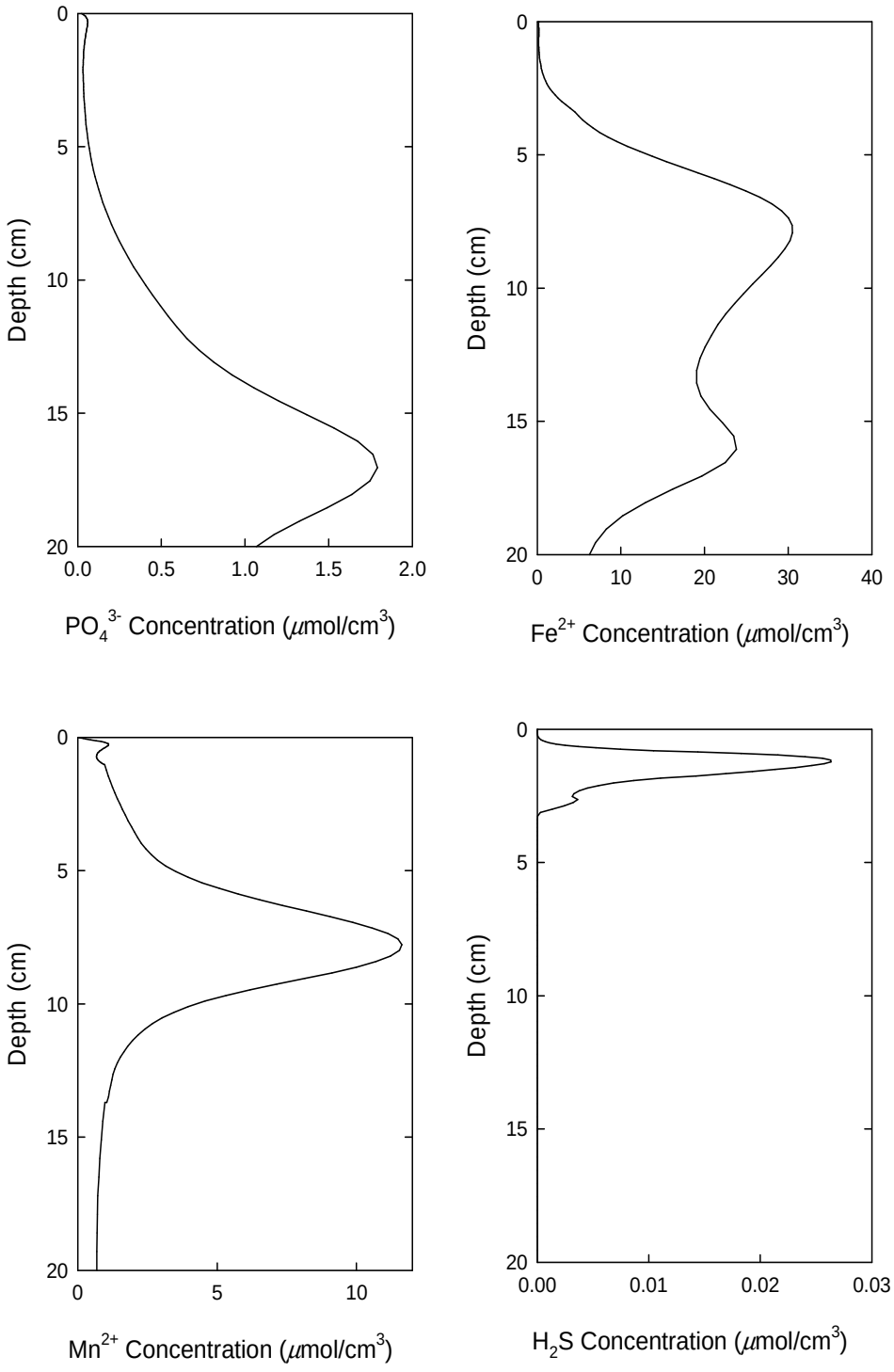

Figure 3.3 b Concentration profiles of Anacostia sediment model as the nitrate rate constant of 0.693

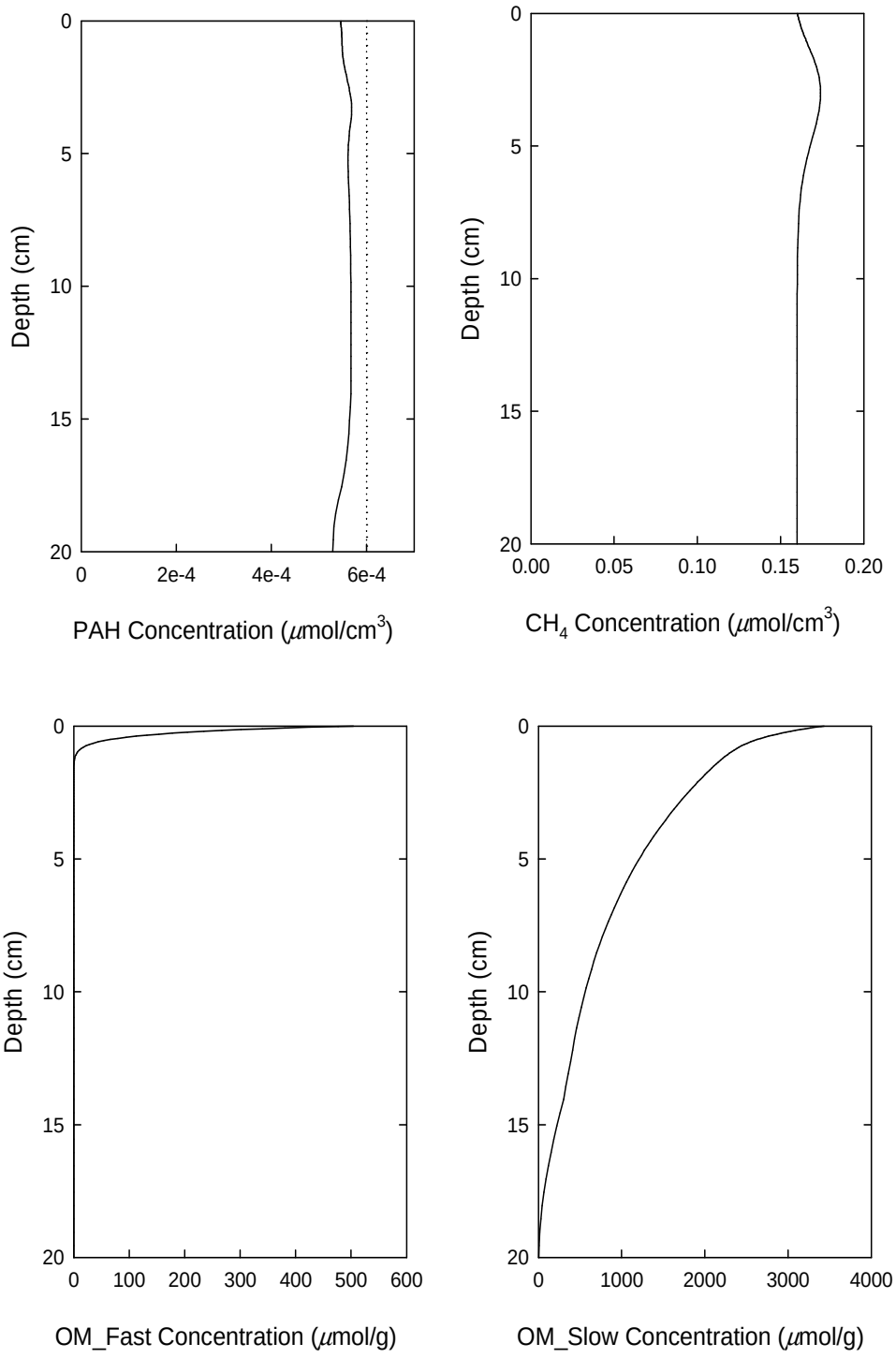

Figure 3.3 c Concentration profiles of Anacostia sediment model as the nitrate rate constant of 0.693

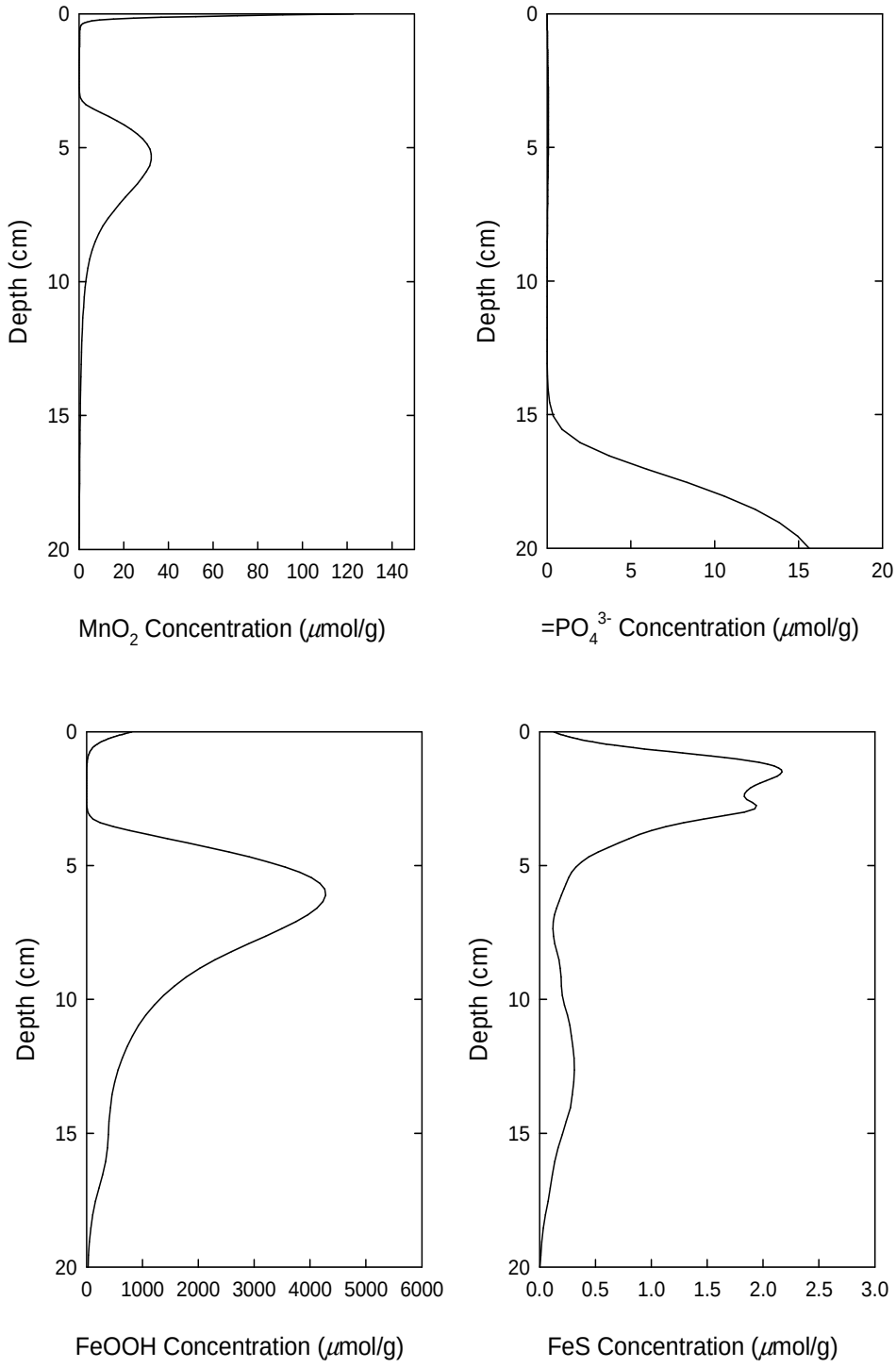

Figure 3.3 d Concentration profiles of Anacostia sediment model as the nitrate rate constant of 0.693

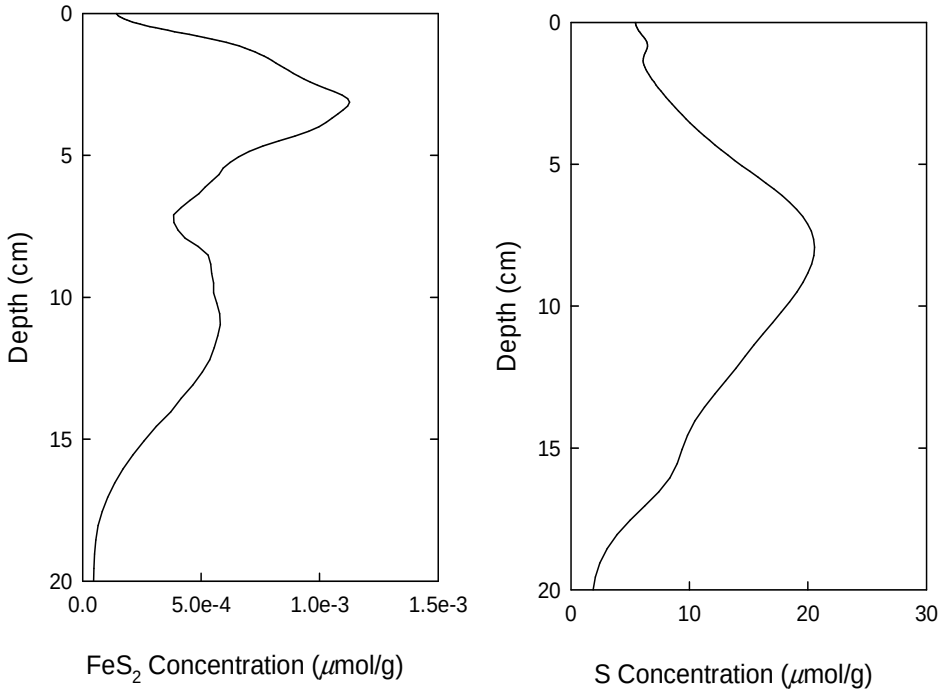

Figure 3.3 e Concentration profiles of Anacostia sediment model as the nitrate rate constant of 0.693

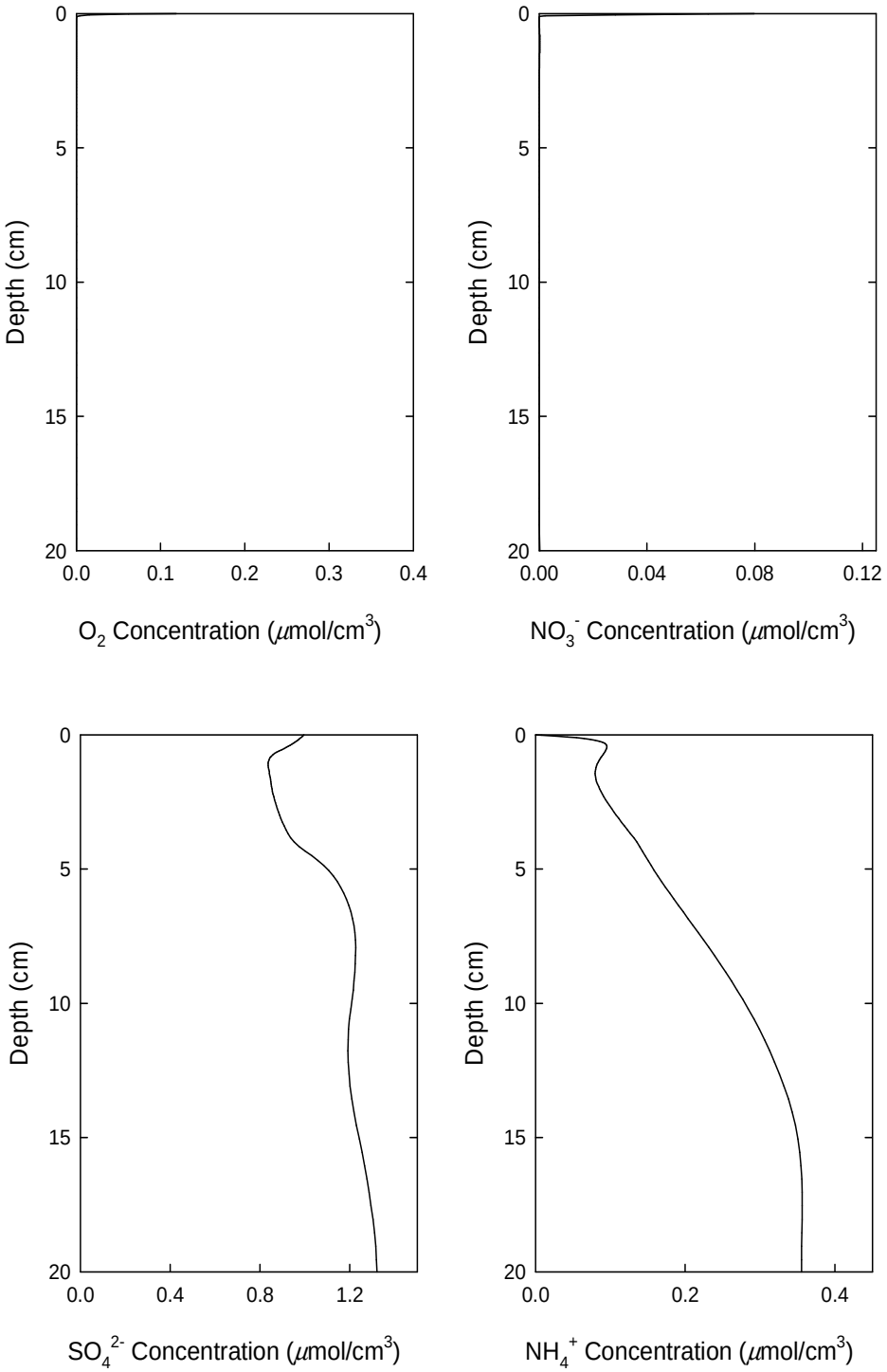

Figure 3.4 a Concentration profiles of Anacostia sediment model as the manganic manganese rate constant of 0.693

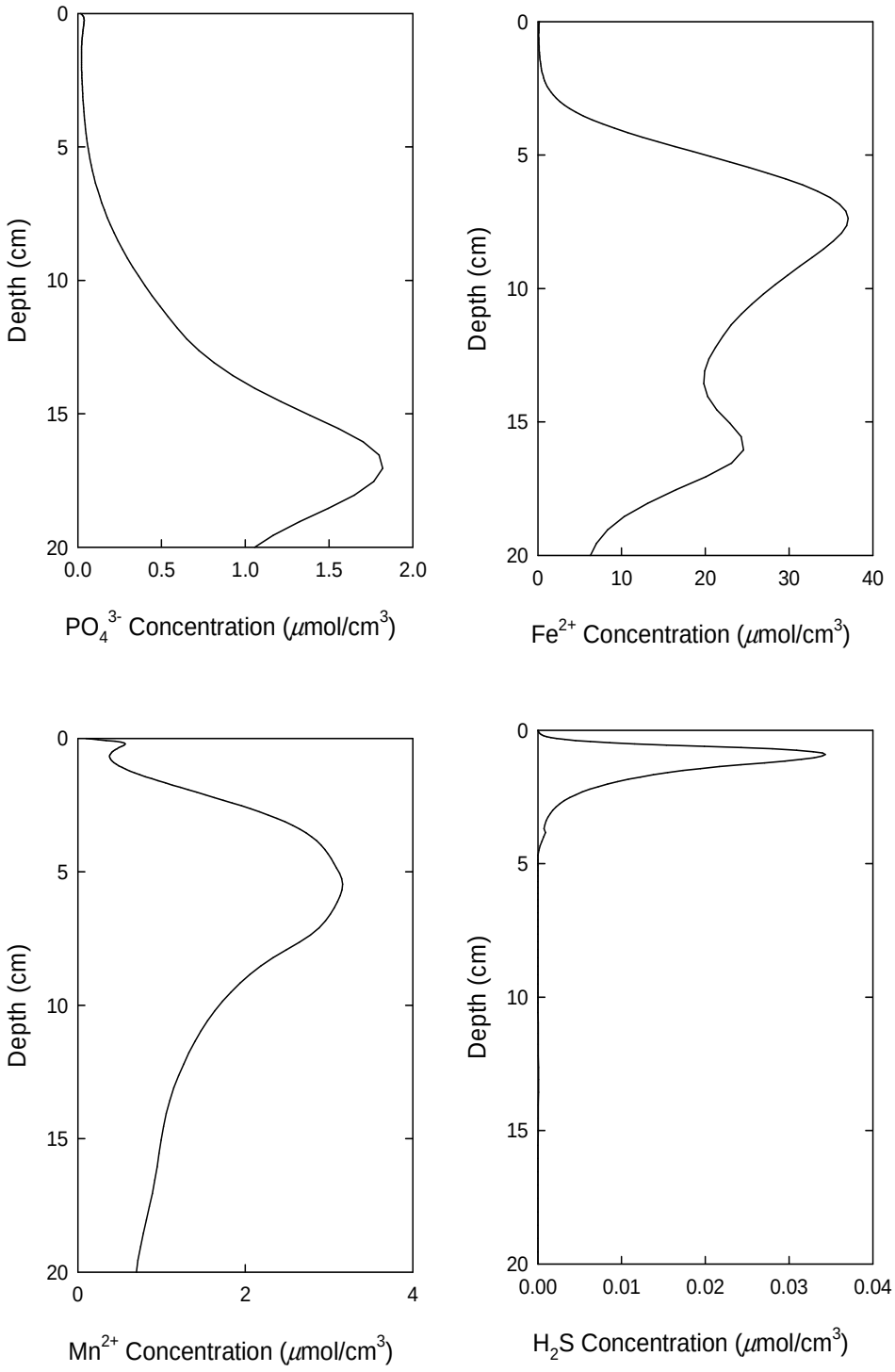

Figure 3.4 b Concentration profiles of Anacostia sediment model as the manganic manganese rate constant of 0.693

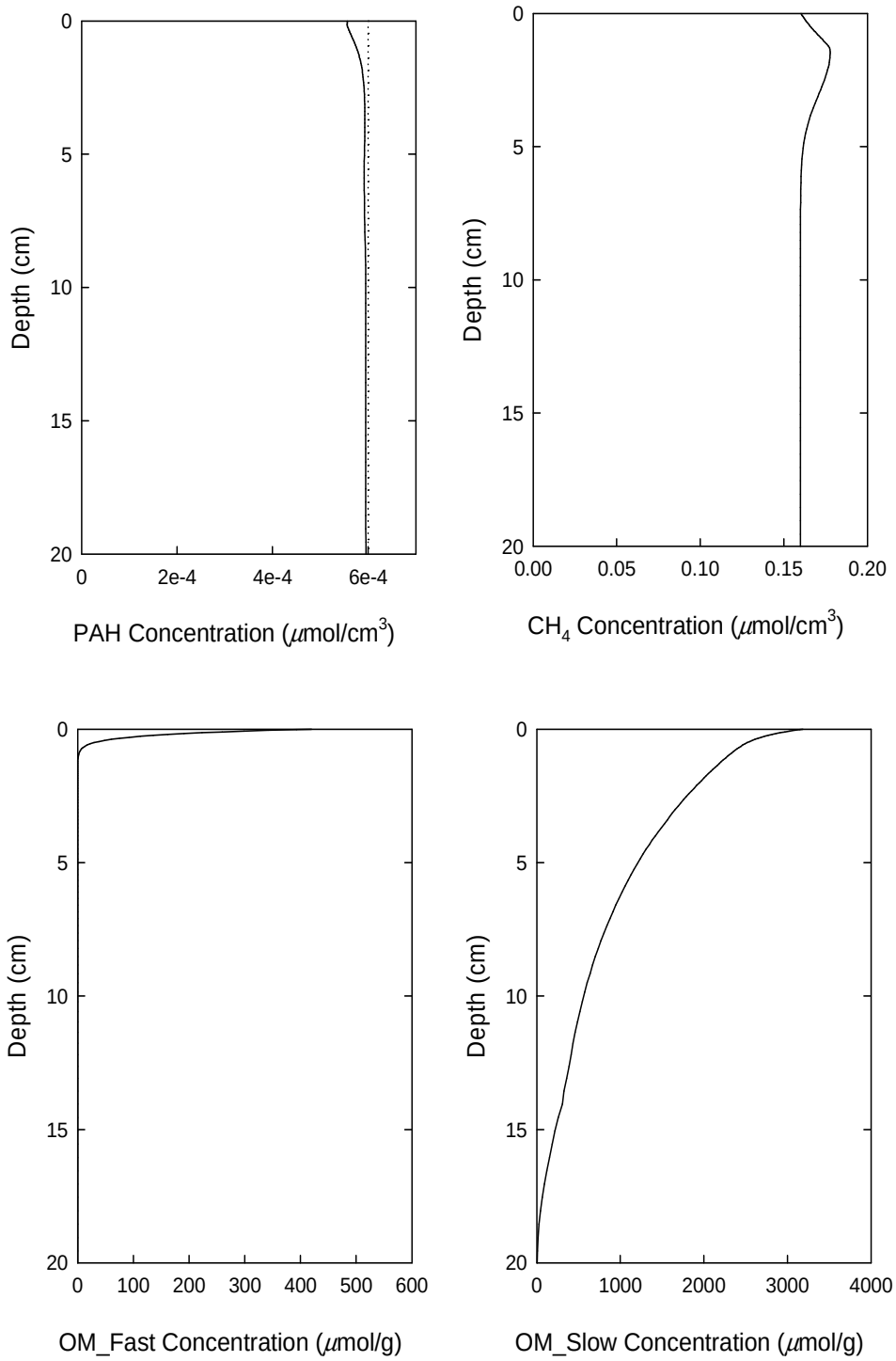

Figure 3.4 c Concentration profiles of Anacostia sediment model as the manganic manganese rate constant of 0.693

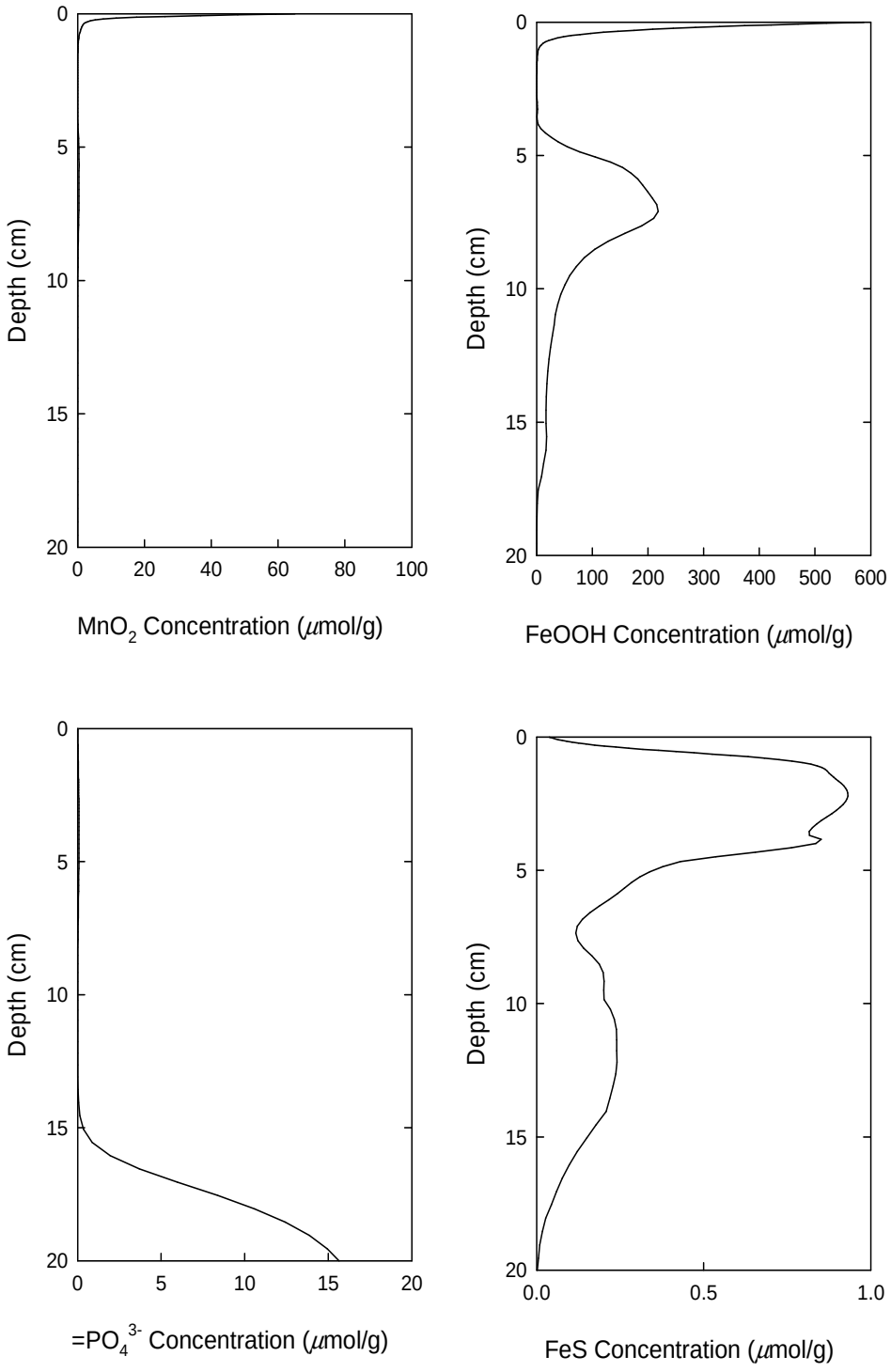

Figure 3.4 d Concentration profiles of Anacostia sediment model as the manganic manganese rate constant of 0.693

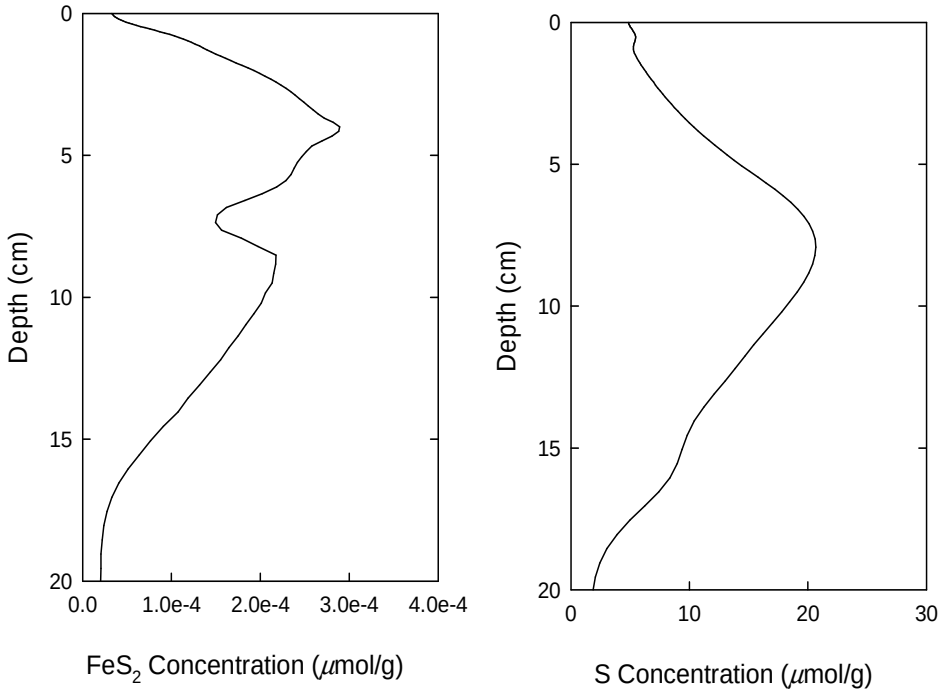

Figure 3.4 e Concentration profiles of Anacostia sediment model as the manganic manganese rate constant of 0.693

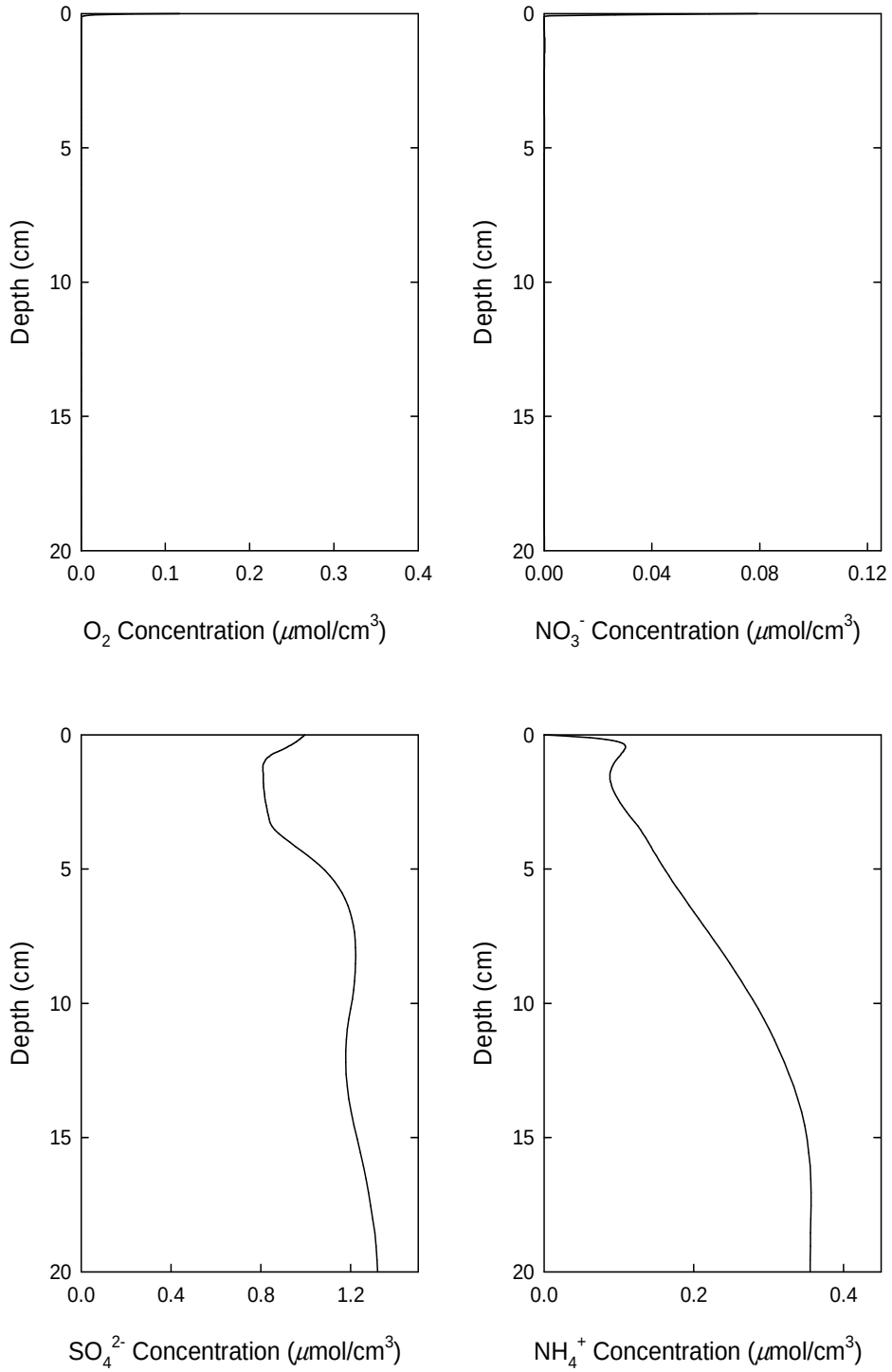

Figure 3.5 a Concentration profiles of Anacostia sediment model as the ferric iron rate constant of 0.693

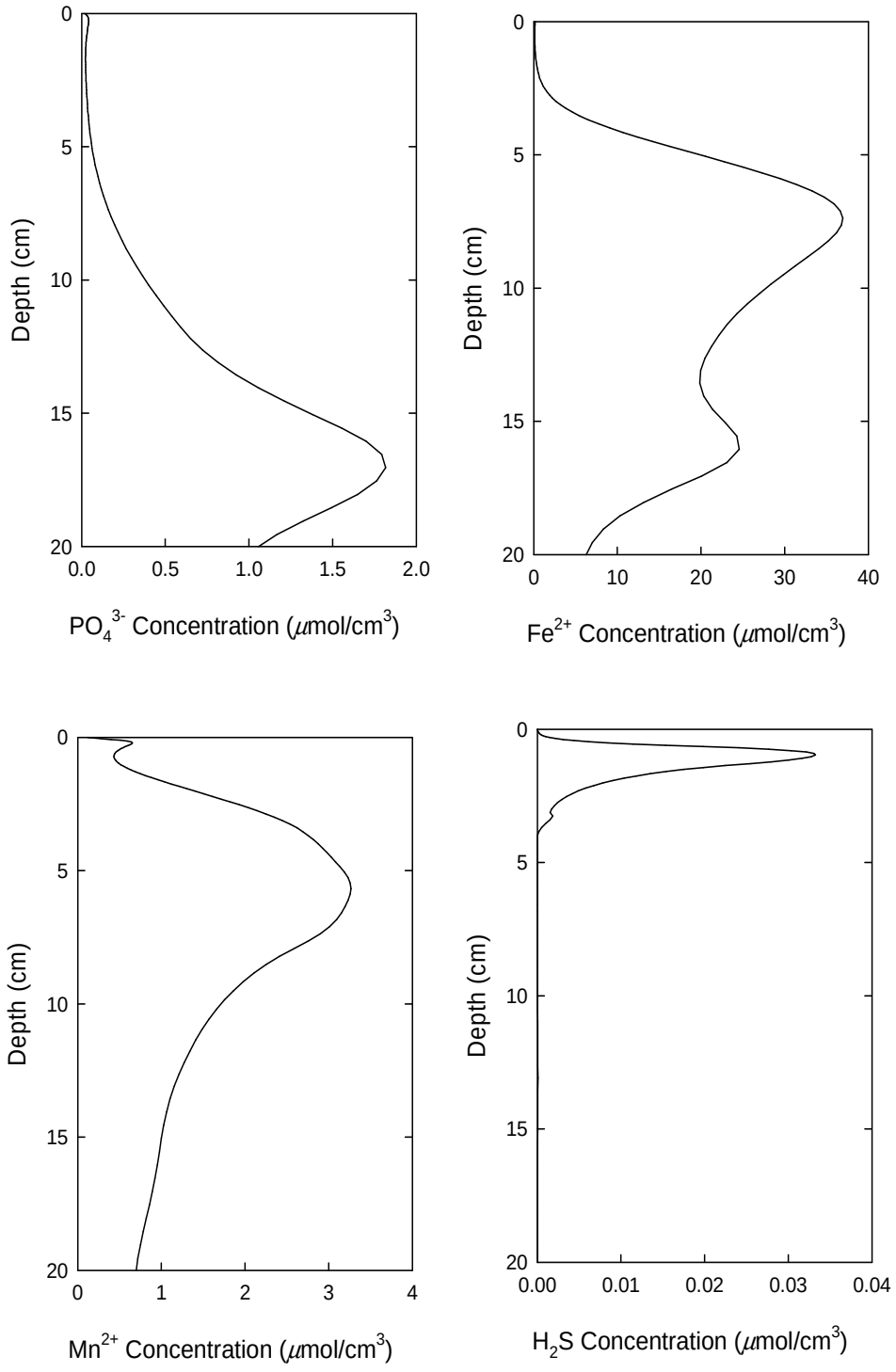

Figure 3.5 b Concentration profiles of Anacostia sediment model as the ferric iron rate constant of 0.693

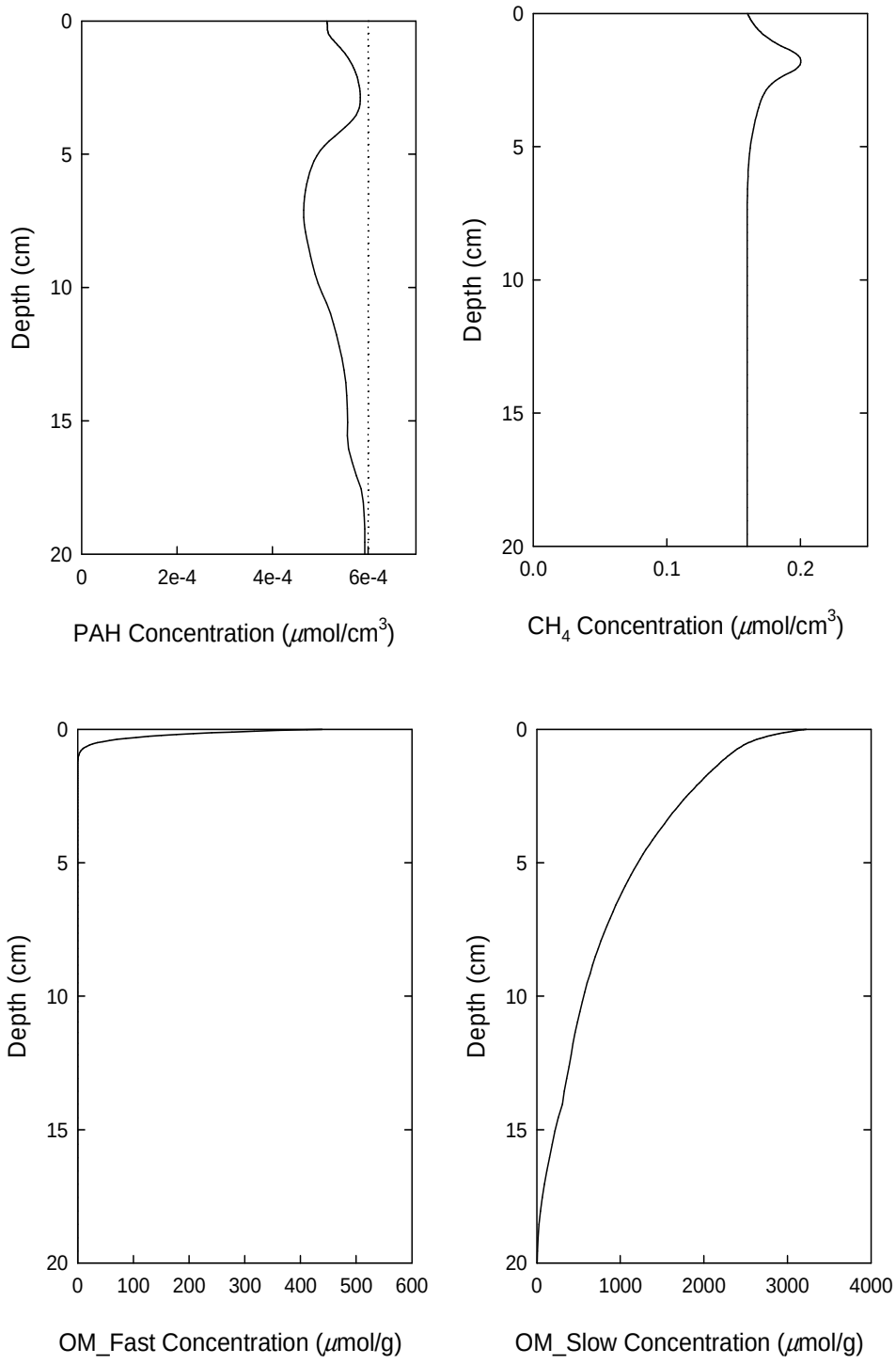

Figure 3.5 c Concentration profiles of Anacostia sediment model as the ferric iron rate constant of 0.693

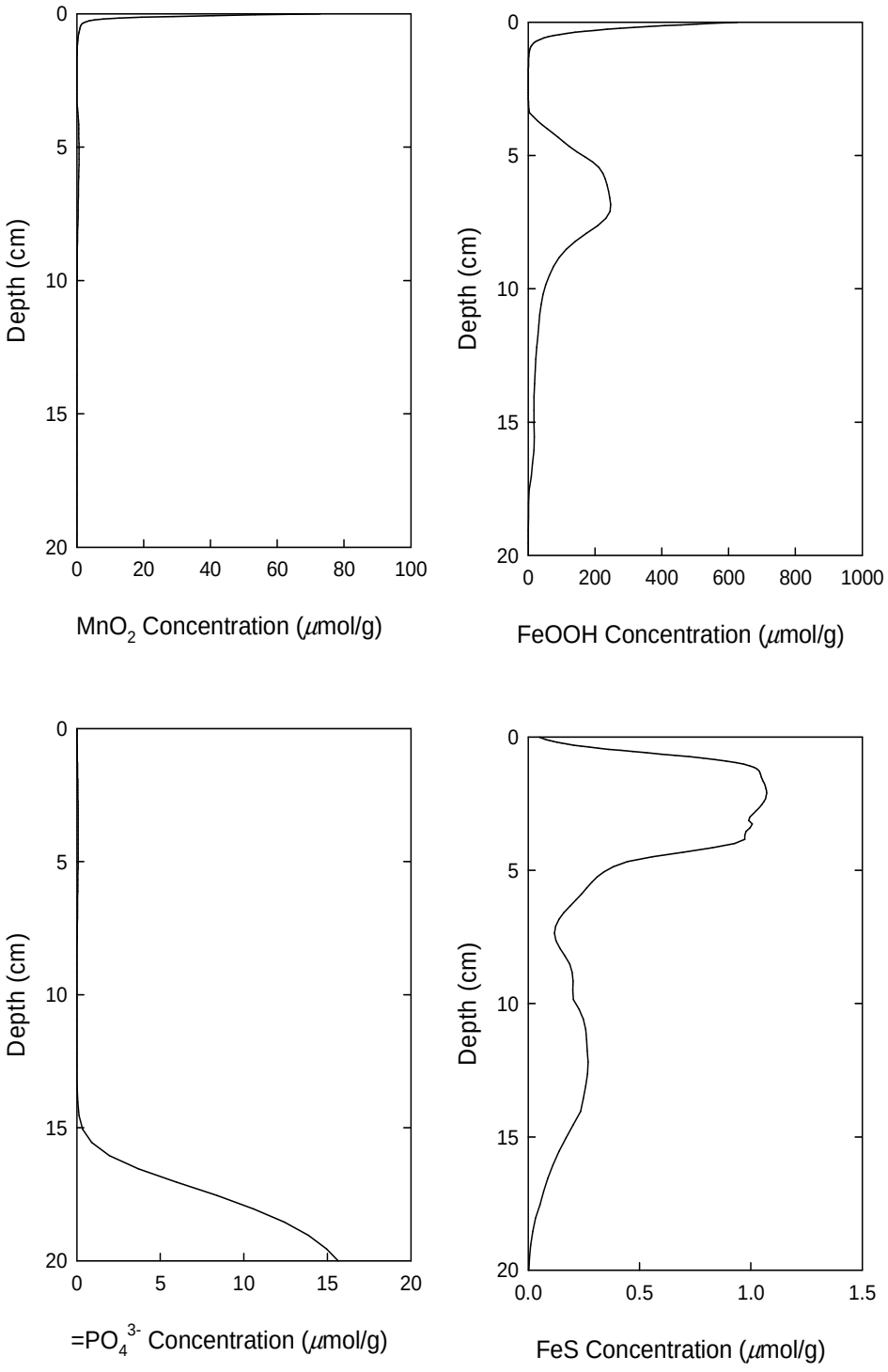

Figure 3.5 d Concentration profiles of Anacostia sediment model as the ferric iron rate constant of 0.693

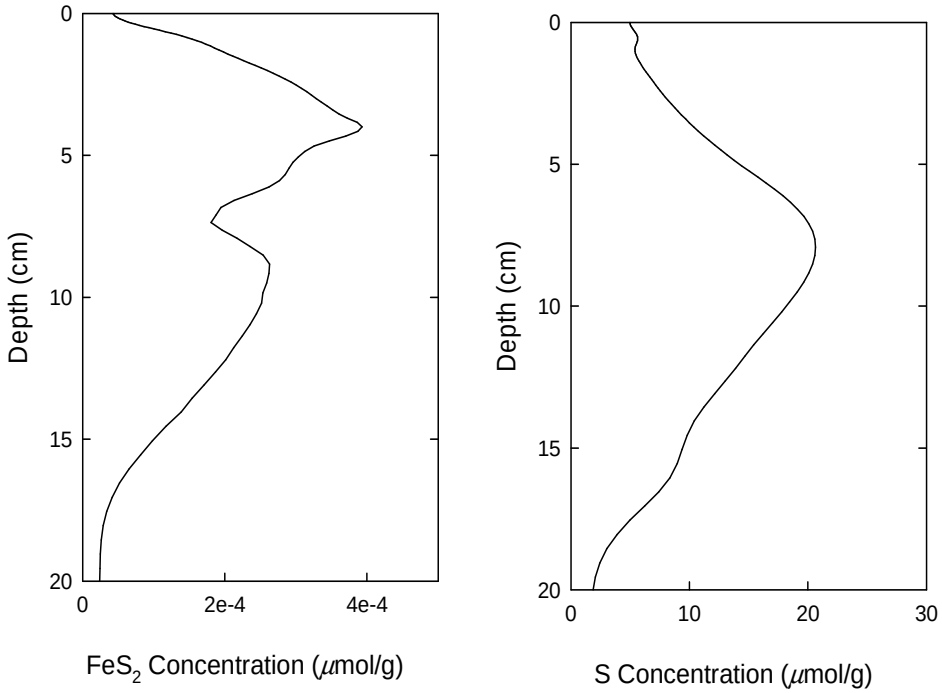

Figure 3.5 e Concentration profiles of Anacostia sediment model as the ferric iron rate constant of 0.693

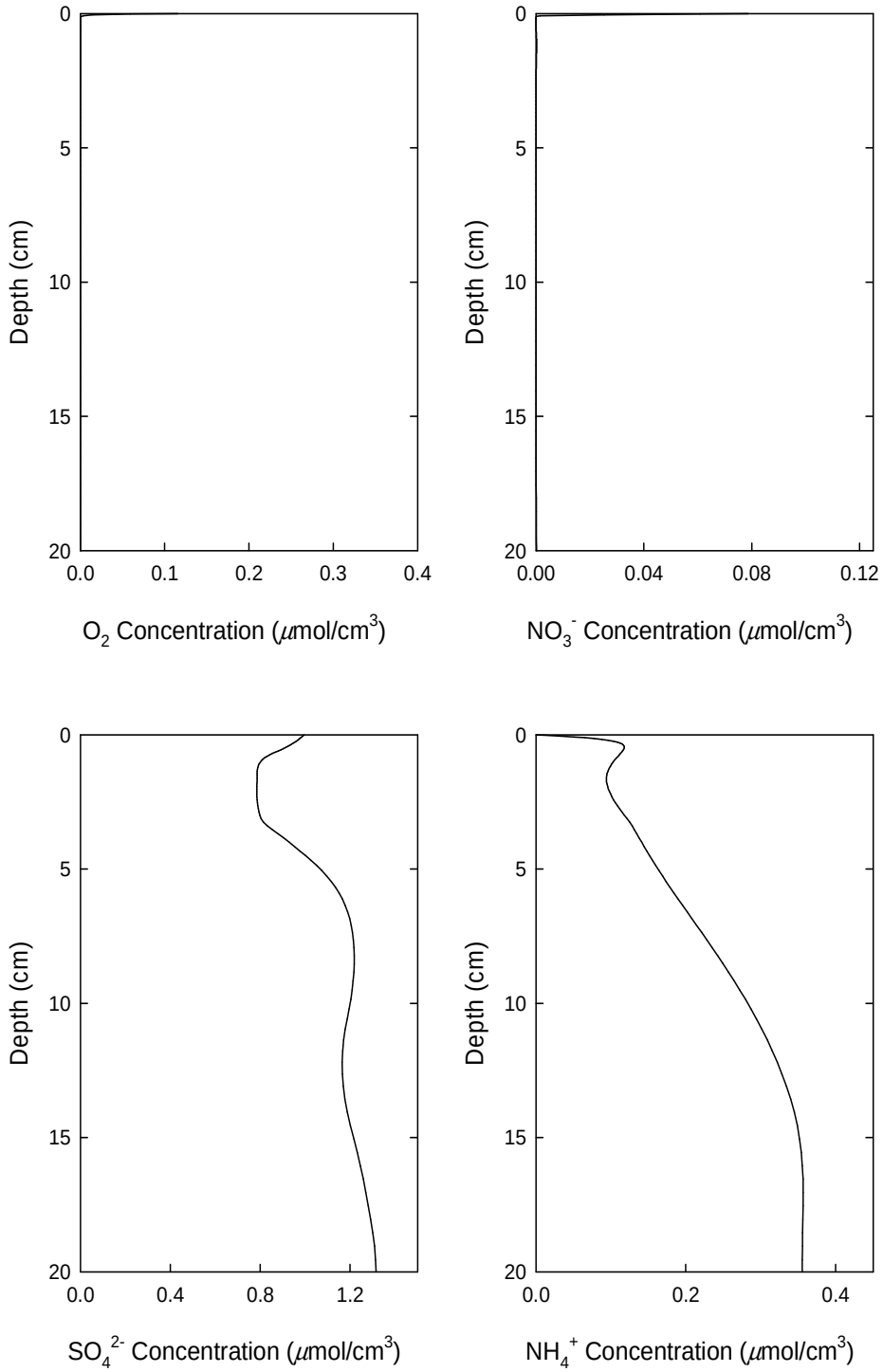

Figure 3.6 a Concentration profiles of Anacostia sediment model as the sulfate rate constant of 0.693

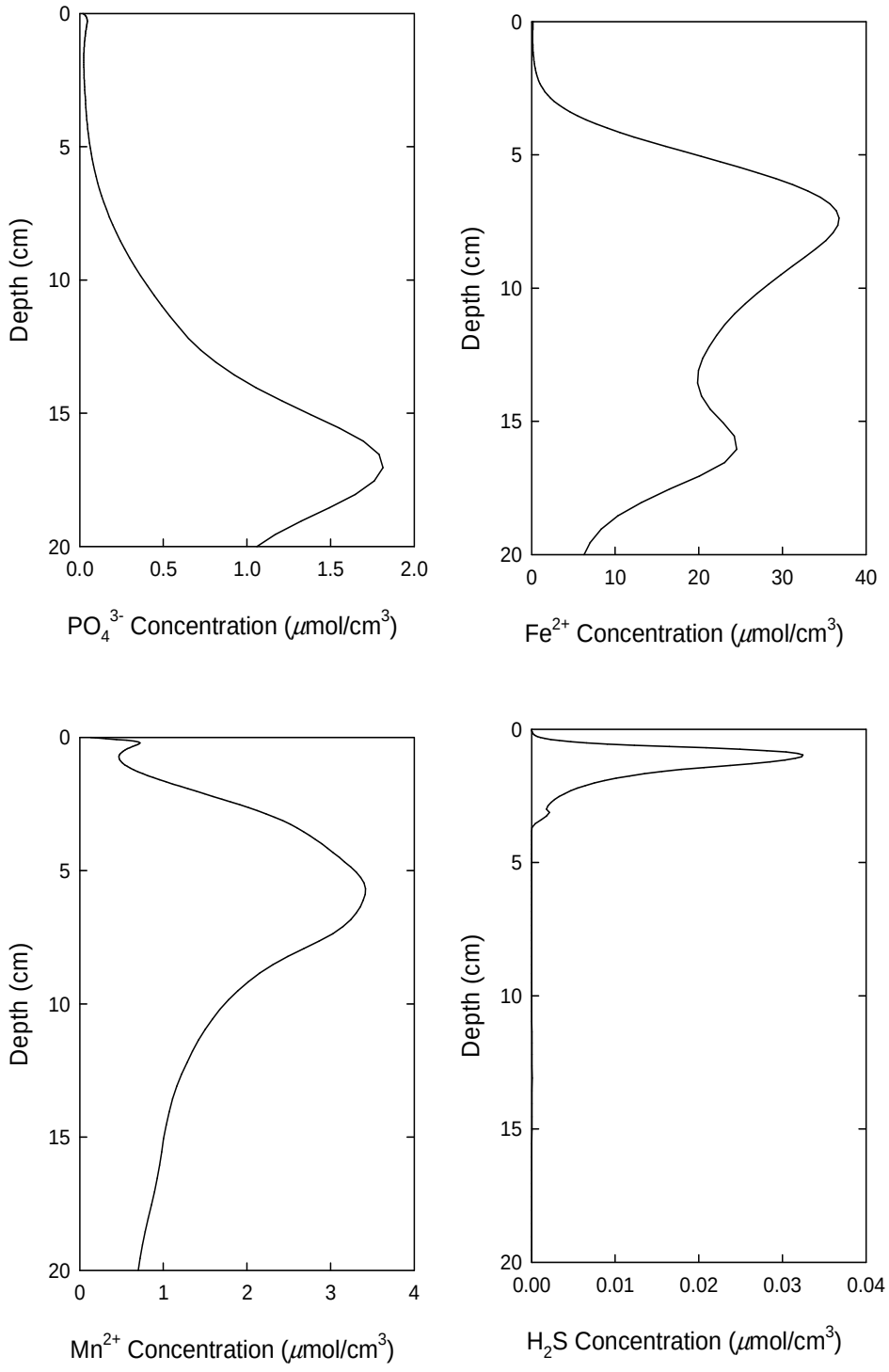

Figure 3.6 b Concentration profiles of Anacostia sediment model as the sulfate rate constant of 0.693

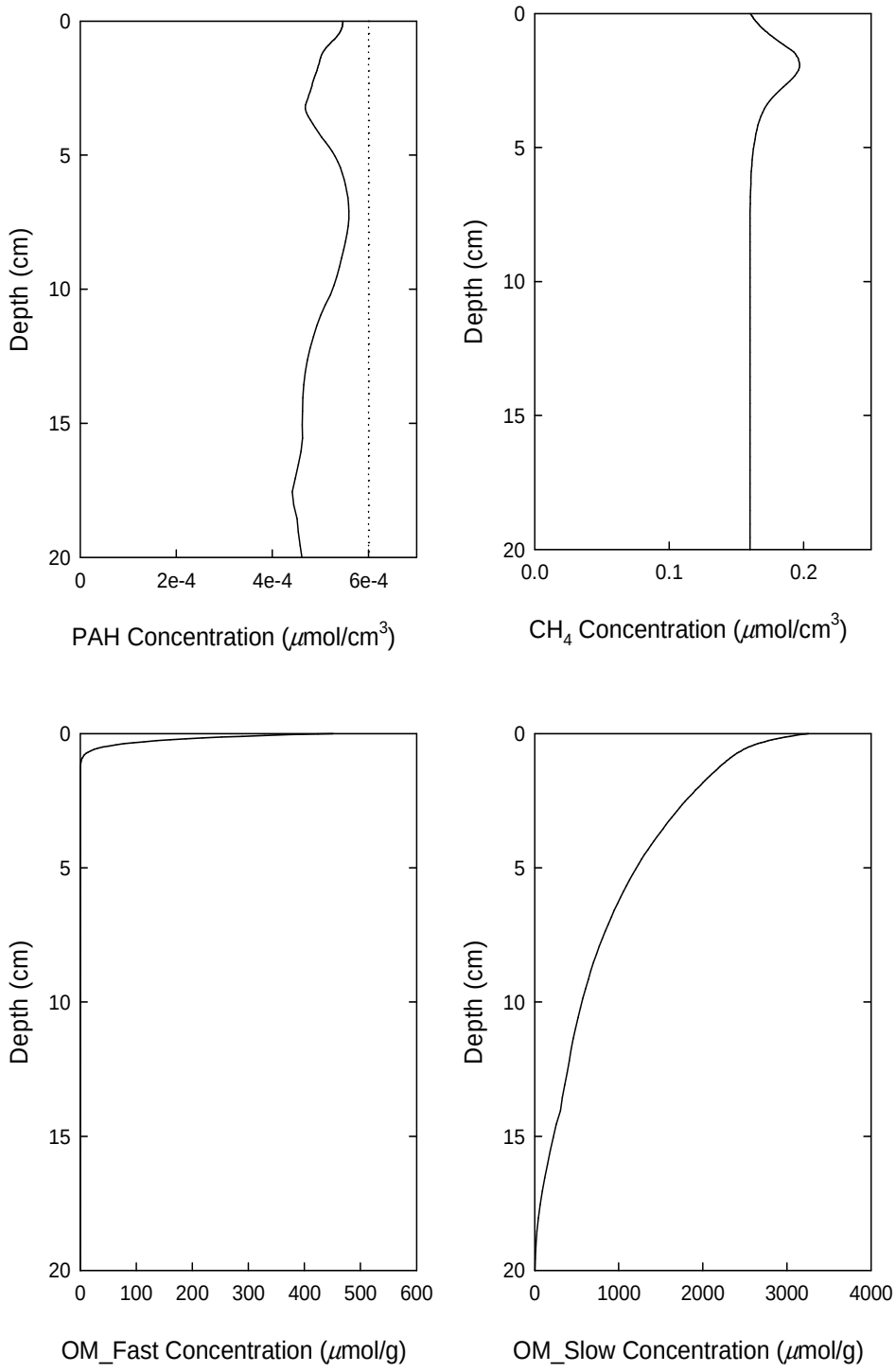

Figure 3.6 c Concentration profiles of Anacostia sediment model as the sulfate rate constant of 0.693

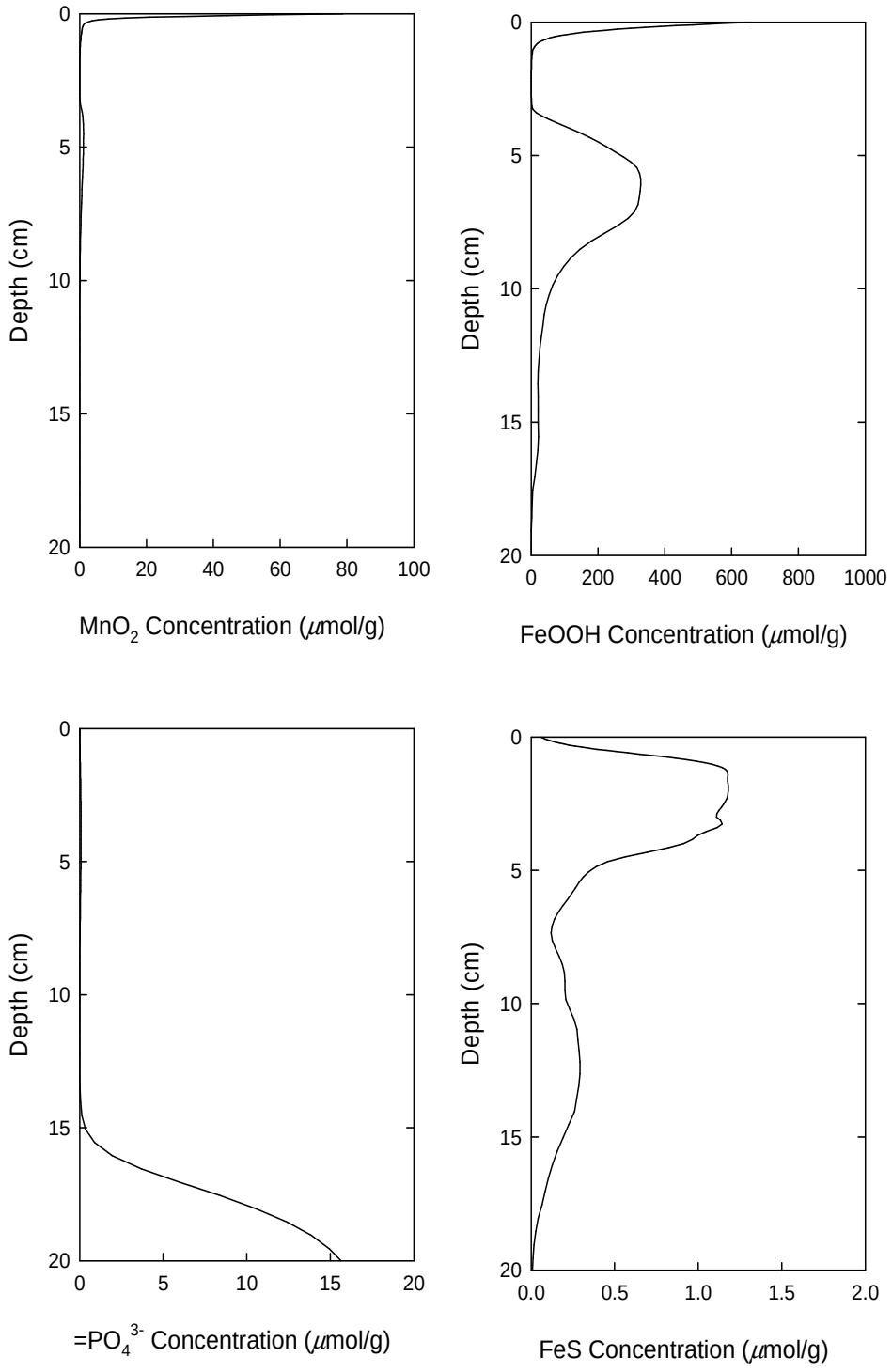

Figure 3.6 d Concentration profiles of Anacostia sediment model as the sulfate rate constant of 0.693

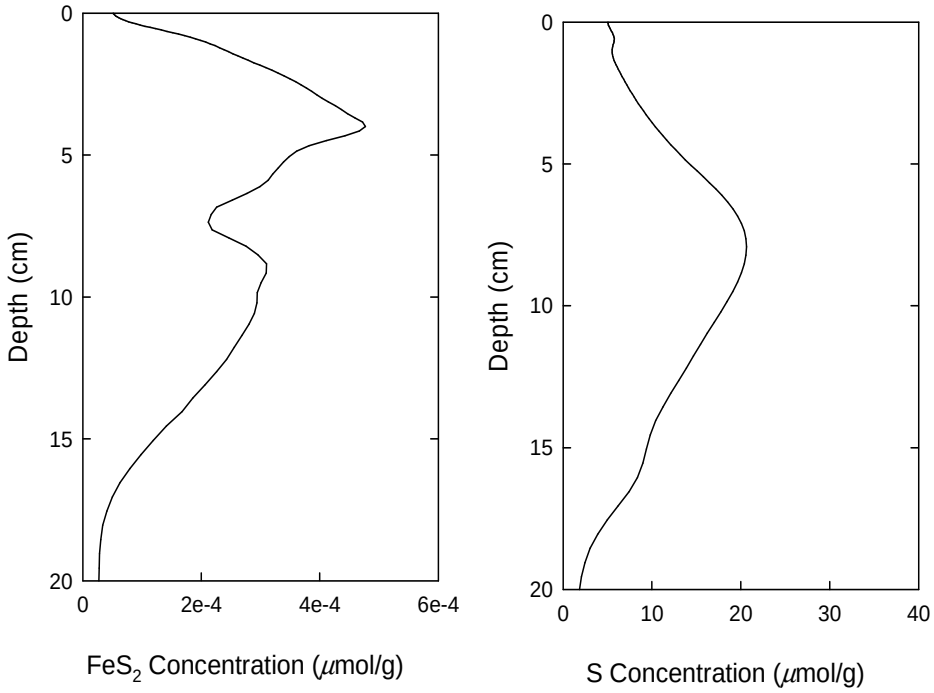

Figure 3.6 e Concentration profiles of Anacostia sediment model as the sulfate rate constant of 0.693

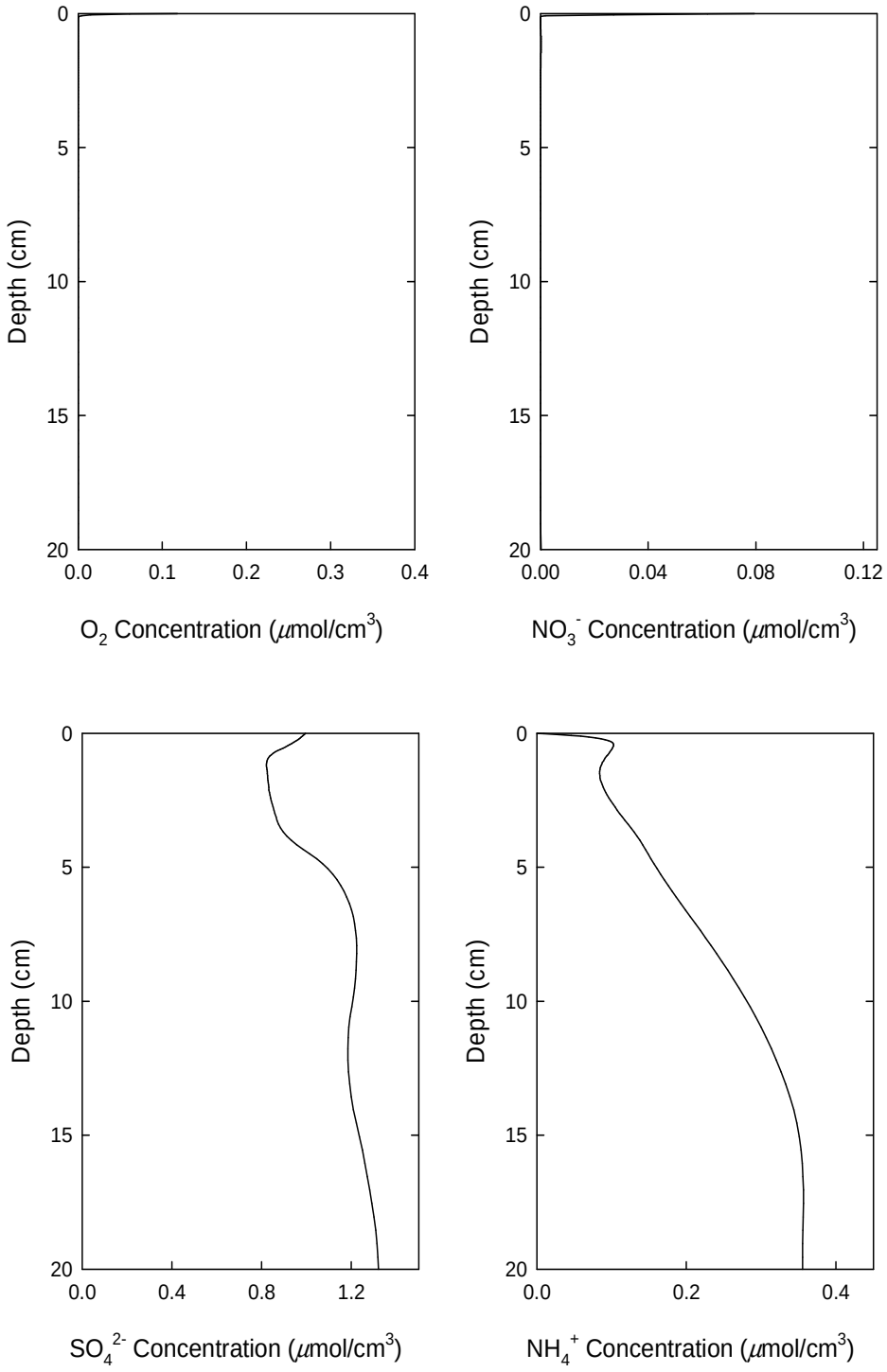

Figure 3.7 a Concentration profiles of Anacostia sediment model as the methane rate constant of 0.693

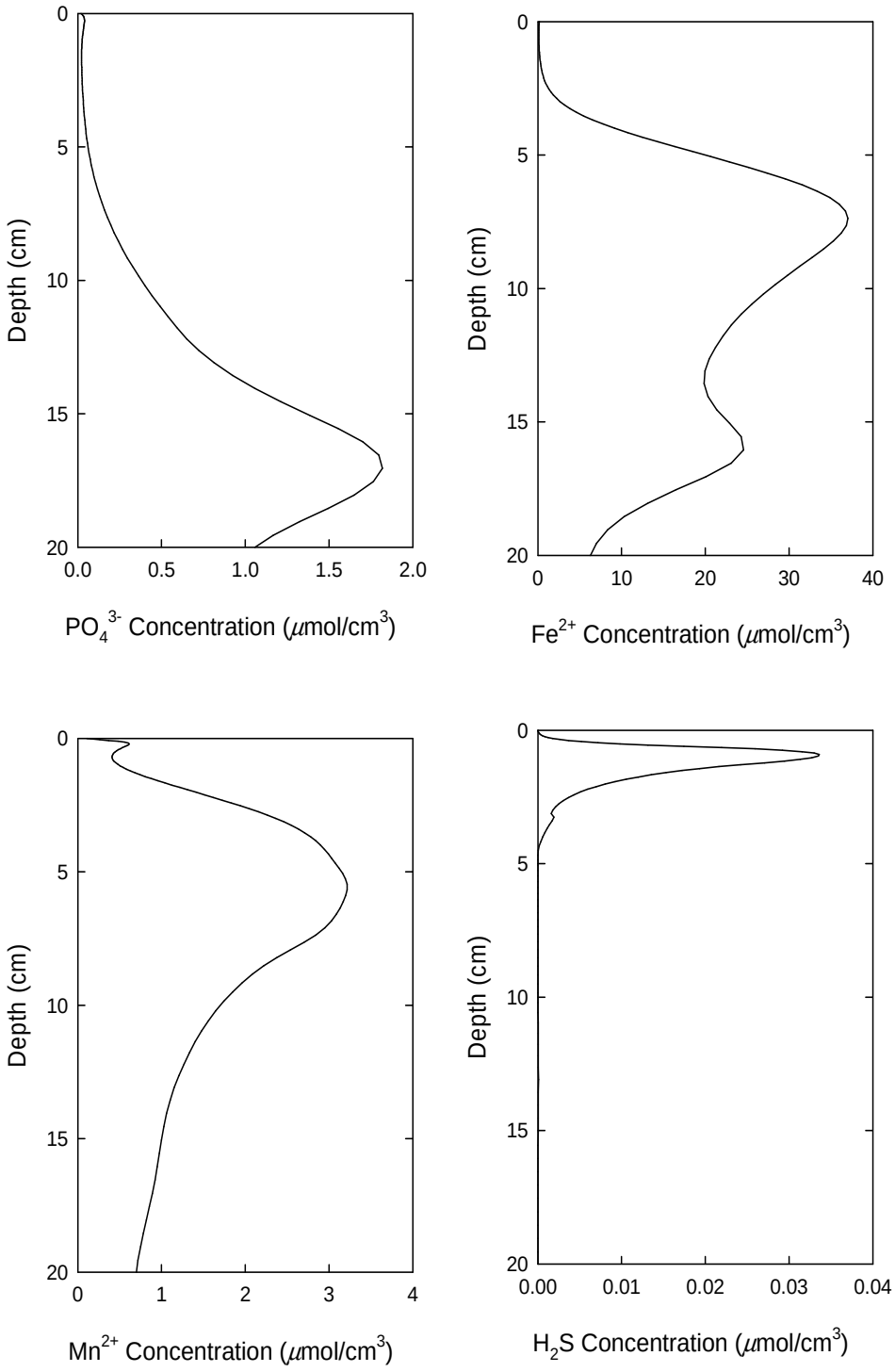

Figure 3.7 b Concentration profiles of Anacostia sediment model as the methane rate constant of 0.693

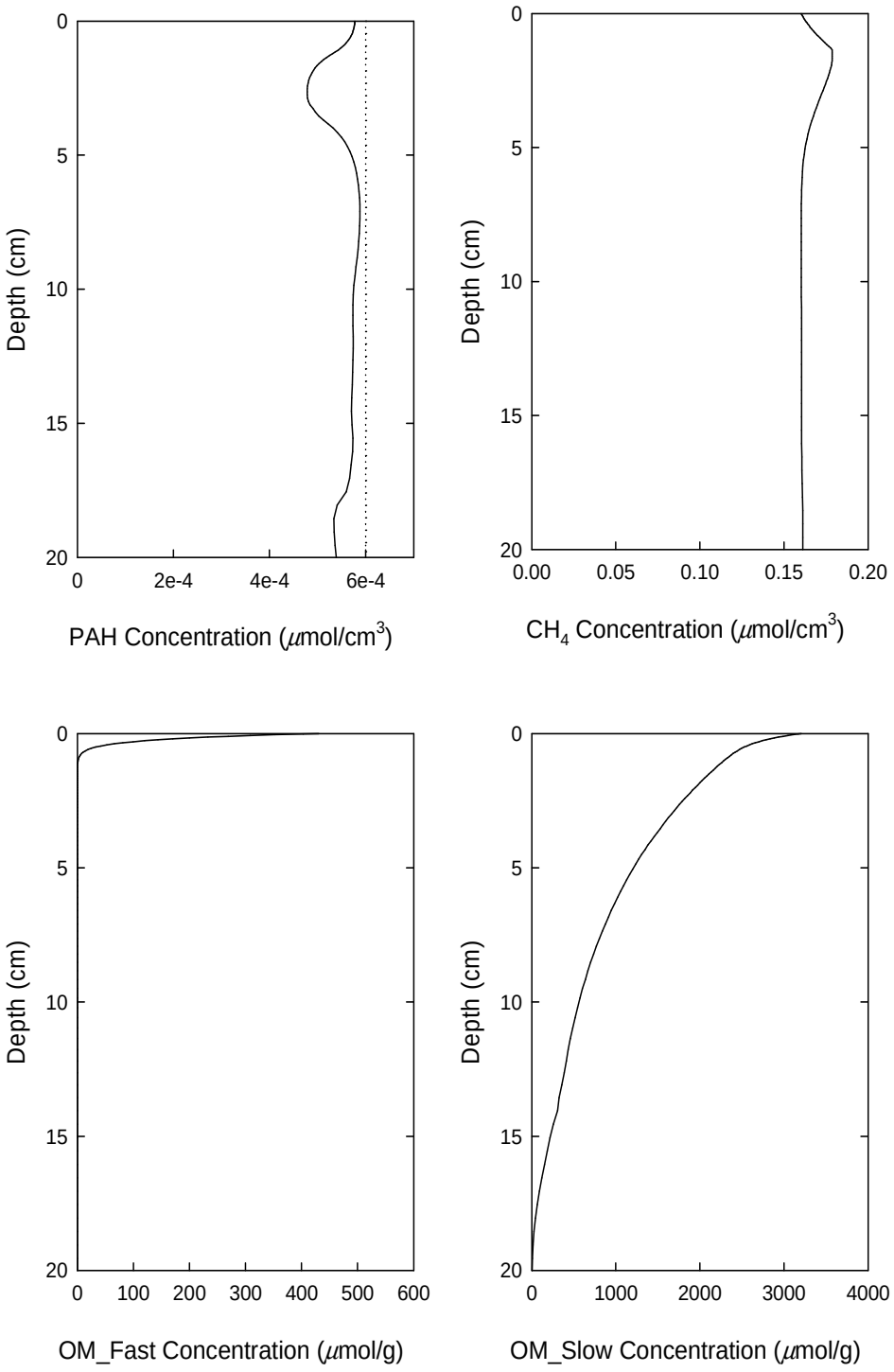

Figure 3.7 c Concentration profiles of Anacostia sediment model as the methane rate constant of 0.693

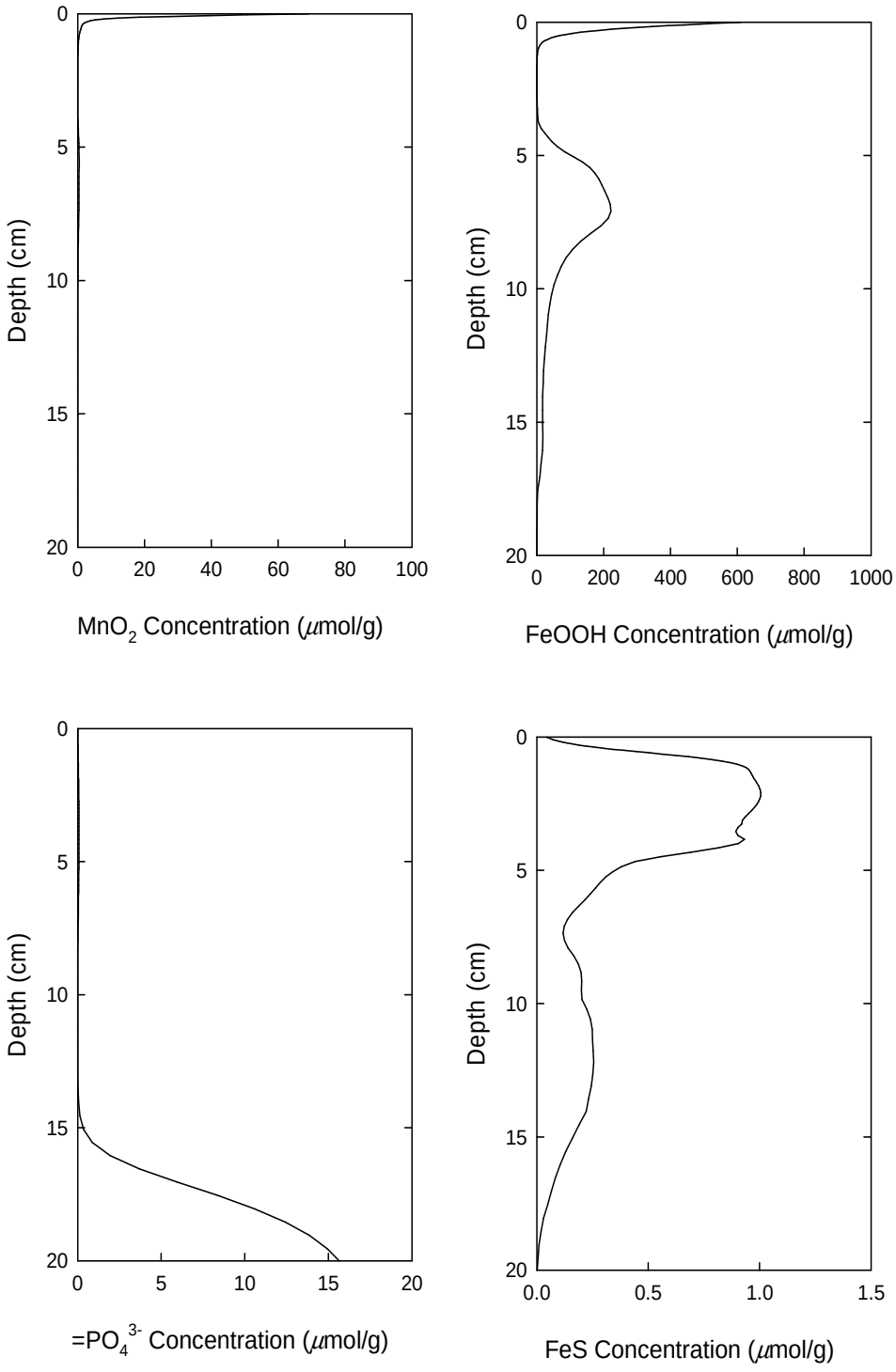

Figure 3.7 d Concentration profiles of Anacostia sediment model as the methane rate constant of 0.693

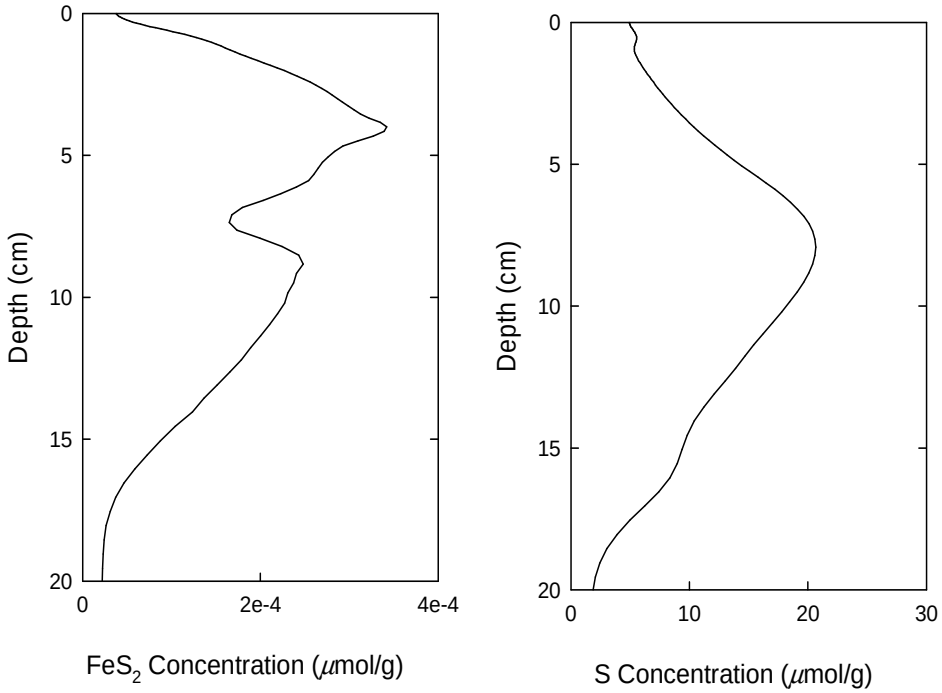

Figure 3.7 e Concentration profiles of Anacostia sediment model as the methane rate constant of 0.693

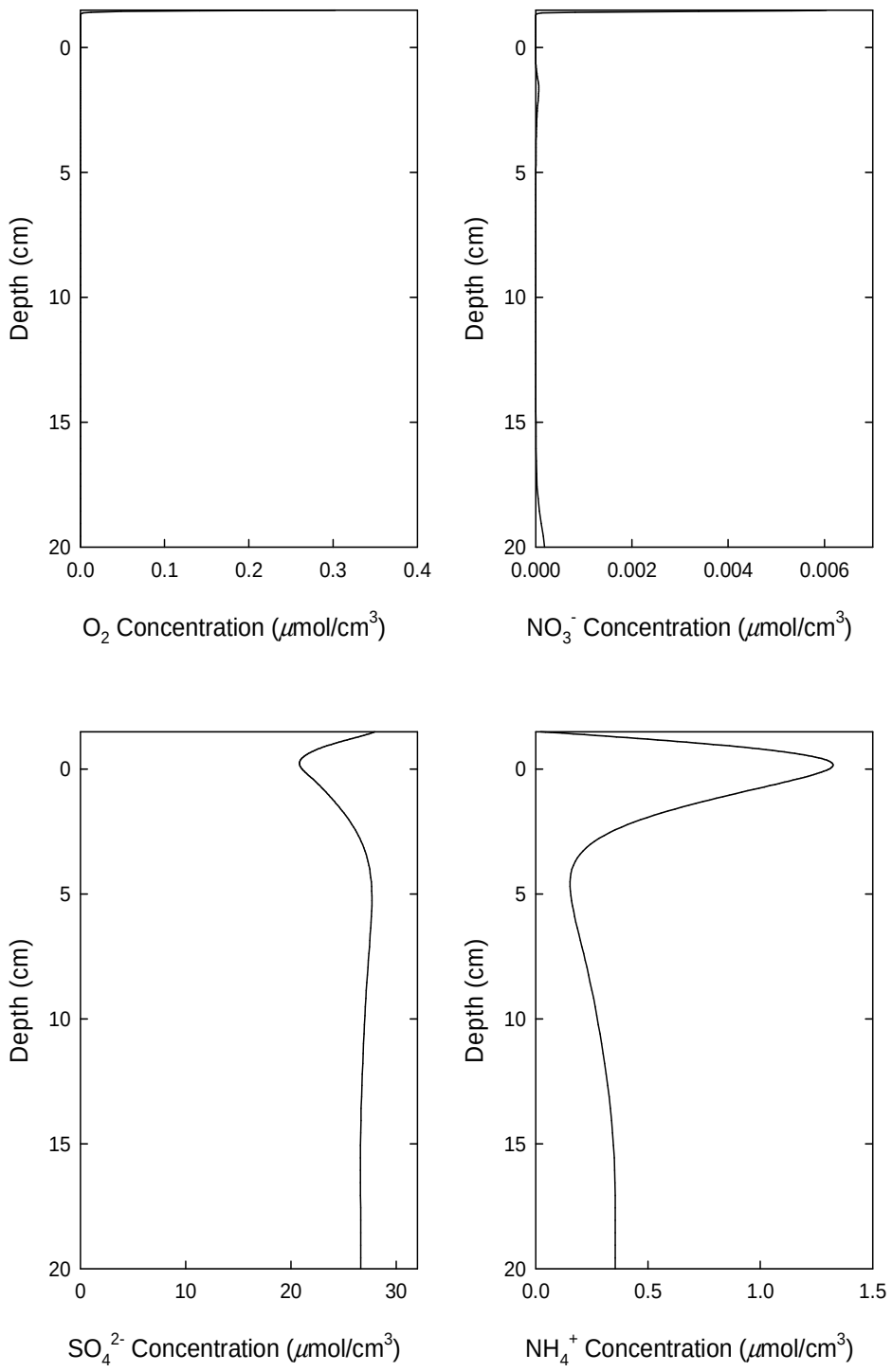

Figure 3.8 a Concentration profiles of capping model

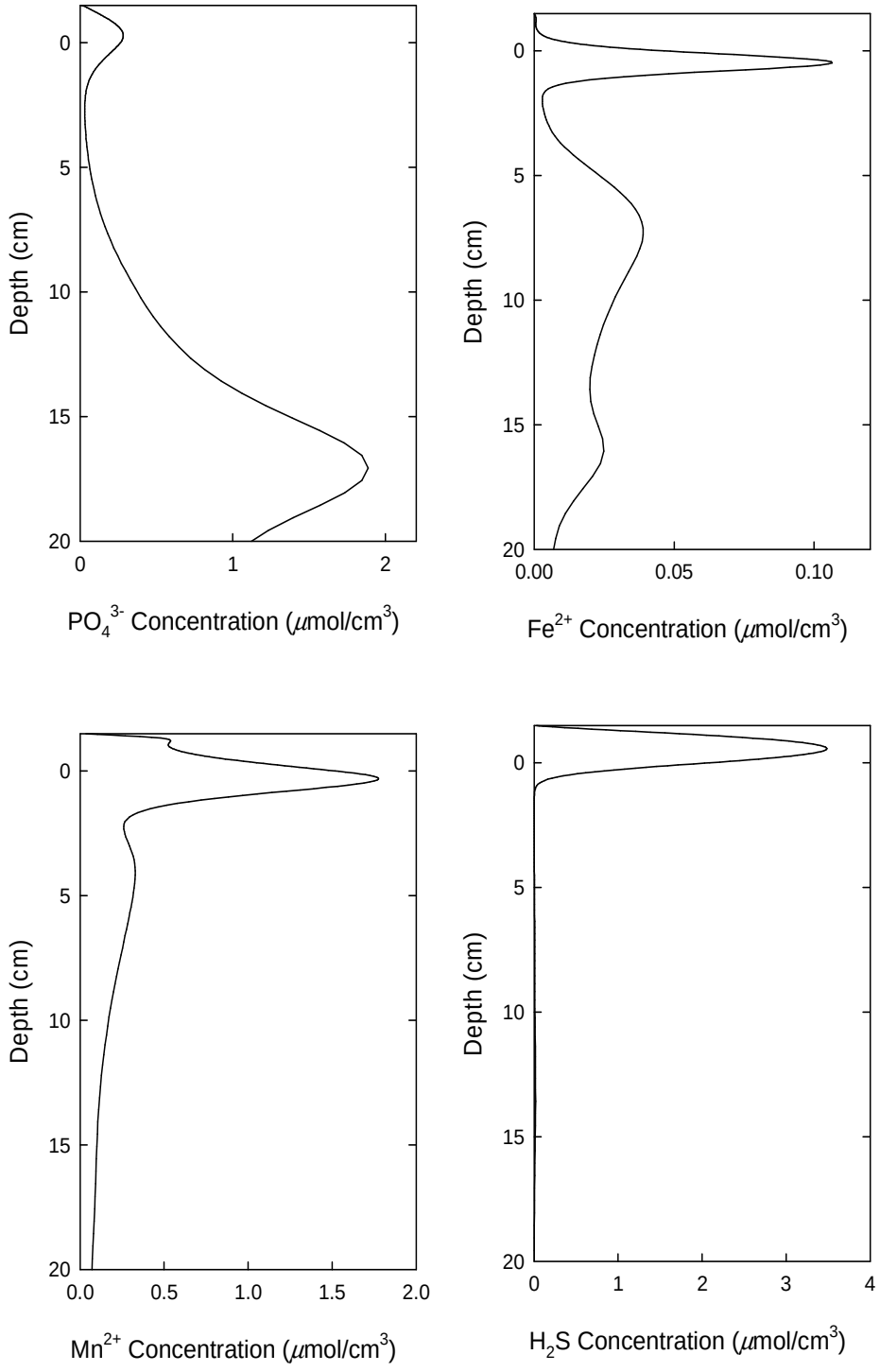

Figure 3.8 b Concentration profiles of capping model

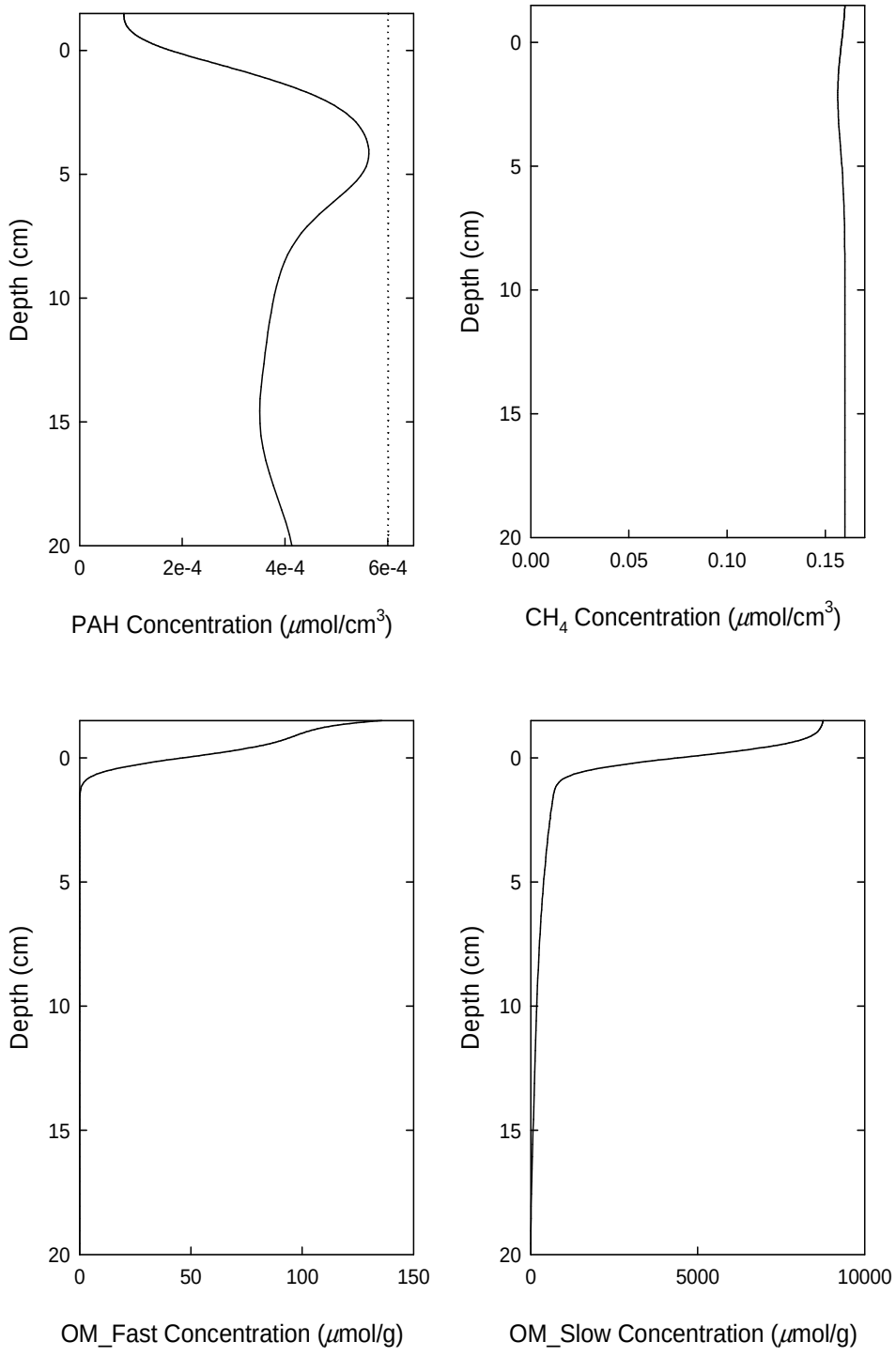

Figure 3.8 c Concentration profiles of capping model

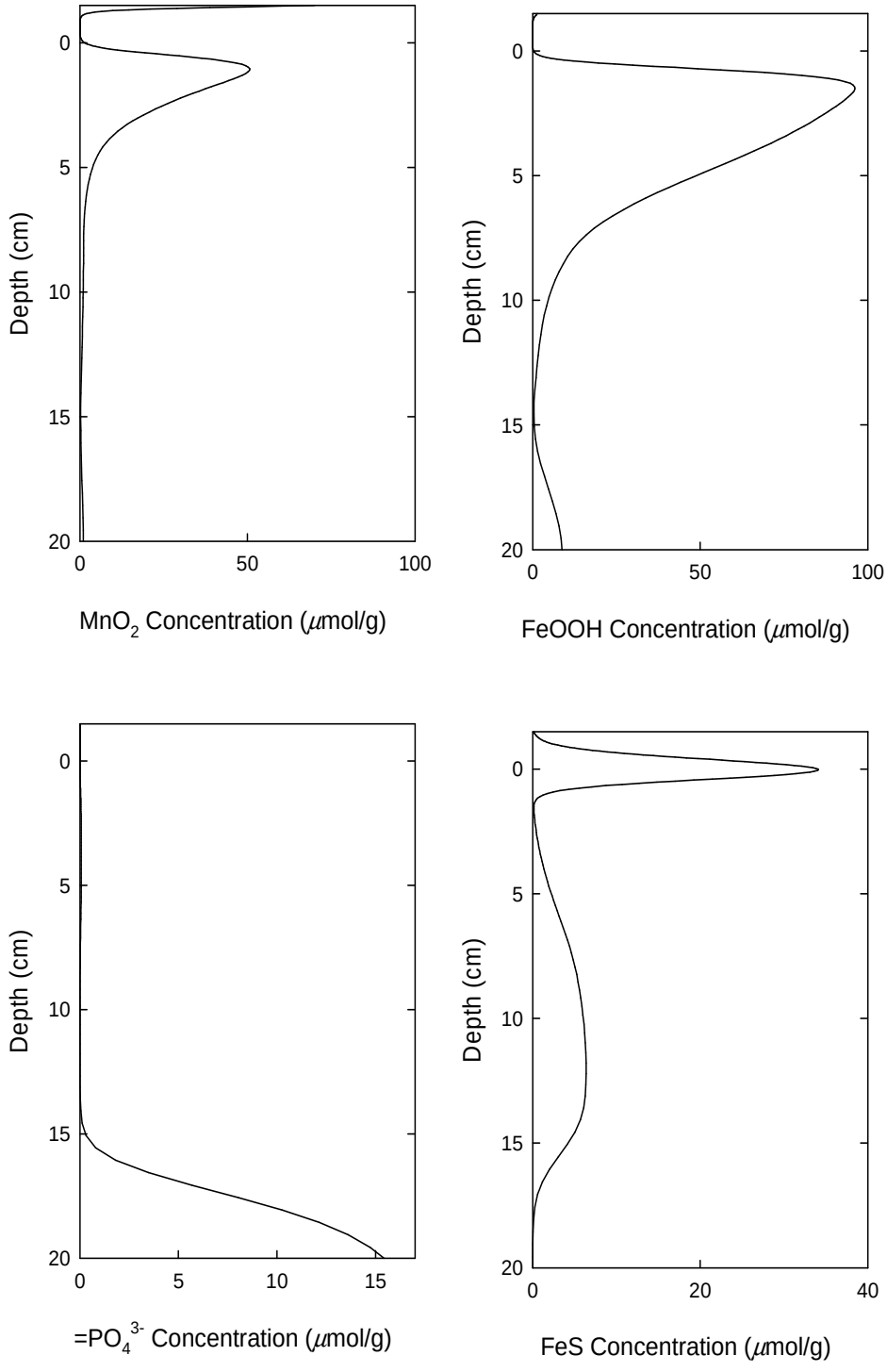

Figure 3.8 d Concentration profiles of capping model

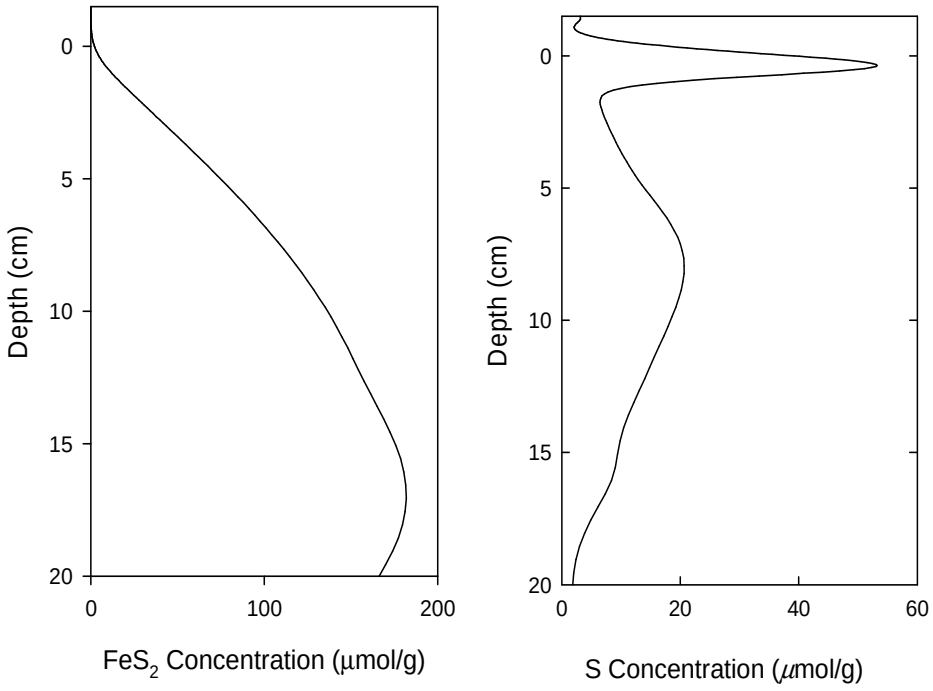

Figure 3.8 e Concentration profiles of capping model

Conclusions

The conclusions may be stated about the development of a numerical diagenetic sediment transport and reaction model. Three different systems were simulated; basic diagenetic model that calibrated using a data set from marine system in Denmark, Anacostia Rive sediment that calibrated for Anacostia conditions adding the PAH reaction into model, and sediment with a cap that simulated with the initial conditions of the marine system plus a cap.

The concentration profiles of basic diagenetic model matched with the realistical data profile by Fossing (2004). Based on developed the diagenetic model, the location of the PAH reactions was identified in the Anacostia River sediment bed using the rate constant of 0.693. The location of PAH degradation was accord with that of sulfate, which reduced on top cemtimeters then slightly decreased below. For the capping simulation, PAHs declined at the surface due to the cap and then degraded in an area just below the cap and deeper below the iron reducing zone. We could not observe differences in the redox conditions from the capping simulation due to simulation time limits.

CHAPTER 4
THE EFFECT OF BIONSOIL ON PAH BIODEGRADATION

Introduction

Polycyclic aromatic hydrocarbons (PAHs) are used as an energy source for industrial production in our lives. However, these energy sources and chemical building blocks can cause serious ecological damage to natural environment and adverse health effects to humans. PAHs are common sediment contaminants and ubiquitously spread worldwide as a petroleum sources. Understanding the fate and transport of PAHs in sediments that are largely aerobic or anaerobic has drawn the interest of many researchers (Coates et al., 1996a; Coates et al., 1996b; Bedessem et al., 1997; Coates et al., 1997; Caldwell et al., 1998; Burland and Edwards et al., 1999; Hayes et al., 1999; Rothermich et al., 2002; Eriksson et al., 2003).

Biodegradation has received particular attention as a clean-up tool for organic compounds because it is not only destroying of contaminants but also transferring mass. Natural degradation processes lead to natural attenuation of pollution (Alexander, 1999). Anaerobic and facultative anaerobic microorganisms have the ability to utilize alternative electron acceptors (AEAs), such as nitrate (NO_3^-), manganic manganese (Mn^{4+}), ferric iron (Fe^{3+}), sulfate (SO_4^{2-}), and carbon dioxide (CO_2), as a substrate in the absence of oxygen (O_2). Microbial transformation of aromatic compounds under denitrifying, sulfate-reducing, and methanogenic conditions have been reported (Lovley and Phillips, 1987; Caldwell et al., 1998; Burland and Edwards et al., 1999). However, the discussion here is more important to anaerobic transformation of PAHs under sulfate reducing conditions and methanogenesis since these are the main terminal electrons accepting conditions, which is studied during the research work.

Researchers reported that sediment maintained the sufficient sulfate to decline the PAHs. In general, PAHs were degraded very slowly due to the number of benzene rings (high molecular

weight) but, PAHs were not decline at all when sulfate was depleted (Rothermich et al., 2002). Ramsay et al. (2003) showed that PAH mineralization can be linked to wide range of terminal electron acceptors (TEAs): oxygen, nitrate, Fe (Ⅲ) and sulfate reduction. PAH can be degraded when any of these TEAs were available.

Isolation of microorganisms in the biodegradation of PAHs has been interest issues in these days. Recently, isolated microbial species, *Cladosporium sp.*, was able to degrade PAHs and it could be a potential candidate for effective bioremediation of PAH contaminated sites (Potin et al., 2004). Moreover, sulfate-reducing bacteria are the first candidate for the aromatic degrader. They are strict or facultative anaerobes with capacity to reduce sulfate as the terminal electron acceptor in a respiratory mode of metabolism (Odom and Singleton, 1993). The sulfate-reducing bacteria were isolated from oil production and H_2 are potential electron donors for sulfate reduction also hydrocarbons in crude oil are used directly by sulfate-reducing bacteria (Howarth and Hobbie, 1982; Rosnes et al. 1991; Rueter *et al*., 1994).

Laboratory studies have demonstrated that BionSoil (Bion Environmental Technologies, Inc. Old Bethpage, NY) has the capability of PAH biodegradation as capping material in the Anascotia River sediment where heavily contaminated by PAHs, polychlorinated biphenyls (PCBs), and heavy metals. The observed mechanisms were microbial anaerobic degradation for PAH contaminated sediment. These studies suggested that capping using the BionSoil could be effective alternatives to remediation technologies in cleaning the petroleum hydrocarbon contaminated sediments. The study investigated the capability of BionSoil and sediment mixture for construction of reactive cap, capable of long-term attenuation of organic contaminant PAHs. The effectiveness of reactive cap using BionSoil was evaluated in this study. The objectives of the study were (1) to determine and compare degradation kinetics of PAH components with

capping material in laboratory microcosms, (2) to evaluate the related dominant redox status with anaerobic degradation by water analysis, and (3) to identify microorganism responsible for PAH degradation by molecular analysis.

Materials and Methods

Sediments

Sediments were obtained from the Anacostia River which flows from the Maryland suburbs of Washington, DC to its mouth at the Potomac River near downtown Washington. The Anacostia River is one of America's most endangered rivers, with sediments containing significant concentrations of heavy metals, polychlorinated biphenyls (PCBs), hydrocarbons, and chlordane. The sources of these contaminants are long-term military and industrial activity in the Anacostia and Potomac Rivers. Figure 4.1 shows the two study sites (Site 1 and Site 2) on the Anacostia adjacent to the Navy Yard. Sediment samples were collected from Site 2 contaminated with PAHs up to 210 ppm. Site 1, near the old combined sewer overflows on the south end of the Navy Yard has 6-12 ppm of polychlorinated biphenyls (PCBs), 30 ppm of PAHs, and significant level of several metals such as cadmium, chromium, copper, lead, mercury, and zinc.

BionSoil is essentially peat material and a trademark name for a type of processed mixture of animal manure. It facilitates sorption of contaminants and can provide a source of carbon for bacteria in waste treatment systems and BionSoil has high organic matter and nutrient content (www.biontech.com). BionSoil encourages degradation of organic contaminants through enhancement of reductive dechlorination and anaerobic degradation of polyaromatic hydrocarbon (PAH) compounds. The geotechnical characteristics of BionSoil are follows: saturated density 34.6 (pcf), TOC of 57.1 (%), pH of 7.4, and saturated moisture content of 125.4 (%) (Kassenga et al., 2000).

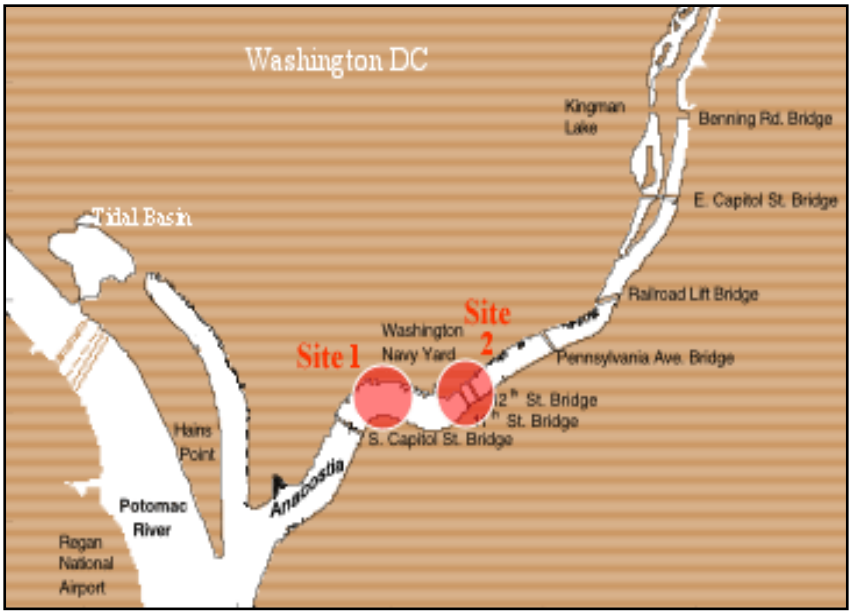

Figure 4.1 Anacostia study sites (From http://www.hsrc-ssw.org/anacostia/)

Chemicals

The test chemicals selected for this study were five major PAH compounds, phenanthrene, fluoranthrene, pyrene, benzo(α)anthracene, and chrysene which present in Anacostia sediments. The properties of these chemicals are listed in Table 4.1.

Table 4.1 Properties of the test contaminants (PAHs) (Maagd et al., 1998)

Property	Phenanthrene	Fluoranthrene
Chemical formula	$C_{14}H_{10}$	$C_{16}H_{10}$
	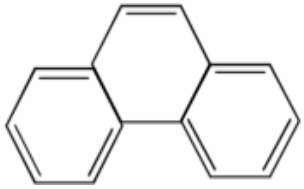	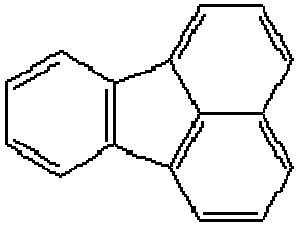
Molecular weight	178.2	202.3
Aqueous solubility (mg/L @ 25ºC)	1.20	0.20-0.26
Vapor pressure (m mHg @ 25ºC)	6.8×10^{-4}	5.9×10^{-6}
Log K_{ow}	4.45	4.90
Density (g/cm^3 @ 20ºC)	0.98	No data

(Table 4.1 cont'd)

Pyrene	Benzo(α)anthracene	Chrysene
$C_{16}H_{10}$	$C_{18}H_{12}$	$C_{18}H_{12}$
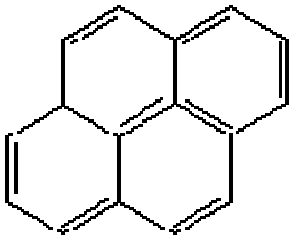	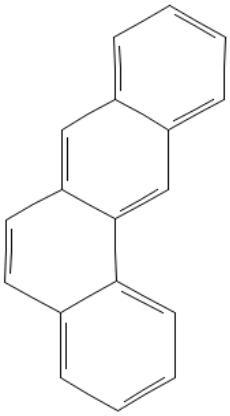	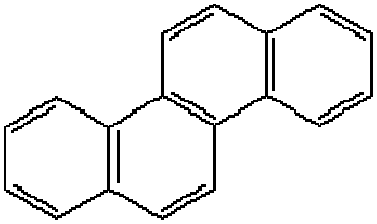
202.3	228.29	228.3
0.077	0.010	$2.8\ e^{-3}$
2.5×10^{-6}	2.2×10^{-8}	6.3×10^{-7}
4.88	5.61	5.16
1.271	1.274	No data

Microcosm Experiments

Anaerobic microcosms were constructed in a glove bag (Cole Parmer Instrument Company, Cheltenham, PA) under an oxygen-free nitrogen atmosphere. Microcosms were prepared using mixtures of Anacostia River sediment and BionSoil, which were then packed in 125 mL clear Wheaton serum bottles (Fisher Scientific, Pittsburgh, PA) with 20 mL head space. The serum bottles were made from borosilicate glass and meet requirements for Class A of the

United States Pharmacopeia for Type I glass. These bottles have a high chemical durability and can be sterilized repeatedly.

Anaerobic microcosms were prepared from the mixture of Anacostia River sediment and BionSoil with different ratios (0 %, 20 %, 40 %, and 60 % (w/w) of BionSoil). All bottles were sealed with Teflon-lined rubber septa and aluminum crimp seals. The sediments from Anacostia River with BionSoil were slurried (1:1.5, w/w %) with deionized water. Microcosms were incubated in an inverted position at 25ºC under static conditions in the dark. To account for abiotic losses, killed controls were prepared by autoclaving the sediment. Two identical sets of bottles were set up, one set of bottles for analysis of indicators of redox status (sulfate, hydrogen and methane) and another set for analysis of test chemicals. PAH concentrations were monitored at regular time intervals using analytical techniques described below.

Sediment Extraction

Ten mL of sediment slurry was subsampled from the serum bottles and transferred into 60 mL Teflon centrifuge tubes containing the same volume of hexane/acetone mixture (50/50, v/v %). Each centrifuge tube was shaken 24 hours to extract the PAH from the slurry then, each tube was centrifuged for 20 minutes at 3000 rpm in Avanti^{TM} J-20 XPI high-performance centrifuge (Beckman Coulter, Fullerton, CA). The liquid was separated into aqueous and nonaqueous phase using a separatory funnel. The nonaqueous phase was passed through sodium sulfate to remove the remaining water. The collected nonaqueous phase of each vial was concentrated to a volume of 1 mL by passing dry N_2 over the surface of the sample. One mL of this extract was transferred to gas chromatography/mass spectrometry (GC/MS) autosampler vials and refrigerated until GC/MS analysis.

Chemical Analysis

The extracts were analyzed using a Hewlett Packard 5890A gas chromatograph (GC) coupled with a HP 5971 mass selective (MS) detector. The GC was equipped with a 30 m × 250 μm × 0.25 μm film thickness capillary column. One μL of the sample was injected automatically onto the column. GC temperature program conditions were 55°C, ramped at 10°C/min to 200°C, then at 4°C/min to 300°C and held for 10 minutes. The mass spectrometer was operated in the selected ion monitoring mode and the ion source temperature was 280°C. PAH components were quantified by using a semivolatile internal standard mixture (Supelco, Bellefonte, PA).

Kinetic Data Analysis

Rate constants for the degradation of PAH compounds were determined using non-linear regression of a first-order exponential decay equation. The degradation rate constant (*k*) was calculated using the following equation:

$$C/C_0 = e^{-kt}$$

where *C* is the substrate concentration t any time t, (mg/Kg dry soil), C_0 is the initial concentration (mg/Kg dry soil), *k* is the pseudo first-order degradation rate constant, (day^{-1}), and *t* is the time, (days). Kinetic data were modeled using SigmaPlot 9.0. A two sample t-test was used to compare the differences in rate constants from different treatments using a significant level of 0.05.

Sulfate and Gas Measurements

A Hach DR 2010 spectrophotometer (Hach Co., Loveland, CO) was used to determine the sulfate concentration. Water from each microcosm was diluted with deoxygenated water to 25 mL to analyze concentration using the spectrophotometer. The Hach DR 2010 is capable of

analyzing for sulfate concentrations within a range of 0 to 70 mg/L SO_4^{2-}. Sulfate concentrations were read directly by adding the Hach, SulfaVer 4 Sulfate Reagent "powder pillow" and inserting the samples into the spectrophotometer. Sulfate ions in the sample react with barium in the SulfaVer 4 Sulfate Reagent "powder pillow", forming insoluble barium sulfate turbidity. A standard calibration was performed for each lot of SulfaVer 4 Reagent Powder Pillows. Standards of 0, 10, 20, 30, 40, 50, and 60 mg/L sulfate were prepared by diluting 0, 0.1, 0.2, 0.3, 0.4, 0.5 and 0.6 mL of the contents of a Sulfate Voluette Ampule standard.

Hydrogen was analyzed using a gas chromatograph/reduction gas detector (GC/RGD) (Trace Analytical, Menlo Park, CA). Headspace samples were injected into 1 mL gas sampling loop and were separated with a molecular sieve analytical column at an oven temperature of 40˚C. Ultrahigh purity nitrogen (BOC Gases, Baton Rouge, LA) was used as a carrier gas after it was passed through a catalytical combustion converter to removes traces of H_2. Aqueous H_2 concentrations were calculated as Löffler et al. (1999).

$$H_2\,(dissolved) = LP/RT$$

where $H_2\,(dissolved)$ is the aqueous concentration of H_2 (in moles/L), L is the Oswald coefficient for H_2 solubility (0.01913 @ 25ºC), R is the universal gas constant (0.0821 L · atm · K^{-1} · mol^{-1}), P is the atmospheric pressure, and T is temperature in Kelvin.

Methane was measured using a gas chromatograph/flame ionization detector (GC/FID). One mL of gas was collected from the headspace of the bottle using a gas tight syringe and injected into GC/FID (HP 5890 series II) equipped with a 2.4 m × 0.32 mm i.d. column packed with Carbopack b/l % SP-1000 (Supelco, Bellefonte, PA). The injector and detector temperatures were 375ºC and 325ºC, respectively. The column temperature was held constant 50ºC for 6.50

min. Ultrahigh purity nitrogen (Grade 5.0, BOC Gases, Baton Rouge, LA) was used as a carrier gas. Headspace methane concentrations were converted to aqueous phase concentrations by Henry's Law constant of 0.6364 atm/mol/m^3 for methane.

Microbial Analysis

Microbial populations were characterized using denaturating gradient gel electrophoresis (DGGE) and real time polymerase chain reaction (RT-PCR). The protocol of Mo Bio Ultraclean Soil DNA Isolation Kit (Mo Bio Laboratories, Inc., Carlsbad, CA) was followed to extract DNA from 0.25 g of wet sediment slurry samples collected from the microcosm bottles. Sediment samples were washed twice with 0.12 M of sodium phosphate buffer to remove extracellular DNA (Lee et al., 1996). Extracted DNA was amplified using PCR using a 20 μL reaction volume. Each reaction contained DNA Polymerase (1 U), 1x Taq Buffer, 3 mM of $MgCl_2$, 1 μM of each primer, 0.2 mM of each deoxynucleoside triphosphate (dNTP) (Promega Corporation, Madison, WI) and 1 μL of extracted DNA. PCR conditions were reported by Hendrickson et al. (2002) for the bacteria group: initial denaturation at 95ºC for 2 min, followed by 30 cycles consisting of denaturation at 94ºC for 1 min, annealing at 55ºC for 1 min, and extension at 72ºC for 1 min. For the archaea group (i.e., methanogens), PCR conditions were : denaturation at 94ºC for 2 min, followed by 30 cycles consisting of denaturation at 94ºC for 30 s, annealing at 60ºC for 45 s, and extension at 72ºC for 2 min (Löffler et al., 1997). PCR amplication was performed using a RT-PCR Detection System iCycler iQ (Bio-Rad Laboratories, Inc., Hercules, CA). The PCR products were purified with MoBio PCR Clean-Up Kit (Mo Bio Laboratories, Inc., Carlsbad, CA). The molecular weight of products was determined by electrophoresing portions of extracts on 1.0 % agarose gels with a 1-kb ladder ((Promega Corporation, Madison, WI) as a size marker. The bacterial 16S rDNA real-time PCR assay was log-linear over 5 orders of magnitude with

DNA standards. The numbers of bacteria and methanogen cells per gram soil was calculated from copies per gram soil. The gene copy number per cell was used 3.6 for bacterial 16S rDNA (Harms et al., 2003). The oligonucleotide primers are listed in Table 4.2. All these primers were obtained from AlphaDNA (Montreal, Quebec, Canada).

DGGE was performed using a D-Code™ Universal Mutation Detection System (Boi-Rad, Hercules, CA). The denaturing gradient gel (6 %, wt/v, acrylamide solution) was used for a particular size ranging between 300 and 1000 base pairs. The acrylamide gels were made with a gradient ranging from 40 % to 70 %, where 100 % denaturant contained 42 % (wt/v) urea and 40 % (v/v) formamide. Polymerization was catalyzed by adding 0.057 % of TEMED (v/v) and 0.85 % of the 10 % ammonium persulfate (v/v) to both denaturant solutions. Gels were cast using a Bio-Rad Model 475 gradient delivery system. Electrophoresis was performed in 1x TAE buffer at 60˚C for 16 hours with an applied current of 0.15 A at 65 V. After electrophoresis, the gel was stained with ethidium bromide (EtBr) for 10 min. then, destained in distilled water for 10 min. The gel was imaged with a UV transilluminator using the Chemidoc XRS system using Quantity One® 1-D Analysis Software (Bio-Rad, Hercules, CA).

DNA was also amplified using PCR with non GC primers, 341F and 907R, for cloning. After check the DNA with gel electrophoresis, a ligation reaction was performed using the pGEμ-T-vector then, transformation was accomplished with *E.coli* competent cells (Promega Coporation, Madison, WI) through manufacturer protocol provided by the manufacturer. LB plates with ampicillin/IPTG/X-Gal and liquid LB media with ampicillin were prepared to plate *E.coli* competent cells. The growing white colonies were selected, and transferred into liquid LB medium with ampicillin, and incubated overnight at 37˚C. The plasmid with inserts was extracted from liquid LB medium using the plasmid preparation kit (Mo Bio Laboratories, Inc.,

Carlsbad, CA). To verify the clone plasmid products, restriction enzyme reactions were conducted and checked with gel electrophoresis. DNA products were purified using the MoBio PCR Clean-Up Kit. Finally, samples were sent to BioMMED (Biotechnology and Molecular Medicine) in the School of Veterinary Medicine (Louisiana State University) for sequencing.

Table 4.2 Oligonucleotide primers used in this study

Primer	Sequence (5´ - 3´)	References
	Universal Primers for 16s rDNA	Lane (1991)
27f	5'-AGAGTTTGATCCTGGCTCAG-3'	
1492r	5'-GGTTACCTTGTTACGACTT-3'	
	Archaea Primers for RT- PCR	Löffler et al. (1997)
340f	5´-GTGCTCCCCCGCCAATTCCT-3´	
915r	5´-CCTACGGGGCGCASCAGGSGC-3´	
	Universal Primers for DGGE (GC clamp)	Schafer and Muyzer
341f	5´-GCCCGCCGCGCCCCGCGCCCGTCCCGCC	(2001)
	GCCCCCGCCCGCCTACGGGAGGCAGCAG-3´	
907r	5´-CCGTCAATTCMTTTRAGTTT-3´	
	Universal Primers for clone (non GC)	Schafer and Muyzer
341f	5´-CCTACGGGAGGCAGCAG-3´	(2001)
907r	5´-CCGTCAATTCMTTTRAGTTT-3´	
	Primers for Sulfate Reducing Bacteria	Daly et al. (2000)
DSV 230	GRG YCY GCG TYY CAT TAG C	
DSV 838	SYC CGR CAY CTA GYR TYC ATC	

Results and Discussion

PAH Biodegradation

The biodegradation of phenanthrene, fluoranthrene, pyrene, benzo(α)anthracene, and chrysene were monitored with mixtures of BionSoil and Anascotia River sediment. PAH components are degraded slowly and the rate constant values varied ranged from 0.0021 day^{-1} to 0.0066 day^{-1} between different treatments after 200 days. The rate constants for the individual PAH compounds and removal efficiency for 200 days are given in Table 4.3. Eighty three percentage of benzo(α)anthracene was removed in 60 % BionSoil microcosms with 0.0066 day^{-1} of decay rate constants. Faster degradation observed in phenanthren and benzo(α)anthracene with 60 % BionSoil treatment but, there are not much different with BionSoil treatment in fluoranthrene, pyrene, and crysene. PAH component degradation trends over 200 days are shown in Figure 4.2 to 4.6.

Table 4.3 First-order rate constants (day^{-1}) and removal efficiency (%) of PAHs

PAHs / Treatments	Control	20 % Bion	40 % Bion	60 % Bion
Phenanthrene	0.0026	0.0024	0.0038	0.0037
	51.5	53.9	67.4	73.6
Fluoranthrene	0.0021	0.0026	0.0021	0.0024
	11.3	24.6	45.4	60.4
Pyrene	0.0026	0.0030	0.0030	0.0030
	16.4	42.1	57.2	62.7
Benzo(α)anthracene	0.0051	0.0049	0.0051	0.0066
	71.4	78.8	81.4	82.9
Chrysene	0.0048	0.0026	0.0046	0.0040
	53.1	56.8	68.2	75.0

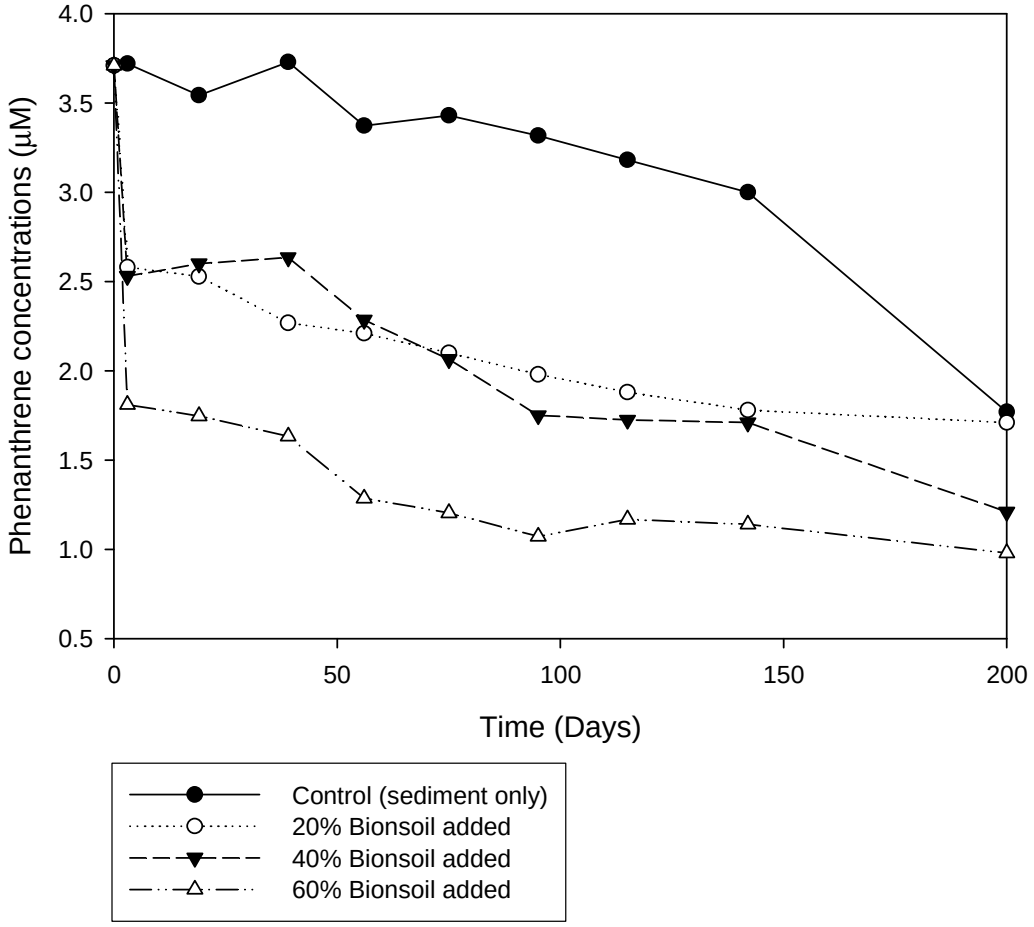

Figure 4.2 Phenanthrene removal in Anacostia sediment microcosm

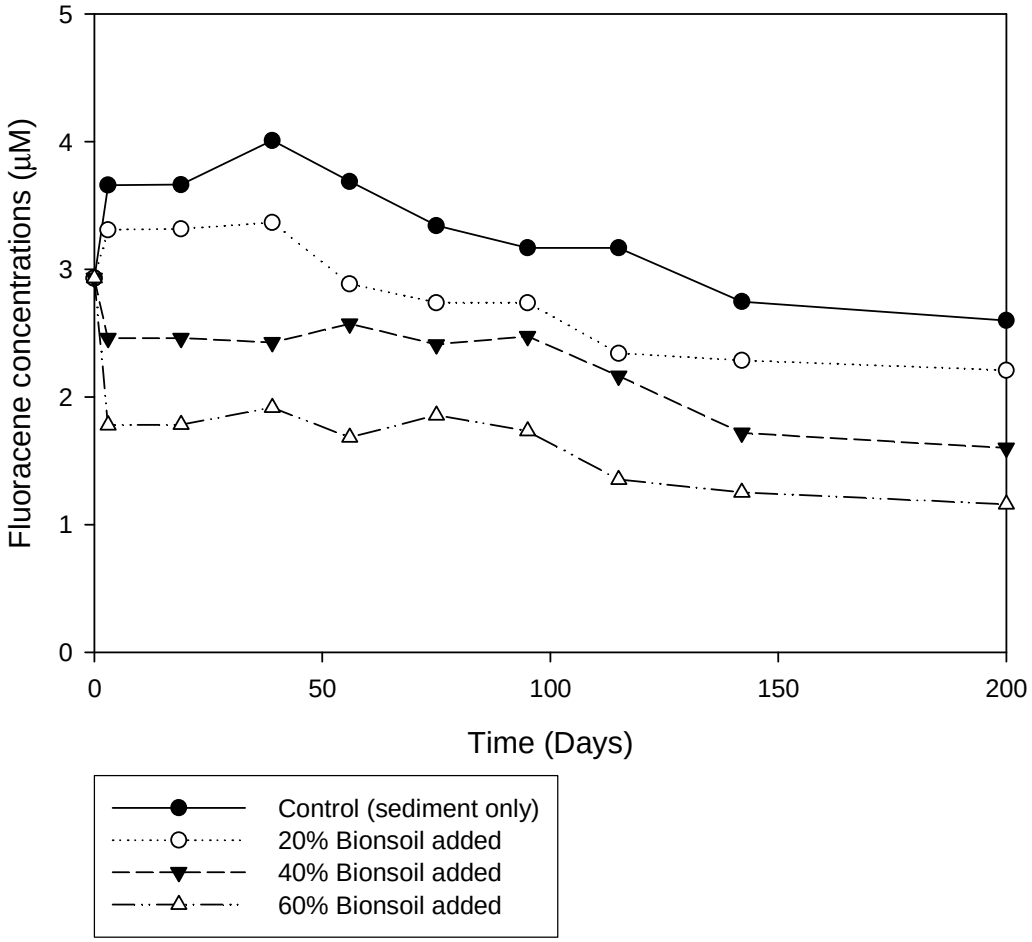

Figure 4.3 Fluoracene removal in Anacostia sediment microcosm

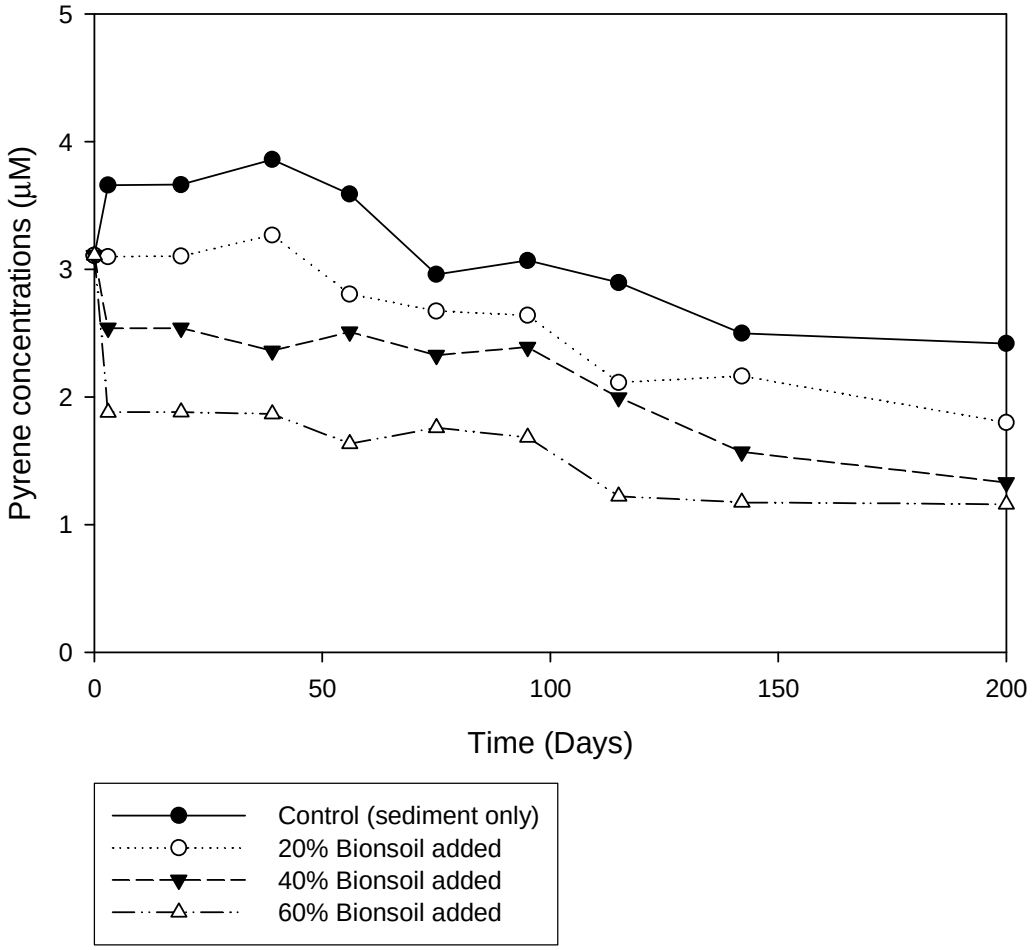

Figure 4.4 Pyrene removal in Anacostia sediment microcosm

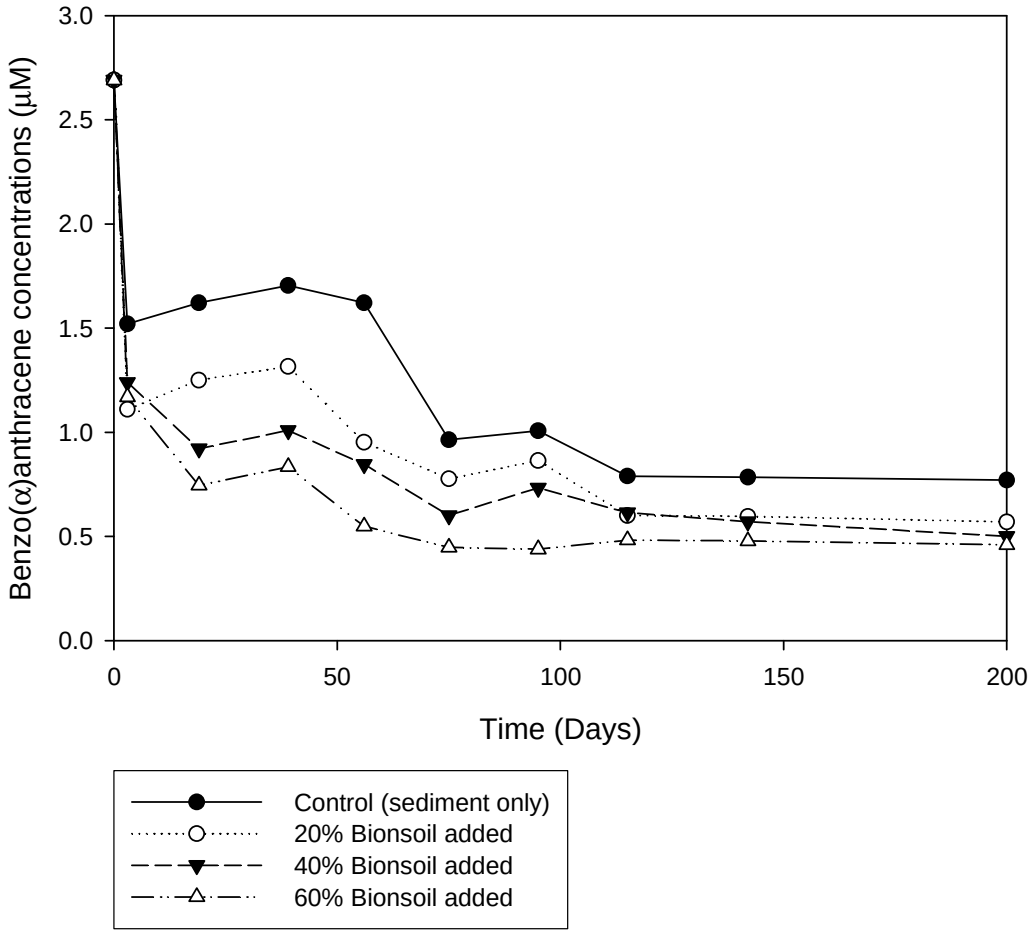

Figure 4.5 Benzo(α)anthracene removal in Anacostia sediment microcosm

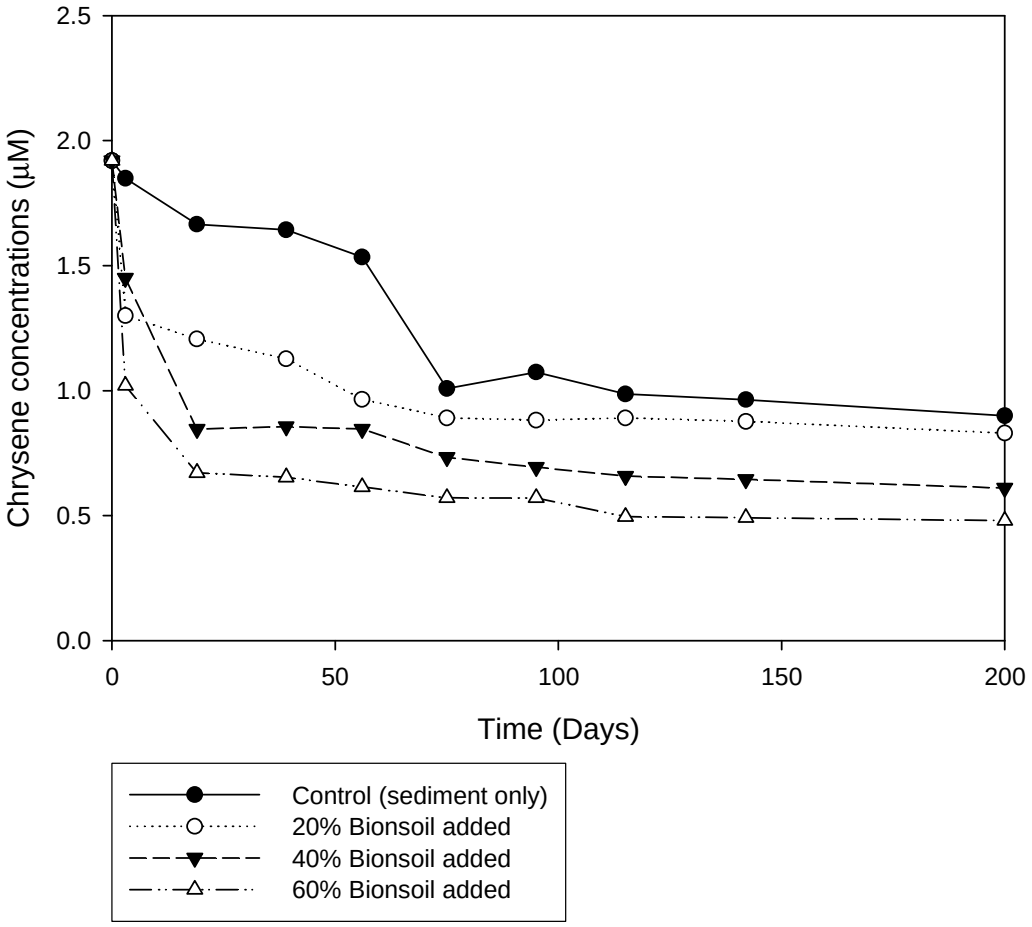

Figure 4.6 Chrysene removal in Anacostia sediment microcosm

Degradation curves were fit by the first order kinetics using non-linear regression. The degradation rates of different PAH components were reported by many researchers as first order rate constants. Augenfeld et al. (1982) observed the PAH loss rate, 0.0069 (day^{-1}) using ^{14}C-labelled phenanthrene. The loss rates of total aromatics were measured over 2 years in Prudhoe Bay crude oil and apparent rate constant was 0.0012 (day^{-1}) (Haines and Atlas, 1982). The value is very similar to this study for PAH component degradation. Appropriate kinetics and rate constants are very critical for accurate predictions and rebuilding of the concentration of contaminant over time after oil spill (Hinga, 2003).

Slow degradation of PAHs was examined for a long time throughout the study. Haines and Atlas (1982) also monitored the decrease of PAHs for 2 years and reported slow degradation with rate constant of 0.0012 (day^{-1}). Rothermich et al. (2002) observed the loss of PAH around 1 year to better evaluate anaerobic biodegradation. Some component of PAH levels, anthracene and fluorine, declined up to 67 % while pyrene and chrysene decreased 13-25 %. Recent researchers examined long term trends in atmospheric PAH concentrations (Prevedouros, 2004). They reported that many PAH concentrations were shown downward trend at some sites, but not all compounds and sites.

Hinga (2003) described that the degradation rate of PAH is correlated with sediment total organic carbon (TOC). He calculated the first order degradation rate constants and compared the correlation of degradation rate with sediment TOC in several stations. Table 4.4 presented the TOC and pH values between different treatments for this study. Higher fraction of BionSoil microcosms shows the greater TOC values.

Table 4.4 Sediment TOC and pH values from Anacostia microcosms

Treatments / TOC & pH	TOC (ppm)	pH
Control	49.31 ± 9.44	7.22
20 % BionSoil	61.63 ± 15.71	7.2
40 % BionSoil	196.27 ± 6.8	7.02
60 % BionSoil	246.5 ± 4.9	8.11

The degradation rate constants of PAHs are not significant between different fractions of BionSoil microcosms in the study because the BionSoil rapidly exhausted the sulfate in the microcosms at 100 days. Degradations of phenanthrene, benzo(α)anthracene, and chrysene in control microcosm are greater than 20 % or 40 % BionSoil treatment microcosms. Bionsoil had a lot organic carbons and consumed in competing with sulfate. Even though BionSoil consumed phenanthrene from 1.8 μm to 1.0 μm in 60 % BionSoil treatment, sorption is greater than degradation. By mixing the BionSoil with Anascotia River sediment, PAH concentrations are immediately diluting the PAHs with clean bion soil. PAH contaminated sediment is initially diluted and equilibrated with BionSoil. PAHs were declined 51.2 %, 39.7 %, 39.7 %, 35.4 %, and 47.1 % of phenanthrene, fluoranthrene, pyrene, benzo(α)anthracene, and chrysene respectively by adding 60 % BionSoil.

The degradation of organic contaminants in soil and sediment is the direct result of microbial activity. The sorption of the organic compounds to soil or sediments reduces availability of the organic molecules to microorganisms and slow biodegradation. In recent bioavailability literature by Lee et al. (2004) explained that biodegradation is limited by sorption. The rate of biodegradation decreased with increasing organic compound hydrophobicity, soil-to-

water ratio, and soil organic carbon content (Zhang and Bouwer, 1997). The biodegradation can be limited by the greater sorption and the slow rate of desorption of organic compounds. The sorption potential of BionSoil as capping material and bioavailability for PAH components are described detail in Chapter 6.

Stoichiometry was used to determine whether the degradation was coupled to sulfate reduction. The amount of sulfate reduced during PAH degradation was compared to the amount predicted from the theoretical stoichiometric equations in Table 4.5. Sulfate consumed 166.6 μM over 180 days in control treatment microcosm. Based on stoichiometry, theoretical sulfate consumed during the major five PAH degradation in Anacostia sediment was 64.2 μM. As increasing the fraction of BionSoil, the amount of sulfate consumed are significantly increased 2.52 mM, 4.08 mM, and 6.41 mM in 20 % BionSoil, 40 % BionSoil, and 60 % BionSoil treatment microcosm, respectively. It indicates that BionSoil contains a lot organics and sulfate itself and consume competing with adding sulfate and its sulfate. For instance, 8.25 mole of sulfate are required to metabolize 1 mole of phenanthrene. On a mass basis, the ratio of sulfate to phenanthrene is followed by

Molecular weights : Phenanthrene 14(12) + 10(1) = 178 gm

Sulfate 8.25(96) = 792 gm

Mass ratio of sulfate to phenanthrene = 792 : 178 = 4.45 : 1

The PAH degradation occurred as sulfate was terminal electron acceptor. Sulfate loss occurred due to metabolism of carbon compounds present in PAH compounds. Results suggested that PAHs mineralized to carbon dioxide and that sulfate reduction is the terminal electron accepting process involved.

Table 4.5 Theoretical stoichiometric equation of PAH compounds

Compound	Theoretical stoichiometric equation	Initial PAH (μM)	Sulfate consumed (μM)
Phenanthrene	$C_{14}H_{10} + 8.25\ SO_4^{2-} + 16.5\ H^+ \rightarrow 14\ CO_2 + 8.25\ H_2S + 5\ H_2O$	3.71	16.51
Fluoracene	$C_{16}H_{10} + 9.25\ SO_4^{2-} + 18.5\ H^+ \rightarrow 16\ CO_2 + 9.25\ H_2S + 5\ H_2O$	2.93	13.15
Pyrene	$C_{16}H_{10} + 9.25\ SO_4^{2-} + 18.5\ H^+ \rightarrow 16\ CO_2 + 9.25\ H_2S + 5\ H_2O$	3.11	13.96
Benzo(α)anthracene	$C_{18}H_{12} + 10.5\ SO_4^{2-} + 21.0\ H^+ \rightarrow 18\ CO_2 + 10.5\ H_2S + 6\ H_2O$	2.69	11.97
Chrysene	$C_{18}H_{12} + 10.5\ SO_4^{2-} + 21.0\ H^+ \rightarrow 18\ CO_2 + 10.5\ H_2S + 6\ H_2O$	1.92	8.62
PAHs			64.21

Redox Studies

For the measurement of methane and hydrogen, the slurry samples were collected at the same time in order to correlate PAH degradation with methane and sulfate concentrations. Initial concentration of sulfate is 2.3 ± 0.29 (mM). Sulfate concentration in six different treatment starts between 2.05 mM and 6.25 mM then, sulfate reduction is occurred 98 % in 60 % BionSoil treatment. Sulfate concentration change is shown in Figure 4.7. Sulfate and carbon dioxide both are electron acceptor in biodegradation processes. When sulfate is terminal electron acceptor, sulfate reducing condition is more energetic than methanogenesis condition. The researcher suggested that PAH degradation is slower under methanogenic conditions than sulfate reducing

condition (Anderson and Lovley, 2000). When sulfate is greater than 1 mg/L, methnogenesis is not occurred. Hydrogen concentration is also low.

Trends of methane and hydrogen concentration in different treatment microcosms are shown in figure 4.8 and Figure 4.9. Hydrogen concentration decreased and sustained at low concentration. Hydrogen produced and consumed through the entire period. These results indicate that hydrogen was probably used as an electron donor during the degradation period. Hydrogen (~5 nM) was purposely added in the middle of time frame (80 days) in order to determine the relative role of PAH degrader in the treatment. In the 60 % BionSoil treatment, hydrogen concentrations decreased and sustain the lower concentrations.

When sulfate was depleted, methane concentrations abruptly increased. It might change the sulfate reducing condition into methnogenesis condition after 100 days. But, Methanogenesis condition does not strongly supported PAH biodegradation since most PAH degradation was slowed down around 100 days. All component of PAH concentrations were steady at this time. Sulfate reducing conditions changed to methanogenesis condition at this point. Some researchers reported that sulfate reducers can outcompete methanogens for hydrogen and substrate (Lovely and Klug, 1983; Lovley and Phillips, 1987). Here, PAH biodegradation was strongly linked to sulfate reduction and sulfate reducers competed with methane producers.

Many previous studies reported that hydrocarbon components were degraded anaerobically when sulfate reduction was the predominant electron-accepting process (Bedessem et al., 1997; Caldwell et al., 1998; Coates et al., 1996a; Anderson and Lovley, 2000; Rothermich et al., 2002) and both sulfate reduction and methane production had competitive Mechanisms (Lovely and Klug, 1983; Lovley and Phillips, 1987; Anderson and Lovley, 2000).

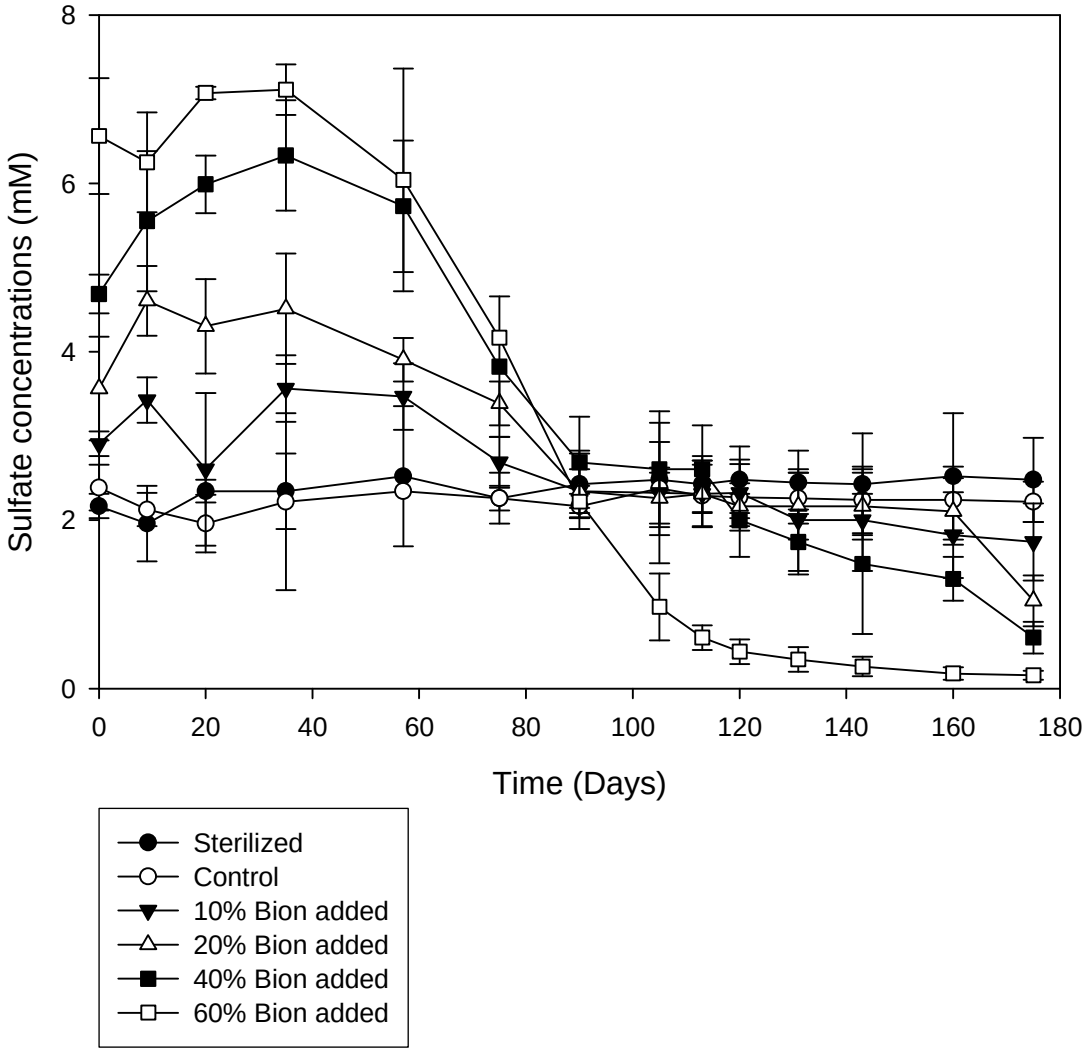

Figure 4.7 Sulfate concentration changes over time

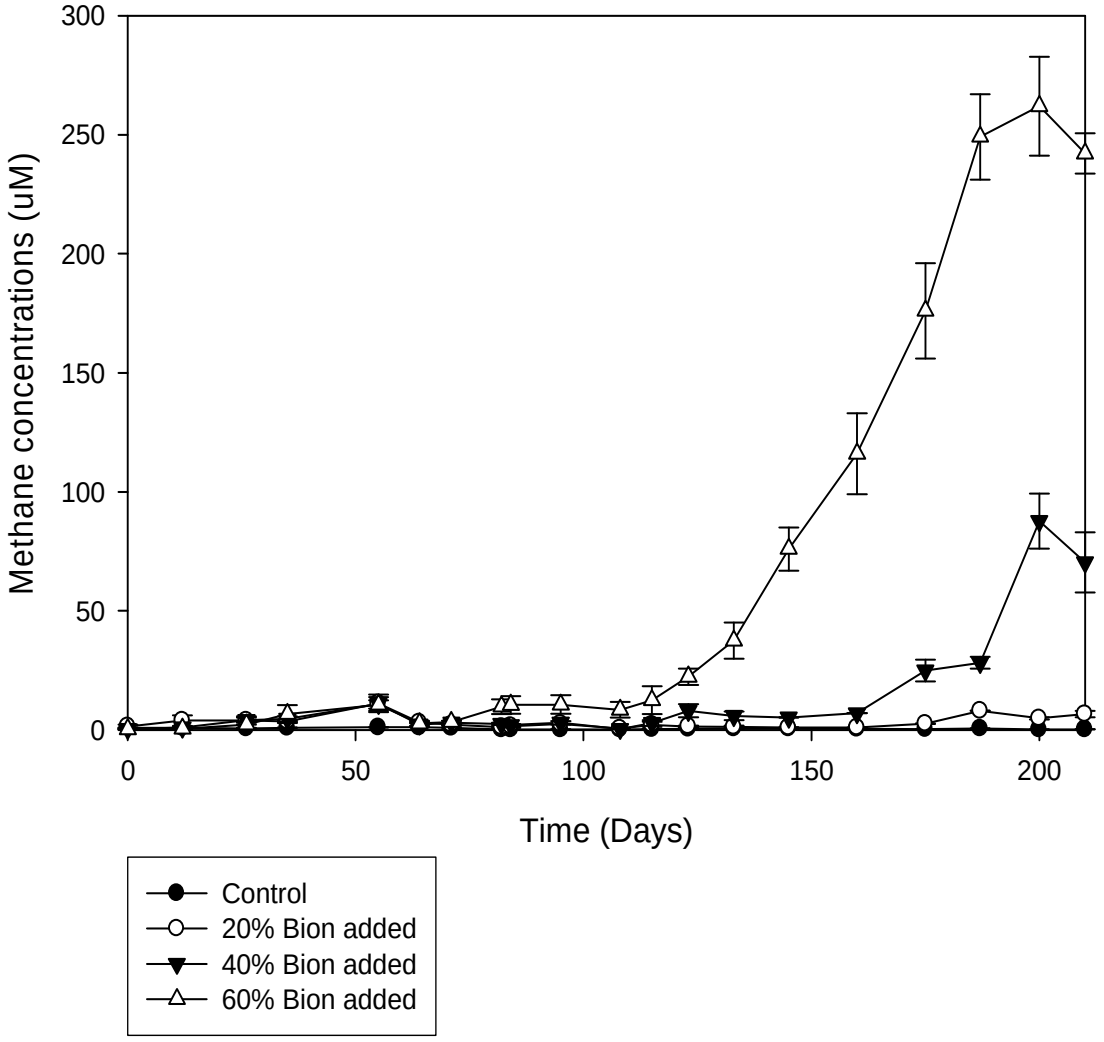

Figure 4.8 Methane concentration changes over time

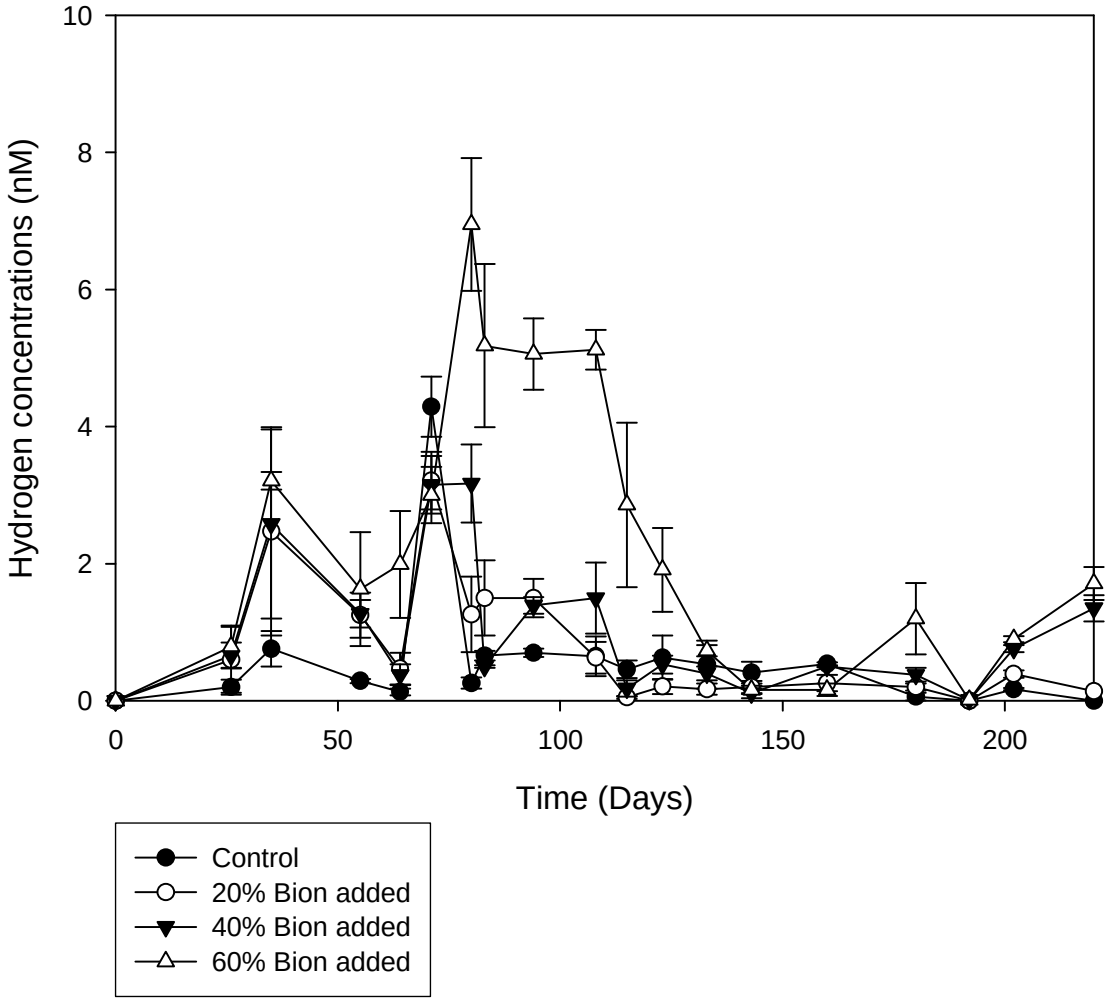

Figure 4.9 Hydrogen concentration changes over time

Microbial Analysis

Real-time PCR assays were developed and optimized for the quantification of total bacteria, and methanogens from microcosms. Real-time PCR quantification of bacteria and methanogen from Anacostia sediment microcosms are shown in Table 4.6. Total bacteria ranged from 1.1×10^6 to 3.8×10^6 and methanogen ranges from 1.8×10^5 to 2.1×10^6 cells per gram soil.

Table 4.6 Real time PCR quantification of bacteria in Anacostia microcosms

Treatments / Target cells	Eubacteria cells/g	Methanogen cells/g
Sediment	1.1×10^6	9.1×10^5
BionSoil	3.8×10^6	2.1×10^6
Control (Sediment only)	7.7×10^5	1.8×10^5
20 % of BionSoil added	7.9×10^5	5.6×10^5
40 % of BionSoil added	1.0×10^6	7.6×10^5
60 % of BionSoil added	1.7×10^6	1.7×10^6

The values were the greater in eubacteria and methanogen as the fraction of BionSoil was increased. BionSoil may enhance the soil microbes and boost soil organic matter. Microbial degradation is the major mechanism for decrease of contaminant. Recently, many researchers explain the biodegradation potential of contaminant degrading bacteria. Potin et al. (2004) demonstrated the ability of PAH degradation using the specific strain, *Cladosporium sphaerospermum*, and they presented that PAH decline was strongly related to this fungus. Kassenga et al. (2004) supported anaerobic degradation by identifying the microbial community. Guo et al. (2005) found that mixed culture or single isolate could facilitate PAH bioremediation.

They isolated three bacterial consortia (*Sphingomonas*, *Rhodococcus*, and *Paracoccus*) to investigate bacterial composition and its degradation ability.

PCR amplification products were tested for presence of bacteria and the concentration of amplified PCR products prior to DGGE analysis. DNA sequences of the cloned DNA fragments were edited using Chromas software downloaded from http://www.mb.mahidol.ac.th/pub/chromas/chromas.htm and was compared using BLAST (http://www.ncbi.nlm.nih.gov/BLAST/) maintained by the National Center of Biotechnology Information (NCBI). *Desulfotomaculum sp*. and *Pelobacter sp*. were dominant bacteria with 98 % of homology from BionSoil treatment microcosm. Identified sequences are listed in Table 4.7. They are preventative sulfate-reducing bacterium (Chang et al., 2001; Rios-Hernandez et al., 2003; Londry et al., 2004). They participate in microbial manganese and sulfate reduction also in degradation processes (Rios-Hernandez et al., 2003; Lorah and Voytek, 2004; Matsui et al., 2004). Theses microbial communities were produced and were able to biodegrade PAH in control and BionSoil treatment microcosms. The microbial communities may participate in biodegrading the PAH components.

Table 4.7 Identification of bacteria from Anacostia microcosms

Treatments	Bacteria species	Similarity (%)
BionSoil	*Desulfotomaculum sp.*	98
	Pelobacter sp.	
Control (Sediment only)	*Clostridium sp.*	92

The SRB specific PCR primer for the 16S rDNA was applied to detect SRB DNA from sediment microcosms. The 16S rDNA-targeted PCR primer sequence, DSV230 and DSV838 (Daly et al., 2000), was used as expected product of 610 (bp). Daly et al., 2000 designed the six groups of PCR primers to detect SRB DNA and evaluate the PCR amplication of SRB 16s rDNA from landfill leachate. DSV230 and DSV838 were selected in this study as a *Desulfovibrio* group. PCR amplication of DNA extracted from sediment and microcosms was conducted with specific primers. *Desulfovibrio*-like amplication products obtained from all samples were shown in Figure 4.10. Sulfate reducers are possibly important factors in process of PAH biodegradation. Some bacteria species, *Desulfovibrio,* can ferment such as lactate and hydrogen in the presence of sulfate (Raskin et al., 1996; Richardson et al., 2002).

A phylogenetic tree is a graphical representation of the evolutionary relationship among taxonomic groups. Taxonomy is the system of classifying plants and animals by grouping them into categories according to their similarities. Phylogenetic tree of microcosm treatments using Quantity One® 1-D analysis software was shown in Figure 4.11. It presents that how much similar in appearance and related patterns among the microcosms. It shows higher similarity of 61 % relationship between 40 % BionSoil treatment and 20 % BionSoil treatment microcosms. These two treatments also have 55 % of similarity with 60 % BionSoil treatment microcosms. It indicated that BionSoil treatment microcosms were affected by adding the BionSoil. It is important to understand that the phylogenetic tree generated by bioinformatics tools is primarily based on sequence data alone. Hence, the sequence relatedness can be one of very powerful methods as a predictor of the relatedness of species.

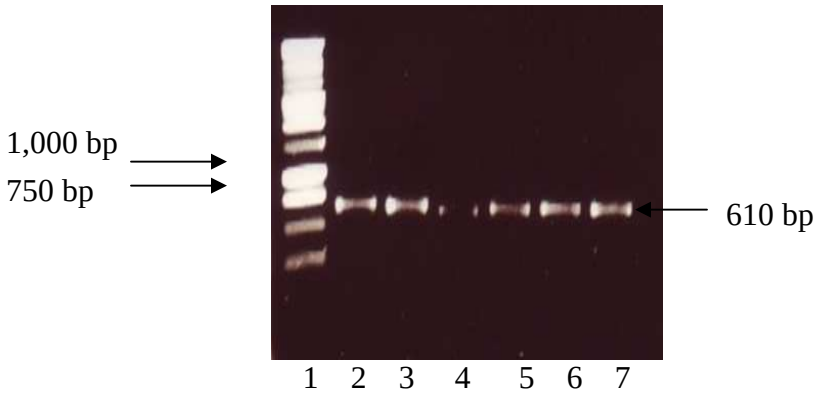

Figure 4.10 PCR amplications of SRB 16S rDNA with SRB specific primers
1: 1Kb DNA ladder, 2: Anacostia sediment 3: BionSoil
4: Control microcosm (sediment only), 5: 20 % of BionSoil added,
6: 40 % of BionSoil added, and 7: 60 % of BionSoil added microcosm

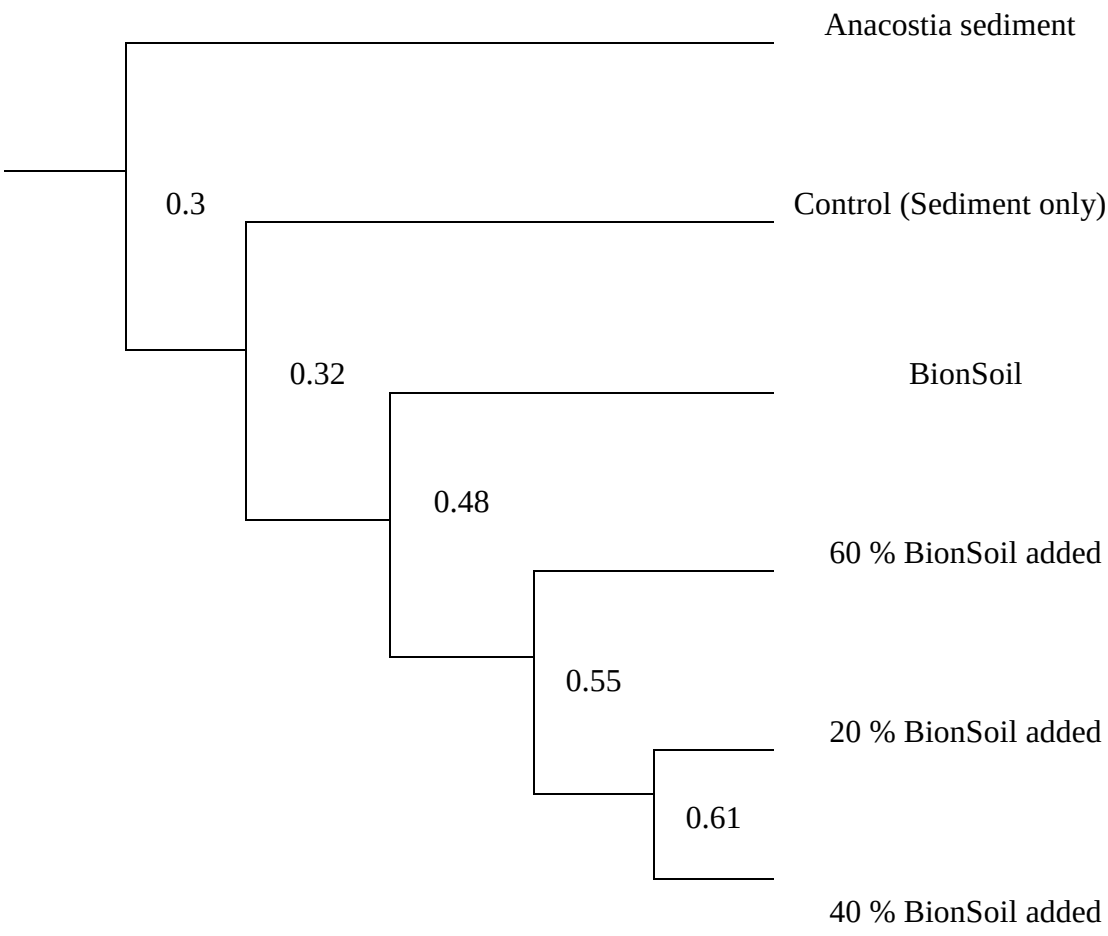

Figure 4.11 Phylogenetic tree using Quantity One® 1-D analysis software

Conclusions

This kinetic study observed the important removal process of PAHs in anaerobic biodegradation. Biodegradation processes were examined the comparable effectiveness in the mixtures of BionSoil and Anascotia River sediment. Since BionSoil enhances soil microbes and contains high sediment total organic carbon (TOC), the correlation between degradation rate and sediment total organic carbon (TOC) are important for PAHs in Anacostia sediment.

Biodegradation of PAHs was strongly linked to sulfate reduction in BionSoil mixtures. Though sulfate and carbon dioxide both are electron acceptor in biodegradation processes, sulfate reduction is the more energetic process than methanogenesis condition. Concentration of hydrogen decreased and maintained low level of concentration, it means, hydrogen was used as an electron donor during the degradation.

Fast degradation of PAHs was possibly mediated by microbial communities such as *Desulfotomaculum sp*., *Pelobacter sp*., and *Desulfuromonas sp*. The microbial consortia may have a relation with the degradation potential. These sulfate-reducing bacteria potentially use hydrocarbon substrates as an electron donors and sulfate is used as an electron acceptor. BionSoil could support the population of sulfate-reducing bacteria.

CHAPTER 5
THE EFFECT OF BIONSOIL ON HCB BIODEGRADATION

Introduction

Hexachlorobenzene (HCB) has been used as both a pesticide and an industrial chemical. While HCB has not been produced commercially since 1982, HCB is also still produced as a by product during the manufacture of several chlorinated chemicals. HCB has been detected in the flue gas and the fly ash of municipal incinerators and other thermal processes (ATSDR, 1996). HCB is a chlorinated hydrocarbon that is very hydrophobic in nature with a low aqueous solubility (0.005 mg/L). The U.S. EPA has classified HCB as a probable human carcinogen and has established a national primary drinking water standard (maximum contaminant level) of 0.001 mg/L (ATSDR, 1996). HCB is a hydrophobic organic chemical that has shown a lack of toxicity in water at concentrations up to and exceeding the solubility limit (Fuchsman et al., 1998). A potential risk is present in the contaminated sediment. HCB is rather persistent and binds to particular matter and easily bioaccumulates into the organism and food chain (Boese et al., 1996; Nakashima et al., 1997; Fuchsman et al., 1998).

Many studies have shown that anaerobic reductive dechlorination of HCB yields lower chlorinated benzenes (Sims et al., 1991; Beurskens, 1995; Middeldorp et al., 1997; Pavlostathis and Prytula, 2000). The most cited predominant pathway of the microbial reductive dechlorination of HCB is as follows: HCB → pentachlorobenzene (PeCB) → 1,2,3,5-tetrachlorobenzene (1,2,3,5-TeCB) → 1,3,5-trichlorobenzene (1,3,5-TrCB). 1,3,5-TrCB usually accumulates, although it can be further reduced via 1,3-dichlorobenzene (1,3-DCB) to monochlorobenzene or even benzene (Beurskens, 1995; Chen et al., 1997; Middeldorp et al., 1997; Pavlostathis and Prytula, 2000). Other possible tetrachlorobenzene (1,2,3,4-TeCB and 1,2,4,5-TeCB), trichlorobenzene (1,2,3-TrCB and 1,2,4-TrCB), and dichlorobenzene (1,4-DCB

and 1,2-DCB) isomers have been observed either less frequently or at low levels as compared with the above-discussed predominant HCB sequential dechlorination pathway (Pavlostathis and Prytula, 2000). Reductive dechlorination appeared to occur in a stepwise fashion until lower chlorinated compounds accumulate. These latter reactions tend to occur much more slowly and result in trace levels of dechlorination products.

Reductive dechlorination of polychlorinated benzene congeners and accumulation of less chlorinated benzene congeners (CBs) has been documented for reduced environments such as soils rich in organic matter and sediments (Sims et al., 1991; Pavlostathis et al., 2000). Since chlorinated compounds are used as electron acceptors during reductive dechlorination, there must be an appropriate source of carbon for microbial growth in order for reductive dehalogenation to occur. Organic matter is one of the potential carbon sources of energy for anaerobic microorganisms. A number of studies have demonstrated that dechlorination kinetics is faster in organic carbon rich soils than in soils poor in organic carbon content because microbial activity depends on the availability of organic carbon (Lorah et al., 1997, Kassenga et al., 2003). Therefore, HCB dechlorination would be expected to accelerate in organic carbon soil.

Redox conditions in soils and sediments can impact HCB dechlorination. Beurskens (1995) reported concomitant dechlorination of HCB with sulfate reduction. The degadation of HCB under sulfidogenesis and methanogenesis is thermodynamically possible since reactions involving HCB conversion to benzene offer more energy (1717.6 kJ/mol) to anaerobic bacteria than the reduction of compounds available naturally in anaerobic environments, such as sulfate to sulfur (551.84 kJ/mol) and carbon dioxide to methane (400.46 kJ/mol) (Sims et al., 1991; Dolfing et al., 1992). Chen et al. (2002) investigated the reductive chlorination of HCB under

various redox conditions. Results indicated that microbial activity caused an effect on dechlorination (Chen et al., 2002). Researchers presented that reductive chlorination of HCB under methanogenic condition (Beurskens et al, 1994; Chang et al., 1997). Beurskens et al. (1994) showed anaerobic dechlorination by determining dechlorination rates and Chang et al. (1997) proved reductive dechlorination of HCB by anaerobic mixed culture using methane producing bacteria. Some researchers reported that sulfate reducers can outcompete methanogens for hydrogen and substrate (Lovely and Klug, 1983; Lovley and Phillips, 1987). The chlororespiring anaerobe *Dehaloccoides* sp. strain CBDB1 can degrade chlorinated benzene (CB) compounds. Strain CBDB1 is capable of coupling growth to dechlorination of CBs (Adrian et al., 2000; Jayachandran et al., 2003; Jayachandran et al., 2004). *Dehaloccoides* sp. is most important on HCB dechlorination.

The study investigated the effect of a compost product BionSoil on HCB degradation in Anacostia sediment. BionSoil was selected as an organic rich material for construction of a reactive sediment cap. The reactive caps are occurred the degradation of contaminants as the contaminated water passes through. The destructive technologies such as biodegradation, sorption, and sequestration take place in permeable reactive caps. The effectiveness of reactive cap using BionSoil was evaluated with HCB dechlorination in this study.

Materials and Methods

Sediments

Sediments were obtained from the Anacostia River which flows from the Maryland suburbs of Washington, DC to its mouth at the Potomac River near downtown Washington. Anacostia River is one of America's most endangered rivers, with sediments containing significant concentrations of heavy metals, polychlorinated biphenyls (PCBs), hydrocarbons, and

chlordane. The sources of these contaminants are long-term military and industrial activity in the Anacostia and Potomac Rivers. Figure 5.1 shows two study sites on the Anacostia adjacent to the Navy Yard. Sediment samples were collected from Site 2 contaminated with PAHs up to 210 ppm. Site 1, near the old combined sewer overflows on the south end of the Navy Yard has 6-12 ppm of polychlorinated biphenyls (PCBs), 30 ppm of PAHs, and significant level of several metals such as cadmium, chromium, copper, lead, mercury, and zinc.

BionSoil is essentially peat material and a trademark name for a type of processed mixture of animal manure. It facilitates sorption of contaminants and can provide a source of carbon for bacteria in waste treatment systems and BionSoil has high organic matter and nutrient content (www.biontech.com). BionSoil encourages degradation of organic contaminants through enhancement of reductive dechlorination and anaerobic degradation of polyaromatic hydrocarbon (PAH) compounds. The geotechnical characteristics of BionSoil are follows: saturated density 34.6 (pcf), TOC of 57.1 (%), pH of 7.4, and saturated moisture content of 125.4 (%) (Kassenga et al., 2000).

Chemicals

The test chemicals selected for this study were hexachlorobenzene (HCB) and daughter compounds, pentachlorobenzene (QCB), tetrachlorobenzene (TeCB), trichlorobenzene (TCB), dichlorobenzene (DCB), monochlorobenzene (MCB), and benzene. HCB was selected as the test chemical because it together with its daughter products can be used a surrogate for polychlorinated biphenyls (PCBs) in reductive dechlorination study. The properties of these chemicals are listed in Table 5.1.

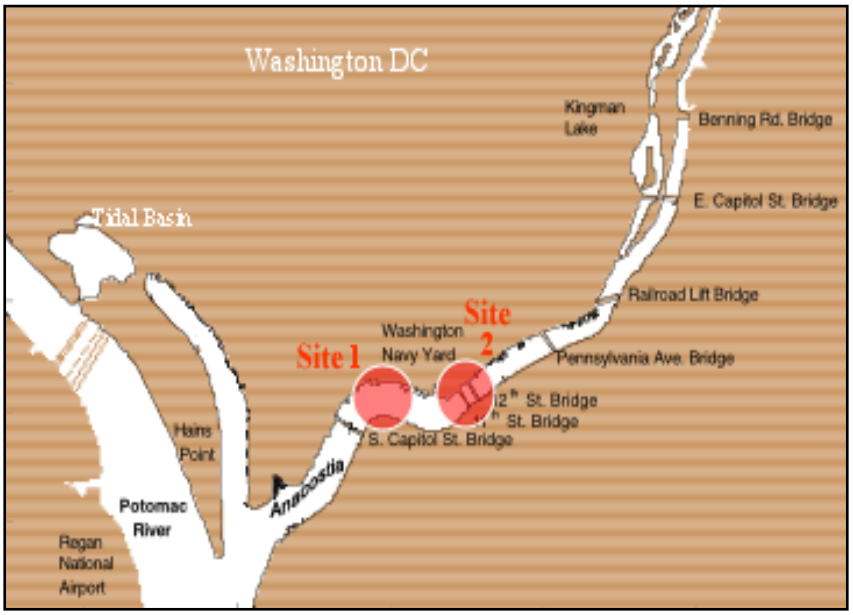

Figure 5.1 Anacostia study sites (From http://www.hsrc-ssw.org/anacostia/)

Table 5.1 Physical and chemical properties of HCB and degradation products (www.inchem.org/pages/icsc.html)

Property	HCB	PCB	TeCB	TCB	DCB	MCB
Molecular weight	284.8	250.3	215.9	181.5	147.0	112.6
Aqueous solubility (mg/L @ 25ºC)	0.005	none			none	499
Vapor pressure (Pa @ 25ºC)	0.001	2	0.7	17.3	286	1170
Log K_{ow}	5.5 – 6.2	5.1 – 5.6	4.9	4.05	3.53	2.2 – 2.8
Density (g/cm^3 @ 20ºC)	1.21	1.8	1.83	1.45	1.29	1.11

Microcosm Experiments

Anaerobic microcosms were constructed inside a glove bag (Cole Parmer Instrument Company, Cheltenham, PA) under an oxygen-free nitrogen atmosphere. Microcosms were prepared using mixtures of Anacostia River sediment and BionSoil, which were then packed in 125 mL Wheaton serum bottles with 20 mL head space. Prior to addition of the selected compost, 50 ppm of HCB was dissolved in diethyl ether added to the serum bottles, and then solvent was flushed away with nitrogen in bottles. The sediments from Anacostia River and sediment with BionSoil were slurried (1:1.5 w/w %) with deionized water. All bottles were sealed with Teflon-lined rubber septa and aluminum crimp seals. Anaerobic microcosms were prepared from Anacostia River sediment and BionSoil mixed with four different volumes (0 %, 20 %, 40 %, and 60 % (w/w) of BionSoil). Microcosms were incubated in an inverted position at 25 ºC under static conditions in the dark. To account for abiotic losses, killed controls were prepared with mercuric chloride (3.89% wt/vol) which inhibits microbial activities. Two

identical sets of bottles were set up for each experiment, one set of bottles for analysis of indicators of redox status by sulfate, hydrogen and methane and another set for analysis of the test chemicals. The concentrations of chlorinated compounds were monitored at regular time intervals using analytical techniques described below. Temporal monitoring of concentrations of the parent compound and degradation daughter products were done for each spike until the concentration of the parent compound drops below the detection limit of the analytical methods.

Sediment Extraction

Five mL of sediment mixture slurry was subsampled from the serum bottles and transferred into 60 mL Teflon centrifuge tubes containing the same volume of hexane/acetone mixture (50/50, v/v, %). Each centrifuge tube was tumbled 24 hours to extract the chlorinated compounds from the slurry then, each tube was centrifuged for 20 minutes at 3000 rpm in Avanti^{TM} J-20 XPI high-performance centrifuge (Beckman Coulter, Fullerton, CA). One mL of hexane/acetone extract was transferred to gas chromatography mass spectrometry (GC/MS) autosampler vials and refrigerated until GC/MS analysis.

Chemical Analysis

The chlorinated extracts were analyzed following EPA Method 8270. Ten μL of semivolatile internal standards mix (Supelco, Bellefonte, PA) was injected into the extract. The sample was analyzed using a Hewlett Packard 5890A gas chromatograph (GC) coupled with a HP 5971 mass selective (MS) detector. The GC was equipped with a 30 m x 250 μm x 0.25 μm film thickness capillary column. One μL of the sample was injected automatically onto the column. GC temperature program conditions were 55°C, ramped at 10°C/min to 200°C, then at

4°C/min to 300°C and held for 10 minutes. The mass spectrometer was operated in the selected ion monitoring mode and the ion source temperature was 280°C.

Analysis of chlorobenzene and benzene were performed by EPA Method 8260B using a purge and trap apparatus attached to HP 5890A GC equipped with a HP 5971 MS detector. A thermal desorption trap (VOCARB 3000; Supelco, Bellefonte, PA) was employed in the purge and trap apparatus. The extracts along with 10 μL of internal standard and 2.5 μL of surrogate (Supelco, Bellefonte, PA) were manually injected into the purge and trap autosampler (Tekmar 2016; Tekmar Dohrmann, Mason, OH) and purged for 11 min then, desorbed for 0.5 min and baked for 13 min at 225°C.

Sulfate and Gas Measurements

A Hach DR 2010 spectrophotometer (Hach Co., Loveland, CO) was used to determine sulfate concentrations. Water from each microcosm was diluted with deoxygenated water to 25 mL in order to measure the concentrations using the spectrophotometer. The Hach DR 2010 was capable of analyzing for sulfate concentrations within a range of 0 to 70 mg/L SO_4^{2-}. Sulfate concentrations were read directly by adding the Hach, SulfaVer 4 Sulfate Reagent "powder pillow" and inserting the samples into the spectrophotometer. Sulfate ions in the sample react with barium in the SulfaVer 4 Sulfate Reagent "powder pillow", forming insoluble barium sulfate turbidity. A standard calibration was performed for each lot of SulfaVer 4 Reagent Powder Pillows. Standards of 0, 10, 20, 30, 40, 50, and 60 mg/L sulfate were prepared by diluting 0, 0.1, 0.2, 0.3, 0.4, 0.5 and 0.6 mL of the contents of a Sulfate Voluette Ampule standard.

Hydrogen was analyzed using a reduction gas chromatograph (Trace Analytical, Menlo Park, CA). Headspace samples were injected into 1 mL gas sampling loop and were separated

with a molecular sieve analytical column (Trace Analytical, Menlo Park, CA) at an oven temperature of 40°C. Ultrahigh purity nitrogen (BOC Gases, Baton Rouge, LA) was used as a carrier gas after it was passed through a catalytical combustion converter to removes traces of H_2. The detection limit for H_2 under these conditions was 1 ppb. Aqueous H_2 concentrations were calculated as Löffler et al. (1999).

$$H_2\,(dissolved) = LP/RT$$

where $H_2\,(dissolved)$ is the aqueous concentration of H_2 (in moles/L), L is the Oswald coefficient for H_2 solubility (0.01913 @ 25ºC), R is the universal gas constant (0.0821 L · atm · K^{-1} · mol^{-1}), P is the atmospheric pressure, and T is temperature in Kelvin.

Methane was measured using a gas chromatography flame ionization detector (GC/FID). One mL of gas was collected from the headspace of the bottle using a gas tight syringe and injected into GC/FID (HP 5890 series II) equipped with a 2.4 m x 0.32 mm i.d. column packed with Carbopack b/l % SP-1000 (Supelco, Bellefonte, PA). The injector and detector temperatures were 375ºC and 325ºC, respectively. The column temperature was held constant 50ºC for 6.50 min. Ultrahigh purity nitrogen (Grade 5.0) was used as a carrier gas. Methane data were reported as aqueous phase concentrations. Headspace methane concentrations were converted to aqueous phase concentrations by Henry's Law constant of 0.6364 atm/mol/m^3 for methane.

Microbial Analysis

Microbial populations were characterized using denaturating gradient gel electrophoresis (DGGE) and real time polymerase chain reaction (RT-PCR). The protocol of Mo Bio Ultraclean Soil DNA Isolation Kit (Mo Bio Laboratories, Inc., Carlsbad, CA) was followed to extract DNA from 0.25 g of wet sediment slurry samples collected from the microcosms. Sediment samples

were washed twice with 0.12 M of sodium phosphate buffer to remove extracellular DNA (Lee et al., 1996). Extracted DNA was amplified using PCR using a 20 μL reaction volume. Each reaction contained DNA Polymerase (1 U), 1x Taq Buffer, 3 mM of $MgCl_2$, 1 μM of each primer, 0.2 mM of each deoxynucleoside triphosphate (dNTP) (Promega Corporation, Madison, WI) and 1 μL of extracted DNA. The conditions PCR amplification program consisted of an initial 5 min denaturation step at 94°C followed by 30 cycles of 94°C for 1 min, 57°C for 1 min, 72°C for 1 min, and a final 10 min extension step at 72°C (Lee et al., 2002).

For real-time PCR, the PCR mixture consisted of 12.5 μl of 2×iQ SYBR Green Supermix, 250 nM of each primer and 1.5 μl of DNA templates. Distilled water was used to bring the volume to 25 μl. PCR conditions were as reported by Hendrickson et al. (2002) for the bacteria: initial denaturation at 95ºC for 2 min, followed by 30 cycles consisting of denaturation at 94ºC for 1 min, annealing at 55ºC for 1 min, and extension at 72ºC for 1 min. For the archaea group (i.e., methanogens), PCR conditions were : denaturation at 94ºC for 2 min, followed by 30 cycles consisting of denaturation at 94ºC for 30 s, annealing at 60ºC for 45 s, and extension at 72ºC for 2 min (Löffler et al., 1997). PCR amplication was performed using a RT-PCR Detection System iCycler iQ (Bio-Rad Laboratories, Inc., Hercules, CA). The PCR products were purified with MoBio PCR Clean-Up Kit (Mo Bio Laboratories, Inc., Carlsbad, CA). The molecular weight of products was determined by electrophoresing portions of extracts on 1.0 % agarose gels with a 1-kb ladder ((Promega Corporation, Madison, WI) as a size marker. The bacterial 16S rDNA real-time PCR assay was log-linear over 5 orders of magnitude with DNA standards. The linear range of detection for real-time PCR assay for bacterial 16S rDNA was from 8.5 to 8.5×10^5 copies per PCR. The regression coefficient value for standard curves for PCR was 0.99. The numbers of bacteria, methanogen, *Dehalococcoides* cells per gram soil were calculated from

copies per gram soil. The gene copy number per cell was used 3.6 for bacterial 16S rDNA (Harms et al., 2003). The oligonucleotide primers are listed in Table 5.2. All these primers were obtained from AlphaDNA (Montreal, Quebec, Canada).

Table 5.2 Oligonucleotide primers used in this study

Primer	Sequence (5´ - 3´)	References
Universal Primers for 16s rDNA		Lane (1991)
27f	5'-AGAGTTTGATCCTGGCTCAG-3'	
1492r	5'-GGTTACCTTGTTACGACTT-3'	
Archaea Primers for RT- PCR		Löffler et al. (1997)
340f	5´ - CCTACGGGGCGCASCAGGSGC - 3´	
915r	5´ - GTGCTCCCCCGCCAATTCCT - 3´	
Universal Primers for DGGE (GC clamp)		Schafer and Muyzer (2001)
341f	5´ - GCCCGCCGCGCCCCGCGCCCGTCCCGC CGCCCCCGCCCGCCTACGGGAGGCAGCAG - 3´	
907r	5´ - CCGTCAATTCMTTTRAGTTT - 3´	
Universal Primers for clone (non GC)		Schafer and Muyzer (2001)
341f	5´ - CCTACGGGAGGCAGCAG - 3´	
907r	5´ - CCGTCAATTCMTTTRAGTTT - 3´	
Dehalococcoides sp. Primers for RT- PCR		Hendrickson et al. (2002)
DHC 1f	GATGAACGCTAGCGGCG	
DHC 1212r	GGATTAGCTCCAGTTCACACTG	

DGGE was performed using a D-Code™ Universal Mutation Detection System (Bio-Rad, Hercules, CA). The denaturing gradient gel (6 %, wt/v, acrylamide solution) was selected for a particular size range between 300 and 1000 base pairs. The acrylamide gels were made with a gradient ranging from 40 % to 70 %, where 100 % denaturant contained 42 % (wt/v) urea and 40 % (v/v) formamide. Polymerization was catalyzed by adding 0.057 % of TEMED (v/v) and 0.85 % of the 10 % ammonium persulfate (v/v) to both denaturant solutions. Gels were cast using a Bio-Rad Model 475 gradient delivery system. Electrophoresis was performed in 1x TAE buffer at 60˚C for 16 hours with an applied current of 0.15 A at 65 V. After electrophoresis, the gel was stained with ethidium bromide (EtBr) for 10 min. then, destained in distilled water for 10 min. The gel was imaged with a UV transilluminator using the Chemidoc XRS system using Quantity One® 1-D Analysis Software (Bio-Rad, Hercules, CA).

DNA was also amplified using PCR with non GC primers, 341F and 907R, for cloning. A ligation reaction was performed using pGEμ-T-vector and transformation was accomplished with *E.coli* competent cells (Promega Coporation, Madison WI) through the protocol provided by the manufacturer. LB (Luria-Bertani) plates with ampicillin/IPTG/X-Gal and liquid LB media with ampicillin were prepared to plate *E.coli* competent cells. The growing white colonies were selected, and transferred into liquid LB medium with ampicillin, and incubated overnight at 37˚C. The plasmid with inserts was extracted from liquid LB medium using the plasmid preparation kit (Mo Bio Laboratories, Inc., Carlsbad, CA). To verify the clone plasmid products, restriction enzyme reactions were conducted and checked with gel electrophoresis. DNA products were purified using the MoBio PCR Clean-Up Kit. Finally, samples were sent to BioMMED (Biotechnology and Molecular Medicine) in the School of Veterinary Medicine (Louisiana State University) for sequencing.

Data Analysis

First-order reaction rate constants were calculated from the first-order kinetic equation. Rate constants for the degradation of HCB compounds were determined using non-linear regression of a first-order exponential decay equation. The degradation rate constant (*k*) was calculated using the following equation:

$$\frac{C}{C_0} = e^{-kt}$$

where *C* is the substrate concentration, (mM/kg dry soil), C_0 is the initial concentration, *k* is the pseudo first-order degradation rate constant, (day^{-1}), and *t* is the time, (days). Kinetic data were modeled using SigmaPlot 9.0. A two sample t-test was used to compare the differences in rate constants from different treatments using a significant level of 0.05. The characteristic half-life period ($t_{1/2}$) was calculated from the first-order reaction rate constant (*k*) using the following equation:

$$t_{1/2} = -\frac{(\ln 2)}{k} = \frac{0.693}{k}$$

where $t_{1/2}$ is the half-life time (days) and *k* is the pseudo first-order degradation rate constant, (day^{-1}).

Results and Discussion

HCB Dechlorination

HCB dechlorination was monitored from the mixtures of BionSoil and Anascotia River sediment at a regular interval. Reductive dechlorination of HCB and daughter product profiles from the different treatments is shown in Figure 5.2 through Figure 5.6.

Parent component HCB was totally degraded after 150 days. Then, daughter products were produced from 30 days in control microcosms. HCB was not degraded and no daughter products detected in the killed control treatment. The inhibition of degradation after addition of mercuric chloride in the killed control treatment strongly suggests that microorganisms in sediment are responsible for degradation since microbial activity is inhibited by mercuric chloride. Faster degradation of HCB was observed in microcosms with the compost mixture rather than in microcosms with sediment alone. HCB was biodegraded at different kinetic rates in the treatments.

HCB was completely removed in all microcosms except the killed control. HCB was reductively dechlorinated to QCB, 1,2,4,5-TeCB and 1,2,3,5-TeCB, which was converted to 1,3,5-TCB, 1,2,4-TCB, 1,3-DCB and 1,4-DCB. The final end products of HCB dechlorination were MCB and benzene. QCB was detected in trace amounts and formation of 1,2,3,4-TeCB was not detected. The observed transformation pathway (HCB → QCB → 1,2,3,5-TeCB and 1,2,4,5-TeCB → 1,3,5-TCB) was very similar to that reported by Chang et al. (1997), Pavlostathis et al. (2002) and Jayachandran et al. (2003). Moreover, 1,2,3,4-TeCB component was not formed at all in Jayachandran et al., (2003). The final products of HCB were 1,3-DCB and 1,4-DCB, or 1,3,5-TCB in previous studies cited. In the current study, MCB and even benzene were formed and dechlorinated and degraded completely in this study. The benzene has been mineralized in sediment and was converted to CH_4 and CO_2 (Lovley et al., 1994; Weiner and Lovley, 1998b). Benzene was degraded with steady production of CO_2 over time under anaerobic condition (Weiner and Lovley, 1998a).

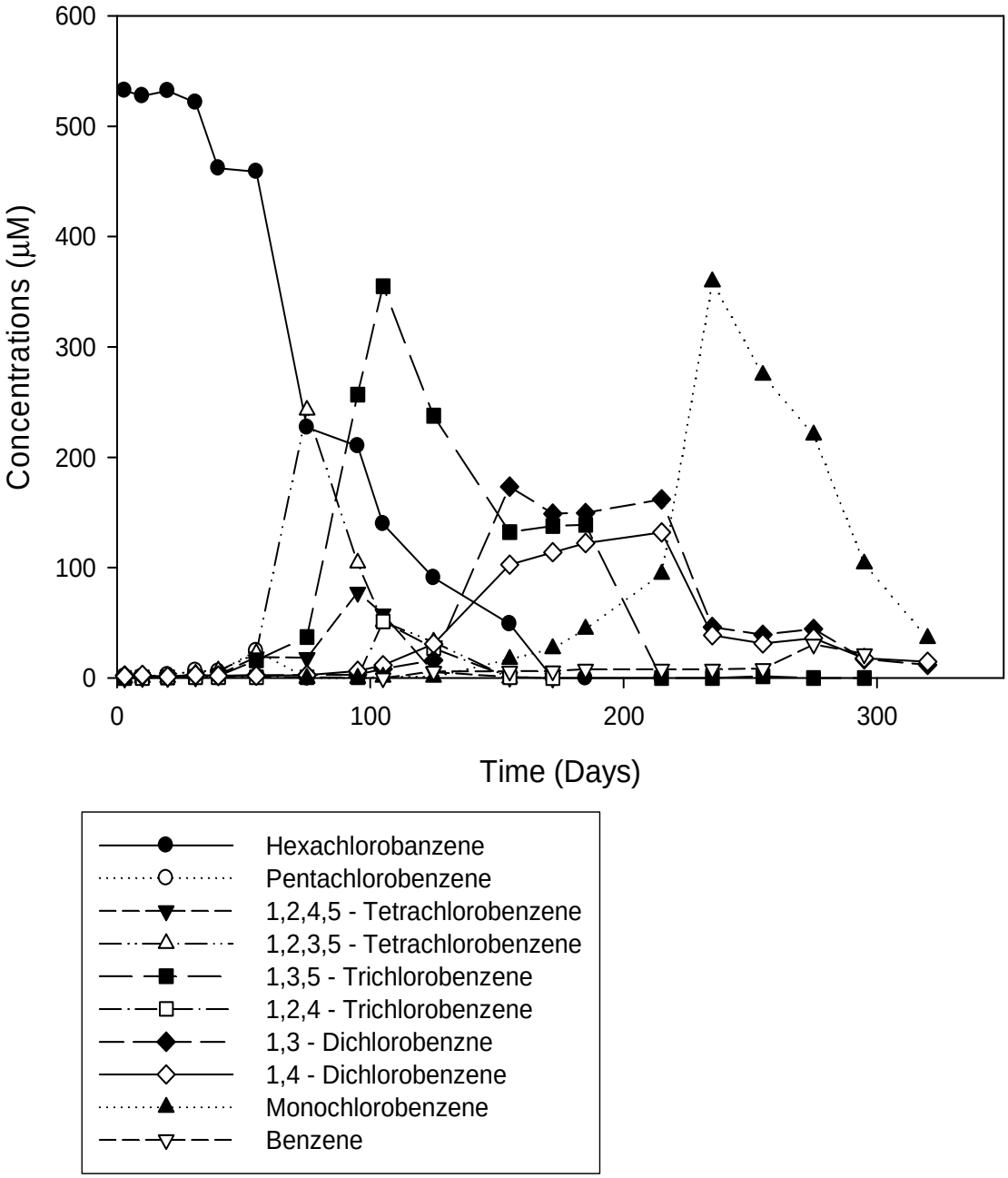

Figure 5.2 HCB dechlorination in control microcosm

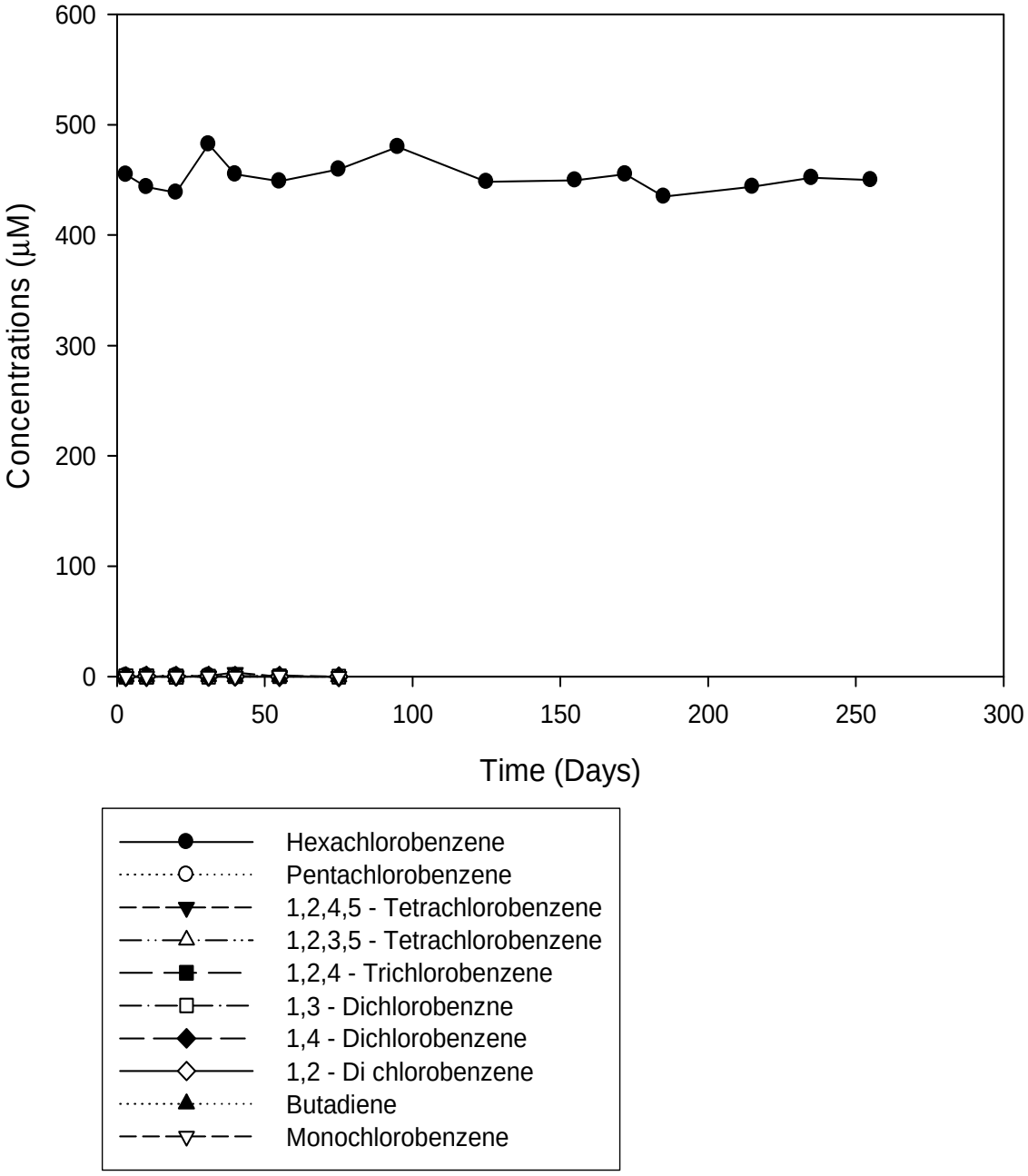

Figure 5.3 HCB dechlorination in killed control microcosm

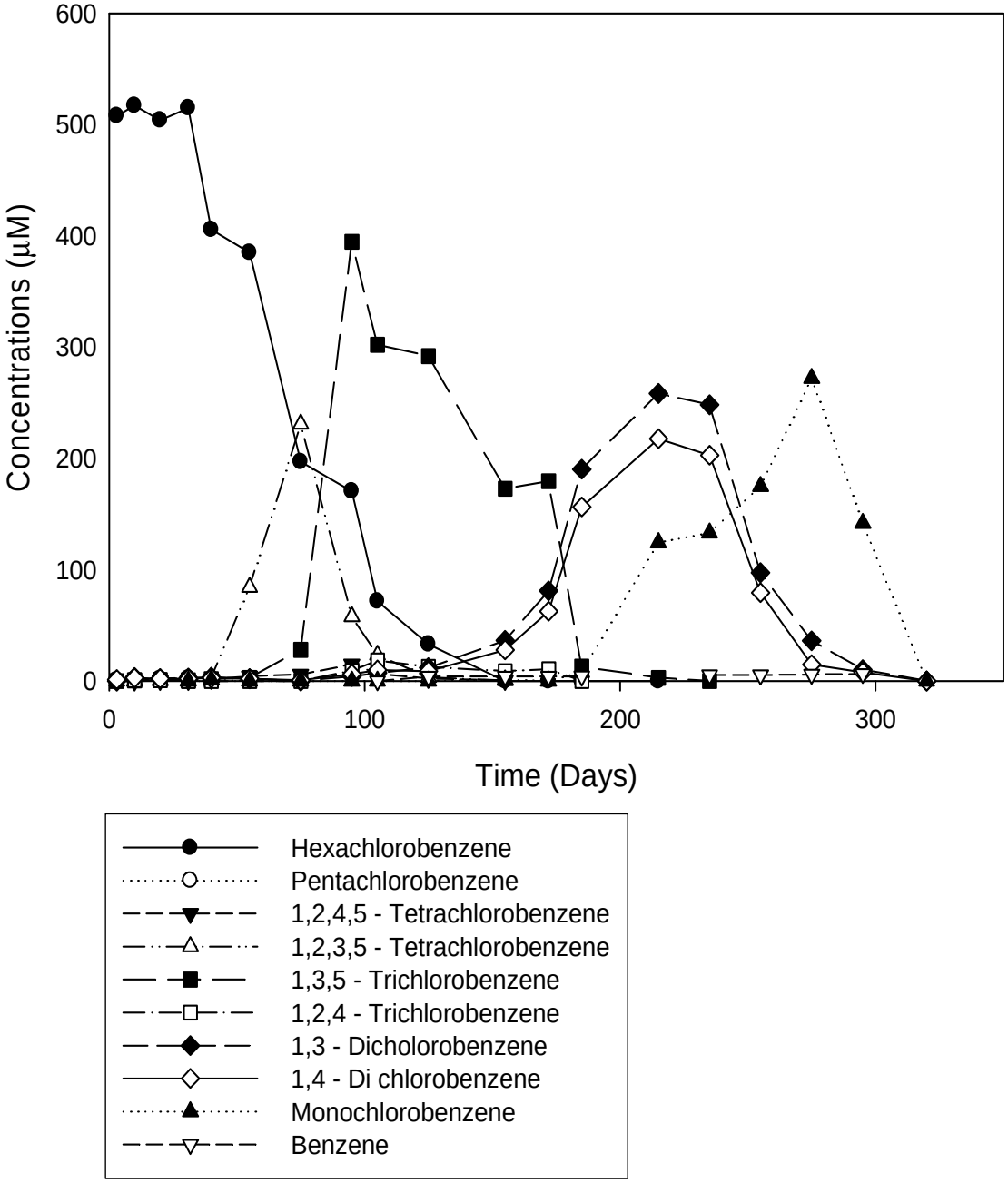

Figure 5.4 HCB dechlorination in 20 % BionSoil added microcosm

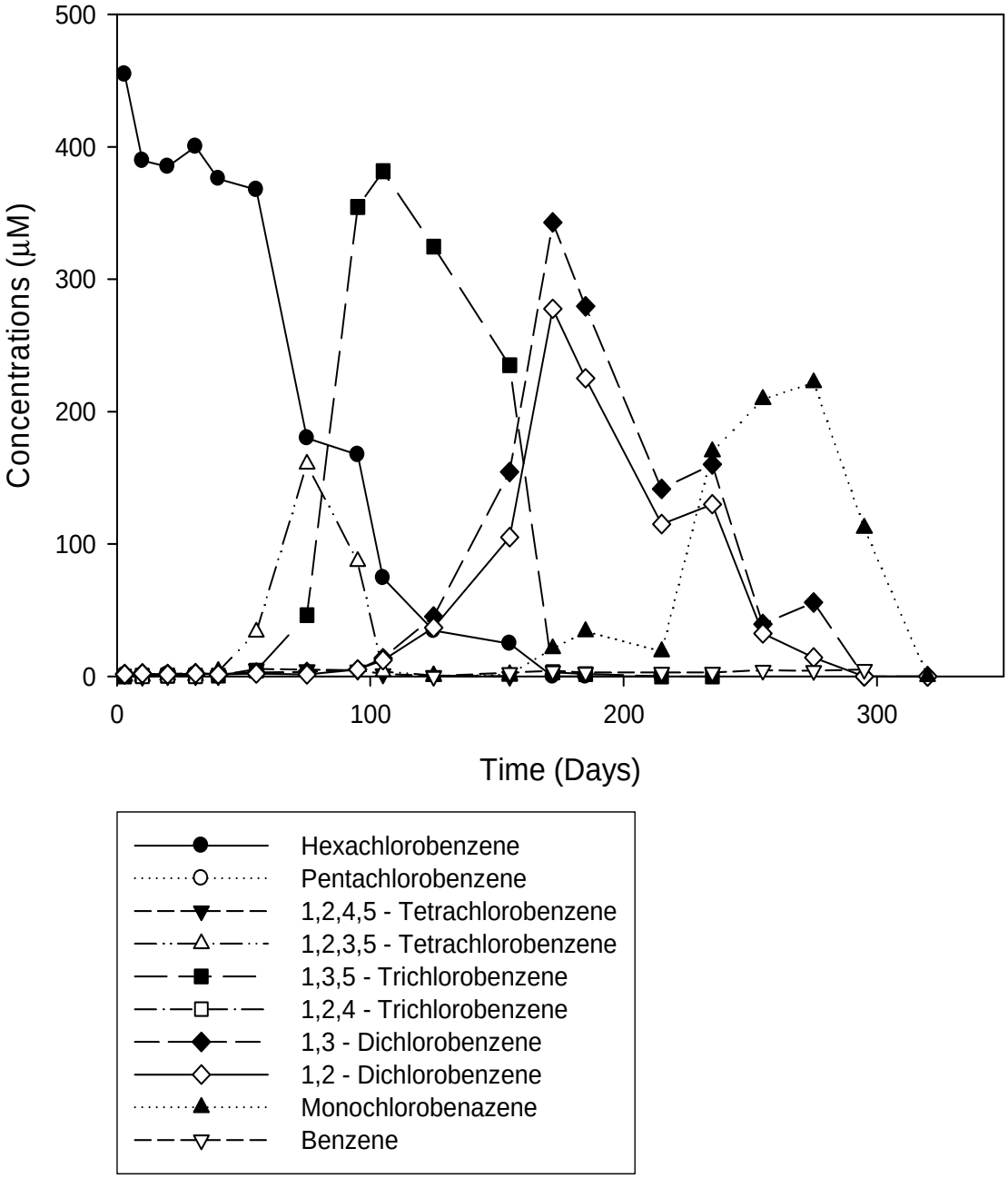

Figure 5.5 HCB dechlorination in 40 % BionSoil added microcosm

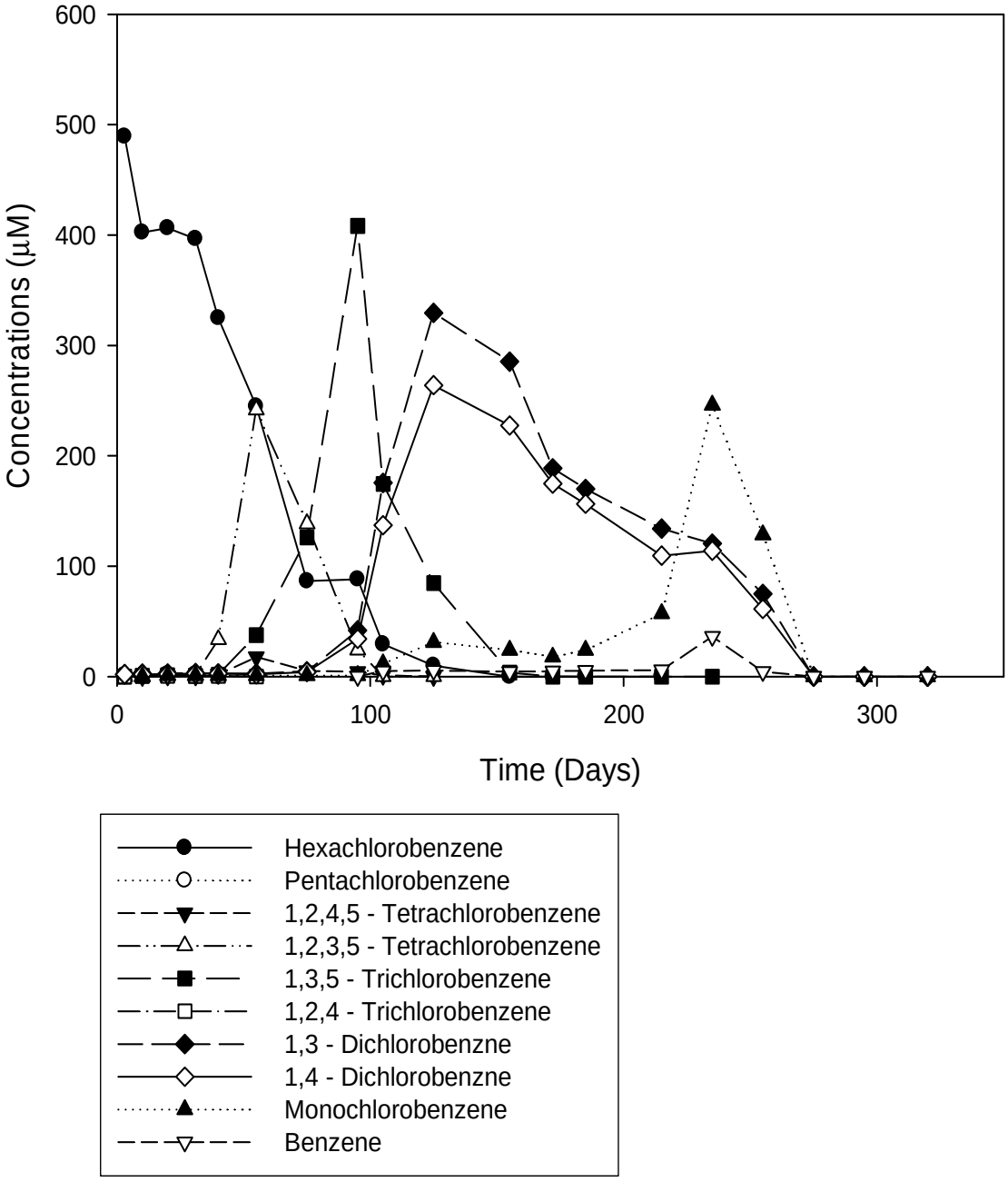

Figure 5.6 HCB dechlorination in 60 % BionSoil added microcosm

The kinetic rate constants and half-life times of HCB dechlorination are listed in Table 5.3. The first-order kinetic model is able to describe degradation kinetics in most microcosms reasonably well as coefficient of determination (R^2) values shown in Table 3.3. The rate constants of different treatment microcosms are 0.0058 (day^{-1}), 0.0068 (day^{-1}), 0.0085 (day^{-1}), and 0.0138 (day^{-1}) in control microcosms, 20 %, 40 % and 60 % of BionSoil treatments, respectively. The value of the rate constant increased as fraction of BionSoil increased in microcosms. The rate constant in 60 % of BionSoil treatment is 2.5 times greater than sediment control treatment. Corresponding half-lives vary from 50 days to 119 days.

Table 5.3 First-order rate constants (day^{-1}) of HCB

Treatment	degradation rate constant (k)	$t_{1/2}$	R^2
Control	0.0058	119	0.98
20 % Biosoil	0.0068	102	0.97
40 % Bionsoil	0.0085	82	0.97
60 % Bionsoil	0.0138	50	0.98

Mass balances were calculated to verify the disappearance of parent compound due to biodegradation. Mass balance for HCB was found to be 86 - 103 %. The dechlorination was completely occurred in parent compound and intermediate daughter products in microcosms. The observations further imply that it is feasible to apply in-situ or ex-situ bioremediation for cleaning up chlorinated compound contaminated sites since no accumulation of intermediate daughter products, TeCB, TCB, and DCB is anticipated.

Redox Studies

Sulfate concentration change is shown in Figure 5.7. In the 60 % of Bionsoil treatment, 95 % of sulfate was removed over 225 days while it was not consumed in the killed control treatment. Sulfate concentrations significantly decreased until 120 days which corresponds with the HCB dechlorination period. This indicated that HCB dechlorination occurred when the redox status was sulfate-reducing. Sulfate was completely depleted at 200 days followed by rapid increases in methane concentration. Sulfate reducing conditions changed to methanogenesis condition at this point. After 200 days, the daughter products, MCB and benzene, produced and these compounds degraded under methanogenic condition (Figure 5.8). Methanogenesis was limited during the dechlorination periods of parent and intermediate compounds (0 to 200 days) and methane concentration increased after the parent compound and intermediate daughter products were completely dechlorinated. Sulfate reducing bacteria was the predominant population over methanogens when the electron donor was sufficient for dechlorination of HCB (Channg et al., 1996 and Chen et al., 2002). However, the studies have reported that methanogenesis was the dominant redox status where reductive dechlorinative occurred (Middeldorp et al., 1997; Pavlostathis and Prytula, 2000).

Methane and hydrogen concentration trends in different treatment microcosms are shown in Figure 5.8 and Figure 5.9. Methane concentrations increased slightly from 0 to 150 days when HCB were dechlorinated completely. The methane production rates were lowest when dechlorination rates were highest (Brahushi et al., 2004). Methane concentrations increased tremendously after 170 days in accordance with sulfate depletion. Dechlorination of daughter products (TCB, DCB, and CB) were found to correlate with methane production in microcosms after 170 days.

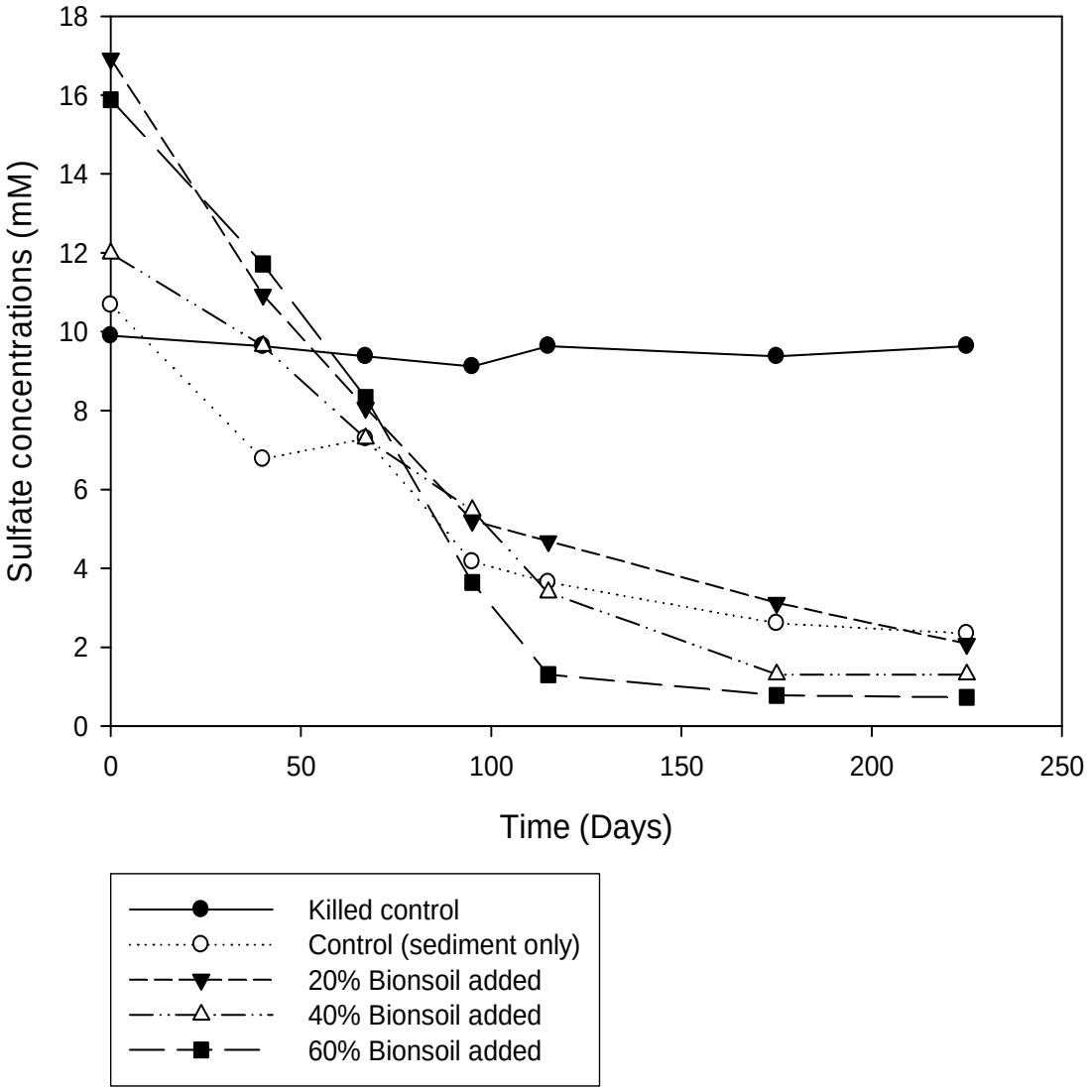

Figure 5.7 Sulfate monitoring with time in Anacostia sediment

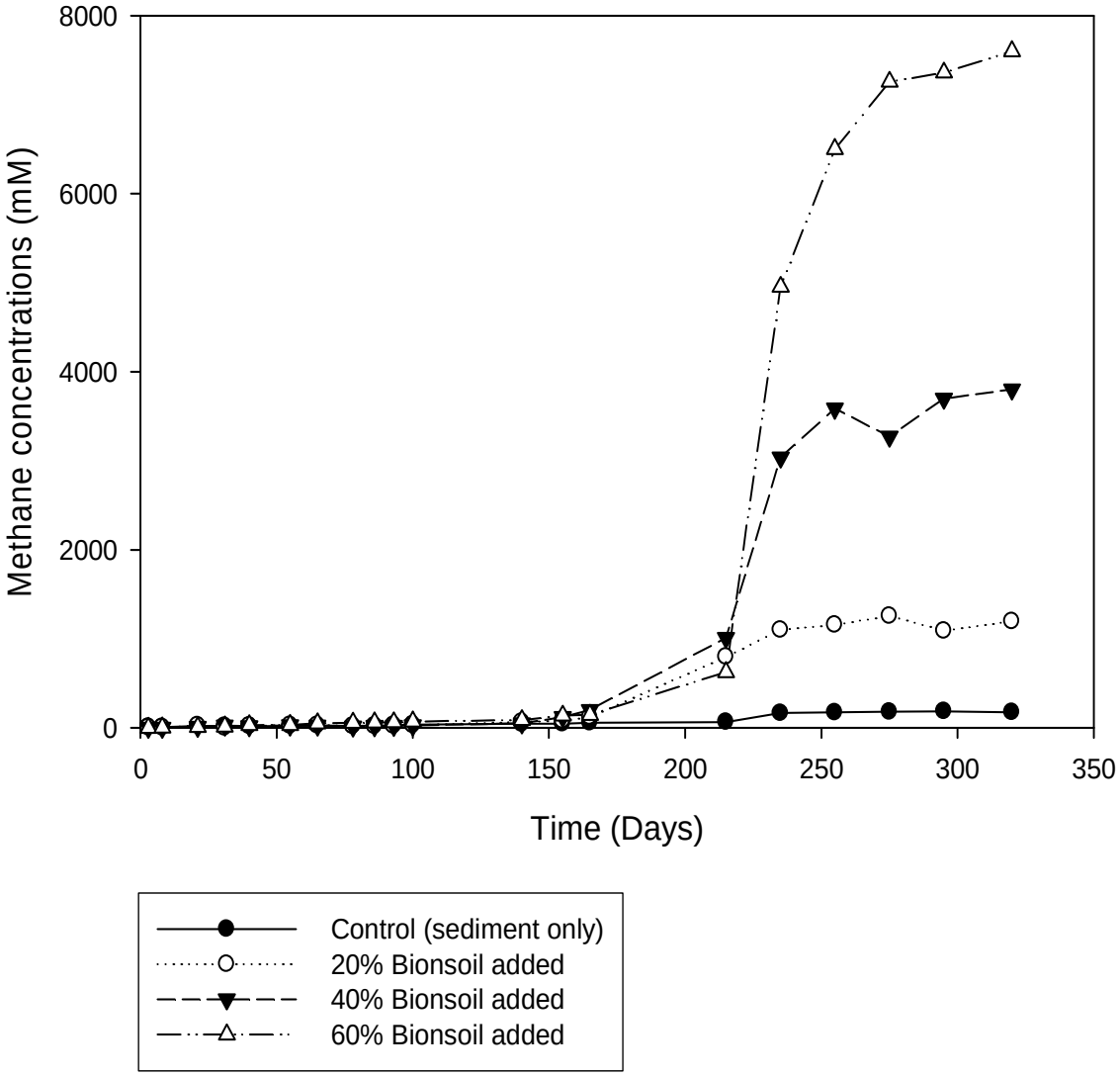

Figure 5.8 Methane productions with time in Anacostia sediment

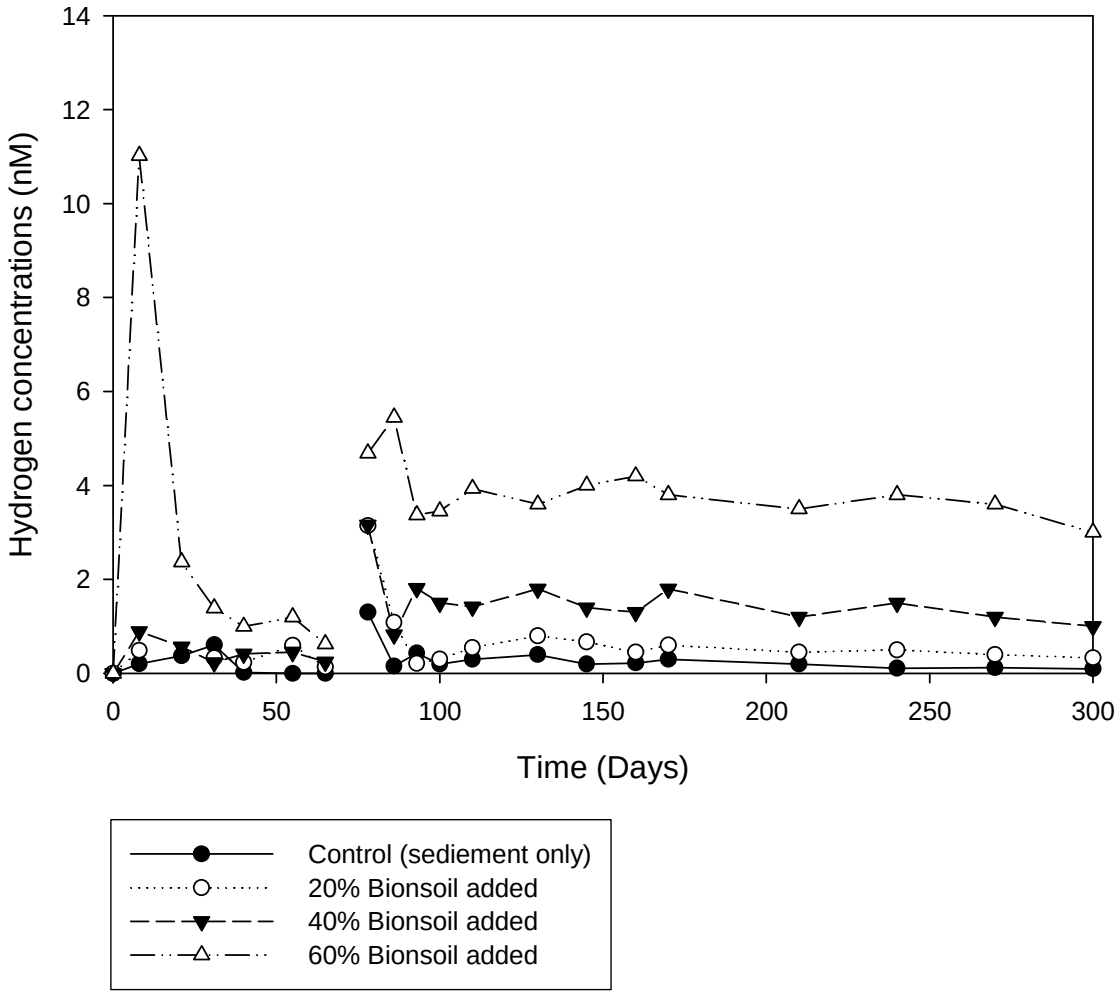

Figure 5.9 Hydrogen monitoring with time in Anacostia sediment

Hydrogen concentration decreased initially while methane slightly increased. During the dechlorination period, hydrogen concentration decreased and sustained at low concentration. Hydrogen was used initially then fluctuated and sustained approximately 4 nM. These results indicated that hydrogen was probably used as an electron donor during methanogenesis for driving dechlorination reactions (Middeldrop et al., 1997; Löffler et al., 1997; Adrian et al., 2000). Hydrogen concentration decreased when dechlorination started and remained constant in microcosms. Methane and hydrogen concentrations were significantly related with the fraction of BionSoil. Methane production and hydrogen activity were accelerated in the larger fraction of BionSoil added treatment.

Microbial Analysis

Soil slurry samples from microcosms were collected and analyzed to compare the diversities of microbial communities in sediment and to investigate the effect of BionSoil on microbial consortia. Soil slurry samples were taken for DNA extraction and amplification. Real-time PCR assays were developed and optimized for the quantification of total eubacteria, methanogen, and *Dehalococcoides* from microcosms. The targets for the real-time PCR assays were the 16S rDNA for bacteria, methanogen, and *Dehalococcoides*. Real-time PCR quantification of bacteria, methanogen, and *Dehalococcoides* from Anacostia sediment microcosms are shown in Table 5.4. Eubacteria ranged from 9.1×10^5 to 4.7×10^6, Methanogen ranges from 2.6×10^6 to 1.3×10^7, and *Dehalococcoides* ranged from 2.4×10^3 to 3.4×10^3 cells per gram soil. Methanogens in the 60 % of BionSoil treatment is five times greater than sediment control treatment based on the real time PCR quantification. *Dehalococcoides* populations were not much different between the treatments.

Table 5.4 Real-time PCR quantification of bacteria, methanogen, and *Dehalococcoides*

	Eubacteria (cells/g)	Methanogen (cells/g)	*Dehalococcoides* (cells/g)
Sediment	9.1×10^5	2.6×10^6	3.4×10^3
BionSoil	4.7×10^6	4.2×10^6	2.8×10^3
Control	1.9×10^6	2.8×10^6	2.4×10^3
20 % of BionSoil	1.5×10^6	3.4×10^6	3.2×10^3
40 % of BionSoil	2.2×10^6	9.1×10^6	2.3×10^3
60 % of BionSoil	2.5×10^6	1.3×10^7	2.8×10^3

DGGE band profiles of the PCR amplification products extracted from microcosms and Anacostia sediment are shown in Figure 5.10. Comparing the banding patterns, BionSoil only, BionSoil treatment microcosm, control microcosm, and Anacostia sediment show different microbial compositions. The band (a) was significantly visible in the control microcosm and BionSoil treatment microcosm. The band (d) was prominent in the control treatment but not in any other microcosms. The band (e) was very intensive in BionSoil treatment microcosm and little in in the control treatment but not in any other microcosms. Different microbial communities were able to dechlorinate HCB and daughter products in control and BionSoil treatment microcosms. Microbial degradation could be occurred by different microbial consortia since HCB and daughter products dechlorinated in both control microcosms and BionSoil treatment.

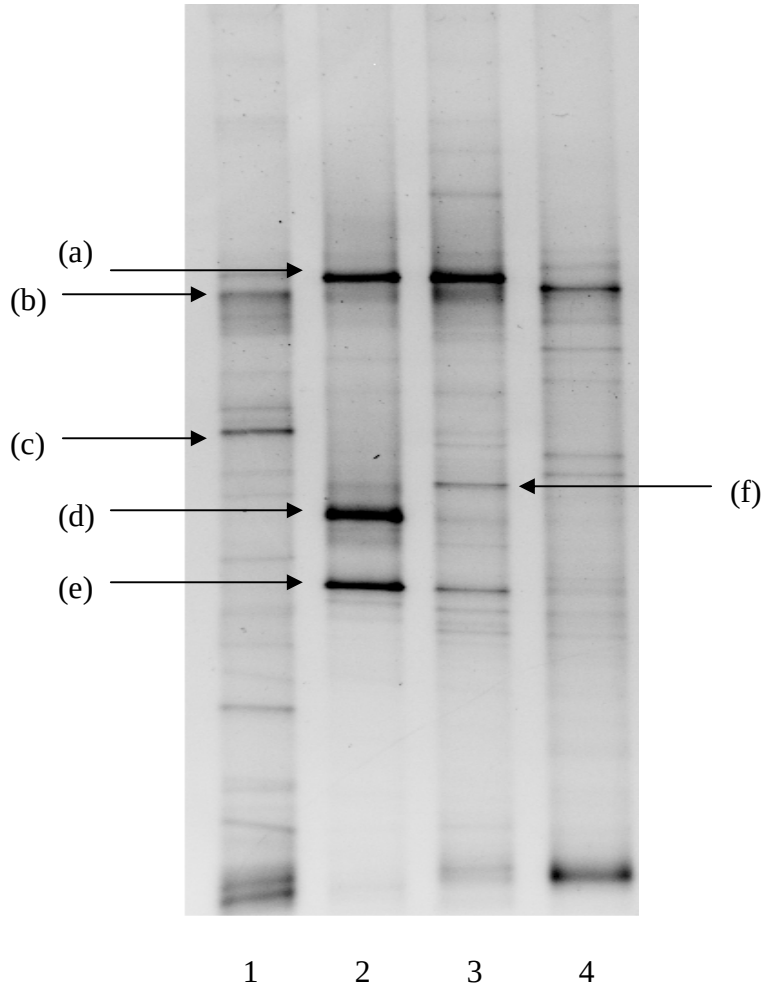

Figure 5.10 DGGE band – 1: BionSoil, 2: BionSoil treatment microcosm 3: Control microcosm (sediment only), and 4: Anacostia sediment

DNA sequences of the cloned DNA fragments were edited using Chromas software (http://www.mb.mahidol.ac.th/pub/chromas/chromas.htm) and was compared using BLAST (http://www.ncbi.nlm.nih.gov/BLAST/) maintained by the National Center of Biotechnology Information (NCBI) database. Table 5.5 shows that only one or two HCB dechlorinating bacterial strains was identified from sediment and microcosms.

Table 5.5 Bacterial identification by DNA sequencing

Starins (DGGE band)	Bacterial species (% homology)
(a)	*Actinomycete, Actinobacteria*
(b)	*Lactobacillus sp.* (100 %)
(c)	*Bacteroidetes bacterium, Pseudomonas synxantha*
(d)	*Desulfotomaculum sp., Clostridia bacterium*
(e)	*Pelobacter sp., Desulfuromonas sp.* (98 %)
(f)	*Clostridium sp.* (96 %)

The result of the microbial identification and DGGE profile indicated that microcosms closely related to bands (d) and (e) were present in BionSoil treatment microcosms. *Desulfotomaculum sp*. is representative of sulfate-reducing bacterium (Chang et al., 2001; Rios-Hernandez et al., 2003; Londry et al., 2004) that uses a plenty of substrates as electron donors from simple organic compounds to aromatic compounds. Sulfate, thiosulfate and sulfite are used as an electron acceptor. (Kuever et al., 1999). The characterization of both strains *Pelobacter sp*. and *Desulfuromonas sp.* are very similar. They participate in microbial manganese and sulfate

reduction also in dechlorination processes (Lorah and Voytek, 2004; Matsui et al., 2004). Bands (d) and (e) were may contributed the faster HCB dechlorination as BionSoil treatment microcosms in this study.

A phylogenetic tree is a graphical representation of the evolutionary relationship between taxonomic groups according to their similarities. Phylogenetic tree between microcosm treatments using Quantity One® 1-D analysis software was shown in Figure 5.9. It presents that how much similar in appearance and relatedness patterns between the microcosms. The higher similarity is 85 % of relationship between 60 % BionSoil treatment and 20 % BionSoil treatment microcosms. These two treatments also have 82 % of similarity with BionSoil. It indicated that BionSoil treatment microcosms were affected by adding the BionSoil. It is important to understand the phylogenetic tree generated by bioinformatics tools. And it is also true that sequence relatedness can be very powerful as a predictor of the relatedness of species.

Implication of BionSoil

BionSoil causes an effect on dechlorination in this study since it boosts soil organic matter and enhances soil microbes that facilitate HCB degrdation. These observations suggest that BionSoil has a capability to accelerate degradation by providing microbial source. Therefore, BionSoil ingredient probably changes microbial community. Many researches have been added nutrients or microbes to enhance the dechlorination ability. They presented that dechlorinating microbes, electron suppliers, sulfate reducers and denitrifying bacteria, all possibly caused a great effect on dechlorination (Chang et al., 1997; Chen et al., 2002). The microbial communities were important to dechlorinate HCB. And it is likely that other organisms were also involved, either directly or indirectly, in declining the HCB.

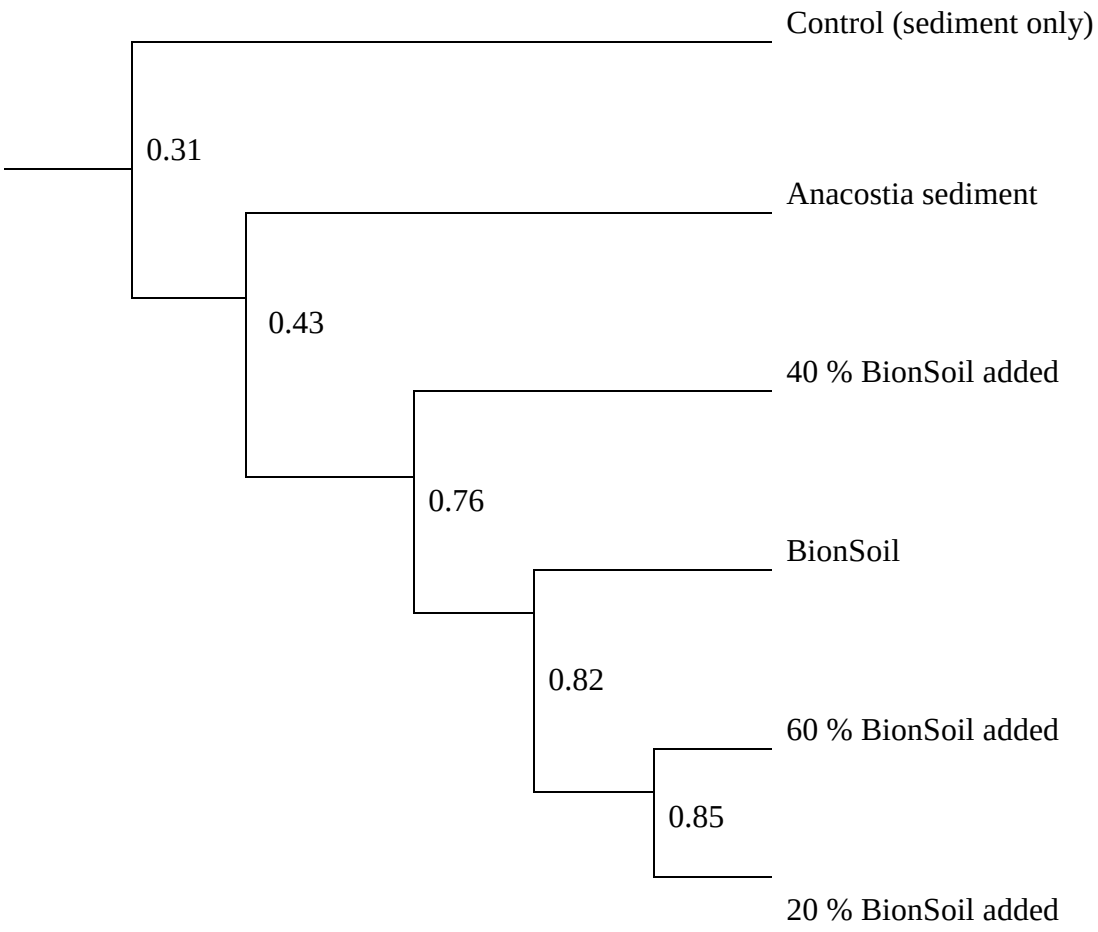

Figure 5.11 Phylogenetic tree using Quantity One® 1-D analysis software

Conclusions

The transformation of HCB in Anacostia was mainly due to reductive dechlorination. The complete dechlorination of the parent compound and daughter products were observed and proceeded faster as the percentage of the compost increased. The first order rate constants of parent compound in the sediment ranged 0.0058 to 0.0138 day^{-1}. The dominant pathway of HCB was: QCB → 1,2,4,5-TeCB + 1,2,3,5-TeCB → 1,3,5-TCB + 1,2,4-TCB → 1,3-DCB + 1,4-DCB → MCB and benzene. Degradation of parent and intermediate compounds (HCB, PCB, TeCB, TCB, and DCB) were observed faster under sulfate reducing conditions followed by methanogenic conditions while end product (MCB and benzene) degradation was occurred under methanogenesis. Hydrogen concentration trends also suggested that hydrogen was probably used as an electron donor during both sulfate reduction and methanogenesis to drive dechlorination.

The results of microbial analysis showed that different microbial composition and diversities were able to dechlorinate HCB under anaerobic condition. Highly organic rich soil, BionSoil, probably changed the microbial community and facilitated dechlorination. HCB was able to dechlorinate completely in BionSoil treatment microcosms. These observations provide strong evidence for the application of bioremediation. In addition, BionSoil was found to be a very promising material for *ex-situ* bioremediation of chlorinated solvents contaminated sites.

CHAPTER 6
SORPTIVE REACTIVE CAPPING OF PHENANTHRENE IN ANACOSTIA SEDIMENTS

Introduction

Polycyclic aromatic hydrocarbons (PAHs) have been widely distributed in the environment as a product of incomplete combustion of fossil fuels, vehicular emissions, coal and oil burning, wood combustion, coke plants, aluminum plants, iron and steel works, foundries, municipal incinerators, and oil shale plants and has been identified in ambient air, surface water, tap water, wastewater, drinking water, and dried lake sediments. The pollution of PAHs causes a serious risk to environment, and to human health due to direct exposure or through the food chain (U.S. EPA, 1987; Gao and Zhu 2004, 2005; Saison et al., 2004). Understanding of the fate of organic contaminants such as phenanthrene in environment is important to remediation strategies for contamination.

Reactive capping techniques, both containment and treatment, are very effective of managing the sediments that risk the health of national waterways (Reible et al, 2004; Reible and Lowry, 2005). Reactive capping designed to allow contaminants to pass through. The sediment-water interface provides opportunities for economic placement of a treatment barrier to encourage contaminant degradation, sorption or sequestration prior to release to the overlying water (Reible and Lowry, 2005). The contaminants with alternative materials, such as AquaBlook, Zero-valent iron, Apatite, and BionSoil, can degrade or control more efficiently than sand. Capping with sand are not considered in many areas subject to groundwater upwelling or tidal pumping due to the potential for contaminant mobility and flux to the overlying water. Sand caps are used to retard migration of contaminants from sediments by physically separating contaminants from organisms and the water column (Palermo et al., 1998). Reactive caps

encourage the fate processes such as degradation or sequestration of the contaminants beneath cap and discourage recontamination of cap. The reactive capping can be extremely effective at reducing the exposure and risk of contaminated sediments. Such a cap is to ensure elimination of migration through a cap or sorption, chemical fixation or degradation of any contaminants that may migrate.

The effectiveness of reactive cap using BionSoil on bioavailability of phenanthrene in the Anacostia River sediment was investigated in this study. BionSoil has potential for nutrient release and is effective primarily against chlorinated organics and hydrocarbons so, contaminants subject to anaerobic degradation. BionSoil facilitates sorption of contaminants and can provide a source of carbon for bacteria in waste treatment systems and it has high organic matter and nutrient content. BionSoil encourages degradation of organic contaminants through enhancement of reductive dechlorination and anaerobic degradation of PAH compounds.

Adsorption isotherms were determined for phenanthrene in mixtures of different ratios of BionSoil and Anacostia River sediment in order to evaluate the effect of BionSoil as a sorbent. The objective of these experiments was to determine the partiotion coefficient of phenanathrene in the target sediment and water. In addition, fluxes of phenanthrene from Anacostia River sediment were measured to evaluate the bioavailability of the contaminants.

Materials and Methods

Sediments and Chemicals

The Anacostia River in Washington, DC is a freshwater, tidal river draining an urban watershed encompassing 176 square miles in Maryland and the District of Columbia. The site sampled is the location of a field reactive capping experiment conducted through the EPA-fended Hazardous Substance Research Center-South & Southwest (http://www.hsrc-ssw.org/ana-

index.html). The site is near the combined sewer overflow at the western end of the Washington Navy Yard. The Anacostia River watershed has historically included unacceptable industrial, municipal, and military activities, which have resulted in levels of PAHs, polychlorinated biphenyls (PCBs), metals, and other contaminants. The sediments used in this study were collected from the Anacostia River and delivered to the laboratory in sealed five gallon buckets. Sediment preparation was described in detail in Chapter 4.

The total PAH concentrations raging from 1366 to 2350 (μg/Kg) were detected in the Anacostia sediment. The major components, 200 (μg/Kg) of phenanthrene, 360 (μg/Kg) of pyrene, 280 (μg/Kg) of chrysene, 220 (μg/Kg) of fluoranthene, and 36 (μg/Kg) of benzo(α)pyrene were measured from Anacostia sites (Phelps, 2002). Significant PAH contamination appeared widespread in the Anacostia sites. Phenanthrene was selected as test chemical of representative PAH in this reactive capping study. Phenanthrene (CAS No. 85-01-8) is a polycyclic aromatic hydrocarbon (PAH) with three aromatic rings. It has a chemical formula of $C_{14}H_{10}$, a molecular weight of 178.22, and exists as a colorless crystalline solid (U.S. EPA, 1987). It has a density of 1.179 (g/cm^3) and a vapor pressure of 6.8×10^{-4} mmHg at 25ºC. Phenanthrene is almost insoluble in water (1-1.6 mg/L), but is soluble in glacial acetic acid and a number of organic solvents including ethanol, benzene, carbon disulfide, carbon tetrachloride, diethyl ether, and toluene. Phenanthrene has a log octanol/water partition coefficient of 4.45-4.57 (U.S. EPA, 1987).

Sorption and Desorption Experiments

Batch experiments were conducted to determine phenanthrene sorption in slurries prepared by mixing various concentrations of sediment and the proposed capping material, BionSoil. Varied volumes of BionSoil were added to 50 mL Teflon tubes to measure the sorption

potential of this product. Approximately 5 g (dry weight) of Anacostia sediment was placed in a Teflon test tube followed by a 100 ppm of phenanthrene-spiked electrolyte solution (0.01 M $CaCl_2$), 10 mM of sodium azide, and 5 mM of sodium molybdate inhibitor to prevent phenanthrene biodegrading through sulfate reduction. Teflon centrifuge tubes were sealed with Teflon caps to minimize headspace and tumbled for 48 hours. Following that, the test tubes were centrifuged and the supernatant was extracted to remove the water and analyzed with gas chromatography mass spectroscopy (GC/MS) to determine the phenanthrene concentrations. Four phenanthrene concentrations were used to develop the isotherm. Concentrations were generated by diluting phenanthrene solutions with the electrolyte solution described above to the following ratios 1:1, 1:2, 1:5, and 1:10. Three replicate vials were used for each isotherm point. The amount of PAH sorbed in the sediment was estimated by subtracting the measured final PAH concentration of the aqueous-phase from the initial PAH aqueous-phase concentration.

Sorption experiments were conducted in solutions of initial concentrations which were well below the limit of solubility at 20°C, obtained by dilution of stock solutions. The criteria for selection of the concentrations was that the highest concentration was at least 20 times greater than the lowest concentration, and that the highest concentration did not exceed two third of the solubility of the test chemical. The aqueous solubility of phenanthrene is 1170 μg/L. (Maad et al. 1998). Because phenanthrene has a low solubility, solvents were used to prepare initial stock solutions. Methanol was used in this study. To minimize the effects of solvents on the sorption of the test chemicals, minimum amounts of solvent were used in preparing solutions. Total methanol or methylene chloride solvent in each centrifuge tube was below 0.02 % of total solution volume (Zhao et al., 2002). The measurement of partitioning of phenanthrene was performed. Mass of the chemical adsorbed was calculated a using mass balance equation:

$$q_e = \frac{(C_0 - C_i)}{W} V$$

where q_e is the mass of chemical sorbed per unit mass of soil, C_0 is the initial aqueous-phase concentration of the chemical, C_i is the equilibrium aqueous-phase concentration of the chemical, W is dry weight of the sediment; and V is the volume of solution. A plot of the concentration of contaminant sorbed, q_e versus dissolved equilibrium concentration C_e, was made using the data for each reaction vial. The isotherms were used to describe the data; a linear isotherm and the Freundlich isotherm. The sorption distribution coefficient K_d in a linear sorption model can be described by

$$K_d = \frac{q_e}{C_e}$$

where q_e is the mass of chemical sorbed per unit mass of soil and C_e is the equilibrium concentration. Nonlinear isotherms can be described by the Freundlich equation.

$$q_e = K_F C_e^N$$

where K_d is the Freundlich sorption constant and N is the Freundlich exponent.

The retardation coefficient R is calculated as follows

$$R = \left(1 + \frac{\rho_b}{\eta} K_d \right)$$

where ρ_b is the bulk density of the medium, η is the porosity, K_d is the linear distribution coefficient.

Desorption of the phenanthrene from Anacostia sediment and BionSoil mixture was determined with various phenanthrene concentrations using the same batch technique. The

concentrations of phenanthrene desorbed from the originally PAH-contaminated river sediment were monitored over time. After adsorption was completed, the tube was centrifuged and the electrolyte solution was replaced every 24 hours. Teflon tubes were sealed with Teflon caps and tumbled for 24 hours. The analytical procedures for phenanthrene are as described above for the sorption experiments.

Flux Measurements

Laboratory scale flux chambers illustrated in Figure 6.1 were used to evaluate the potential fluxes of PAHs with BionSoil as a capping material under continuous flow. The two flux chambers; one for uncapped Anacostia River sediment and one for BionSoil-capped Anacostia River sediments were set up based on a previous design (Qaisi et al., 1996). The dimensions of the flux chamber (Figure 6.1) were 5 cm depth, 5 cm width, and 50 cm in length. The chambers were first packed as sediment bed, 1.5 cm of contaminated sediment layer and the followed by 1.5 cm of BionSoil as a cap layer. The control uncapped bed chamber was packed as 3 cm of contaminated sediment layer. As the water flowed over and through the bed, contaminants leached from the sediment into the water. Water was pumped onto the chamber at a flow rate of 3.0 ± 0.15 mL/min. An outlet was located at the end of the bed for sampling. Experiments were continued until parameters reached steady state for 160 hours.

The experimental flux rates ($g \cdot m^{-2} \cdot d^{-1}$) were calculated based on concentrations in the overlying water using the following equation.

$$Flux(g \cdot m^{-2} \cdot d^{-1}) = Q \cdot C/A$$

where Q is the volumetric flow rate (L/hr), C is concentration (mg/L), A is area of the bed surface (cm^2). The experimental flux rates were compared between uncapped Anacostia River sediment and sediments with BionSoil caps.

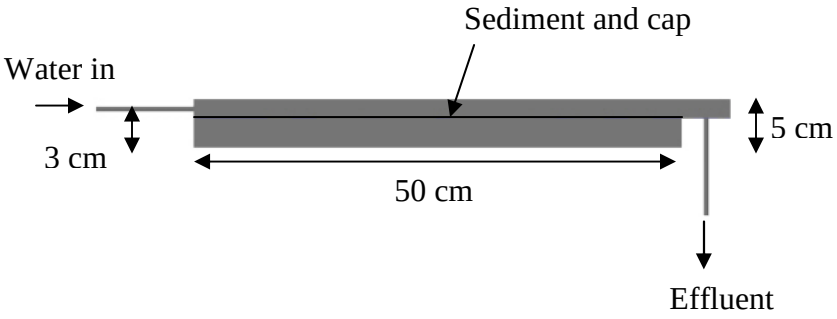

Side View

Top View

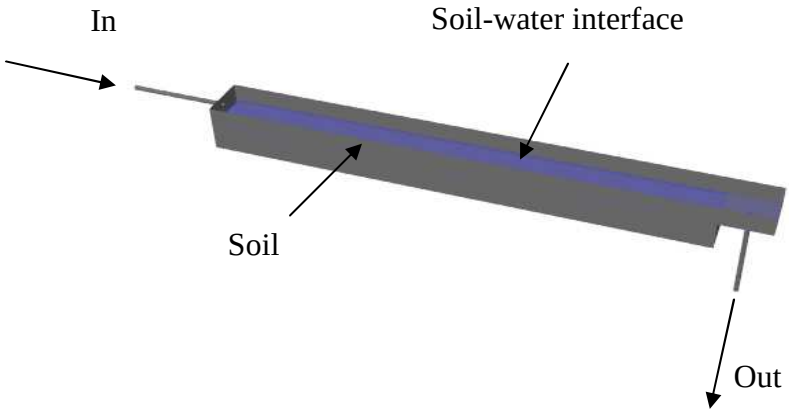

Figure 6.1 Laboratory Flux Chamber

Samples were taken from the overlying water, capping layer, and sediment every 6 hours to monitor the migration of contaminants and degradation of contaminants in each layer. Sediment samples were taken spoonful of soils from cap layer using the spatula and dug under the cap and scooped out from sediment. Sampling was conducted from three positions for triplicate analyses. Soil and sediment samples were transferred into scintillation vials and analyzed for phenanthrene, pyrene and chrysene concentrations as described below. Effluent samples were collected from the outlet of the flux chamber to monitor the potential for fluxes of nitrate, ferric iron, manganic manganese and sulfate at regular intervals.

Analyses

Sediment samples were mixed with a hexane/acetone mixture (1:1 (v/v)) in 50 mL Teflon centrifuge tubes. The mixture was tumbled to homogenize for 24 hrs. After centrifugation, the supernatant was passed through sodium sulfate to remove the remaining water. Samples were transferred into glass scintillation vials and concentrated for GC analyses. PAH extracts were analyzed using a Hewlett Packard 5890A gas chromatograph (GC) coupled with a HP 5971 mass selective (MS) detector equipped with a 30 m $\times$ 250 μm $\times$ 0.25 μm film thickness capillary column. One μL of the sample was injected automatically onto the column. GC temperature program conditions were 55°C and ramped at 10°C/min to 200°C then at 4°C/min to 300°C and held for 10 minutes. The mass spectrometer was operated in the electron impact ionization mode and the ion source temperature was 280°C. PAH components were quantified in the selected ion monitoring mode with a semivolatile internal standard (Supelco, Bellefonte, PA).

The concentrations of nitrate, ferric iron, manganic manganese, and sulfate were measured by colorimetric methods. The Hach 2010 analyzes for nitrate concentrations within range of 0 to 45 mg/L NO_3^--N. Concentrations of NO_3-N were read directly by adding the Hach,

NitroVer5 “powder pillow” to the samples and inserting them into the spectrophotometer. The ferric iron concentrations are differences between total iron concentrations and ferrous iron concentrations. Total iron concentrations were read directly by adding the Hach, FerroVer Iron Reagent and ferrous iron concentrations were read by adding the Hach, Ferrous Iron Reagent. The manganic manganese concentrations are differences between total manganese concentrations and manganous manganese concentrations. Total manganese concentrations were measured by PAN method and soluble manganese concentrations were measured by periodate oxidation method. The Hach 2010 analyzes for sulfate concentrations within range of 0 to 70 mg/L SO_4^{2-}-. Sulfate concentrations of were read directly by adding the Hach, SulfaVer4 “powder pillow” to the samples and inserting them into the spectrophotometer.

Modeling

Contaminants in the sediment will dissolve and desorb in the water, migrate, and contaminate surface or ground waters. The diffusive transport processes of phenanthrene release from sediment were examined using the laboratory scale flux chamber and compared the efficiency between sediment with BionSoil cap and sediment without cap. Here, RECOVERY version 4.3.1 developed by U.S. army engineer research and development center (Vicksburg, MS), mathematical model was used to predict the temporal response of surface water to contaminated sediments. A modeling framework designed to assess the impact of contaminated bottom sediment on surface waters. The analysis is limited to cases where the overlying water is well-mixed. In addition, the contaminant is assumed to be organic and to follow reversible linear equilibrium sorption and first-order decay kinetics (Luiz and Terry, 2001). A list of assumptions used in the development of this model is shown in Table 6.1.

Table 6.1 Assumptions used in the development of RECOVERY (Luiz and Terry, 2001)

Assumptions
Contaminant is of organic nature.
The water body is well-mixed.
The mixed layer is well-mixed.
In the deep sediments, contaminant concentration varies in the vertical direction only.
The initial concentration of the contaminant in the region below the contaminated region is zero.
The contaminant follows a linear reversible equilibrium sorption mechanism.
The contaminant decays according to first-order kinetics.
There is no compaction in the sediments.
The system is isothermal.
The water body is at 25 ˚C.
Flowthrough is constant.
Only single-component mass transfer is described. The movement of the contaminant is independent of the presence of other contaminants.

The contaminant mass balance in the water can be written as

$$V_w \frac{dc_w}{dt} = Qc_i - Qc_w - k_w V_w c_w - k_v V_w c_w - v_s A_w F_{pw} c_w + v_r A_m c_m + v_d A_m \left(F_{dp} c_m - F_{dw} c_w\right) + W$$

where V_w = volume of water body (m^3), c_w and c_m = concentrations of contaminant in water and mixed sediments, respectively ($\mu g/m^3$), c_i = inflow concentration ($\mu g/m^3$), t = times (years), Q = flow rate (m^3/yr), k_w = decay rate constant of contaminant in water (yr^{-1}), k_v = volatilization rate of contaminant (yr^{-1}), v_s = settling velocity of particulate matter (m/yr), A_w and A_m = surface areas of water and mixed sediment, respectively (m^2), F_{pw} = fraction of

contaminant in particulate form in the water, v_r = resuspension velocity of sediments (m/yr), v_d = diffusion mass-transfer coefficient at the sediment-water (m/yr), F_{dp} = ratio of contaminant concentration in the sediment pore water to contaminant concentration in total sediment, F_{dw} = fraction of contaminant in dissolved form in the water, W = external loads (μg/yr).

A mass balance for the mixed-sediment layer can be written as

$$V_w \frac{dc_m}{dt} = k_m V_m c_m + v_s A_w F_{pw} c_w - v_r A_m c_m - v_b A_m c_m + v_d A_m \left(F_{dw} c_w - F_{dp} C_m\right) + v_d A_m \left(F_{dp} c_s(0) - F_{dp} c_m\right)$$

where V_m = volume of mixed layer (m^3), k_m = decay rate constant of contaminant in the mixed layer (yr^{-1}), v_b = settling velocity (m/yr), $c_s(0)$ = the contaminant concentration at the top of the deep contaminated layer (($\mu g/m^3$).

The contaminated sediment can be modeled with one-dimensional advection-diffusion-decay equations of the form

$$\frac{\partial c_s}{\partial t} = \phi F_{dp} D_s \frac{\partial^2 c_s}{\partial z^2} - v_b \frac{\partial C_s}{\partial z} - k_s c_s$$

where c_s = the contaminant concentrations in the sediments ($\mu g/m^3$), ϕ = sediment porosity, D_s = diffusion rate in the sediment pore water (m^2/yr), z = depth into the sediment, k_s = decay rate constant of contaminant in the sediments (yr^{-1}).

The differential equations are solved numerically. Recovery version 4.3.1 is written in Fortran 77. The calibrated models to experimental data could estimate contaminant release rates in similar system and Anacostia River condition. The parameters used in model in laboratory scale flux chamber, Anacostia reactive caps, and Anacostia sand caps are listed in Table 6.2, 6.3, and 6.4, respectively.

Table 6.2 Input parameters for phenanthrene transport mathematical model (Lab scale)

	Parameters	Value
Water layer	suspended solid concentrations (mg/L)	0.0001
	weight fraction carbon	0.0001
	water surface area (m^2)	0.026
	water depth (m)	0.002
	flow (m^3/yr)	1.58
	residence time (yr)	3.29 e^{-5}
Mixed (cap) layer	contaminated sediment depth (m)	0.03
	mixed sediment depth (m)	0.015
	surface area (m^2)	0.026
	carbon fraction	0.4
	porosity	0.5
	specific gravity	1.2
Contaminated sediment	porosity	0.3
	specific gravity	2.04
System properties	wind (m/s)	0.0001
	resuspension velocity (m/yr)	0.0002
	burial velocity (m/yr)	0.00064
	settling velocity	5040000
phenanthrene	initial concentration	0
	initial concentration in mixed	0
	initial concentration in contaminated (mg/Kg)	17
	diffusion coefficient	5 E-6
	Henry's	2.3 E-5
	molecular weight	178
	octanol water partition	28800
Model	simulation (yrs)	1
	time steps	100

Table 6.3 Input for phenanthrene transport mathematical model (Anacostia reactive caps)

	Parameters	Value
Water layer	suspended solid concentrations (mg/L)	30
	weight fraction carbon	0.05
	water surface area (m^2)	10000
	water depth (m)	3
	flow (m^3/yr)	0.001
	residence time (yr)	30000000
Mixed (cap) BionSoil	contaminated sediment depth (m)	1
layer	mixed sediment depth (m)	0.01, 0.05, 0.1, 0.2
	surface area (m^2)	10000
	carbon fraction	0.4
	porosity	0.5
	specific gravity	1.2
Contaminated sediment	porosity	0.3
	specific gravity	2.04
System properties	wind (m/s)	1
	resuspension velocity (m/yr)	0.0002
	burial velocity (m/yr)	0.00064
	settling velocity	16.8
phenanthrene	initial concentration	0
	initial concentration in mixed	0
	initial concentration in contaminated (mg/Kg)	100
	diffusion coefficient	5 E-6
	Henry's	2.3 E-5
	molecular weight	178
	octanol water partition	28800
Model	simulation (yrs)	200
	time steps	100

Table 6.4 Input for phenanthrene transport mathematical model (Anacostia sand caps)

	Parameters	Value
Water layer	suspended solid concentrations (mg/L)	30
	weight fraction carbon	0.05
	water surface area (m^2)	10000
	water depth (m)	3
	flow (m^3/yr)	0.001
	residence time (yr)	recalculate
Mixed (cap) layer	contaminated sediment depth (m)	1
	mixed sediment depth (m)	0.01, 0.1
	surface area (m^2)	10000
	carbon fraction	0
	porosity	0.5
	specific gravity	2.65
Contaminated sediment	porosity	0.3
	specific gravity	2.04
System properties	wind (m/s)	1
	resuspension velocity (m/yr)	0.0002
	burial velocity (m/yr)	0.00064
	settling velocity	37.1
phenanthrene	initial concentration	0
	initial concentration in mixed	0
	initial concentration in contaminated (mg/Kg)	100
	diffusion coefficient	5 E-6
	Henry's	2.3 E-5
	molecular weight	178
	octanol water partition	28800
Model	simulation (yrs)	200
	time steps	100

Results and Discussion

Sorption and Desorption Potential

Sorptive potential of the sediment and BionSoil was determined using the batch technique. Batch testing involved adding soil to a number of vials, adding solutions prepared using various concentrations (0.1, 0.2, 0.5, and 1 ppm) of phenanthrene to produce varying solute concentrations, sealing the vial and shaking it until equilibrium is reached, analyzing the solute concentration remaining in solution, and calculating the amount of contaminant sorbed to the soil matrix using mass balance equations. A plot of the concentration sorbed versus dissolved equilibrium concentration was made using the data for each reaction vial (Wiedemeier et al. 1996). The slope of the line (linear model) formed by linear regression was the sorption distribution coefficient. Alternatively, the Freundlich sorption model was used when non-linear relationships between sorbed and aqueous concentrations of the contaminant of interest were encountered. Sorption data was modeled using either linear or Freundlich sorption models.

Results of the linear K_d values (sediment:water partition coefficients) for phenanthrene from different BionSoil and Anacostia sediment mixtures are presented in Table 6.5. The K_d value of BionSoil (127.4 L/Kg) exceeded the K_d of Anacostia sediment alone by a factor of ~6. This is due to the presence of much high organic carbon content in the BionSoil matrix resulting in much higher sorption potential for this material.

Retardation coefficient of contaminant for phenanthrene in the sediment mixtures ranges from 139.72 to 351.78. Computed retardation coefficients of sediment for phenanthrene are similar to those reported by Dohse and Lion (1994) from low-carbon sand. Hydrophobic compounds tends to have high sorption coefficient, it means, have high retardation coefficients (PAH and PCB: greater than 100) rather than those of soluble compounds (TCE: 1-5 and PCE: 1-

3.78). It was observed that higher ratios of BionSoil have significantly higher retardation coefficients than lower ratios of BionSoil.

Table 6.5 K_d value for phenanthrene among different treatments using linear model

Treatments	Sediment	20 % BionSoil	40 % BionSoil	60 % BionSoil	BionSoil only
$K_d\ (L/Kg)$	20.4	52.7	88.9	112	127.4
R^2	0.88	0.98	0.92	0.95	0.89
R	139.72	199.36	307.53	351.78	318.99

Table 6.6 K_F value for phenanthrene among different treatments using nonlinear Freundlich model

Treatments	Sediment	20 % BionSoil	40 % BionSoil	60 % BionSoil	BionSoil only
$K_F\ (L/Kg)$	11.37	33.41	96.20	97.81	152.9
N	0.74	0.85	0.86	0.75	0.64
R^2	0.93	0.97	0.95	0.98	0.99

The nonlinear Freundlich sorption models are presented in Table 6.6 and nonlinear model of BionSoil is shown in Figure 6.2. Both the linear and nonlinear Freundlich models fit well (R^2>0.88). The K_F value for BionSoil is taken from Figure 6.6 as follows: 152.9 of K_F, 0.64 of N, and 0.99 of R^2. Again, the behavior is similar with highest K_d value in BionSoil treatment and Anacostia sediment having the lowest. This is attributed to the effect of the organic BionSoil. The organic matter plays a significant role in sorptive behaviors of sediments.

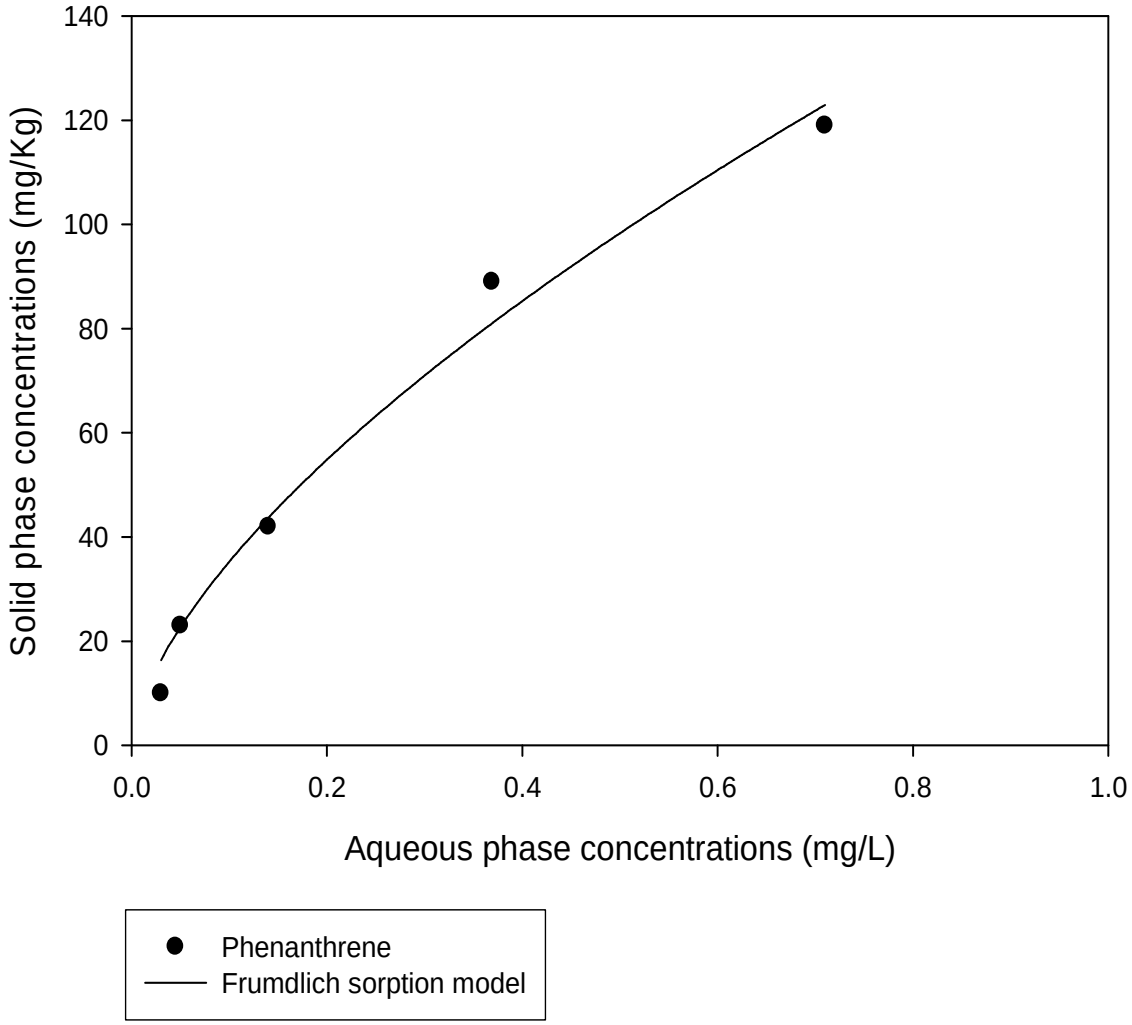

Figure 6.2 Nonlinear Freundlich sorption model for Bionsoil

Additional experimental K_d values using the ^{14}C-phenanthrene are presented in Table 6.7. The K_d value for Anacostia sediment is shown as 34.6 L/Kg and BionSoil had a 51.9 L/Kg using the linear model while K_F values were 12.5 L/Kg of Anacostia sediment and 102.7 L/Kg of BionSoil using the nonlinear Freundlich model using the ^{14}C-phenanthrene. The nonlinear Freundlich sorption fit is better for BionSoil sorption. The nonlinear Freundlich sorption model using the ^{14}C-phenanthrene is presented in Figure 6.3.

Table 6.7 Sediment and water partition coefficient using ^{14}C-phenanthrene

Treatments	Linear model		Nonlinear Freundlich model		
	$K_d\ (L/Kg)$	R^2	$K_F\ (L/Kg)$	N	R^2
Sediment	34.55	0.97	12.46	1.42	0.99
BionSoil	51.87	0.90	102.70	0.70	0.98

Studies of sorption and desorption of phenanthrene showed that an apparent steady state was reached within 3 days in Figures 6.4 and 6.5. The sediment and water partition coefficients were examined between Anacostia sediment and BionSoil at different concentration of phenanthrene in Figure 6.4. The comparison of the higher concentration to the lower concentration for phenanthrene component indicates a higher K_d value for the higher concentration of chemicals. In other words, more water per mass was required to move the same amount of contaminants.

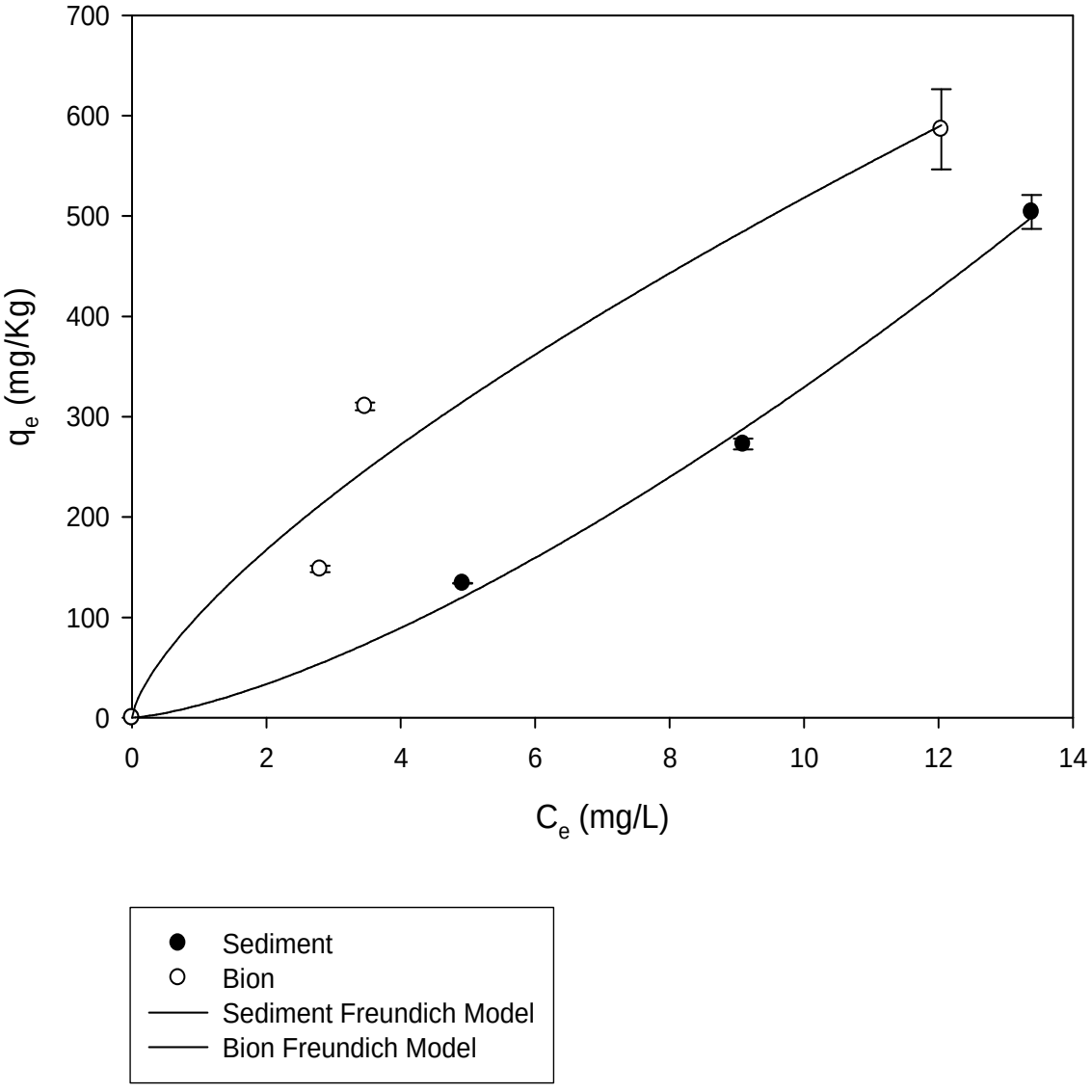

Figure 6.3 Freundlich sorption model using ^{14}C-phenanthrene

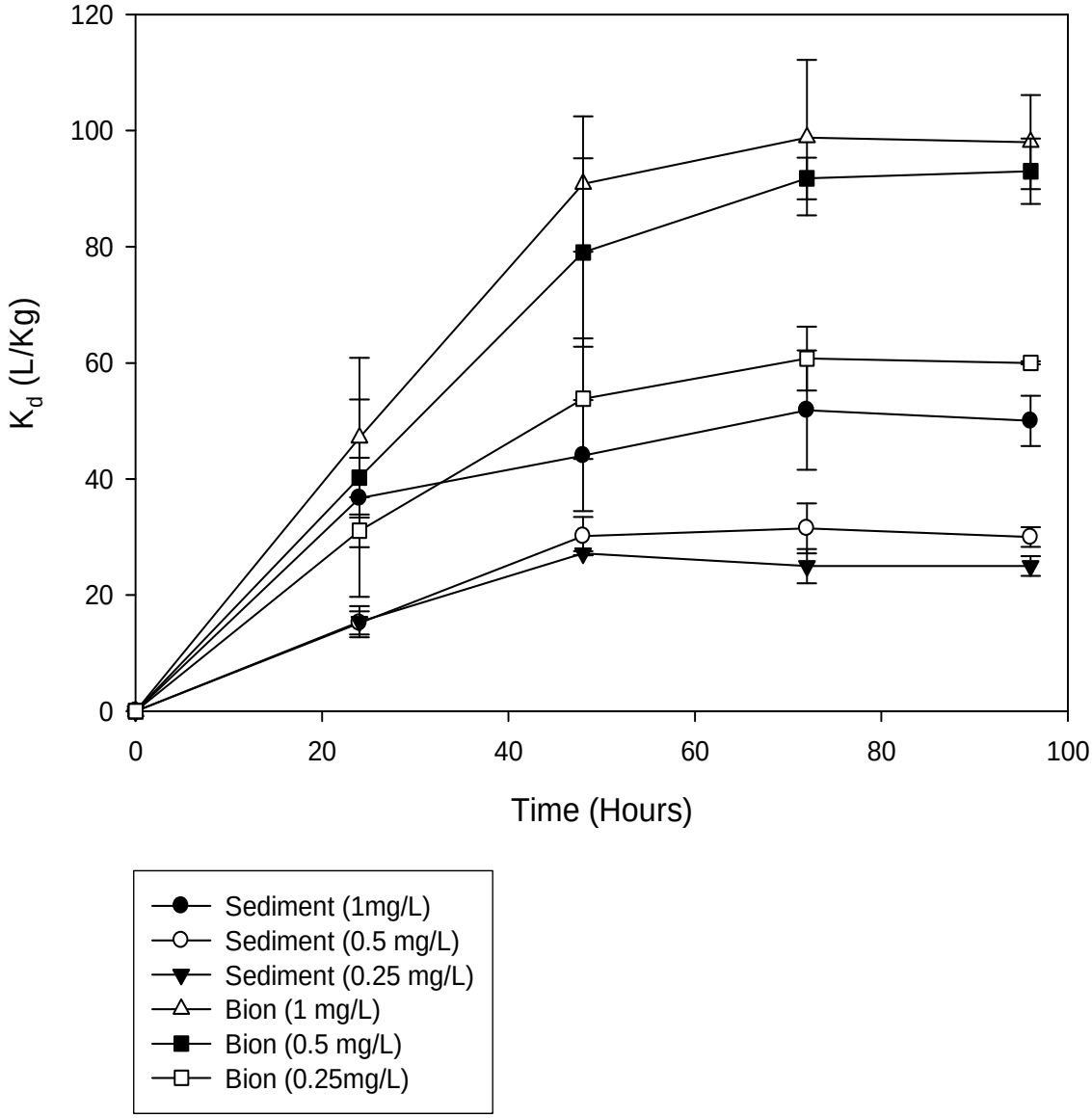

Figure 6.4 Partition coefficients as function of time

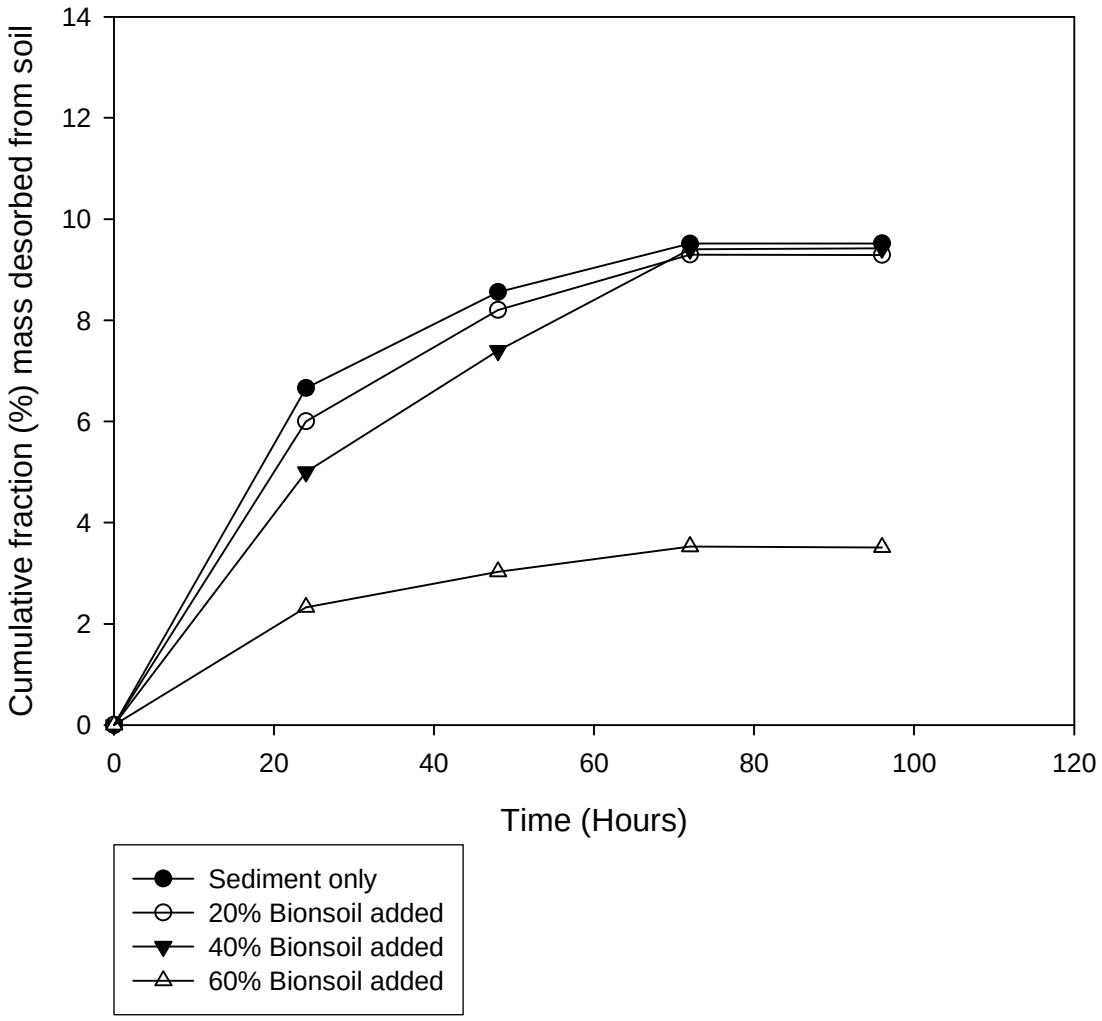

Figure 6.5 Desorption in different treatments

Desorption behavior for phenanthrene among different treatments was shown in Figure 6.5. At the apparent steady state, approximately 9 % of phenanthrene was desorbed from Anacostia sediment while only 3 % of phenanthrene was desorbed from the 60 % of BionSoil and sediment mixture treatment. As shown, as the BionSoil percentage in the treatment decreased, greater desorption occurred. Release of phenanthrene from the Anacostia sediment was faster than the release of phenanthrene from the BionSoil and sediment mixture treatments.

Flux Measurements

As previously mentioned, the experimental flux rates were compared between Anacostia River sediment and sediments with BionSoil caps. The aqueous samples and sediment samples were analyzed for the phenanthrene, pyrene and chrysene concentrations. The release of contaminants was quantified by computing flux rates. The goal of study was to quantify the diffusion flux rates of nitrate, nitrite, manganese, ferric iron, and sulfate from a bed of Anacostia sediment and sediment with BionSoil cap. The aqueous samples were analyzed for nitrate, manganic manganese, ferric iron, and sulfate concentrations and fluxes.

The PAH concentrations were observed both lower concentrations in BionSoil cap layer and higher concentrations in sediment layer in Figure 6.6 and 6.7 respectively. The concentration plots follow a similar pattern which PAH components are degraded efficiently. Around 75 % of PAHs were removed in sediment layer in the bed composed of sediment with BionSoil cap. In addition, around 85–100 % of PAHs were removed in the BionSoil cap layer. The degradation occurred not only in the sediment layer but also in BionSoil cap layer. The BionSoil cap layer was expected clean initially but, there are PAHs in the cap layer. The BionSoil appeared to sorb the contaminant initially during the sediment and cap bed were settled down. Based on biodegradation microcosms (Chapter 4), PAH concentration decreased in sediment mixing with

BionSoil because the PAH contaminant transferred into BionSoil matrix by its high sorption potential and degradation capability. While PAH degradation occurred significantly in the sediment with BionSoil cap layer, PAHs were not changed in the sediment only without cap (Figure 6.9). In addition, trace of PAH was detected in the water column in the BionSoil cap shown in Figure 6.8.

The spikes in the concentrations of the PAHs, especially phenanthrene (Figures 6.8) of the experiment are contrary to what was expected. The concentrations were expected to decrease with time until they reached non-detectable levels. Considering that within the cap and sediment materials water was practically stationary during the experiment, the main mechanism for the transfer of the PAHs within these layers was diffusion, which is concentration gradient-controlled. On the other hand, within the water column both diffusion and advection are likely to have been effective (Charbeneau, 2000).

Therefore, the spikes in PAH concentrations can be attributed to: 1) changes in geotechnical and hydrodynamic properties of the cap and sediment materials under the influence of the column of flowing water; 2) scouring and channeling of the cap layer with resultant preferential flows, which coupled with heterogeneities within the cap and sediment materials would have resulted in a temporal variation in the fluxes of the PAHs; and 3) changes in water flow rate due to blockage and wear and tear as well as manufacturing defects of the water conveyance tubing. The changes in the geotechnical and hydrodynamic properties of the cap and sediment materials would have affected, among others, water content, effective porosity, and density.

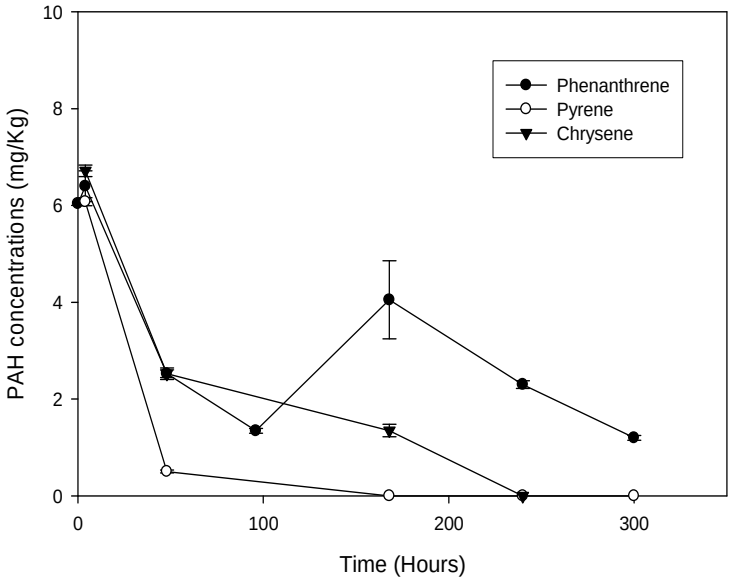

Figure 6.6 PAH concentrations of cap layer in the sediment with BionSoil cap

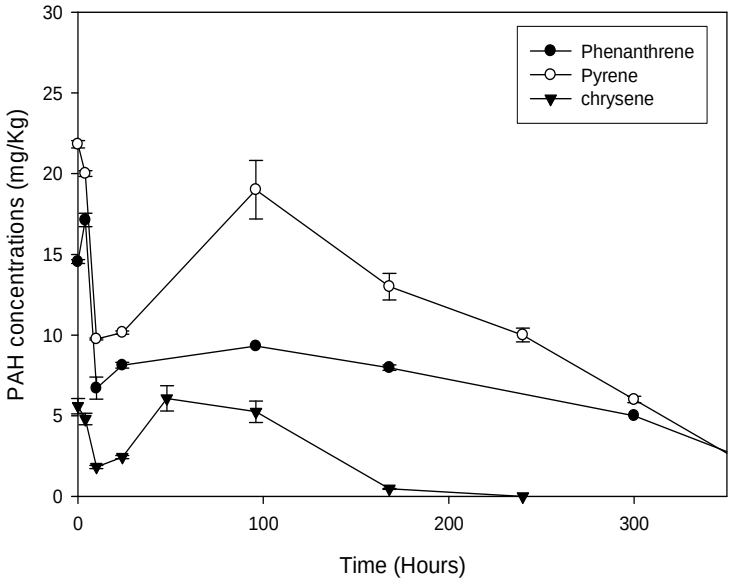

Figure 6.7 PAH concentrations of sediment layer in the sediment with BionSoil cap

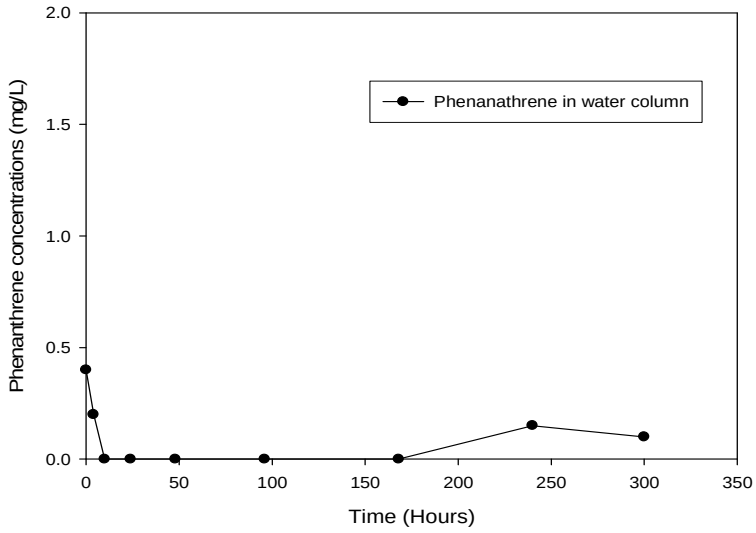

Figure 6.8 PAH concentrations of water column in the sediment with BionSoil cap

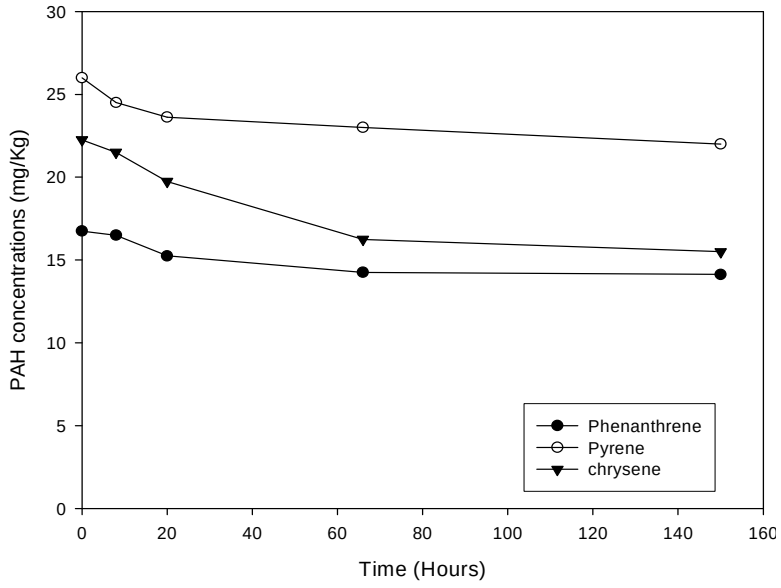

Figure 6.9 PAH concentrations in sediment only without cap

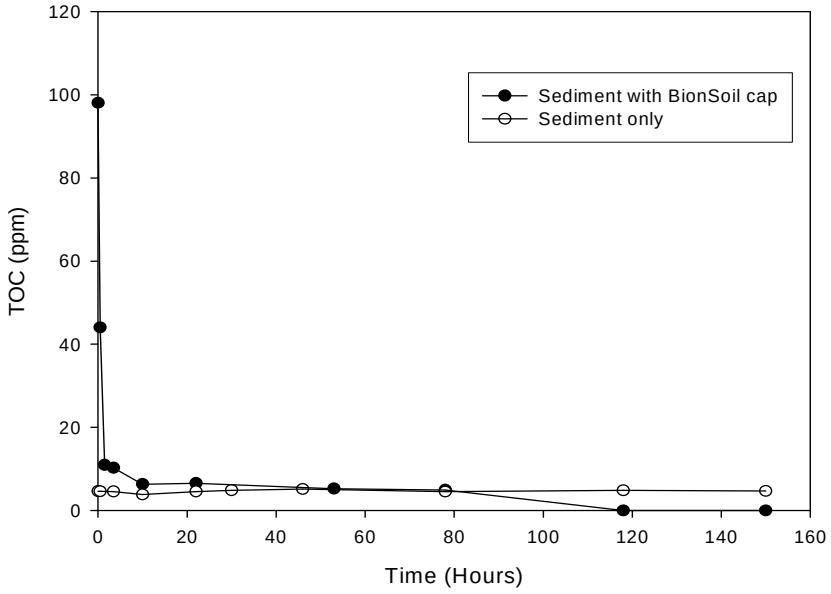

Figure 6.10 Aqueous TOC concentrations

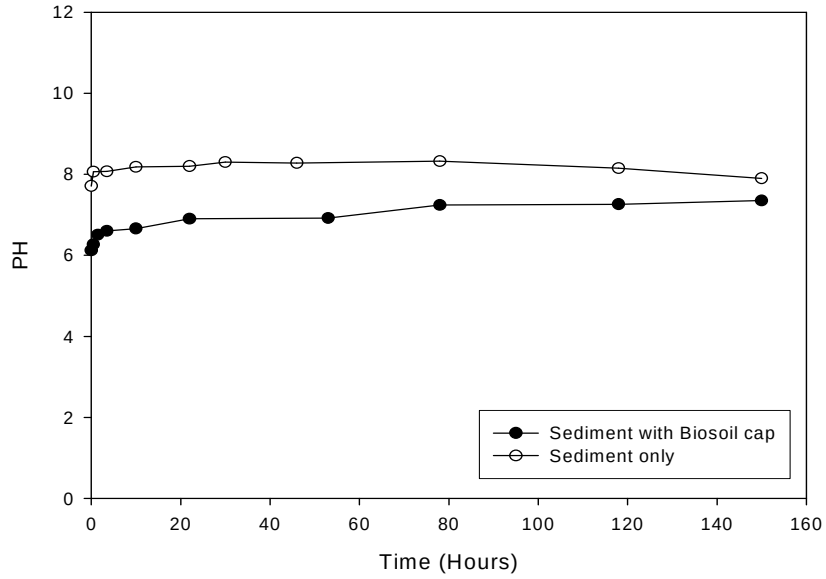

Figure 6.11 pH value comparisons

Aqueous total organic carbon (TOC) concentration and pH values are compared between Anacostia sediment with a BionSoil cap and Anacostia sediment alone in Figures 6.9 and 6.10. BionSoil is nutrient rich product and is sued as an organic soil amendment and fertilizer. It contains around 40-55 % of organic matter. Aqueous TOC concentrations are high initially in sediment with BionSoil cap treatment in comparison with the sediment only treatment. pH values in the BionSoil capped system averaged 6.2. BionSoil lowers the pH of the Anacostia sediment. pH in BionSoil cap is slightly lower because of organic acids from the biological processes.

The graphs are shown the nitrate flux, manganese flux, ferric iron flux, and sulfate flux in Anacostia sediment with BionSoil cap treatment in Figure 6.12, 6.13, 6.14, and 6.15 respectively. Figures show the typical shape of diffusion curves, with initially higher concentrations rapidly decreases to a steady state. They look very similar trends which decrease flux rate initially less than 10 hours and reached steady state flux rate. The plot is described by the transient initial desorption and advection removal of nitrate, manganese, ferric iron, and sulfate followed by steady state desorption flux rate. The Anacostia sediment and BionSoil release sulfate more rapidly as seen around 21 ($g \cdot m^{-2} \cdot d^{-1}$) the initial flux rate in the Figure 6.15. The sulfate flux rate value is high compared with manganese and iron. The flux rate points in the graphs are the average of three triplicates. The steady state concentrations of nitrite, manganese, and ferric iron are non detectable after 120 hours, with the final flux rates about 0.01 ($g \cdot m^{-2} \cdot d^{-1}$). In nitrate, around 0.65 ($g \cdot m^{-2} \cdot d^{-1}$) of flux rate was observed. Nitrate flux, manganese flux, ferric iron flux, and sulfate flux in Anacostia sediment without BionSoil cap treatment are shown in Figure 6.16 to 6.19. Initial flux rates are not changed to the end of monitoring time. The flux rate is significantly different between sediment with cap treatment and sediment without cap.

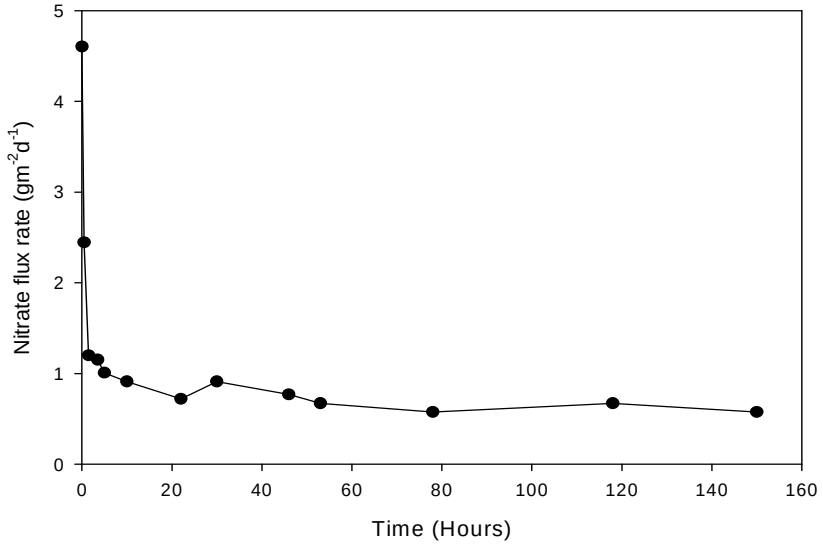

Figure 6.12 Variation of nitrate flux in sediment with BionSoil cap

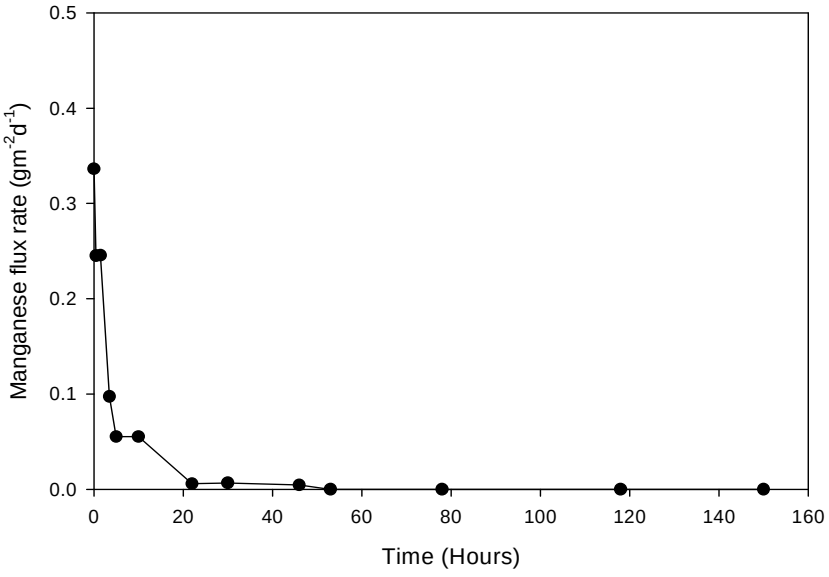

Figure 6.13 Variation of manganese flux in sediment with BionSoil cap

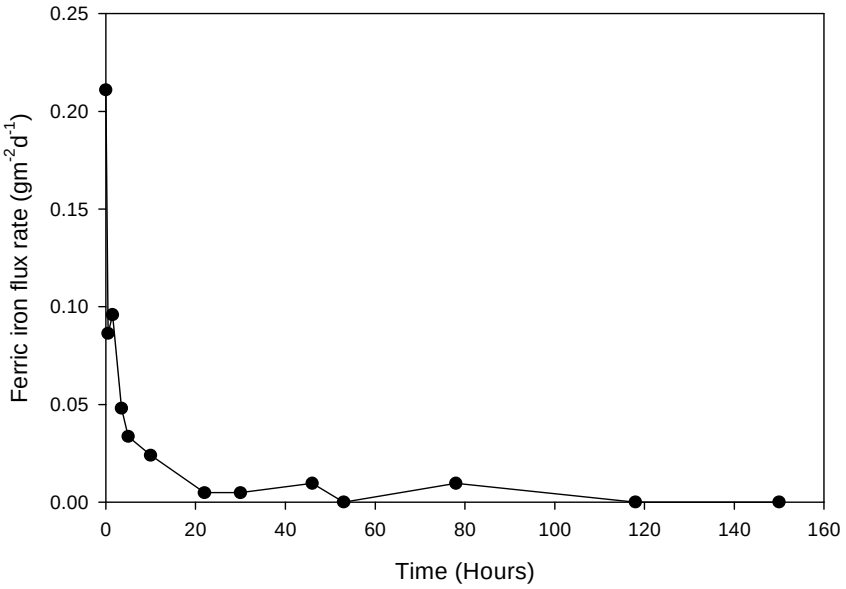

Figure 6.14 Variation of ferric iron flux in sediment with BionSoil cap

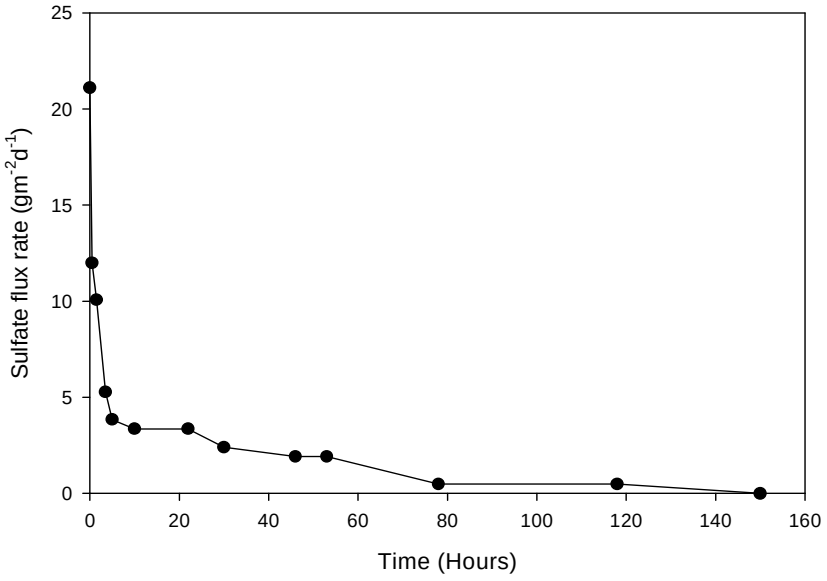

Figure 6.15 Variation of sulfate flux in sediment with BionSoil cap

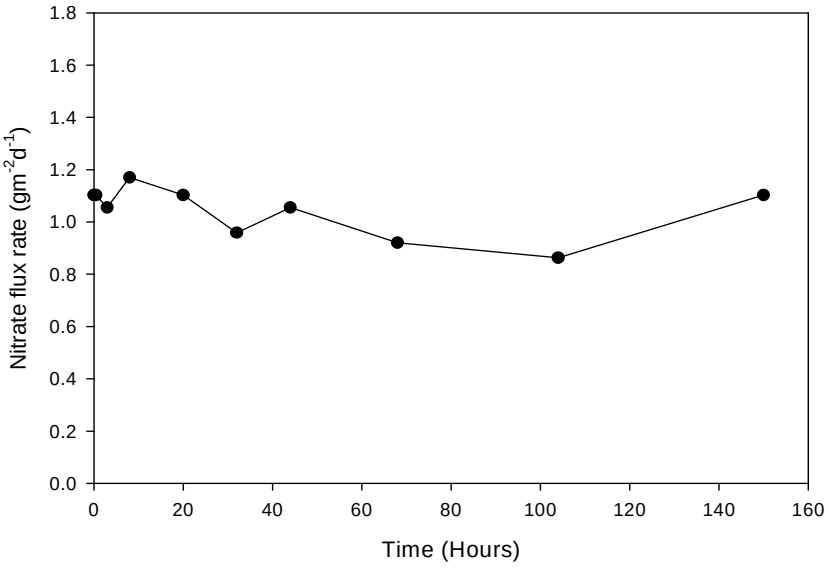

Figure 6.16 Variation of Nitrate flux in sediment only without cap

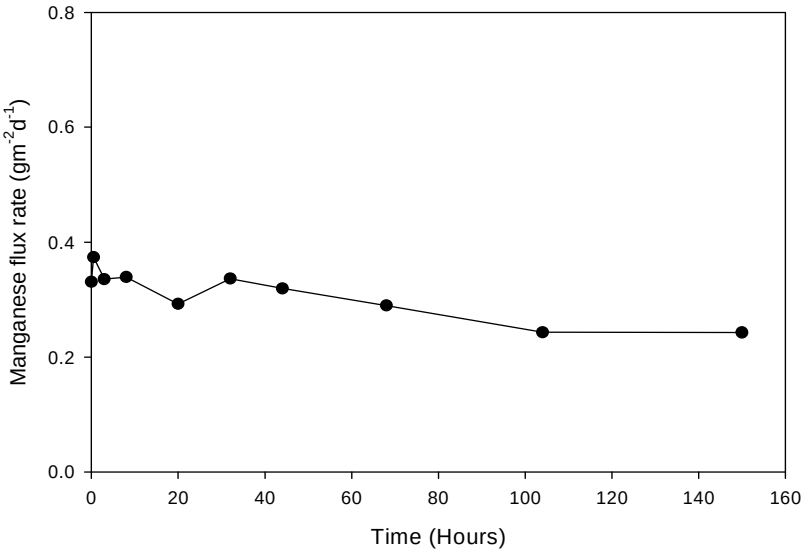

Figure 6.17 Variation of manganese flux in sediment only without cap

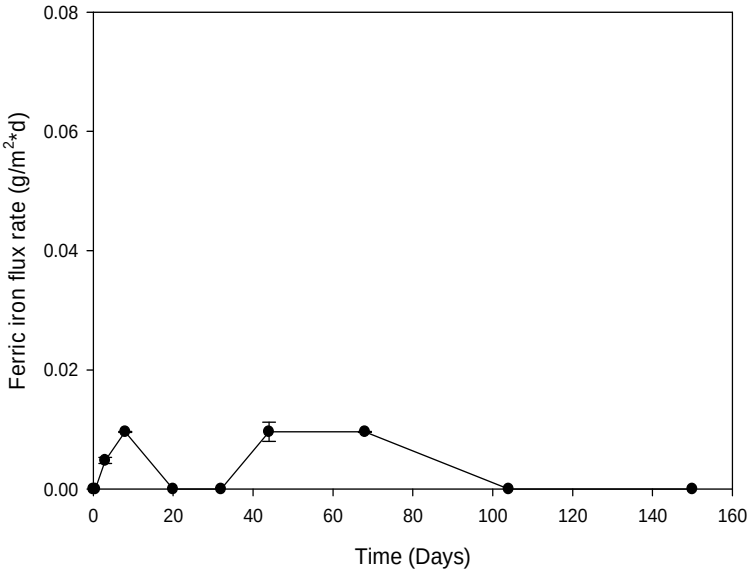

Figure 6.18 Variation of ferric iron flux in sediment only without cap

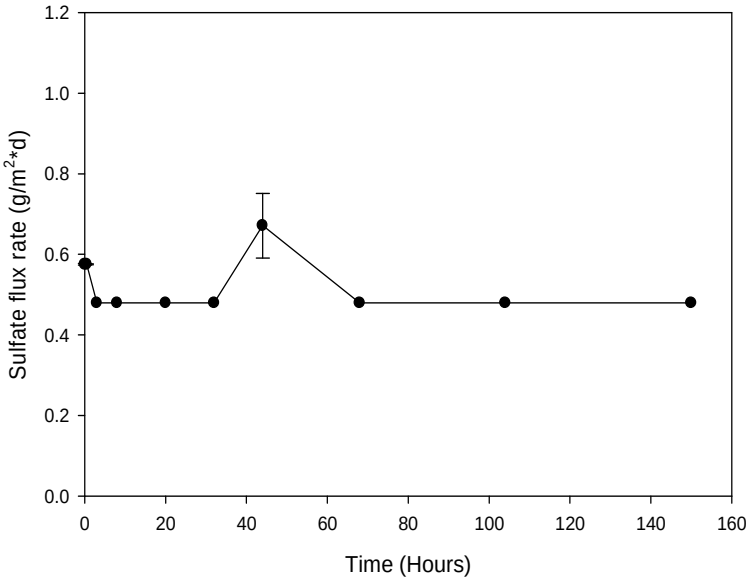

Figure 6.19 Variation of sulfate flux in sediment only without cap

Modeling

The flux of phenanthrene from sediment into the water column was modeled mathematically using RECOVERY version 4.3.1. both laboratory scale and Anacostia River conditions. These models are intended to describe diffusion in a finite layer with uniform initial concentration, and zero flux at the base. The laboratory scale of flux model shown in Figure 6.20 was run in order to compare the experimental flux data. The flux of phenanthrene increased linearly with time frame, it means, phenanthrene was released into the water body from sediment as time passes in direct proportion. The phenanthrene was detected in the water column while phenethrene concentration decreased from sediment layer in experimental data from Figures 6.7 and 6.8.

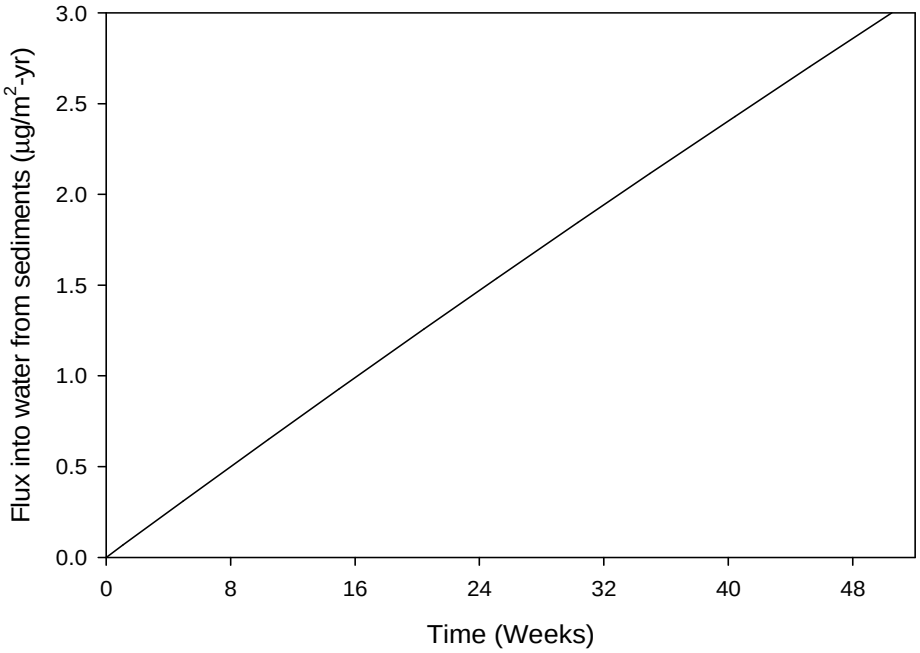

Figure 6.20 Flux of phenanthrene from sediment into water in laboratory scale

Model scenarios are run in order to compare the effectiveness of reactive capping material, BionSoil. The flux of phenanthrene into the water column from sediment was modeled in different cap thickness with Anacostia River conditions. Sand caps provide the basis of comparison. Results of the reactive cap and sand cap simulations with different cap thickness are shown from Figure 6.21 to 6.26, flux into water from sediments without cap, 1 cm of BionSoil cap, 5 cm of BionSoil cap, 10 cm of BionSoil cap, 1 cm of sand cap, and 10 cm of sand cap, respectively.

For each case of cap has a time before phenanthrene has transported through the cap layer, followed by increasing flux through the cap until a maximum is reached, then decrease in flux over time until the phenanthrene is depleted in the underlying sediment layer. The trends are shown to be intimately related to the sorption characteristics of the reactive cap. Sand caps show a flux more than forty times that of reactive BionSoil cap. Sand has little sorptive capacity for phenanthrene.

The results show that contaminant flux through sand quickly approaches its maximum value rather than that of reactive caps. Reactive caps, 5 cm of BionSoil cap and 10 cm of BionSoil cap, improved mitigation by increasing the time before phenanthrene has transported through the cap layer by approximately 20-30 years, and then reduced the phenanthrene release. Ten centimeters of BionSoil cap (Figure 6.24) shows a highly effective ability to reduce flux and phenanthrene release. The cap placement will inhibit the flux of organic matter to contaminated sediments and will biodegrade contaminant in this region. The anaerobic metabolism of organic contaminant is considered a first order process as consistent with nutrient flux models (Chapter 3).

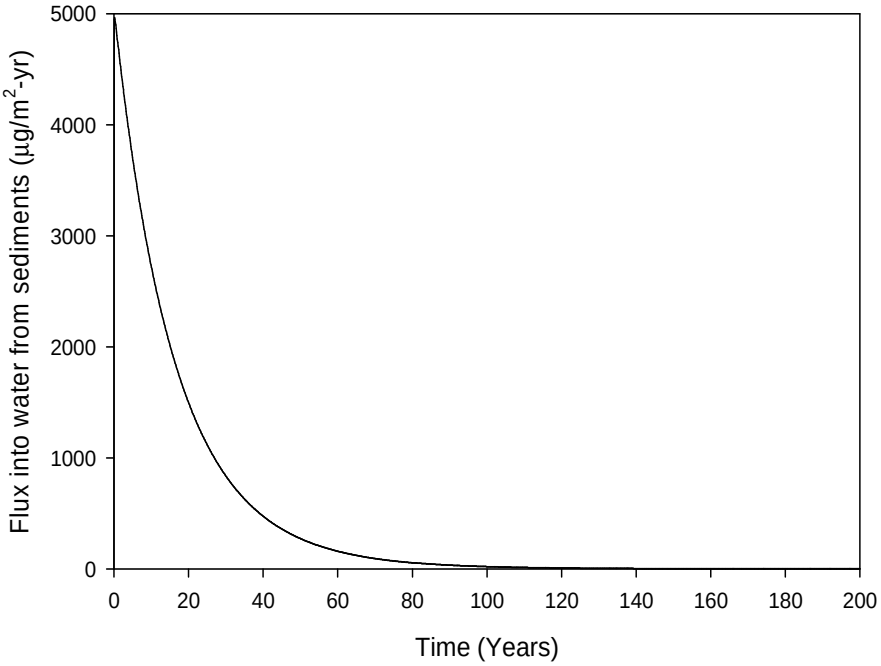

Figure 6.21 Flux of phenanthrene from sediment into water without cap

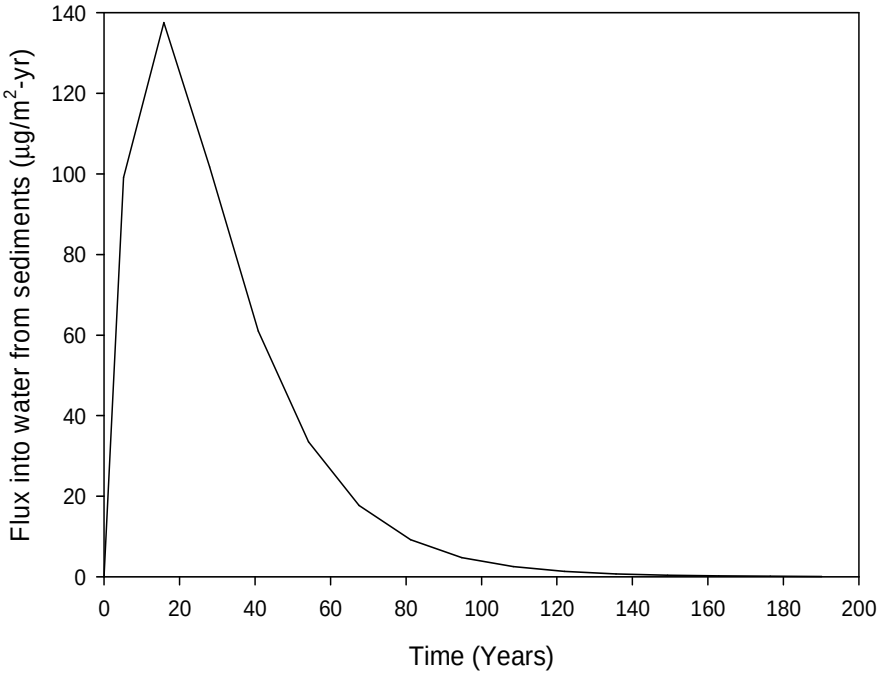

Figure 6.22 Flux of phenanthrene from sediment into water with 1 cm BionSoil cap

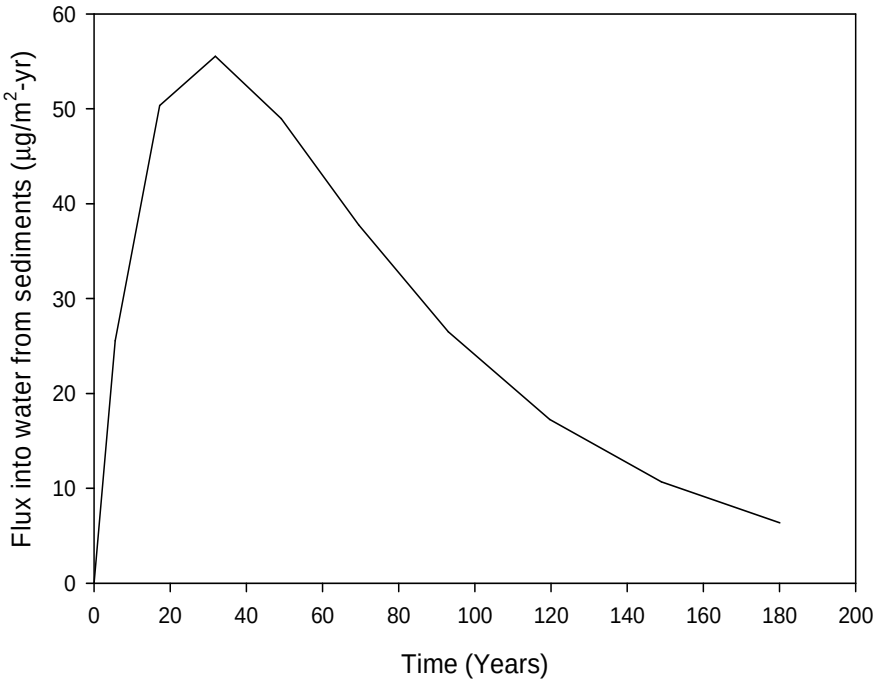

Figure 6.23 Flux of phenanthrene from sediment into water with 5 cm BionSoil cap

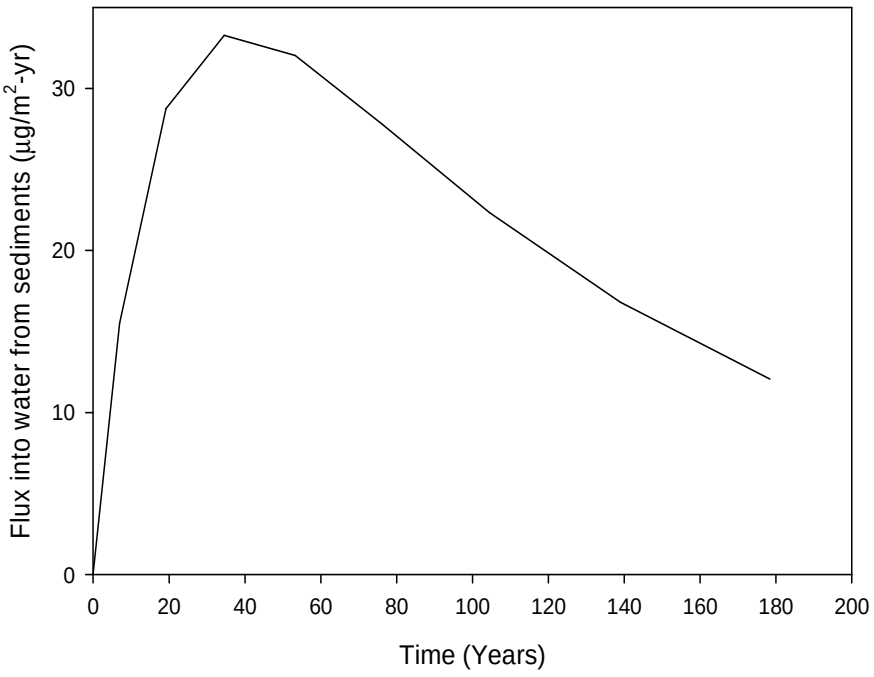

Figure 6.24 Flux of phenanthrene from sediment into water with 10 cm BionSoil cap

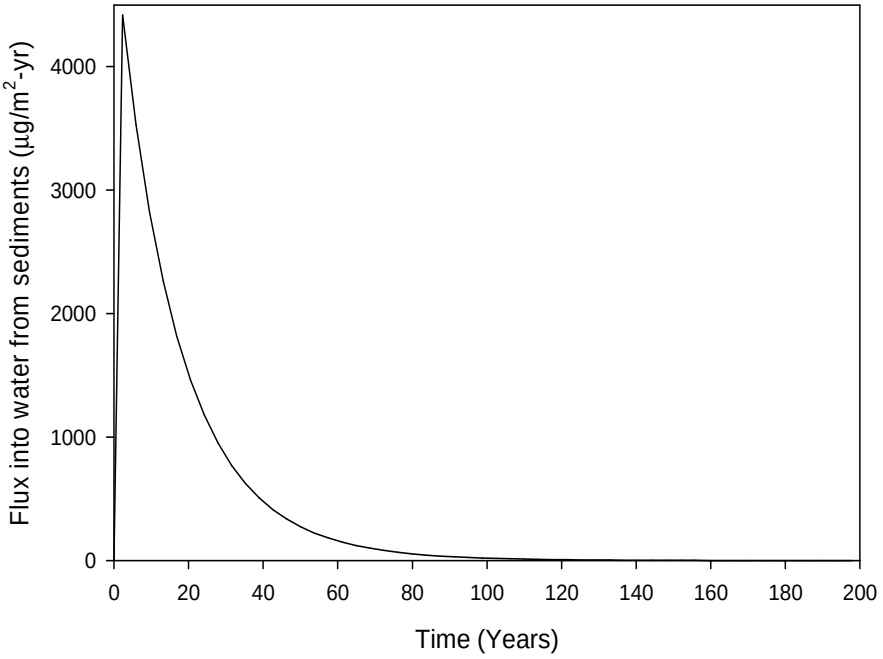

Figure 6.25 Flux of phenanthrene from sediment into water with 1 cm sand cap

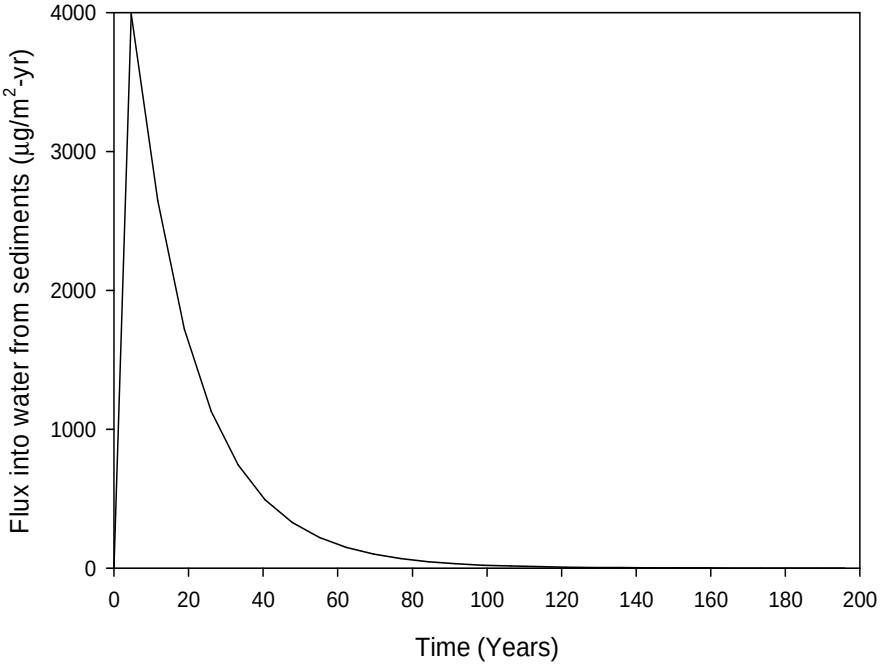

Figure 6.26 Flux of phenanthrene from sediment into water with 10 cm sand cap

Settling Data from Previous Study

Simulation of the placement of the cap material under water at the target site was done using glass columns (diameter: 150 mm, effective height: 500 mm). Two types of experiments were done. The first was meant to simulate what would occur when the cap material was placed at the target remediation site for the first time. The second experiment was meant to simulate the situation when the cap material already placed at the target site was re-suspended due to disturbance occurring within the cap or turbulence in the water column above it.

For both the placement and re-suspension experiments, monitoring was done for: changes in the clarity of the supernatant water in the column in Figure 6.27; variation of total suspended solids (TSS) with time in the supernatant water in Figure 6.28 and 6.29; and build up of the settled cap material in the column in Figure 6.30 and 6.31. The variation of TSS was assessed by taking samples of water from the columns through sampling ports placed at different levels along the height of the column. The build up of the cap was assessed by measuring the depth of the settled cap material, whereas the changes in the clarity of the supernatant water was assessed visually and recorded by photography. TSS was analyzed as recommended in the Standard Methods for the Examination of Water and Wastewater (APHA et al., 1998). I acknowledge Dr. Gabriel R. Kassenga and Mr. Stephen Mbuligwe performed experiments and discussion for simulation of the cap placements.

The photographs shown in Figures 6.27 show clearly that, upon pouring the cap material (T = 0), almost the whole of the water column was laden with the cap material. Nonetheless, there were signs of partial clearing of the cap material from the top most part of the water column even at T = 0. The largest extent of the effects of the clarification process in the supernatant water took place immediately after placement of the cap material then, later,

clarification proceeded much more slowly. For instance, the visual difference between the clarity of the water at T = 0 minutes and T = 12 minutes is very significant. This is in stark contrast with the difference for between T = 12 minutes and T = 180 minutes, which is hardly noticeable.

As intended, during pouring, the bulk of the cap material went straight to the bottom of the column. As such, the suspended solids profiled in Figures 6.28 a and b, formed from the portion of the cap material that separated from the rest. Consequently, the reduction in total suspended solids (TSS) corresponds to the sedimentation of the suspended solids. The settlement profiles are in agreement with the sedimentation profiles reported in the literature for similar conditions (Metcalf and Eddy, 2003). It is evident that effects of the cap material by way of TSS formation after both the initial placement and re-suspension, are most serious within the initial few (four) minutes. The highest recorded TSS levels were about 3100 mg/L after initial placement and 3500 mg/L after re-suspension. In both the initial placement and re-suspension experiments, TSS concentration was reduced to practically the same level (of about 200 mg/L) at all depths within the water column after only 12 minutes. Furthermore, about 30 minutes after placement or re-suspension of the cap material, the TSS levels with the whole water column had been reduced to almost zero. Drinking water guidelines specify 500 mg/L as the highest desirable level of TSS in drinking water (Hammer and Hammer, 1996). It is apparent from Figures 6.28 a and b that clarification of the water can be attained much faster after re-suspension than after the initial placement of the cap material. This suggests that careful placement of the cap material, as outlined earlier, can go a long way towards minimizing the unintended effects of the operation in the water column.

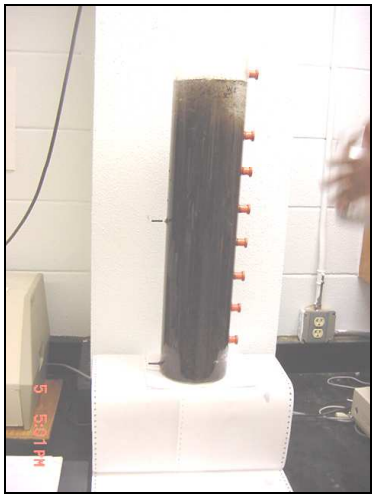

T = 0

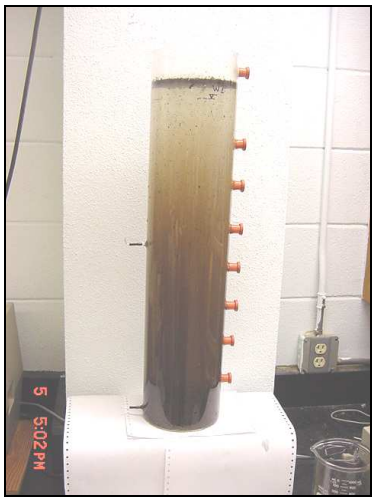

T = 1.5 min

Figure 6.27 a Settling test of BionSoil

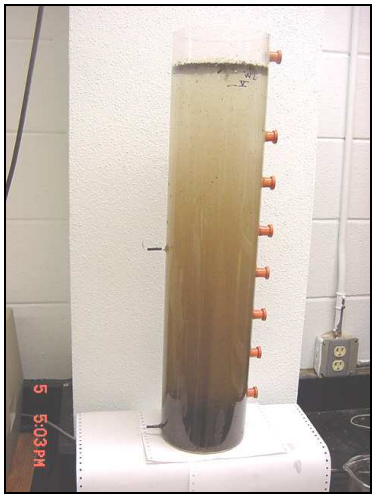

T = 2.2 min

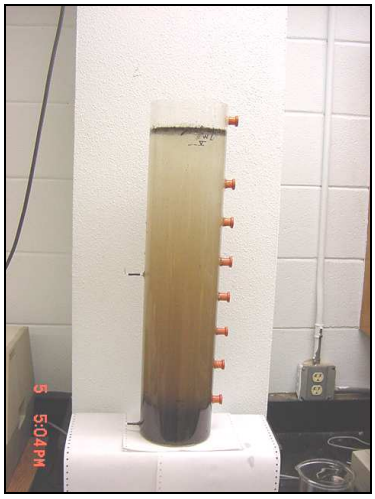

T = 4.0 min

Figure 6.27 b Settling test of BionSoil

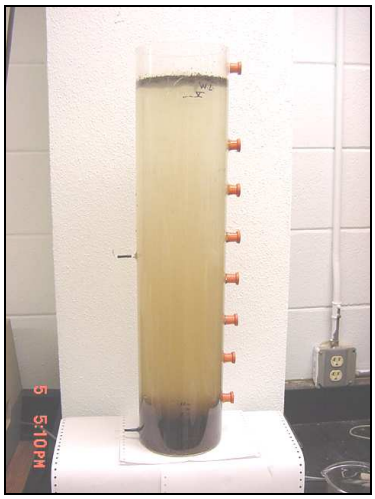

T = 12.0 min

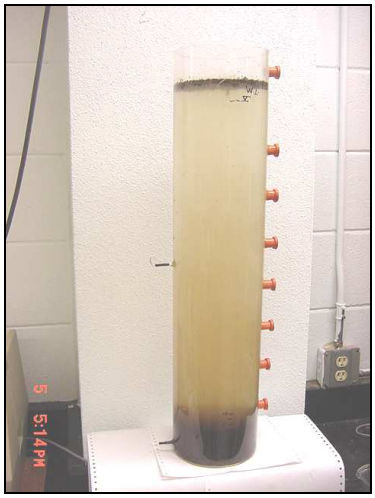

T = 180.0 min

Figure 6.27 c Settling test of BionSoil

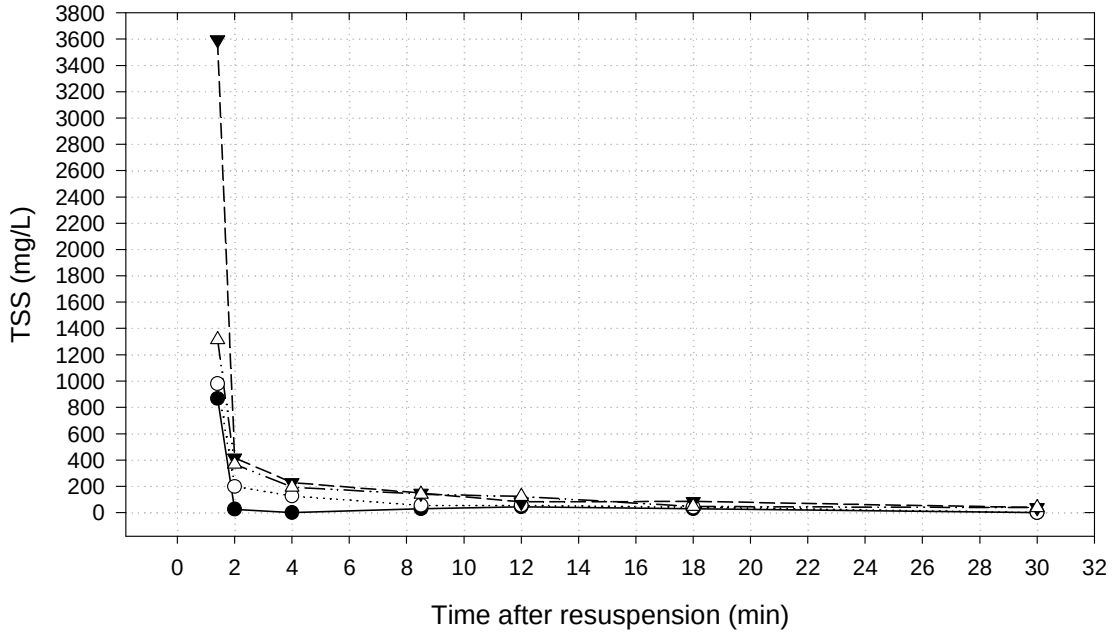

Figure 6.28 a Variation of TSS concentrations after re-suspension of BionSoil

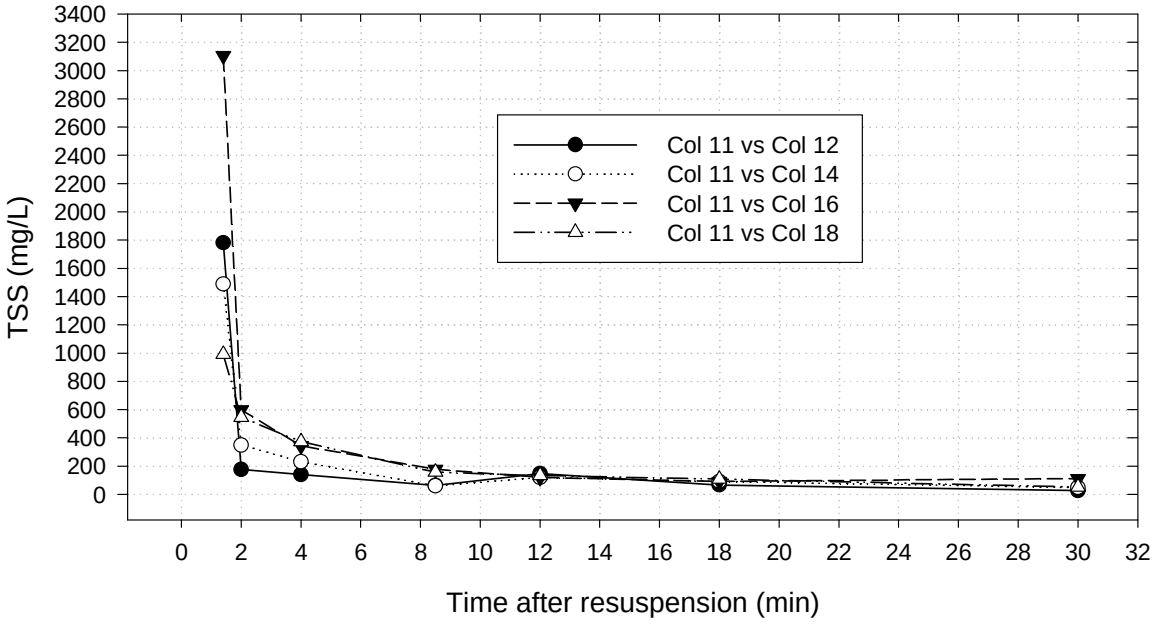

Figure 6.28 b Variation of TSS concentrations after pouring of BionSoil

Figures 6.29 a and b show that the pattern of the build up of the cap material after the initial placement corresponds to the one exhibited following re-suspension of the cap material. This observation reinforces the predictability of the cap material placement operation. As observed with respect to the TSS removal process, the bulk of the cap thickness, both following the initial placement and after re-suspension, developed within a short time after commencement of the process. Notably, more that 91 % of the total thickness of the cap layer was built up within the first 5 minutes (300 s). Within about 20 minutes (1200 s) almost 100 % of the cap thickness was already in place. With respect to the build up of the cap material after re-suspension, more than 92 % of the cap layer was in place after about 5 minutes (300 s), whereas the whole cap layer was built up in about 25 minutes (1500 s).

The fact that the cap layer was thicker after re-suspension than after the initial placement of the cap material can be attributed to two main things. First, the cap material expanded due to absorbing water, and thus the swelling resulted from the net increase in water content within the cap material (Sharma and Reddy, 2004). Second, consolidation of the cap material was slow, and within the scope of the monitoring for this study the process was still incomplete. Consolidation, which squeezes out the absorbed water under the weight of the cap material, is a slow process, and can proceed slowly for a long time depending on the type of material under consideration (Sharma and Reddy, 2004). It is also noteworthy that the correspondence of the cap material settling patterns observed above parallels the correspondence of TSS removal patterns. The inverse correspondence between the build up of the cap layer and removal of TSS from the water column (supernatant water) is due to the fact that both processes resulted from the same settling process.

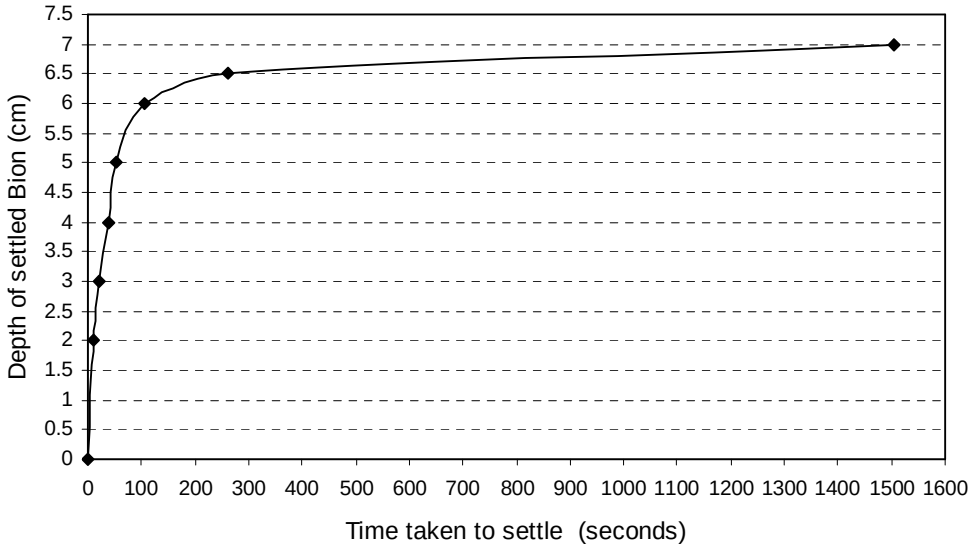

Figure 6.29 a Build up of settled BionSoil layer after re-suspension of previously settled BionSoil

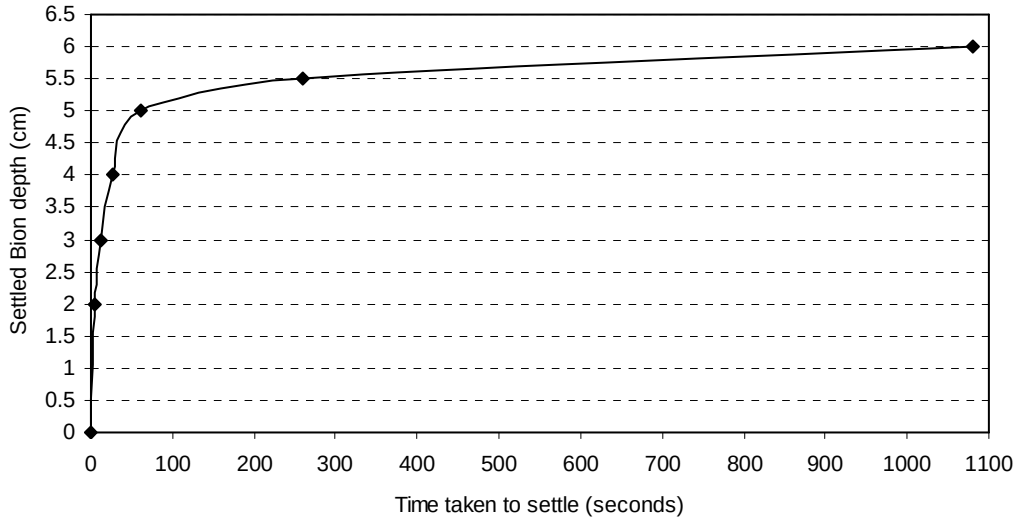

Figure 6.29 b Build up of settled BionSoil layer after pouring fresh BionSoil

Conclusions

Sorption and flux chamber studies indicate that concentration of contaminants from the sediment beds and flux of nitrate, manganic manganese, ferric iron, and sulfate from sediment was investigated. Effect of capping was estimated by comparison between Anacostia sediment with BionSoil cap and sediment without BionSoil cap. BionSoil was selected as a capping material.

Sediment and water partition coefficient of BionSoil (112 L/Kg) is six times greater than that of Anacostia River sediment (20.4 L/Kg) using the linear sorption model. BionSoil has high sorption ability and acts a good sorbent. The nonlinear model K_d value of ^{14}C-phenanthrene in the Anacostia sediment has been found to be 12.46 L/Kg whereas that of BionSoil is 102.70 L/Kg. Studies of sorption and desorption of phenanthrene showed that an apparent steady state was effectively reached in 2-3 days. At the apparent steady state, approximately 9 % of phenanthrene was desorbed from the soil phase in Anacostia sediment while only 3 % of phenanthrene was desorbed from soil phase in 60 % of BionSoil and sediment mixture treatment. This indicates that BionSoil is good capping material. This observation is reinforced by the fact that the release of phenanthrene from the Anacostia sediment was faster than release of phenanthrene from the BionSoil and sediment mixture treatment.

In the flux chamber, PAH components degraded efficiently. Around 75 % of PAHs were removed in sediment layer in the bed composed of sediment with the BionSoil cap. The degradation occurred not only in the sediment layer but also in the BionSoil cap layer. TOC concentration was high initially in the sediment with BionSoil cap treatment but it was low in the sediment without cap. The flux rates of nitrate, manganese, ferric iron, and sulfate showed the typical shape of diffusion curves, with initially higher concentrations which rapidly decreased to

a steady state. The flux rates were significantly different between the sediment with cap treatment and sediment without cap. This indicates that BionSoil improved the characteristics of the sediment enhancing its sorption ability and facilitation of microbial activities. These activities slowed down the release of contaminants and nutrients. The model simulation shows the inherent advantage of using the reactive cap. BionSoil (10 cm) cap is shown to be the most effective scenario for reducing the flux mitigation.

CHAPTER 7
OVERALL CONCLUSIONS

^{14}C–Phenanthrene study observed ^{14}C–Phenanthrene mineralization under various redox conditions in Anacostia river sediments with providing TEAs. Mineralization was examined to demonstrate the comparable effectiveness using the nitrate-reducing, ferric iron-reducing, manganese-reducing, sulfate-reducing, and methane production conditions. Mineralization of phenanthrene component was strongly linked to sulfate reduction since 34 % of mineralization was occurred when sulfate was provided as TEA. The mineralization of phenanthrene was less than 10 % in other treatments entire study period. The sulfate was electron acceptor in biodegradation processes. Sulfate reduction was the more energetic process than any other condition in Anacostia sediments. Sulfate treatment had more microbial ability to degrade phenanthrene than other treatments. Faster degradation of phenanthrene was possibly mediated by microbial communities such as *Pelobacter sp*. and *Desulfuromonas sp*. in the sulfate treatment microcosms. The microbial consortia may have a relation with the degradation potential and these organisms can possibly help facilitate PAH mineralization. *Pelobacter sp*. and *Desulfuromonas sp*. are members of the *Geobacteraceae* family which have an important role in the anaerobic degradation of PAHs. These sulfate reducers use hydrocarbon substrates as an electron donors and sulfate is used as an electron acceptor. Mineralization monitoring data suggested that the population of sulfate-reducing bacteria were involved with PAH degradation. Therefore, sulfate is a more promising TEA for intrinsic degradation in Anacostia River and other PAH contaminated sites.

A model simulating nutrient flux through sediment was developed the model framework of simulation and for the future use in the field of environmental remediation. The model can be

used to predict the response of the primary nutrients and overall sediment redox state after step changes in boundary conditions on the sediment.

The kinetic study observed the important removal process of PAH components in anaerobic biodegradation. Biodegradation processes were examined to show the comparable effectiveness in the mixtures of BionSoil and Anascotia River sediment. A Biodegradation of PAH compound was strongly linked to sulfate reduction in BionSoil mixtures. Though sulfate and carbon dioxide both are electron acceptor in biodegradation processes, sulfate reduction is the more energetic process than methanogenesis condition. More fraction of BionSoil made these reactions or mechanisms vigorous in sediments. The degradation of PAHs was most likely mediated by microbial communities such as *Desulfotomaculum sp.*, *Pelobacter sp*. and *Desulfuromonas sp.* The microbial consortia may have a relation with the degradation potential and they possibly help facilitating PAH decline. These sulfate-reducing bacteria use substrate as electron donors from hydrocarbons.

The transformation of HCB in Anacostia was mainly due to reductive dechlorination. The complete dechlorination of the parent compound and daughter products were observed and proceeded faster as the percentage of the compost increased. The first order rate constants of parent compound in the sediment ranged 0.0058 to 0.0138 day^{-1}. The dominant pathway of HCB was: QCB → 1,2,4,5-TeCB + 1,2,3,5-TeCB → 1,3,5-TCB + 1,2,4-TCB → 1,3-DCB + 1,4-DCB → MCB and benzene. Degradation of parent and intermediate compounds (HCB, QCB, TeCB, TCB, and DCB) were observed faster under sulfate reducing conditions followed by methanogenic conditions while end product (MCB and benzene) degradation was occurred under methanogenesis. Hydrogen concentration trends also suggested that hydrogen was probably used as an electron donor during both sulfate reduction and methanogenesis to drive dechlorination.

The results of microbial analysis showed that different microbial composition and diversities were able to dechlorinate HCB under anaerobic condition. Highly organic rich soil, BionSoil, probably changed the microbial community and facilitated dechlorination. HCB was able to dechlorinate completely in BionSoil treatment microcosms. These observations provide strong evidence for the application of bioremediation. In addition, BionSoil was found to be a very promising material for *ex-situ* bioremediation of chlorinated solvents contaminated sites.

Sorptive reactive capping studies indicate that concentration of contaminants from the sediment beds and flux of nitrate, manganic manganese, ferric iron, and sulfate from sediment was investigated. Effect of capping was estimated by comparison between Anacostia sediment with BionSoil cap and sediment without BionSoil cap. Sediment and water partition coefficient of BionSoil (112 L/Kg) is six times greater than that of Anacostia River sediment (20.4 L/Kg) using the linear sorption model. BionSoil has high sorption ability and acts a good sorbent. The nonlinear model K_d value of ^{14}C-phenanthrene in the Anacostia sediment has been found to be 12.46 L/Kg whereas that of BionSoil is 10.2.70 L/Kg. Studies of sorption and desorption of phenanthrene showed that an apparent steady state was effectively reached in 2-3 days. At the apparent steady state, approximately 9 % of phenanthrene was desorbed from the soil phase in Anacostia sediment while only 3 % of phenanthrene was desorbed from soil phase in 60 % of BionSoil and sediment mixture treatment. This observation is reinforced by the fact that the release of phenanthrene from the Anacostia sediment was faster than release of phenanthrene from the BionSoil and sediment mixture treatment. In the flux chamber, PAH components were removed efficiently. Around 75 % of PAHs were removed in sediment layer in the bed composed of sediment with the BionSoil cap. TOC concentration was high initially in the sediment with BionSoil cap treatment but it was low in the sediment without cap. The flux rates

of nitrate, manganese, ferric iron, and sulfate showed the typical shape of diffusion curves, with initially higher concentrations which rapidly decreased to a steady state. The flux rates were significantly different between the sediment with cap treatment and sediment without cap. This indicates that BionSoil improved the characteristics of the sediment enhancing its sorption ability and facilitation of microbial activities.

LITERATURE CITED

Adrian, L., Szewzyk, U., Wecke, J., and Görisch, H. 2000. Bacterial Dehalorespiration with Chlorinated Benzenes. *Nature* 408 (6812):580-583.

Alexander, M. 1999. *Biodegradation and Bioremediation*, 2nd Ed. Academic Press, New York.

Anderson, R.T., and Lovley D.R., 2000 Anaerobic Bioremediation of Benzene under Sulfate-Reducing Conditions in a Petroleum-Contaminated Aquifer. *Environ. Sci. Technol.,* 34,2261-2266.

Anderson, R.T., Rooney-Varga, J.N., Gaw, C.V., and Lovley, D.R. 2007. Aromatic and Polyaromatic Hydrocarbon Degradation under Fe (III)-Reducing Conditions. In Press.

ASTM International. 100 Barr Harbor Drive, PO Box C700, West Conshohocken, PA 19428-2959, United States. Designation: E 1195-01, p.1-9. Standard Test Method for Determining a Sorption Constant (K_{oc}) for an Organic Chemical in Soil and Sediments.

ATSDR (Agency for Toxic Substances and Disease Registry). 1990. Toxicological Profile for Polycyclic Aromatic Hydrocarbons. Acenaphthene, Acenaphthylene, Anthracene, Benzo(a)anthracene, Benzo(a)pyrene, Benzo(b)fluoranthene, Benzo(g,i,h)perylene, Benzo(k)fluoranthene, Chrysene, Dibenzo(a,h)anthracene, Fluoranthene, Fluorene, Indeno(1,2,3-c,d)pyrene, Phenanthrene, Pyrene. Prepared by Clement International Corporation, under Contract No. 205-88-0608. ATSDR/TP-90-20.

Augenfeld, J.M., Anderson, J.W., Riley, R.G., Thomas, B.L., 1982. The fate of polyaromatic hydrocarbons in an intertidal sediment exposure system: bioavailabiliy to *Macoma inquinata* (Mollusaca: Pelecypoda) and *Abarenicola pacifica* (Annelida: Polychaeta). *Marine Environmental Research* 7:31-50.

Azcue, J.M., Zeman, A.J., Mudroch, A., Rosa, F., and Patterson, T. 1998. Assessment of Sediment and Porewater after One Year of Subaqueous Capping of Contaminated Sediments in Hamilton Harbour, Canada. *Water Science and Technology.* 37: 323-329.

Bedessem, M. E., Swoboda-Colberg, N. G., Colberg, P. J. S. 1997. Naphthalene Mineralization Coupled to Sulfate Reduction in Aquifer-Derived Enrichments, *FEMS Microbiology Letters*. 152: 213-218.

Berg, P., Rysgaard, S., and Thsmdrup, B. 2003. Dynamic Modeling of Early Diagenesis and Nutrient Cycling. A Case Study In an Arctic Marine Sediment, American Journal of Science. 303: 905-955.

Berner, R.A. 1980. Early Diagenesis: A Theoretical Approach, Princeton University Press.

Beurskens, J. E. M., 1995. Microbial transformation of chlorinated aromatics in sediments. Dissertation, Wageningen University, Netherlands.

Beurskens, J. E. M., Dekker, C. G. C., Heuvel, H., Swart, M., and Wolf, J., 1994. Dechlorination of Chlorinated Benzenes by an Anaerobic Microbial Consortium That Selectivity Mediates the Thermodynamic Most Favorable Reactions, *Environ. Sci. Technol*., 28: 701-706.

Blad, M., 2001. Mass Transfer of 2,4,6,-Trinitrotoluene and Lower Chlorinated Benzenes from Sediment into Water. Dissertation, Louisiana University, Baton Rouge.

Boudreau, B. P. 1996. A Method-of-Lines Code for Carbon and Nutrient Diagenesis in Aquatic Sediments. *Computers and Geosciences*, 22:479-496.

Boese, B.L., Lee, H., Specht, D.T., Pelletier, J., and Randall, R. 1996. Evaluation of PCB and Hexachlorobenzene Factors Based on Ingested Sediment in a Deposit-Feeding Clam. *Environmental Toxicology and Chemistry*, 15 (9):1584-1589.

Brannon, J. M., Hoeppel, R. E., Sturgis, T. C., Smith, I., and Gunnison, D. 1986. Effectiveness of Capping in Isolating Dutch Kills Sediment from Biota and The Overlying water. Technical Report, D-86-2, US Army Engineer Waterways Experiment Station, Vicksburg, Mississippi.

Brannon, J.M., Hoeppel, R.E., and Gunnuson, D. 1987. Capping Contaminated Dredged Material. *Mar. Pollut. Bull.*, 18:175-179.

Burland, S. M., and Edwards, E. A. 1999. Anaerobic Benzene Biodegradation Linked to Nitrate Reduction, *Appl. Environ. Microbiol*., 65: 529-533.

Caldwell, M. E., Garrett, R. M., Prince, R. C. and Suflita, J. M. 1998. Anaerobic Biodegradation of Long-Chain *n*-Alkanes under Sulfate-Reducing Conditions, *Environ. Sci. Technol*., 32: 2191-2195.

Canfield, D.E., Thamdrup, B., and Hansen, J.W., 1993. The Anaerobic Degradation of Organic Matter in Danish Coastal Sediments: Iron Reduction, Manganese Reduction, and Sulfate Reduction. *Geochim. Cosmochim. Acta*., 57: 3867-3883.

Chang, B. V., Chen, I. M., Yuan, S. Y., and Wang, Y. S., 1997. Reductive Chlorination of Hexachlorobenzene by an Anaerobic Mixed Culture. *Water, Air, and Soil Pollution,* 100: 25-32.

Charbeneau, R.J. 2000. Groundwater Hydraulics and Pollutant Transport. Prentice-Hall, Inc. Upper Saddle River, New Jersey 07458.

Chen, I. M., Chang, B. V., Yuan, S. Y., and Wang, Y. S., 2002. Reductive Chlorination of Hexachlorobenzene Under Various Additions. *Water, Air, and Soil Pollution,* 139: 61-74.

Choi, J.W., Choi, N.C., Mahendran, B., Kim, D.J., Lee, C.E., 2007. Sorption kinetics of aqueous benzene for attached bacteria on sorbents. *Current Applied Physics* 7, 13-17.

Choy, B. and D.D. Reible. 2000. Diffusion Models of Environmental Transport. Lewis Publishers, Boca Raton, FL.
Coates, J. D., Anderson, R. T., and Lovley, D. R. 1996a. Oxidation of Polycyclic Aromatic Hydrocarbons under Sulfate-Reducing Conditions, *Appl. Environ. Microbiol*., 62: 1099-1101.

Coates, J. D., Anderson, R. T., Woodward, J. C., Phillips, E. J. P., and Lovley, D. R. 1996b. Anaerobic Hydrocarbon Degradation in Petroleum-Contaminated harbor Sediments under Sulfate-Reducing and Artificially Imposed Iron-Reducing Conditions, *Environ. Sci. Technol*., 30: 2784-2789.

Coates, J. D., Woodward, J. C., Allen, J., Philp, P., and Lovley, D. R. 1997. Anaerobic Degradation of Polycyclic Aromatic Hydrocarbons and Alkanes in Petroleum-Contaminated Marine Harbor Sediments, *Appl. Environ. Microbiol*., 63: 3589-3593.

Cummings, D.E., Snoeyenbos-West, O.L., Newby, D.T., Niggemyer, A.M., Lovley, D.R., Achenbach, L.A., and Rosenzweig, R.F. 2003. Diversity of Geobacteraceae Species Inhabiting Metal-Polluted Freshwater Lake Sediments Ascertained by 16S rDNA Analyses. *Microb. Ecol.* 46:257-269.

Daly, K., Sharp, R.J., and McCarthy, A.J. 2000. Development of olegonucleotide Probes and PCR Primers for Detecting Phylogenetic Subgroups for Sulfate-Reducing Bacteria. *Microbiology* 146:1693-1705.

Deane, G., Z. Chroneer, and W. Lick. 1999. Diffusion and Sorption of Hexachlorobenzene in Sediments and Saturated Soils. *Journal of Environmental Engineering*. 125 (8): 689-696.

Dhakar, S.P., and Burdige, D.J. 1996. A Coupled, Non-Linear, Steady State Model for Early Diagenetic Processes in Pelagic Sediment. Americal Journal of Science. 296: 296-330.

Dohse, D.M., and Lion, L.W. 1994. Effect of Microbial Polymers on the Sorption and Transport of Phenanthrene In a Low-Carbon Sand. *Environ. Sci. Technol*. 28: 541-548.

Dolfing, J., and Harrison, B.K., 1992. Gibbs Free Energy of Formation of Halogenated Aromatic Compounds and their Potential Role as Electron Acceptors in Anaerobic Environments. *Environ. Sci. Technol*., 26: 2213-2218.

Eriksson, M., Sodersten, E., Yu, Z., Dalhammar, G., and Mohn, W.W., 2003. Degradation of Polycyclic Aromatic Hydrocarbons at Low Temperature Under Aerobic and Nitrate-Reducing Conditions in enrichment Cultures from Northern Soils. *Appl. Environ. Microbiol.*, 69: 275-284.

Fossing, H., Berg, P., Thamdrup, B., Rysgaard, S., Sorensen, H.M., and Nielsen, K., 2004. A Model Set-Up for an Oxygen and Nutrient Flux Model for Aarhus Bay (Denmark). National Environmental Research Institute, Ministry of Environment, Denmark. *NERI Technical Report*, No. 483.

Fuchsman, P.C., Barber, T.R., Sheehan, P.J. 1998. Sediment Toxicity Evaluation for Hexachlorobenzene: Spiked Sediment Tests with Leptocheirus Plumulosus, Hyalella Azteca, and Chironomus Tentans. *Arch. Environ. Contam. Toxicol*. 35 (4): 573-579.
Gao, Y.Z., Zhu, L.Z., 2004. Plant uptake, accumulation and translocation of phenanathrene and pyrene in soils. *Chemosphere.* 55: 1169-1178.

Gao, Y.Z., Zhu, L.Z., 2005. phytoremediation for phenanathrene and pyrene contaminated soils. *J. Environ. Sci*., 16: 12-18.

Guo, C.L., Zhou, H.W., Wong, Y.S., Tam, N.F.Y., 2005 Isolation of PAH-degrading Bacteria from Mangrove Sediments and Their Biodegradation potential. *Marine Pollution Bulletin* 51: 1054-1061.

Haines, J.R., Atlas, R.M., 1982. In Situ microbial degradation of Purdhoe Bay crude oil in Beaufort Sea sediments. *Marine Environmental Research* 7, 91-102.

Hammer, M.J. and Hammer, M. J (Jr). 1996. Water and wastewater technology (3rd ed.). Prentice Hall, New Jersey.

Harms, G., Layton, A.C., Dionisi, H.M., Gregory, I.R., Garrett, V. M., Hawkins, S.A., Robinson, K.G., and Sayler, G.S. 2003. Real-Time PCR Quantification of Nitrifying Bacteria in a Municipal Wastewater Treatment Plant. *Environ. Sci. Technol.*, 37: 343-351.

Hayes, L.A., Nevin, K.P., and Lovely, D.R., 1999. Role of Prior Exposure on Anaerobic Degradation of Naphthalene and Phenanthrene in Marine Harbor Sediments. *Organic Geochemistry*, 30: 937-945.

Hendrickson, E. R., J. A. Payne, R. M. Young, M. G. Starr, M. P. Perry, S. Fahnestock, D. E. Ellis, and R. C. Ebersole. Molecular Analysis of Dehaloccccoides 16S Ribosomal DNA from Chloroethene-Contaminated Sites Throughout North America and Europe. *Appl. Environ. Microbiol*., 68 (2): 485-495.

Hinga, K.R., 2003. Degradation rates of low molecular weight PAH correlate with sediment TOC in marine subtidal sediments. *Marine Pollution Bulletin.* 46, 466-474.

http://www.biontech.com/product/ (Apr. 06,2007)

http://www.hsrc-ssw.org/anacostia/ (Sep. 04, 2007)

Jackson, W. A., Pardue, J. H. and Araujo, R. 1996. Monitoring Crude Oil Mineralization in Salt Marshes: Use of Stable Carbon Isotope Ratios, *Environ. Sci. Technol*., 30: 1139-1144.

Jacobs, P.H. and Förstner, U. 1999. Concept of Subaqueous Capping of Contaminated Sediments with Aactive Barrier Systems (ABS) Using Natural and Modified Zeolites. *Water Researsh.* 33: 2083-2087.

Jayachandran, G., Görisch, H., and Adrian, L. 2003. Dehalorespiration with Hexachlorobenzene and Pentachlorobenzene by *Dehaloccoides* sp. strain CBDB1. *Archives of Microbiology*. 180 (6): 411-416.

Jayachandran, G., Görisch, H., and Adrian, L. 2004. Studies on Hydrogenase Activity and Chlorobenzene Respiration in *Dehaloccoides* sp. strain CBDB1. *Archives of Microbiology*. 182 (6): 498-504.

Kao, C. M., and Lei, S.E., 2000. Using a Peat Barrier to Remediate PCE/TCE Contaminated Aquifers. *Wat. Res.*, 34(3): 835-845.
Kassenga, G., Pardue, J.H., Moe, W.M., and Bowman, K.S. 2004. Hydrogen Threshold as Indicators of Dehalorespiration in Constructed Treatment Wetlans. *Environ. Sci. Technol*. 38: 1024-1030.

Kassenga, G.R., Pardue, J.H., Blair, S., and Ferraro, T., 2003. Treatment of Chlorinated Volatile Organic Compounds in Upflow Wetland Mesocosms. *Ecol. Eng*., 19: 305-323.

Lane, D. J. 1991. 16S/23S rRNA sequencing, p. 115-175. *In* E. Stackebrandt and M. Goodfellow (ed.), Nucleic acid techniques in bacterial systematics. Academic Press, Chichester, England.

Lee, H. W., S. Y. Lee, J. W. Lee, J. B. Park, E. S. Choi, and Y. K. Park. 2002. Molecular characterization of microbial community in nitrate-removing activated sludge. *FEMS Microbiol. Ecol*. 41: 85–94.

Lee, S.Y., Bollinger, D. Bezdicek and Ogram, A. 1996. Estimation of the Abundance of an Uncultured Soil Bacterial Strain by a Competitive Quantitative PCR Method. *Appl. Environ. Microbiol*., 62: 3787-3793.

Lee, S.J., Kommalapati, R.R., Pardue, J.H., and Constant, W.D., 2002. Rate-Limited Desorption of Volatile Organic Compounds from Soils and Implications for the Remediation of a Louisiana Superfund Site. *Environmental Monitoring and Assessment.* 75: 87-105.

Lee, S.J., Kommalapati, R.R., Valsaraj, K.T., Pardue, J.H., and Constant, W.D., 2004. Bioavailability of Reversibly Sorbed and Desortion-Resistant 1,3-Dichlorobenzene from a Louisiana Superfund Site Soil. *Water, Air, and Soil Pollution.,* 158: 207-221.

Li, H., Teppen, B. J., Johnston, C.T., Boyd, S.A., 2004. Thermodynamics of nitroaromatic compound adsorption from water by smectite clay. *Environ. Sci. Technol*., 38: 5433-5442.

Ling, W.T., Xu, J.M., Wang, H.Z., Gao, Y.Z., 2005 Sorption of dissolved organic matter and its effects on the atrazine sorption on soils. *J. Environ. Sci.*, 16: 478-482.

Löffler, F. E., K. M. Ritalahti, and J. M. Tiedje. Dechlorination of Chloroethenes is Inhibited by 2-Bromoethanesulfate in the Absence of Methanogens. *Appl. Environ. Microbiol*., 63: 4982-4985.

Löffler, F.E., Tiedje, J.M., and Sanford, R.A. 1999. Fraction of Electrons Consumed in Electron Acceptor Reduction and Hydrogen Thresholds as Indicators of Halorespiratory Physiology. *Appl. Environ. Microbiol*. 65: 4049-4056.

Lorah, M.M., Olsen, L.D., Smith, B.L., Johnson, M.A., and Fleck, W.B., 1997. Natural Attenuation of Chlorinated Volatile Organic Compounds in a Freshwater Tidal Wetland, Aberdeen Proving Ground, Maryland. USGS Water Resources Investigations Report, 97-4171.

Lovely, D.R., 1985. Minimum Threshold for Hydrogen Metabolism in Methanogenic Bacteria. *Appl. Environ. Microbiol*., 49: 1530-1531.

Lovely, D.R., and Klug, M. J., 1983. Sulfate Reducers Can Outcompete Methanogens at Freshwater Sulfate Concentrations. *Appl. Environ. Microbiol*., 45: 187-192.

Lovley D.R., and Goodwin, S. 1988. Hydrogen Concentrations as an Indicator of the Predominant Terminal Electron-Accepting Reactions in Aquatic Sediments. Geochim. Cosmochim. Acta 52: 2993-3003.

Lovley D.R., Woodward, J.C., and Chapelle, F.H. 1994. Stimulated Anoxic Biodegradationof Aromatic Hydrocarbons Using Fe(III) Ligands. Nature 370: 128-131.

Lovley, D.R., and Phillips, E.J.P., 1987. Competitive Mechanisms for Inhibition of Sulfate Reduction and Methane Production in the Zone of Ferric Iron Reduction in Sediments. *Appl. Environ. Microbiol.*, 53: 2636-2641.

Lovley, D.R., Chapelle, F.H., and Woodward, J.C., 1994. Use of Dissolved H_2 concentrations to Determine Distribution of Microbially Catalyzed Redox Reactions in Anoxic Groundwater. *Environ. Sci. Technol.*, 28: 1205-1210.

Maagd, P.G., Hulscher, D.T., Heuvel, H., Opperhuizen, A., and Sijm, D. 1998. Physicochemical Properties of Polycyclic Aromatic Hydrocarbons: Aqueous Solubilities, *n*-Octanol/water Partition Coefficients, and Henry's Law Constants. *Environ Toxicol Chem.*, 17(2): 251-257.

Middeldorp, P. J. M., De Wolf, J., Zehnder, A. J. B., and Schraa, G. 1997. Enrichment and Properties of a 1,2,4-Trichlorobenzene Dechlorination Methanogenic Microbial Consortium. *Appl. Environ. Microbiol.*, 63(4): 1225-1229.

Mihelcic, J.R., and Luthy, R.G., 1988. Degradation of Polycyclic Aromatic Hydrocarbons Compounds Under Various Redox Conditions in Soil-Water Systems. *Appl. Environ. Microbiol.*, 54: 1182-1187.

Nakashima, Y., Ohsawa, S., Umegaki, K., Ikegamin, S. 1997. Hexachlorobenzene Accumulated by Dams During Pregnancy is Transferring to Suckling Rates During Early Lactation. *J. Nuti*., 127: 648-654.

Nevin, K.P., Homes, D.E., Woodard, T.L., Hinlein, E.S., Ostendorf, D.W., and Lovley, D.R. 2005. *Geobacter bemidjiensis* sp. nov. and *Geobacter psychrophilus* sp. nov., Two Novel Fe (III)-Reducing Subsurface Isolates. *International Journal of Systematic and Evolutionary Microbiology*. 55: 1667-1674.

Odom, J.M. and Singleton, R. Jr. 1993. The Sulfate-Reducing Bacteria: Contemporary Perspectives. Springer-Verlag New York Inc..

Palermo, M., Maynord, S., Miller, J., and Reible, D. 1998. Guidance for In-Situ Subaqueous Capping of Contaminated Sediments. EPA 905-B96-004. Great Lakes National Program Office, Chicago, IL.

Pardue, J.H., Jackson, W.A., Shin, W.S., Adrian, D.D., and DeLaune, R.D. 1998. Biodegradation of Petroleum Hydrocarbons in Wetlands: Constraints on Natural and Engineering Remediation, EPA, Grant # CR822271.

Pavlostathis, S.G., and Prytula, M.T., 2000. Kinetics of the Sequential Microbial Reductive Dechlorination of Hexachlorobenzene. *Environ. Sci. Technol.*, 34 (18): 4001-4009.

Phelps, H.L. 2002. Sources of Bioavailabe Toxic Pollutants in the Anacostia. Final Report to the DC Water Resources Research Center.

Potin, O., Veignie E., and Rafin, C., 2004. Biodegradation of Polycyclic aromatic Hydrocarbons (PAHs) by *Cladosporium sphaerospermum* Isolated from an aged PAH contaminated soil. *FEMS Microbiology Ecology* 51(1): 71-78.

Prevedouros, K., Brorström-Lunden, E., Halsall, C.J., Jones, K.C., Lee, R.G.M., Sweetman, A.J., 2004. Seasonal and long-term trends in atmospheric PAH concentrations: evidence and implications. *Environmental Pollution* 128: 17-27.

Qaisi, K.M., K.S. Ro, D. Reible, L.J. Thibodeaux, K.T. Valsaraj, and W.D. Constant. 1996. Transport Process of TNT from Flooded Highly Contaminated Surface Soil Bed. *Journal of Environmental Science and Health*, Part A, Vol. 10: 2512-2532.

Qaisi, K.M., L.J. Thibodeaux, K.S. Ro, K.T. Valsaraj, and D.D. Adrian. 1996. A Proposal for a Field-Scale Pilot Demonstration Unit for Bioremediation of TNT Contaminated Soil. *Journal of Environmental Science and Health*, Part A, Vol. 9: 2287-2294.

Ramsay, J.A., Li, H., Brown, R.S., and Ramsay, B.A., 2003. Naphthalene and Anthracene Mineralization Linked to Oxygen, Nitrate, Fe(III) and Sulphate Reduction in a Mixed Microbial Population. *Biodegradation*. 14: 321-329.

Ravikrishna, R., Choy, B. C., Valsaraj, K. T., Reible, D. D., Thibideaux, L. J., Price, C. B., and Brannon, J. M. 2000. The Efficiency of Capping to Control Air Emissions from Exposed Contaminated Sediments and Dredged Material. *Environ. Eng. Sci.*, 17 (2): 97-106.

Reible, D.D., Hayes, D., Lue-Hing, C., Patterson, J., Bhowmik, N., Johnson, M., and Teal, J. 2003. Comparison of the Long-Term Risks of Removal and In-Situ Managemanet of Contaminated Sediments in the Fox River. *J. Soil Sed. Contam*., 12: 325-344.

Reible, D.D. and Lowry, G.V. 2005. Active Capping of Contaminated Sediments. 05AIChE: 2005 AIChE Annual Meeting and Fall Showcase, Conference Proceedings, p 5934

Reible, D.D., Constant, D.W., Roberts, K., and Zhu, Y. 2004. Active capping demonstration project in anacostia DC. Remediation of Contaminated Sediments : Proceedings of the Second International Conference on Remediation of Contaminated Sediments, p 925-931

Rothermich, M.M., Hayes, L.A., and Lovely, D.R., 2002. Anaerobic, Sulfate-Dependent Degradation of Polycyclic Aromatic Hydrocarbons in Petroleum-Contaminated Harbor Sediment. *Environ. Sci. Technol,* 36 (22): 4811-4817.

Ruiz, C.E., and Gerald, Terry. (2001). RECOVERY version 2.0, a mathematical model to predict the temporal response of surface water to contaminated sediments. ERDC/EL TR-01-3, U.S. Army Engineer Research and Development Center, Vicksburg, MS.

Saison, C., Perrin-Ganier, C., Amellal, S.,Morel, J.L., Schiavon, M., 2004. Effect of metals on the adsorption and extractability of ^{14}C-phenanthrene in soils. *Chemosphere*. 55: 477-485.

Sanderson, W. H. and Mcknight, A. L. 1986. Survey of Equipment and Construction Techniques for Capping Dredged Material. Technical Report, D-86-6, US Army Engineer Waterways Experiment Station, Vicksburg, Mississippi.

Schafer, H., and G. Muyzer. 2001. Denaturing gradient gel electrophoresis in marine microbial ecology. *Methods Microbiol*. 30: 425-468.

Schnoor, Jerald L. Environmental modeling: fate and transport of pollutants in water, air, and soil. 1996. John Wiley & Sons, Inc. New York.

Sharma, H.R. and Reddy, K. R. 2004. Geoenvironmental engineering; site remediation, waste containment, and emerging waste management technologies. John Wiley & Sons, New Jersey.

Simpson, S. L., Pryor, I. D., Mewburn, B. R., Batley, G. E., and Jolley, D. 2002. Considerations for Capping Metal-Contaminated Sediments in Dynamic Estuarine Environments. *Environ. Sci. Technol*., 36 (17): 3772-3778.

Sims, J.L., Suflita, J.M., and Russell, H.H., 1991. Reductive Dehalogenation of Organic Contaminants in Soils and Ground Water. Ground Water Issue, EPA/540/4-90/054.

Soetaert, K., Herman, P.M.J., and Middelburg, J.J. 1996. A Model of Early Diagenetic Processes from the Shelf to Abyssal Depths. *Geochim. Cosmochim. Acta*., 60: 1019-1040.

Takahashi, T. and Yabuta, K., 2002. New Applications for Iron and Steelmaking Slag. NKK Technical Review, 87: 38-44.

Thibodeaux, L. J. Environmental Chemodynamics: Movement of Chemicals in Air, Water, and Soil. 1996. John Wiley & Sons, Inc. New York.

Thoma, G.J., Reible, D.D., Valsaraj, K.T., and Thibodeaux, L.J., 1993. Efficiency of Capping Contaminated Sediments In Situ: 2. Mathematics of Diffusion-Adsorption in the Capping Layer. *Environ. Sci. Technol*, 27 (12): 2412-2419.

U.S. EPA (U.S. Environmental Protection Agency). 1987. Health and Environmental Effects Profile for Phenanthrene. Prepared by the Environmental Criteria and Assessment Office, Office of Health and Environmental Assessment, U.S. Environmental Protection Agency, Cincinnati, OH, for the Office of Solid Waste and Emergency Response. ECAO-CIN-P226.

U.S. EPA. Assessment and Remediation of Contaminated Sediments (ARSC) Program; Guidance for in-situ subaquous Capping of Contaminated Sediments. Assessment and Remediation of Contaminated Sediments Program, Great Lakes National Program Office; Chicago, IL, 1998.

Valsaraj, K.T., Qaisi, K.M., Constant, W.D., Thibodeaux, L.J. and Ro. K.S. 1998. Diffusive Transport of 2,4,6 – Trinitrotoluene (TNT) from Contaminated Soil to Overlying Water. *Journal of Hazardous Materials*. 59: 1-12.

Van Capellen, P. and Wang Y. 1996. Cycling of Iron and Manganese in Surface Sediments: A General Theory for the Coupled Transport and Reaction of Carbon, Oxygen, Nitrogen, Sulfur, Iron and Manganese. *American Journal of Science*, 296: 197-243.

Wang, X.Q., Thibodeaux, L.J., Valsaraj, K.T., and Reible, D.D., 1991. The Efficiency of Capping Contaminated Sediments in Situ. I. Lab-scale Experiments of Diffusion/Adsorption in the Capping Layer. *Environ. Sci. Technol.*, 25 (9): 1578-1584.

Weiner, J.M. and Lovley D.R. 1998a. Anaerobic Benzene Degradation in Petroleum-Contaminated Aquifer Sediments after Inoculation with a Benzene-Oxidizing Enrichment. *Appl. Environ. Microbiol*. 64:775-498.

Weiner, J.M. and Lovley D.R. 1998b. Rapid Benzene Degradation in Methanogenic Sediments from a Petroleum-Contaminated Aquifer. *Appl. Environ. Microbiol*. 64:1937-1939.

Wiedemeier, T.H., Swanson, M.A., Moutoux, D.E., and Gordon, E.K., 1996. Technical Protocol for Evaluating Attenuation of Chlorinated Solvents in Ground water. Air Force Center for Environmental Excellences, Technology Transfer Division, San Antonio.

www.inchem.org/pages/icsc.html (Nov. 23, 2005)

Yang, Y., and McCarty. 1998. Competition for Hydrogen within a Chlorinated Solvent Dehalogenating Anaerobic Mixed Culture. *Environ. Sci. Technol*. 32:3591-3597.

Zhang, W. and Bouwer, E.J. 1998. Biodegradation of Benzene, Toluene and Naphthalene in Soil-Water Slurry Microcosms. *Biodegradation*. 8:167-175.

Zhao, D., Hunter, M. Pignatello, J.J., and J. C. White. (2002). Application of the dual-mode model for predicting competitive sorption equilibria and rates of polycyclic aromatic hydrocarbons in estuarine sediment suspensions. *Environ Toxicol Chem.* 21(11):2276-2282.

VITA

Eun Ju Lee was born in September, 1972, in Korea, where she grew up and pursued a bachelor's degree in microbiology from Gyeong Sang National University, graduating from there in 1995. She worked a position as a research associate at macromolecular chemistry laboratory in Gyeong Sang National University then, she became interested in applied microbiology and she decided to study in United States. She entered Louisiana State University in 1998 and completed her master's degree in engineering science in 2000. She continued her study to pursue a Doctor of Philosophy Degree in the Department of Civil and Environmental Engineering. She is now a doctoral candidate and engineer with completing her research on "Effect of Capping on Biodegradation of Organic Contaminants in Sediments".